12-2014

USING GIS TO PRIORITIZE GREEN INFRASTRUCTURE INSTALLATION STRATEGIES IN AN URBAN WATERSHED

Lauren Owen
Clemson University, LOWEN@g.clemson.edu

USING GIS TO PRIORITIZE GREEN INFRASTRUCTURE INSTALLATION STRATEGIES IN AN URBAN WATERSHED

A Thesis
Presented to
The Graduate School of
Clemson University

In Partial Fulfillment
of the Requirements for the Degree
Master of Science
Biosystems Engineering

By
Lauren Alyssa Owen
December 2014

Accepted by:
Dr. Tom Owino, Co-Advisor
Dr. Daniel R. Hitchcock, Co-Advisor
Dr. David L. White
Dr. Christophe Darnault

ABSTRACT

This study seeks to quantify runoff volume generation and peak flow rates from the urban Sand River Headwaters to determine the most effective placement of additional green infrastructure in Aiken, SC. ArcMap 10.1, HEC-GeoHMS, and HEC-HMS were used to delineate a total outlet watershed along with subwatershed(s) for urban stormwater infrastructure system by "burning" the stormwater system at an artificial elevation below the existing topologically-based Digital Elevation Model (DEM). The result was a higher resolution DEM that allowed for storm routing and subsequent volume and flow predictions compared to that based on the original DEM created by using Light Detecting and Ranging (LiDAR) surface elevation data.

Ten key monitoring locations were identified for flow accumulation determination within the total watershed area, not only at the outlet for the entire watershed but also at inclusive subwatersheds that were selected based on City Engineer recommendations and field evaluations of the complex piped urban stormwater network. Stage data collected from SonTek™IQ-Pipe® acoustic Doppler sensors at each monitoring location were used to calculate flow rates and volumes based on flow through the pipe and Manning's n derived from the material of the conduit. Calculated volumes and flow rates at each subwatershed were used for calibration and validation of both ArcMap 10.1 and HEC-HMS based prediction models. HEC-HMS outputs underestimated runoff generation and peak flow rates over all storm events while ArcMap output volumes demonstrated underestimation for smaller storm events but overestimation for larger storms.

Runoff volume generation and peak flow rate were then used, along with percent impervious surface and average curve number (CN) based on subwatershed data, to determine the location recommendations for additional green infrastructure within the urban Aiken watershed (which also serves as the Sand River Headwaters) to allow for the greatest influence on stormwater quantity reduction and water quality improvement.

Results demonstrated that the most effective placement for additional green infrastructure upon landscapes was within Subwatersheds 3 and 9 with the largest amount of runoff flow and least amount of percent impervious surface out of the four subwatersheds contributing to the 67 percent area of the total watershed. The most effective place to install additional green infrastructure upon hardscapes was within Subwatershed 2 with one of the largest amounts of individual runoff flow and highest amount of impervious surface of the subwatersheds with the highest individual area contribution. An additional space for landscape green infrastructure installations may also exist within Subwatersheds 6 and 7 closer to the natural areas near the watershed outlet with very low percent impervious surface, but significantly smaller area for placement.

ACKNOWLEDGEMENTS

This project is funded through a City of Aiken, SC research grant to the Institute of Computational Ecology. I would like to give a huge thank you to the City for their funding and support. A gigantic thank you to Dr. Daniel Hitchcock for always encouraging me and providing me with this opportunity and all the guidance I needed to complete my research. Thank you to Dr. David White for all of his guidance and expert advice on all GIS work and flow routing analysis and for always being available for help. Many thanks to Dr. Tom Owino and Dr. Christophe Darnault for taking me under their wing and allowing me to complete my degree under their guidance and support. Special thanks to all who have made amazing efforts to make this project a success, specifically: Dr. Gene Eidson, Kelly Kruzner, Alex Pellett from Clemson University, and George Grinton, Ben Smith, Pearce Atkins, Nica Loving, and Ron Mitchell from the City of Aiken.

TABLE OF CONTENTS

Page

TABLE OF CONTENTS (CONT)

Page

LIST OF FIGURES

Figure Page

LIST OF FIGURES (CONT)

Table Page

LIST OF FIGURES (CONT)

Figure Page

LIST OF FIGURES (CONT)

Figure Page

LIST OF FIGURES (CONT)

Figure Page

LIST OF TABLES

CHAPTER 1: INTRODUCTION

1.1 PROBLEM STATEMENT

For over 30 years, the City of Aiken, South Carolina has proactively attempted to utilize stream stabilization techniques and upstream stormwater management practices – including green infrastructure installations – to address erosion issues due to high stormwater flows being discharged from its highly urbanized watershed. A typical issue with urban watersheds is the increased runoff and peak flow rates leading to stream bank erosion downstream of the watershed discharge point. This project employed a modeling and monitoring approach to determine which subwatershed(s) within the greater Aiken watershed most significantly contributed to stormwater flows, thus these areas would be targeted for green infrastructure installations to reduce event-based discharges.

1.2 SITE DESCRIPTION

In Aiken (Figure 1.1), the 1,080 acre watershed has an extensive stormwater pipe system that drains to a single 10 foot pipe outlet. It is a highly connected system in which runoff flows immediately from rooftops to parking lots or driveways to gutters and then to pipes resulting in extremely "flashy" hydrographs during and after a storm event; flow in the system rapidly peaks and then recedes (Woolpert, 2003). The stormwater outflow from the urbanized Aiken watershed drains to the headwaters of

the Sand River, and then flows to Horse Creek and eventually into the Middle Savannah River. The erosion at this outlet is so extensive, that the resulting bank erosion has formed a canyon with depths measuring up to 70 feet in some locations. Upon reaching the outlet, upper reaches are experiencing the greatest erosion, while there is only minor erosion along the middle reaches with considerable sediment transport from upstream sources, and sediment is being deposited in the main channel and in flood plains along the lower reaches (Meadows et al., 1992). With the majority of soils in the Sand River watershed being of sandy texture, the banks and stream beds have no protection from erosion and subsequent sediment transport and downstream loading which can potentially lead to water quality impairments.

A major impact from poorly managed land development and land use/land cover change from forested to urban landscapes within a watershed can be the loss of natural hydrology. According to reports, in 1983, much of downtown Aiken was in-place and two branches to the Sand River systems, Sand River and the southern branch, were visible. By 1951, development had begun to expand westward along Richland Avenue, southward along Whiskey Road, and into the Houndslake area (Figure 1.1). A tributary to Sand River from the vicinity of Palmetto Golf Club to Sand River was now apparent. In 1961, further evolution in the tributary system to Sand River was obvious, and the main channel was more clearly defined, having become deeper and wider. Later evidence shows continued build-out along Richland Avenue and in the Houndslake area, and further expansion of Sand River and its tributaries (Meadows et al., 1992). Since then development has continued and further

erosion has caused further expansion, deepening, and widening of the Sand River and its tributaries.

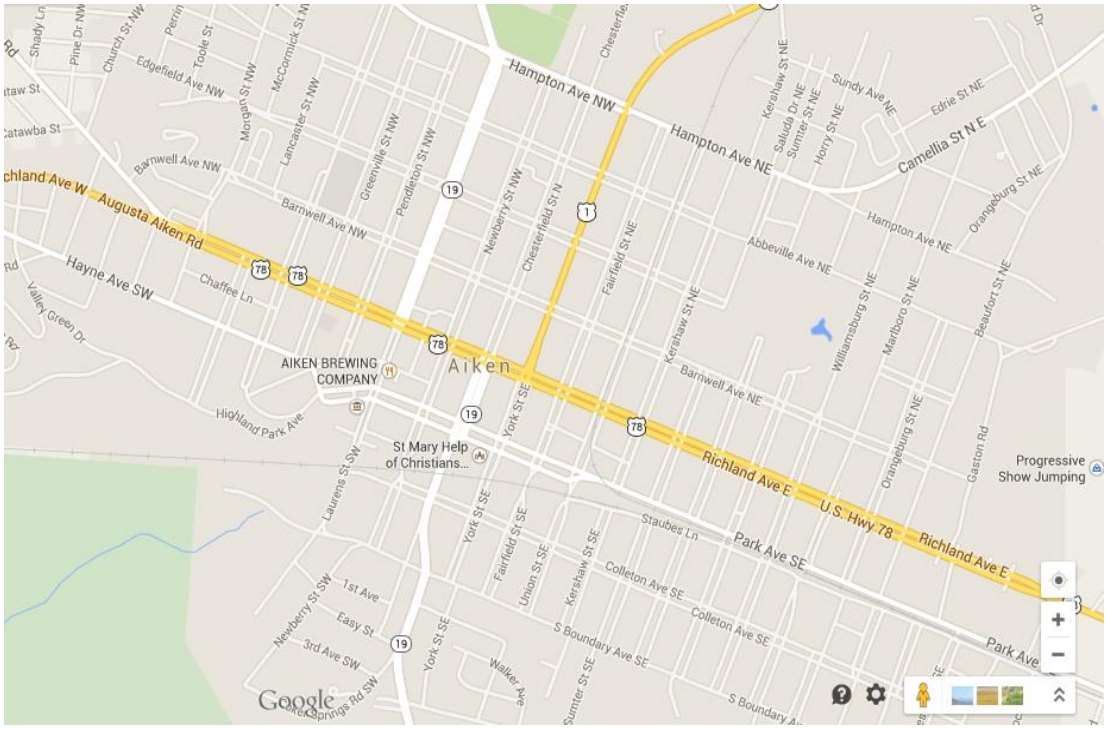

Figure 1.1: Map of the City of Aiken with labeled roads, specifically Richland Avenue and Whiskey Road to demonstrate where expansion occurred

Due to increasing areas of paved surfaces, both the permeability of soil and infiltration capacity decreases, and surface runoff increases; such changes of natural regime on a comparatively small area of a city bring significant and often adverse effects on the whole river basin downstream of the city (Niemczynowicz, 1999). Due to the relatively small size of the Sand River watershed and the City of Aiken, the land use changes and impervious percent increase of development have had an adverse impact on downstream flows from small to large storm events. The direct

connection of impervious surfaces to streams means that even small rainfall events can produce sufficient surface runoff to cause frequent disturbance through regular delivery of water and pollutants (Walsh et al., 2005). A relatively recent study has shown that the smaller, more frequent storms cause the most damage to the Sand River (Woolpert, 2003). It has been demonstrated that existing infrastructure cannot support effective stormwater management in downtown Aiken and adjacent residential and commercial areas. Historically, several solutions were discussed and modeled in previous studies including: diversion, bank stabilization, detention, green infrastructure installation, extension of the outflow, etc.

1.3 PROJECT DESCRIPTION

A Clemson University research team was asked to design a solution to the degradation problem incorporating green infrastructure. In 2009, the resulting project plan finalized by Clemson University's Center for Watershed Excellence incorporated bioretention cells, bioswales, permeable pavement, and a cistern in its green infrastructure solution and the effectiveness of these management practices to capture, store, infiltrate, and treat downtown stormwater (Clemson University, 2013). In January 2012, Phase 1 of the project was completed seeking to examine the effectiveness of bioretention cells and porous pavement in Aiken, SC to reduce stormwater runoff volumes and improve water quality downstream. On April 1, 2013 Phase 2 of the project began set to conclude on March 31, 2015. The objectives of Phase 2 include:

1. Quantify hydrologic flows during storm events draining to and within the downtown Aiken stormwater sewer system that constitutes Sand River headwaters.
2. Based on storm event flows, evaluate and optimize potential locations for further green infrastructure (GI) installation including analysis for hydrology and cost-effectiveness.
3. Enhance site-level remote data acquisition capabilities throughout the Sand River watershed and integrate associated collection, transmission, display, and archival facilities into the *Intelligent River*® network.

There were four main steps to completing these objectives. The first was to gain a better understanding of the existing stormwater network within the watershed and its drainage boundaries based on increased interaction with the public and City officials along with field studies to determine flow accumulation and connectivity of the urban stormwater system. The second step required quantification of volume and routing, with specific tasks that included: review of existing survey information of the water network, trunk line instrumentation with level/flow sensors in which ten monitoring locations were selected, and watershed scale modeling to effectively examine the overall efficiency of existing or future green infrastructure installation. Third, spatial analyses using Geographic Information Systems (GIS) were utilized to delineate watersheds and derive characteristics such as impervious surface and curve number (CN) per watershed. Lastly, an optimal location for future green infrastructure installation would be determined based on steps two and three, along with a cost

benefit analyses and a decision matrix-based on existing infrastructure, contributing area to stormflow and discharge, water volume availability, and proximity. Once all of these steps have been completed and all the parameters determined the subwatershed that contribute to high stormwater flows and subsequently to downstream erosion can be identified. Once this is determined, then additional green infrastructure can be installed within these subwatershed(s) to effectively and efficiently decrease runoff and peak flow rate at the Sand River headwaters. If successful, this research approach and modeling methodology can then be used as a tool in other urban or developing areas.

1.5 REFERENCES

Institute of Applied Ecology/Center for Watershed Excellence. Sand River Headwaters Green Infrastructure Project. Rep. Clemson: n.p., 2013. Print.

Meadows, Michael E., Katalin B. Morris, and William E. Spearman. Stormwater Management Study for the City of Aiken: Sand River Drainage Basin. Rep. Columbia: Department of Civil Engineering at U of South Carolina, South Carolina Land Resources Conservation Commission, 1992. Print.

Niemczynowicz, Janusz. "Urban Hydrology and Water Management – Present and Future Challenges." *Urban Water* 1.1 (1999): 1-14. Web.

Walsh, Christopher J., Tim D. Fletcher, and Anthony R. Ladson. "Stream Restoration in Urban Catchments through Redesigning Stormwater Systems: Looking to the Catchment to save the Stream." *Journal of the North American Benthological Society* 24.3 (2005): 690. Web.

Woolpert. Sand River Watershed Study. Rep. Aiken: n.p., 2003. Print.

CHAPTER 2: PROJECT BACKGROUND AND LITERATURE REVIEW

2.1 URBAN HYDROLOGY

Urban hydrology is typified by very high level of human interference with natural processes and high amounts of land use and land cover changes. All hydrological sub-processes in urban areas must be considered in much smaller temporal and spatial scales than those in rural areas (Niemczynowicz, 1999). This requirement is due to the negative impacts downstream of the urban watershed caused by increased runoff volumes and peak flow rates from even small storm events. Moreover, the installation of storm sewers, storm drains, and piped networks for stormwater management can accelerate runoff (Goudie, 1990). Any construction of urban water related infrastructure, channels, pipes, conduits and even shaping of streets must be based on good knowledge of what will be the effect of these structures on water flows in the city and what is necessary to avoid damage on man-made constructions; increasing imperviousness of an urban city area can lead to generation of stormwater flows that may significantly influence the flow regime in the entire river downstream (Niemczynowicz, 1999). Many published studies exist related to stormwater management in rural areas, but far less studies in urban areas such as the City of Aiken. In order to understand stormwater reduction strategies for urban areas, it is necessary to understand urban hydrology-a growing field of scientific research.

Stormwater management can be difficult to measure and model in urban areas due to lack of permeable surfaces for the installation of management practices and the existence of enough surface area to make a decrease in the runoff at the outlet of the watershed. It is considered more effective to treat stormwater at its source i.e. small units of impermeable surfaces where urban runoff is first generated and where stormwater runoff can accumulate pollutants on the streets, roofs, etc. (Niemczynowicz, 1999) as opposed to treating downstream water bodies after they have already been impacted . Innovative urban water management strategies with more sustainable configurations should be integrated with the planning and management of water supply, wastewater services, and stormwater (Brown, 2005). Urban stormwater management should emphasize the restoration or protection of natural hydrologic processes at small scales, with the aim of restoring natural flow regimes at larger scales downstream (Burns et al., 2010).

There is now widespread recognition of the degrading influence of urban stormwater runoff on stream ecosystems and of the need to mitigate these impacts using stormwater control measures (Fletcher et al., 2014). Stormwater runoff from roads, rooftops, parking lots, and other impervious cover in urban and suburban environments is a well-known cause of stream degradation, commonly referred to as urban stream syndrome with common impacts of stormwater runoff including increased flooding, channel instability, water quality impairment, and disruption of aquatic habitats (Pyke et al., 2011). The collapse of healthy freshwater ecosystems in urban environments is the result of stormwater management policies that emphasize

expedient removal of stormwater from communities for the protection of human health and property, but place a low priority on ecosystem preservation (Roy et al., 2008). A balance of ecology and engineering is necessary to develop urban stormwater management solutions that mimic natural settings and achieve watershed restoration by targeting runoff and peak flow rate.

2.2 LOW IMPACT DEVELOPMENT

Increasingly, cities are experimenting with approaches that reduce runoff and pollution by increasing managed infiltration through natural hydrologic features, often referred to as green infrastructure or low-impact development (LID) considering energy use, ecology, and landscape design to mitigate pollution, reduce consumption, and improve social equity in cities (Porse, 2013). LID is designed to imitate natural hydrologic processes while improving environmental quality of the surrounding watershed. LID strategies are being encouraged in many communities as an approach to reduce potential adverse impacts of development on receiving streams, as LID sites attempt to mimic predevelopment site hydrologic conditions by controlling runoff close to its source, post construction best management practices (BMPs) are typically dispersed throughout a development site (Clary et al., 2011). LID applies principles of green infrastructure to bring together site-planning and stormwater-management objectives, while using LID philosophy to retrofit existing development and to plan new sites (Wang et al., 2010). The main principles of LID-BMP planning usually

include (1) preserve the original terrain, (2) limit the ratio of impervious surface areas, (3) avoid the direct connection of impervious areas, (4) select the most suitable BMP types according to local conditions in terms of both technical and social/economic factors, and (5) set an appropriate goal for the LID-BMP implementation (Jia et al., 2012). Jia et al. (2012) goes on to explain that social/economic conditions include land use, natural hydrology and soil features, areas of sub-watersheds, slope of the development region, and the desired effects of development, also noting public acceptance as an important consideration. LID and BMP practices focus on enhancing infiltration and evapotranspiration to maximize stormwater retention/detention to decrease pressure on downstream water quantity and quality loads.

2.3 LID CLASSIFICATIONS

LID strategies can be classified into various categories including structure versus nonstructural practices. Structural practices consist of bioretention, infiltration well/trenches, stormwater wetlands, wet ponds, level spreaders, permeable pavements, swales, green roofs, vegetated filter/buffer strips, sand filters, smaller culverts, and water harvesting systems (rain barrels/cisterns) while nonstructural practices include minimization of site disturbance, preservation of natural site features, reduction and disconnection of impervious surfaces (i.e., elimination of curbs and gutters), strategic grading, native vegetation utilization, soil amendment

and aerification, and minimization of grass lawns (Ahiablame et al., 2012). LID strategies can also be classified into various performance categories: individual LID practice monitoring in which an individual LID practice (e.g., a bioretention cell, a biofilter, or permeable pavement parking lot) is isolated to monitor its performance, overall site-level performance in which multiple distributed controls are monitored, and hybrid LID traditional site-level monitoring in which a site to be monitored may include multiple distributed controls and LID principles, but it may also incorporate some traditional larger-scale stormwater management components at the downstream end of the study site, particularly for flood control (Clary et al., 2011). There are also various focuses for different BMPs including water quality and water quantity, which can be further developed into peak flow reduction and volume reduction. Runoff can be reduced via canopy interception, soil infiltration, evaporation, transpiration, rainfall harvesting, engineered infiltration, or extended filtration while peak flow reduction is accomplished by providing watershed storage and runoff attenuation; additional BMPs that serve to remove the pollutants from stormwater through settling, filtering, adsorption, biological update, or other mechanisms can be combined with the volume reduction strategy to further reduce the pollutant load (Battiata et al., 2010).

2.4 REDEFINING LID

Expanding on these LID-BMP approaches, as a whole LID practices have shifted focus from only water quality or only volume reduction to combine both approaches into the same implementation strategy. Stormwater management goals are evolving beyond conveyance and flood control, to include pollution abatement, runoff retention, urban landscape improvements, and reduced infrastructure costs creating stormwater systems that are expected to serve more functions, while still remaining cost-effective (Porse, 2013). Combining various LID practices and taking a more holistic, or total watershed, approach is more effective than isolated BMPs. The thrust of watershed-based BMP planning analysis is the evaluation of the "combined", or synergic, effect of all the BMPs installed in the watershed at a prescribed evaluation point or points (Jia et al., 2012). Despite recent advances, in managing stormwater to reduce pollutant loads and peak flow rates, a more complete approach is needed, one which includes as a goal the restoration or protection of ecologically important elements of the pre-development hydrograph and uses a holistic approach to implement LID practices throughout the entire contributing watershed (Burns et al., 2012, Younos, 2011, Ray et al., 2008, Yang and Li, 2013).

Under appropriate conditions, rainwater harvesting systems can complement the other LID-BMPs to attain optimum effect for urban stormwater management and can alleviate the impact of stormwater runoff, save potable water, reduce energy use, and contribute to groundwater preservation (Younos, 2011). Rainwater harvesting is used

to describe the collection of rainwater from roofs; all other runoff in urban areas, such as from roads, contributes to stormwater flows (Inamdar et al., 2013). In order to decrease the effect of urbanization on the city of Aiken, SC rainwater harvesting and innovative stormwater management techniques based on green infrastructure were used. Green infrastructure development integrates a suite of on-site, infiltration-based stormwater management designs, and integrated green infrastructure practices can be effective in stormwater runoff reduction and water quality enhancement at watershed-scale community development (Yang and Li, 2013). Rainwater harvesting in Aiken involved the collection of rain water from roofs through the use of gutters and flow routing, along with road runoff, to permeable pavement plots where it congregated with the stormwater runoff and travelled to bioretention cells, a cistern, or followed the stormwater flow through the urban piping system.

2.5 FURTHER LID RESEARCH

Advances in the field of urban hydrology, urban stormwater, and LID-BMP strategies continue to develop; however, more research is needed to quantify their effectiveness and develop a range of metrics used to do so. More holistic or total watershed, implementation strategies are necessary and development of adequate regulations for these strategies is required as well. There are seven major impediments to sustainable urban stormwater management including: (1) uncertainties in performance and cost, (2) insufficient engineering standards and

guidelines, (3) fragmented responsibilities, (4) lack of institutional capacity, (5) lack of legislative mandate, (6) lack of funding and effective market incentives, and (7) resistance to change (Roy et al., 2008). Metrics to demonstrate effectiveness and performance assessment are also lacking in LID-BMP strategies (Ahiablame et al., 2012, Roy et al., 2014, Pyke et al., 2011, Wang et al., 2012, Clary et al., 2011, Battiata et al., 2010, Qui, 2013). A tentative set of metrics developed through Clay et al.'s research includes: Metric 1: presence/absence of discharge (practice & site), Metric 2: absolute surface runoff volume reduction (practice), Metric 3: relative volume reduction (practice), Metric 4: discharge volume per area (site & practice), Metric 5: discharge volume per impervious area (site & practice). Literature suggests that all LID practices could perform efficiently as long as proper design, implementation, and maintenance are followed (Ahiablame et al., 2012).

2.6 HYDROLOGIC MODELING

The terms effective imperviousness (EI) and directly connected imperviousness (DCI) are thus used to describe the proportion of a catchment made up of impervious areas directly connected to receiving waters via a constructed drainage system; with advances in GIS and spatial modeling capability, more precise means for estimating effective imperviousness have developed (Fletcher et al., 2014). Recent progress observed in development of GIS brings possibility to use hydrological data more efficiently; formalized mathematical models are becoming increasingly important

tools for management of urban water resources as well as for assessment of their environmental impacts (Niemczynowicz, 1999). In order to increase knowledge and understanding of these advances an extensive literature review was done on the new techniques. The specific techniques that were focused on were terrain analysis from Digital Elevation Models (DEMs), watershed delineation, and subwatershed categorization. This specific study focused on the programs ArcMap 10.1, HEC-HMS, and its pre-processer HEC-GeoHMS. The area of focus in this study was the stormwater system located in the city of Aiken, South Carolina and the effect of urbanization in this area on the Sand River Headwaters watershed and the Sand River.

2.6.1 LIDAR DEM TERRAIN ANALYSIS

Various studies have been done on the impacts of urbanization and land use alteration due to the growing need for understanding on the subject. Bhaduri et al. (2000), Weng (2001), Niemczynowicz (1999), Walsh et al. (2005), Ali et al. (2011), Du et al. (2012), Chen et al. (2009), and many others have expressed their concern over the impacts associated with the effects of increased runoff associated with land use change. There has been an abundance of studies on these impacts in natural settings and rural areas; however, there is a great need for further understanding on the subject in fully developed urban areas such as Aiken, SC. A growing field of interest is developing in the study of terrain analysis in these urban areas, specifically focusing on their stormwater management and runoff modeling. Several watershed models have been utilized to further this interest including but not limited to:

Geographic Information Systems/Hydrologic Engineering Center (GIS/HEC-1), StormWater Management Model (SWMM), Hydrologic Engineering Center-Geospatial Hydrologic Modeling (HEC-GeoHMS), Hydrologic Engineering Center Pre-Processor (HECPrePro), Topographic Parameterization (TOPAZ), Watershed Modeling System (WMS), Agricultural Non-Point Source model (AGNPS 98), CASCade of planes using 2 dimensions (CASC2D), Hydrologic Engineering Center-River Analysis System (HEC-RAS), Hydrologic Engineering Center-Hydrologic Modeling System (HEC-HMS), Modular Modeling System/Precipitation Runoff Modeling System (MMS/PRMS), Systeme Hydrologique European (SHE), Soil and Water Assessment Tool (SWAT), and TOPography based hydrologic model (TOPMODEL) (Ogden et al., 2001). For ease of use and access specific to land development and runoff modeling, along with spatial representation and data manipulation capacities, ArcMap 10.1, HEC-HMS, and HEC-GeoHMS were chosen for this project. These three programs also work very well when used in conjunction and ArcMap and HEC-GeoHMS achieve the necessary outputs needed for the inputs into the HEC-HMS model.

Originally, terrain analysis simply involved the physical viewing of maps and hand digitalization. Now, with the creation of various GIS modules that can handle large data sets, terrain analysis means much more. With the use of DEMs in urban and rural areas, hydrologic models can now be created that provide a variety of functions including watershed analysis and characterization. DEMs are becoming more widespread with most areas providing them to the public for further use. A

growing development in the field of hydrologic modeling is the use of LiDAR (Light Detection And Ranging) data to create a more useful and hydrologically correct DEM; While there are several methods to create DEMs that are fairly accurate and useful, compared to other DEMs a LiDAR DEM has higher accuracy and resolution resulting in more detailed drainage networks and subcatchment delineation leading to a higher quality of hydrological features (Lui et al., 2005). LiDAR technology collects elevation data by shooting a laser to the ground and measuring the amount of time it takes to return to its place of origin. There are two different types of elevation models available from LiDAR which are first return, including tree canopies and buildings and referred to as a Digital Surface Model (DSM), or the ground model which contains only the topography and referred to as the DEM (DeLoza and Lee, 2013).

Methods using ArcHydro can be used after the DEM is created, and the depressions and sinks in the DEM can be filled to prevent pits or areas of lower elevation in the DEM from rerouting hydrologic flows on the surface (Maidment, 2002). Flow direction and flow accumulation for the area can be established from the reconditioned DEM. Both of these tools can be computed using a surrounding 8 point grid, but each tool has its own calculation method. The flow direction grid uses slopes of its surrounding cells, and water will follow the path with the steepest slope; from this grid, the flow accumulation grid is created and calculated by recording the number of cells that drain into each cell on the grid (Maidment, 2002). Streams can be digitalized from the flow accumulation grid and watersheds along with

subwatersheds can be created using snap pour points, or cells with the highest flow accumulation, and the ArcHydro tools in ArcMap 10.1. These methods work great for rural settings and develop the natural streams and watersheds of the DEM; however, for this research new methods were needed to create a system that was contrived from the underground routing of an urban area. To summarize, urban stormwater systems, such as Aiken, SC need to be recognized in ArcGIS as the natural streams of the DEM so that watersheds can be created for the pipe network and not the existing geographical elevations.

Modeling urban systems as a natural element of a surrounding area is of growing interest in recent research areas. Several studies have been done on modeling these stormwater systems including but not limited to Gironás et al. (2010), Inamdar et al. (2013), Luzio et al. (2004), Holder et al. (2002), Paz and Collischonn (2007), Maidment (1996), Cantone and Schmidt (2009), Emerson et al. (2003), and Brock (2006). Modeling urban areas is more complicated due to the fact that when the DEM is created and watershed delineation begins, the model determines the watersheds based on the natural streams created by the pre-existing elevations of the DEM. Watersheds are a subdivision of a basin into drainage areas selected for a particular hydrologic purpose while catchments are a subdivision of a basin into elementary drainage areas defined by a consistent set of physical rules; the distinction is drawn between catchments, whose layout can be automatically determined using a set of rules applied to a digital elevation model, and watersheds, whose outlets are chosen manually to serve a particular hydrologic purpose (Maidment, 2002). For urban

projects, the watershed boundaries for the pipe network need to be accepted as the catchment boundaries of the DEM if the stormwater system is added to the natural stream layer correctly. In order to achieve this, a unique method is needed to recreate the urban stormwater systems in the model as the natural element so the watersheds created are delineated based on the pipe system and are equivalent to the catchments delineated from the streams.

There are several different methods to modeling stormwater systems in urban terrain including: use of the raw DEM, street and pipe burning, variable burning of pipes and streets, and surface and subsurface layers (Gironás et al., 2010). The method using the raw DEM designates watershed delineations based on selected pour points, or outlets; however, these watersheds are based on natural elevations-not the stormwater pipe system and will develop the correct areas needed for this research. While these watersheds may be similar to those generated from the stormwater system if the piping follows the natural layout of the area, in most cases this will not be an accurate method for modeling underground schemes. The second method of street and pipe burning will give a much more accurate representation of the underground system. This method involves "burning" the pipes and street layers at an artificial elevation that is lower than the lowest elevation of the DEM. The model is then forced to recognize the pipes and street layers as the natural stream element and delineate the watersheds accordingly. Streams can also be burned as pipes to prevent missing any water flow along the model, and two alterations can be used during the burn using different burn elevations for the streets and the pipes. Method 3 requires

knowing all elevations of streets and pipes within the model. First, the streets are burned into the DEM using their actual elevations. Then, using the DEM with the streets already burned in, the pipes are burned into this DEM using their actual elevations below the ground. Burning the streets and pipe systems into the DEM eliminates the problem in method 2 using the slope of the natural ground surface (Gironás et al., 2010). Method 4 uses the streets and the pipe system as two separate layers in GIS. This method allows flow to travel between the two layers in GIS at set inlet locations, but once flow enters the pipe system it is assumed to stay there permanently. This method also requires all pipe and inlet locations and elevations to be accurate. If all tools perform as they should and all data is manipulated correctly, the watershed for the chosen locations and the adjoint catchment for the natural streams should adhere to the same boundary.

2.6.2 ARCGIS AND HEC-GeoHMS

HEC-HMS and ArcGIS efforts can be combined through HEC's preprocessor HEC-GeoHMS. This preprocessor takes ArcMap outputs from ArcHydro and helps to convert them into HEC inputs through the use of a toolbar extension in ArcMap 10.1. This toolbar processes various shapefiles by placing each one from ArcHydro into data management categories and placing an outlet along a streamline to generate a project point and project area. The preprocessor will then delineate the outlet's basin according to the contributing drainage line and the project can be accepted or the outlet can be relocated to create an acceptable watershed area. Prior to using the

model (HEC-HMS), a DEM should be used to define a stream network and to disaggregate the watershed into a series of interconnected subbasins by HEC-GeoHMS, the GIS preprocessor for HEC-HMS and be coupled to ESRI's ArcMap GIS program. An added capability of version 1.1 allows users to use a more sophisticated "burning in" technique to impose the stream onto the terrain (USACE, 2003). This allows the outlet watershed area generated to include the stormwater system and create all basin characteristics as though it were the natural streams in HEC-GeoHMS.

The process is broken down into five various categories in order of: data management, terrain preprocessing, basin processing, hydrologic parameter estimation, and HMS model support (USACE, 2003). The ArcHydro toolbox in ArcGIS is used to create all the input layers needed for the data management including: the raw DEM or Burned DEM, the Filled DEM or Hydro DEM, the Flow Direction, the Flow Accumulation, the Stream Definition grid, the Stream Link grid, the Catchment grid, the Catchment polygon, the Drainage Line, and the Adjoint Catchment polygon. Burning the stormwater system to the drainage layer allows ArcHydro to manipulate the catchment grid, catchment polygon layer, and the adjoint catchment polygon to essentially accept the pipe system as the natural streams and create a watershed based on the additional flow. This also allows for subbasins to be delineated using HEC-GeoHMS following the divisions of the stormwater network.

All of the terrain preprocessing can be performed using ArcHydro in ArcMap 10.1 along with the slope grid, but the basin processing can be performed using HEC-GeoHMS. River and subbasin layers can be created combining the shapefiles from the data management toolbox in HEC-GeoHMS. Subbasins can then be merged to match the subwatersheds already delineated previously from ArcHydro using the basin merge tool in HEC-GeoHMS. This basin processing allows modeling variables to be calculated from the GIS data and spatially averaged such that a single measure represents an entire subarea (Beighley et al., 2003). The inputs to the model include land use information, hydrologic soil groups, and the DEM. Then, based on the land use data and the hydrologic soil groups, the lumped CN value for each sub-basin can be generated by HEC-GeoHMS (Ali et al, 2011). Impervious percentage can also be lumped per subbasin using HEC-GeoHMS and an impervious surface grid created and clipped in ArcMap from the NLCD. The soil data is gathered from SSURGO data provided by NRCS and converted into a format accepted by HEC-GeoHMS using ArcMap 10.1. The land cover grid from USGS and the SSURGO soil data can be combined to create the soil land use polygon needed for HEC-GeoHMS (Merwade, 2012). The land use soil polygon can then be used in the create curve number grid tool in HEC-GeoHMS to establish the average curve number per subbasin.

Following the methods outlined in the USACE HEC-GeoHMS user's manual the basin characteristics can be extracted to include: River Length, River Slope, Basin Slope, Longest Flow Path, Basin Centroid, Basin Centroid Elevation, and Centroidal Longest Flow Path (Merwade, 2012). These outputs can then be used along with the

curve number and impervious raster sets created to calculate all the various inputs needed to create the HEC-HMS model. HMS process selections can be made in HEC-GeoHMS or chosen later once the model has been created and opened in HEC-HMS. SCS methods are usually chosen for lag method, transform method, and channel routing due to the popularity of the method and the small watershed areas (Costache, 2014). The curve number lag tool can be used to calculate the basin lag time as an input into HEC-HMS based on the curve number grid and impervious grid per subbasin (Merwade, 2012). The "Map to HMS units" tool can be used along with the raw DEM, Subbasin, Longest Flow Path, Centroidal Longest Flow Path, River, and Centroid layers to convert the data into usable HMS units. The HMS link and HMS node layers can be created using the HMS schematic tool to show how the model will look when opened in HEC-HMS after the data has been checked. The check data tool can be used to check any problems involving unique names, river containment, center containment, and river connectivity, all of which will result in errors when uploaded into HEC-HMS (Merwade, 2012). The three main types of input data are: basin input data (loss rate method, transform method, and baseflow method), meteorological data that includes rainfall and evaporation data, and control data that identifies the timing of the analysis, start and finish dates (Al-Abed et al., 2005). These layers can all be derived in HEC-GeoHMS and made ready to import directly in HEC-HMS for flow rate and volume hydrograph generation.

2.6.3 ARCGIS AND HEC-HMS

Now that the stormwater pipe system can be burned in and recognized as the natural stream element, watersheds and subwatersheds can be delineated for specified pipe outlets throughout urban cities using the ArcHydro extension as detailed above. Subwatershed areas can then be calculated and exported through ArcMap 10.1 and used along with rainfall data to calculate runoff volumes for each subwatershed and the total watershed area. These volumes can be used to compare to sensor volume calculations derived from stage data and used for calibration and validation of prediction models. There is a lack of research on peak flow determination directly from ArcMap outputs, but there is not a lack of research determining peak flows using ArcGIS and HEC-HMS in conjunction. Knebl et al. (2005), Chen et al. (2009), Du et al. (2012), Ali et al. (2012), Verma et al. (2010), Beighley et al. (2003), Al-Abed et al. (2005), McColl and Aggett (2007), and many others have all done studies on the use of GIS and HEC-HMS working together to achieve watershed parameter outputs. After the subwatersheds are established for the urban area using ArcMap 10.1, HEC-HMS can be used along with impervious percentage, soil group, and land use data converted in ArcMap and HEC-GeoHMS to create hydrographs showing peak flow for each outlet of each subwatershed and the total watershed. The major datasets needed for manipulation in ArcGIS and input into HEC-HMS are: rainfall inputs, the DEM, stream gage sensor locations and discharge measurements, soil data, land cover including land use, and drainage network and geometry (Knebl et al, 2005). The spatial data (DEM, soils, and land use) can be input into ArcGIS or HEC-

HMS's pre-processer HEC-GeoHMS and manipulated into acceptable outputs that can be used as inputs into HEC-HMS as outlined in the previous section. The spatial hydrologic drainage network can then be placed as an input into HEC-HMS. This input, along with the measured stream flow and channel data, the basin data, the rainfall data, and the control specifications, can be converted within HEC-HMS to output simulated event hydrographs for each specified location (McColl and Aggett, 2007). Curve number and lag time can then be calculated outside of ArcGIS and used to calibrate the model. To summarize all of the inputs and outputs of the three programs working together, spatial data and measured data can be input into ArcMap to create inputs for HEC-GeoHMS whose outputs are output drainage network, streams, catchments, flow lengths, and slopes. These outputs can then be used as inputs into the rainfall runoff model HEC-HMS along with distributed basin data, rainfall data, and control specifications to derive the output stream and hydrographs at specified locations (Knebl et al., 2005).

There have been some issues with HEC-HMS that need to be addressed. One of the main problems with HEC-HMS modeling is that it uses the SCS curve number method to generate hydrograph outputs for various input parameters. This is inaccurate, because the curve number method is not an infiltration method, which can lead to significant errors in peak discharge (Eli and Lamont, 2010). Although this method has been further developed into several different models today, including TR-55 for urban areas (USDA, 1986), it was never intended to create hydrographs. There are three main problems with this method: the tabulated CN values are just estimates

only to be used in the absence of local data, CN values can be inverse calculated and is a variable function of storm depth and rainfall distribution creating a lot of range between numbers, and the CN method is not an infiltration equation nor was it established to predict runoff peak discharges (Eli and Lamont, 2010). The solution to this problem is to use the Green-Ampt method option within the HEC-HMS system versus the CN method. The Green Ampt method is an actual infiltration model and is better suited for use in construction of runoff hydrographs. When using the CN method, the peak discharges are always lower than they should be without manipulation of the inputs; however, the SCS Curve Number (CN) model is usually chosen to estimate precipitation because new land use distribution scenarios and associated curve number can be easily developed and hydrologically assessed (Chen et al., 2009). It is also a highly popular and accepted model within research and literature despite the above concerns. Another solution to this problem would be to use another runoff model to calculate peak discharge such as the second most common runoff model Water Erosion Prediction Project (WEPP). There was a study done by Arbind K. Verma et al. (2010) in Eastern India on rainfall-runoff modeling and remote sensing using HEC-HMS and WEPP demonstrating that the main difference between the two models is that HEC is designed to include multiple watersheds connected if necessary along with subwatersheds, reaches, junctions, etc., and WEPP is designed for only one watershed; HEC-HMS also simulates stream flow peaks and recessions more accurately then WEPP, but WEPP simulates total runoff

volumes better than HEC-HMS in large developing watersheds with relatively low slopes (Verma et al., 2010).

2.7 PROJECT BACKGROUND

Phase 1 of this project focused on the install and analysis of rainwater and stormwater harvesting through the use of green infrastructure such as: bioretention cells, permeable pavement, and a cistern. Phase 2, or the current phase, of this project focuses on the site analysis and discovery of the most beneficial placement of additional green infrastructure through the use of remote sensing and GIS runoff models. Integration of GIS and remote sensing (RS) in runoff modeling involves two processes: (1) hydrological parameter determination using GIS, and (2) hydrological modeling within GIS. Hydrological parameter determination using GIS entails preparing land-cover, soil, and precipitation data that go into the SCS model, while hydrological modeling within GIS automates the SCS modeling process using generic GIS functions (Weng, 2001). Modeling of stormwater flows in a city has recently become a standard routine performed in order to design the city and its infrastructure so that possible damages to the city itself and to the entire river basin downstream are minimized (Niemczynowicz, 1999).

Several previous studies have been performed on the Sand River Headwaters to quantify stormwater flows and enhance the knowledge of the urban stormwater system in Aiken, SC. In 1992, Meadows et al performed a study (Stormwater

Management Study for the City of Aiken: Sand River Drainage Basin) to determine the capacity of drainage networks in the Wise Hollow and Sand River basins to investigate ways to mitigate current and forecasted stormwater problems. They proposed to extend the storm sewer well downstream of the current outfall into an area where the channel is less erodible and/or a regional detention pond could be constructed. Woolpert completed a study in 2003 (Sand River Watershed Study) to examine the pollutant trends in each of these watersheds and assess potential erosion sites along tributaries within Hitchcock woods. The company proposed increased public involvement, a series of detention ponds on roadway medians in the downtown area, extending the gabion structures to protect susceptible areas further downstream, and diversion piping. In 2009, Eidson et. al. performed research (Sand River Ecological Restoration Preferred Alternative) to provide a "blue print" for the remediation of the stormwater canyon and restoration of natural communities and ecosystem processes within the greater Sand River watershed and to implement a long-term strategy to protect and maintain the restored sites. They proposed a combination of the following: upstream filtration and detention options, earthen dam, pond, wetland remediation, Sand River dual pipe system, wetlands, energy dissipation area, and tributary stabilization. Clemson University completed a study in 2013 (Sand River Headwaters Green Infrastructure Project) to summarize research associated with the Sand River Headwaters Green Infrastructure project, conducted in partnership with the City and Woolpert Inc., which incorporated sustainable development practices to capture and treat stormwater within downtown watersheds,

including the use of bioswales and bioretention, multiple applications of pervious pavement, and a cistern. They determined from analysis of green infrastructure installation and efficiency studies and analysis of storm events at monitoring stations including the 10 foot pipe outlet that the current green infrastructure installations were not making a significant impact on stormwater quantity and water quality downstream at the outlet. Phase 2 of the Aiken Project began in December, 2013 to continue these efforts to enhance understanding of the urban stormwater system and assess the most effective placement for additional green infrastructure within the subwatershed(s) to decrease stormwater volume quantity and flow rates downstream.

2.8 REFERENCES

Ahiablame, Laurent M., Bernard A. Engel, and Indrajeet Chaubey. "Effectiveness of Low Impact Development Practices: Literature Review and Suggestions for Future Research." Water, Air, & Soil Pollution 223.7 (2012): 4253-73. Print.

Al-Abed, N., F. Abdulla, and A. Abu Khyarah. "GIS-hydrological Models for Managing Water Resources in the Zarqa River Basin." *Environmental Geology* 47.3 (2005): 405-11. Web.

Ali, Muhammad, Sher Jamal Khan, Irfan Aslam, and Zahiruddin Khan. "Simulation of the Impacts of Land-use Change on Surface Runoff of Lai Nullah Basin in Islamabad, Pakistan." *Landscape and Urban Planning* 102.4 (2011): 271-79. Web.

Battiata, Joseph, et al. "The Runoff Reduction Method." Journal of Contemporary Water Research & Education 146.1 (2010): 11-21. Print.

Beighley, R. Edward, John M. Melack, and Thomas Dunne. "Impacts Of California's Climatic Regimes And Coastal Land Use Change On Streamflow Characteristics." *Journal of the American Water Resources Association* 39.6 (2003): 1419-433. Web.

Bhaduri, Budhendra, Jon Harbor, Bernie Engel, and Matt Grove. "Assessing Watershed-Scale, Long-Term Hydrologic Impacts of Land-Use Change Using a GIS-NPS Model." *Environmental Management* 26.6 (2000): 643-58. Web.

Bo Yang and Shujuan Li. "Green Infrastructure Design for Stormwater Runoff and Water Quality: Empirical Evidence from Large Watershed-Scale Community Developments." Water 5 (2013): 2038-57. Print.

Brock, Larissa Mason. *Water Quality, Nutrient Dynamics, Phytoplankton Ecology and Land Uses within Defined Watersheds Surrounding Six Detention Ponds on Kiawah Island, South Carolina*. Thesis. The Graduate School of the College of Charleston, 2006. N.p.: n.p., n.d. Print.

Brown, Rebekah R. "Impediments to Integrated Urban Stormwater Management: The Need for Institutional Reform." *Environmental Management* 36.3 (2005): 455-68. Web.

Burns, Matthew J., et al. "Hydrologic Shortcomings of Conventional Urban Stormwater Management and Opportunities for Reform." Landscape and Urban Planning 105.3 (2012): 230-40. Print.

Cantone, Joshua P., and Arthur R. Schmidt. "Potential Dangers of Simplifying Combined Sewer Hydrologic/Hydraulic Models." *Journal of Hydrologic Engineering* 14.6 (2009): 596. Web.

Chen, Ying, Youpeng Xu, and Yixing Yin. "Impacts of Land Use Change Scenarios on Storm-runoff Generation in Xitiaoxi Basin, China." *Quaternary International* 208 (2009): 121-28. Print.

Clary, Jane, et al. "Integration of Low-Impact Development into the International Stormwater BMP Database." Journal of Irrigation and Drainage Engineering 137.3 (2011): 190-8. Print.

Costache, Romulus. "Using Gis Techniques For Assessing Lag Time And Concentration Time In Small River Basins. Case Study: Pecineaga River Basin, Romania."*Geographia Technica* 9.1 (2014): 31-38. Web.

De Loza, Victor, and Nahm H. Lee. "Urban Hydrology Modeling Using GIS." Web log post. *ArcGIS Resources*. ESRI, 26 Aug. 2013. Web. 26 Sept. 2013.

Du, Jinkang, Li Qian, Hanyi Rui, Tianhui Zuo, Dapeng Zheng, Youpeng Xu, and C.-Y. Xu. "Assessing the Effects of Urbanization on Annual Runoff and Flood Events Using an Integrated Hydrological Modeling System for Qinhuai River Basin, China." *Journal of Hydrology* 464-465 (2012): 127-39. Web.

Eidson, Gene, Victoria Chanse, Calvin Sawyer, and Erin Cooke. Sand River Ecological Restoration Preferred Alternative. Rep. no. 2096199. Clemson: Clemson U Center for Watershed Excellence, 2009. Print.

Eli, Robert N., and Samuel J. Lamont. "Curve Numbers and Urban Runoff Modeling-Application Limitations." *Low Impact Development* (2010): 405-18. Web.

Emerson, Clay H., Caire Welty, and Robert G. Traver. "Application of HEC-HMS to Model the Additive Effects of Multiple Detention Basins over a Range of Measured Storm Volumes." *World Water and Environmental Resources Congress* (2003): n. pag. Web.

Erik C. Porse. "Stormwater Governance and Future Cities." Water 5 (2013): 29-52. Print.

Fletcher, Tim D., Geoff Vietz, and Christopher J. Walsh. "Protection of Stream Ecosystems from Urban Stormwater Runoff: The Multiple Benefits of an Ecohydrological Approach." Progress in Physical Geography 38.5 (2014): 543-55. Print.

Gironás, Jorge, Jeffrey D. Niemann, Larry A. Roesner, Fabrice Rodriguez, and Hervé Andrieu. "Evaluation of Methods for Representing Urban Terrain in Storm-Water Modeling." *Journal of Hydrologic Engineering* 15.1 (2010): 1. Web.

Goudie, Andrew. *The Human Impact on the Natural Environment*. 3rd ed. Oxford: Basil Blackwell, 1990. Print.

Holder, Anthony W., Eric J. Stewart, and Philip B. Bedient. "Modeling an Urban Drainage System with Large Tailwater Effects Under Extreme Rainfall Conditions." *Global Solutions for Urban Drainage* (2002): n. page. Web.

Inamdar, P.m., S. Cook, A.k. Sharma, N. Corby, J. O'connor, and B.j.c. Perera. "A GIS Based Screening Tool for Locating and Ranking of Suitable Stormwater Harvesting Sites in Urban Areas." *Journal of Environmental Management* 128 (2013): 363-70. Web.

Institute of Applied Ecology/Center for Watershed Excellence. Sand River Headwaters Green Infrastructure Project. Rep. Clemson: n.p., 2013. Print.

Jia, Haifeng, et al. "Planning of LID–BMPs for Urban Runoff Control: The Case of Beijing Olympic Village." Separation and Purification Technology 84 (2012): 112-9. Print.

Knebl, M.r., Z.-L. Yang, K. Hutchison, and D.r. Maidment. "Regional Scale Flood Modeling Using NEXRAD Rainfall, GIS, and HEC-HMS/RAS: A Case Study for the San Antonio River Basin Summer 2002 Storm Event." *Journal of Environmental Management* 75.4 (2005): 325-36. Web.

Luzio, Mauro Di, Raghavan Srinivasan, and Jeffrey G. Arnold. "A GIS-Coupled Hydrological Model System for the Watershed Assessment of Agricultural Nonpoint and Point Sources of Pollution." *Transactions in GIS* 8.1 (2004): 113-36. Web.

Maidment, David R. *Arc Hydro: GIS for Water Resources*. Redlands, CA: ESRI, 2002. Print.

Maidment, David R. "GIS and Hydrologic Modeling-an Assessment of Progress." *GIS and Environmental Modeling* 3 (1996): n. page. Web.

Mccoll, Chris, and Graeme Aggett. "Land-use Forecasting and Hydrologic Model Integration for Improved Land-use Decision Support." *Journal of Environmental Management* 84.4 (2007): 494-512. Web.

Meadows, Michael E., Katalin B. Morris, and William E. Spearman. Stormwater Management Study for the City of Aiken: Sand River Drainage Basin. Rep. Columbia: Department of Civil Engineering at U of South Carolina, South Carolina Land Resources Conservation Commission, 1992. Print.

Merwade, Venkatesh. "Creating SCS Curve Number Grid Using HEC-GeoHMS." *Purdue University* (2012): n. pag. Web.

Merwade, Venkatesh. "Downloading SSURGO Soil Data from Internet." *Purdue University* (2012): n. pag. Web.

Merwade, Venkatesh. "Terrain Processing and HMS-Model Development Using GeoHMS." *Purdue University* (2012): n. pag. Web.

Niemczynowicz, Janusz. "Urban Hydrology and Water Management – Present and Future Challenges." *Urban Water* 1.1 (1999): 1-14. Web.

Ogden, Fred L., Jurgen Garbrecht, Paul A. Debarry, and Lynn E. Johnson. "GIS and Distributed Watershed Models. II: Modules, Interfaces, and Models." *Journal of Hydrologic Engineering* 6.6 (2001): 515. Web.

Paz, Adriano Rolim, and Walter Collischonn. "River Reach Length and Slope Estimates for Large-scale Hydrological Models Based on a Relatively High-resolution Digital Elevation Model." *Journal of Hydrology* 343.3-4 (2007): 127-39. Web.

Pyke, Christopher, et al. "Assessment of Low Impact Development for Managing Stormwater with Changing Precipitation due to Climate Change." Landscape and Urban Planning 103.2 (2011): 166-73. Print.

Roy, Allison H., et al. "How Much is enough? Minimal Responses of Water Quality and Stream Biota to Partial Retrofit Stormwater Management in a Suburban Neighborhood: E85011." PLoS One 9.1 (2014)Print.

Roy, Allison H., et al. "Impediments and Solutions to Sustainable, Watershed-Scale Urban Stormwater Management: Lessons from Australia and the United States." Environmental management 42.2 (2008): 344-59. Print.

United States Department of Agriculture (1986). Urban hydrology for small watersheds. Technical Release 55 (TR-55) (Second Edition ed.). Natural Resources Conservation Service, Conservation Engineering Division.

USACE, 2003. Geospatial Hydrologic Modeling Extension. HECGeoHMS: User's Manual. Version 1.1. USACE, Davis, CA, USA.

Verma, Arbind K., Madan K. Jha, and Rajesh K. Mahana. "Evaluation of HEC-HMS and WEPP for Simulating Watershed Runoff Using Remote Sensing and Geographical Information System." *Paddy Water Environ* 8 (2010): 131-44. Web.

Wang, Xinhao, et al. "Low Impact Development Design—Integrating Suitability Analysis and Site Planning for Reduction of Post-Development Stormwater Quantity." Sustainability 2.8 (2010): 2467-82. Print.

Walsh, Christopher J., Tim D. Fletcher, and Anthony R. Ladson. "Stream Restoration in Urban Catchments through Redesigning Stormwater Systems: Looking to the Catchment to save the Stream." *Journal of the North American Benthological Society* 24.3 (2005): 690. Web.

Weng, Qihao. "Modeling Urban Growth Effects on Surface Runoff with the Integration of Remote Sensing and GIS." *Environmental Management* 28.6 (2001): 737-48. Web.

Woolpert. Sand River Watershed Study. Rep. Aiken: n.p., 2003. Print.

X, Liu, J. Peterson, and Z. Zhang. "High-Resolution DEM Generated from LiDAR Data for Water Resource Management." (2005): 1402-408. Web.

Younos, Tamim. "Paradigm Shift: Holistic Approach for Water Management in Urban Environments." Frontiers of Earth Science 5.4 (2011): 421-7. Print.

Zeyuan Qiu. "Comparative Assessment of Stormwater and Nonpoint Source Pollution Best Management Practices in Suburban Watershed Management." Water 5 (2013): 280-91. Print.

CHAPTER 3: GIS MODELING FOR URBAN WATERSHED DELINEATION AND STORMWATER FLOW DETERMINATION IN AIKEN, SC

3.1 ABSTRACT

Urban watershed hydrology is often difficult to evaluate due to variably changing land uses and land cover, modified soils and topography, and subsurface stormwater infrastructure with complex connections and routing. The City of Aiken, SC is highly urbanized with downstream adverse erosion impacts due to high energy stormwater discharges from the Sand River Headwaters watershed. The objective of the study was to quantify runoff volumes and peak flow rates at the subwatershed scale to establish the most effective placement of additional green infrastructure in the larger urban Aiken watershed to reduce stormwater flows. Toward this aim, ten subwatersheds and the total watershed area were delineated from a Digital Elevation Model (DEM) created from Light Detecting and Ranging (LiDAR) data and the ArcHydro toolbox in ArcMap 10.1. A unique technique called "burning" was used to artificially insert the underground stormwater system and allow ArcMap 10.1 to accept the piping as the natural stream element and then delineate subwatersheds based on this new routing structure. The total watershed area was derived along with ten subwatershed areas and combined with rainfall data to develop runoff volumes.

Using ArcMap 10.1 and ArcHydro toolbox extension, 8 subwatersheds and the overall urbanized Aiken watershed were delineated for the 10 foot pipe outlet, with a separate watershed delineated for Coker Springs, or number 11. The total watershed

area was divided into two main contributions of flow equaling 353 acres, or 33.5 percent and 717 acres, or 66.5 percent indicating that it would be most effective to install additional green infrastructure in the largest flow division of 66.5 percent total land area. The largest and smallest volumes over all storm events for the total outlet watershed runoff generation were seen from a rain event of 2.32 inches on May 15, 2014 and May 16, 2014 resulting in 68 million gallons and a storm event of 0.01 inches on July 22, 2014 resulting in 0.3 million gallons respectively.

3.2 BACKGROUND

In Aiken, the 1,080 acre watershed has an extensive stormwater pipe system that drains to a single 10 foot pipe outlet. It is a highly connected system in which runoff flows immediately from rooftops to parking lots or driveways to gutters and then to pipes, including road runoff, resulting in extremely "flashy" hydrographs during and after a storm event; flow in the system rapidly peaks and then recedes (Woolpert, 2003). The stormwater outflow from the urbanized Aiken watershed drains to the headwaters of the Sand River, and then flows to Horse Creek and eventually into the Middle Savannah River. The erosion at this outlet is so extensive, that the resulting canyon that has formed has depths measuring up to 70 feet in some locations. Upon reaching the outlet, upper reaches are experiencing the greatest erosion, while there is only minor erosion along the middle reaches with considerable sediment transport from upstream sources, and sediment is being deposited in the main channel and in flood plains along the lower reaches (Meadows et al., 1992). With the majority of

soils in the Sand River watershed being of sandy texture, the banks and stream beds have no protection from erosion and subsequent sediment transport and downstream loading, which can lead to water quality impairments.

Several previous studies have been performed on the Sand River Headwaters to quantify stormwater flows and enhance the knowledge of the urban stormwater system in Aiken, SC. In 1992, Meadows et al performed a study (Stormwater Management Study for the City of Aiken: Sand River Drainage Basin) to determine the capacity of drainage networks in the Wise Hollow and Sand River basins to investigate ways to mitigate current and forecasted stormwater problems. They proposed to extend the storm sewer well downstream of the current outfall into an area where the channel is less erodible and/or a regional detention pond could be constructed. Woolpert completed a study in 2003 (Sand River Watershed Study) to examine the pollutant trends in each of these watersheds and assess potential erosion sites along tributaries within Hitchcock woods. The consulting group proposed increased public involvement, a series of detention ponds on roadway medians in the downtown area, extending the gabion structures to protect susceptible areas further downstream, and diversion piping. In 2009, Eidson et. al. performed research (Sand River Ecological Restoration Preferred Alternative) to provide a "blue print" for the remediation of the stormwater canyon and restoration of natural communities and ecosystem processes within the greater Sand River watershed and to implement a long-term strategy to protect and maintain the restored sites. They proposed a combination of the following: upstream filtration and detention options, earthen dam,

pond, wetland remediation, Sand River dual pipe system, wetlands, energy dissipation area, and tributary stabilization. Clemson University completed a study in 2013 (Sand River Headwaters Green Infrastructure Project) to summarize research associated with the Sand River Headwaters Green Infrastructure project, conducted in partnership with the City and Woolpert Inc., which incorporated sustainable development practices to capture and treat stormwater within downtown watersheds, including the use of bioswales and bioretention, multiple applications of pervious pavement, and a cistern. They determined from analysis of green infrastructure installation and efficiency studies and analysis of storm events at monitoring stations including the 10 foot pipe outlet that the current green infrastructure installations were not making a significant impact on stormwater quantity and water quality downstream at the outlet. Phase 2 of the Aiken Project began in December, 2013 to continue these efforts to enhance understanding of the urban stormwater system and assess the most effective placement for additional green infrastructure within the subwatershed(s) to decrease stormwater volume quantity and flow rates downstream.

A Clemson University research team was asked to design a solution to the degradation problem incorporating green infrastructure. In 2009, the resulting project plan finalized by Clemson University's Center for Watershed Excellence incorporated bioretention cells, bioswales, permeable pavement, and a cistern in its green infrastructure solution and the effectiveness of these management practices to capture, store, infiltrate, and treat downtown stormwater (Clemson University, 2013). In January 2012, Phase 1 of the project was completed and on April 1, 2013 Phase 2

of the project began set to conclude on March 31, 2015. The objectives of Phase 2 include:

1. Quantify hydrologic flows during storm events draining to and within the downtown Aiken stormwater sewer system that constitutes Sand River headwaters.
2. Based on storm event flows, evaluate and optimize potential locations for further green infrastructure (GI) installation including analysis for hydrology and cost-effectiveness.
3. Enhance site-level remote data acquisition capabilities throughout the Sand River watershed and integrate associated collection, transmission, display, and archival facilities into the *Intelligent River*® network.

There were four main steps to completing these objectives. The first was to gain a better understanding of the existing stormwater network within the watershed and its drainage boundaries. The second step required quantification of volume and routing, with tasks that included: review of existing survey information of the water network, trunk line instrumentation with level and/or flow sensors in which ten monitoring locations were selected, and watershed scale modeling to effectively examine the overall efficiency of existing or future green infrastructure installation. Third, spatial analyses using Geographic Information Systems (GIS) were utilized to delineate watersheds and derive characteristics such as impervious surface and curve number (CN) per watershed. Lastly, an optimal location for future green infrastructure installation would be determined based on steps two and three, along with a cost

benefit analyses and a decision matrix based on existing infrastructure, contributing area to stormflow and discharge, water volume availability, and proximity. Once all of these steps have been completed and all the parameters determined, the subwatershed(s) that may be significantly contributing to high stormwater flows and subsequently to downstream erosion can be identified. If this is determined, then additional green infrastructure can be installed within these subwatershed(s) to effectively and efficiently decrease runoff and peak flow rate at the Sand River headwaters. This research approach and modeling methodology can then be used as a tool in other urban or developing areas.

3.3 METHODS

3.3.1 WATERSHED DELINEATION

In order to delineate watersheds based on the stormwater system, a DEM was created in ArcMap 10.1 from the LiDAR data provided by the City of Aiken, South Carolina using methods described by DeLoza and Lee (2013). This was accomplished by importing the LiDAR data from an ASCII file into a three dimensional X, Y, Z multipoint feature class with an average point spacing of five and projecting the feature class onto the coordinate system NAD 2983 FIPS 3900 in units of US feet. The multipoint dataset was then converted through ArcMap conversion "point to raster" tool into a raster dataset with a cell size of five feet (Crawford, 2008). Using focal statistics and the spatial analyst extension, "No Data" values were filled by

assigning them with a mean value according to their surrounding cell grid. This was performed in the Python window of ArcMap 10.1 using the code below:

(1) >>>from arcpy.sa import *

(2) >>>raster_int1 =

Con(IsNull("aiken_dem_raster"),FocalStatistics("aiken_dem_raster",NbrRectangle(5,5),"MEAN"),"aiken_dem_raster")

Step two of the code was then repeated four more times in order to achieve the final raster output (Crawford, 2008). The final raster was exported as a TIFF file and added to ArcMap 10.1 (Figure 3.5).

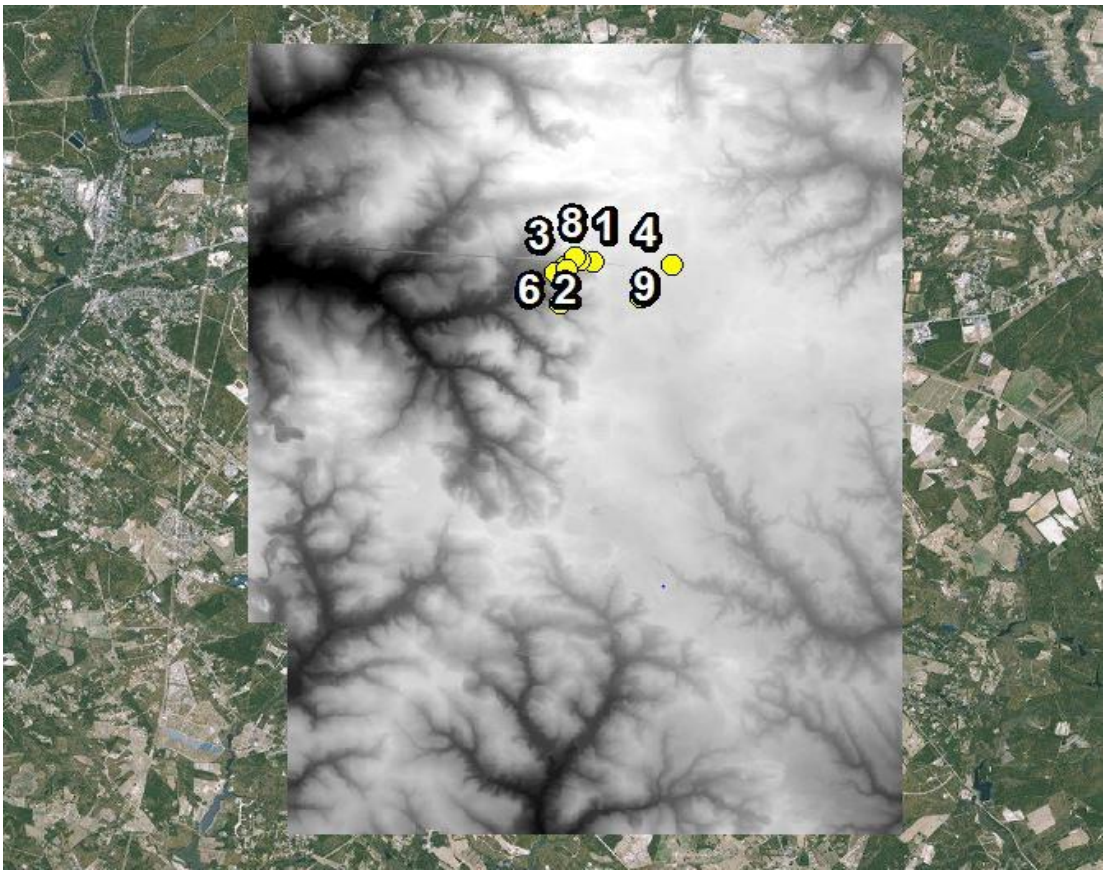

Figure 3.5: DEM raster created from the LiDAR data supplied by the City of Aiken

After DEM creation, the next step in watershed delineation was to import the stormline and monitoring points for the watershed into ArcMap 10.1. The stormline layer was provided by the City of Aiken from existing data, and the monitoring points were created by adding a new multipoint feature class from the GPS points of the sensor monitoring locations (Figure 3.1). The DEM was then clipped to the study area of interest (Figure 3.6). There were several missing areas of piping within the provided stormline shapefile and assumptions were added to the existing map based on the city's stormline outlines and field monitoring of pipe flows (Figure 3.2). The stormline shapefile was finalized using the editor toolbar and adding the assumptions (Figure 3.3). The DEM clip and the stormline were combined using the ArcHydro tool "burn stream slope" and burning the stormline into the DEM at an artificial elevation lower than any existing depressions of the natural DEM (Figure 3.7). After receiving some unrealistic elevation outputs from the "burn stream slope" tool, the "DEM reconditioning" tool (Boucher, 2014) was used instead which completes the same task of burning in the stormline. This "DEM reconditioning" tool had reasonable elevations ranging within the elevations of the original DEM raster and thus was used in further analysis. All stormline pipes were burned below the DEM at the same elevation; however, the streets were excluded from the burn due to interest only in the stormline flow (Gironás et al., 2010). The Burned DEM was filled and any sinks or depressions in the terrain were removed using the fill sinks tool.

Figure 3.1: Existing Stormline shapefile supplied by the City of Aiken

Figure 3.2: Stormline assumptions, in blue, added to the Stormline layer according to project official's hypotheses and field studies

Figure 3.3: Finalized Stormline used for further work in ArcMap 10.1 with added pipeline assumptions

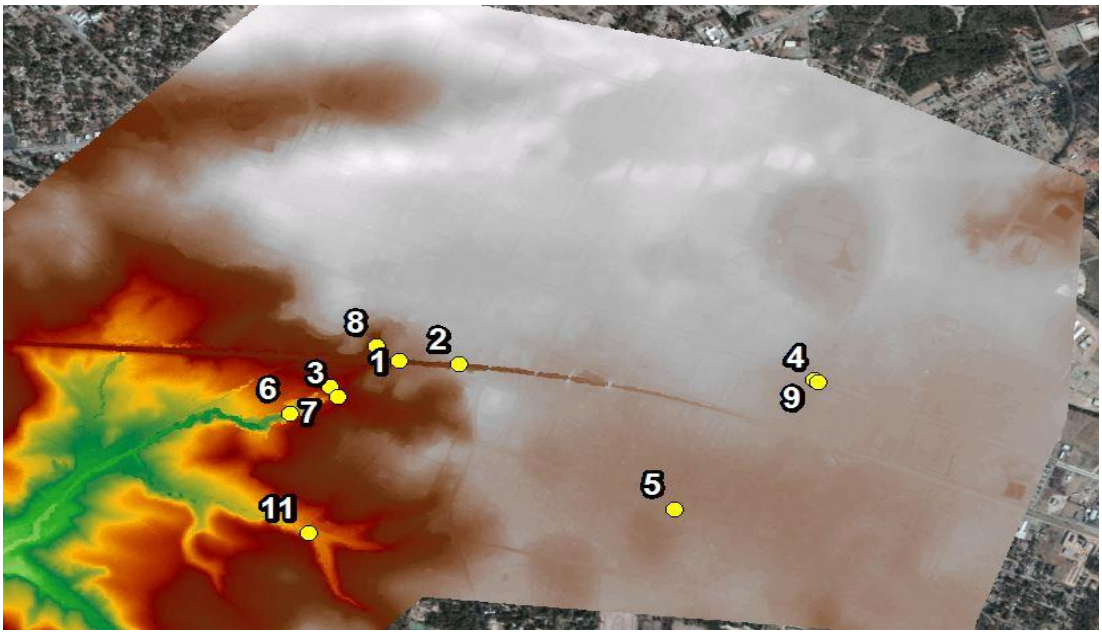

Figure 3.6: DEM raster clipped to the study area, with the highest elevations being light grey and the lowest elevations being bright green

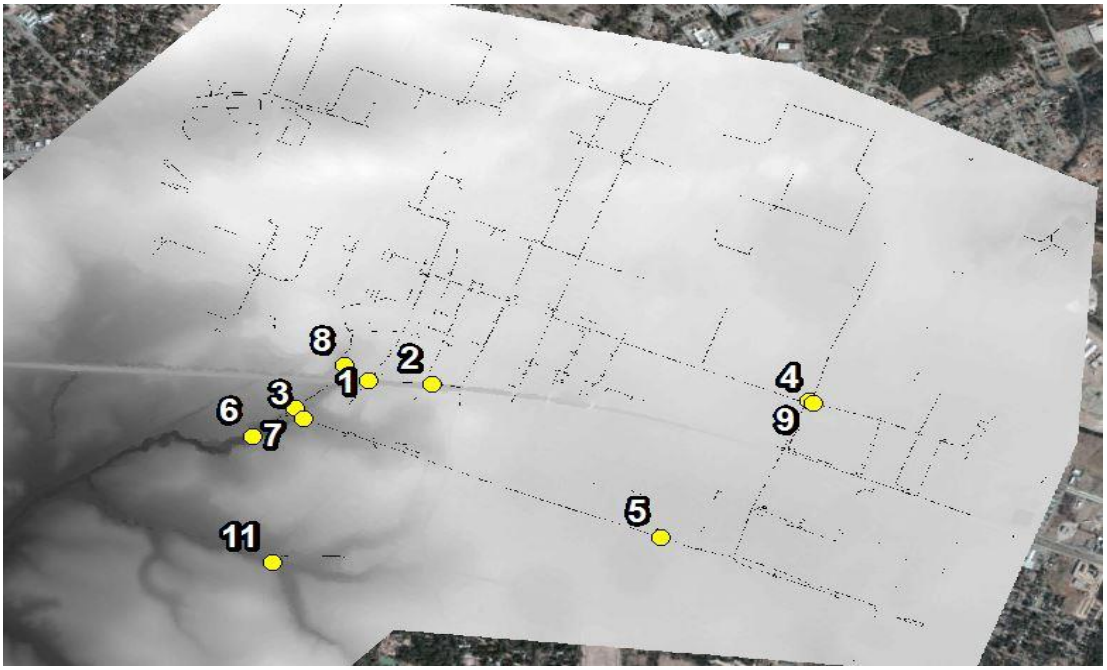

Figure 3.7: DEM after the stormline has been burned in at an artificial elevation and clipped to study area

The "flow direction" tool was used to calculate the Flow Direction grid based on the steepest slope of the surrounding cell grid (Figure 3.8) which was then used to calculate the Flow Accumulation grid based on the surrounding cells with the most flow using the "flow accumulation tool" (Figure 3.9) (Maidment, 2002). The "snap pour point" tool was used separately for all monitoring points and for only the 10 foot pipe monitoring point using a snap distance of zero feet. The snapping distance was set to zero feet, because the monitoring points were snapped on to the flow accumulation grid. Since the stormline was burned into the DEM as natural streams, the Flow Accumulation grid followed the stormline exactly, allowing the snapping distance to be zero feet. Using "snap pour point" allowed the monitoring points to be

recognized as the outlets of the stormline for watershed delineation. The watershed tool delineated the whole watershed outlet raster and all subwatershed rasters based on the outlet monitoring points, now snap pour points, and the Flow Direction raster. Watershed polygon layers were created from the rasters using the "raster to polygon" tool for the total outlet watershed (Figure 3.12) and all subwatersheds (Figures 3.10 and 3.11). Originally, Subwatershed 3 had a different location than the final output, and the original subwatershed delineations are demonstrated in Figure 3.13 and areas in Table 3.3. Further analysis showed that the new location was in fact receiving expected flows and was utilized from July 10, 2014 until the present for calculations and modeling purposes. The "AddField" and "CalculateField" tools were used to add area in hectares and acres to the attribute tables of both the subwatersheds and the outlet watershed (Tables 3.1 and 3.2). These areas were used, along with rainfall data from weather station readings (Weather Underground, 2014), to calculate flow volumes by multiplying the area by the rainfall amount. All rainfall data was gathered from KSCAIKEN3 Weather Station (Latitude: 33.487˚, Longitude: -81.767˚) when available, which uses hardware Vantage Pro Plus (Aiken Standard, 2014). When this station was not available, KSCAIKEN10 was used (Latitude: 33.526˚, Longitude: -81.685˚). Although it is much farther away than the other station, it was the next closest available to the subwatershed location and still allowed for incremental calculations. When neither one of these provided accurate rainfall amounts for certain storm events, a rain gage measurement (Aiken 1.6 NNW) was used from station SC-AK-32; however, this station allowed accurate daily precipitation data reported as a

total of rainfall for the entire day, but it did not allow hourly incremental data not permitting for multiple storm per day calculations (CoCoRaHs, 2014). Model builder (Figure 3.4) within ArcMap 10.1 was used for all ArcHydro tools, which provided the benefit of running all tools together in order sequentially if a single layer was changed as opposed to running each tool separately from Arc Toolbox. The Model Builder process was used to allow for more efficient analyses of watershed delineation results when changing pipeline assumptions and analyzing the outcome of their results on the watershed delineation. Model Builder is recommended for any string of tools always used in sequential order due to more expedient and efficient alteration of shapefiles within ArcMap 10.1.

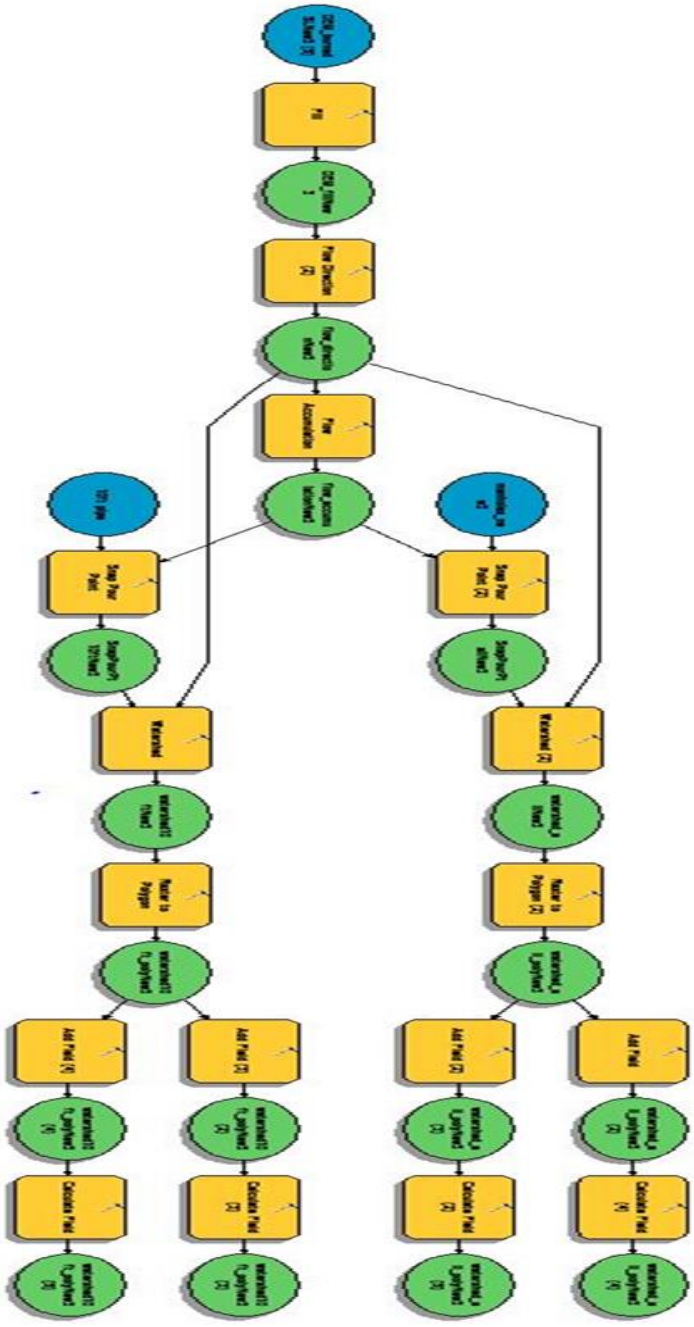

Figure 3.4: Model Builder layout for watershed delineation with tools demonstrated in yellow and input and output files indicated in yellow and blue

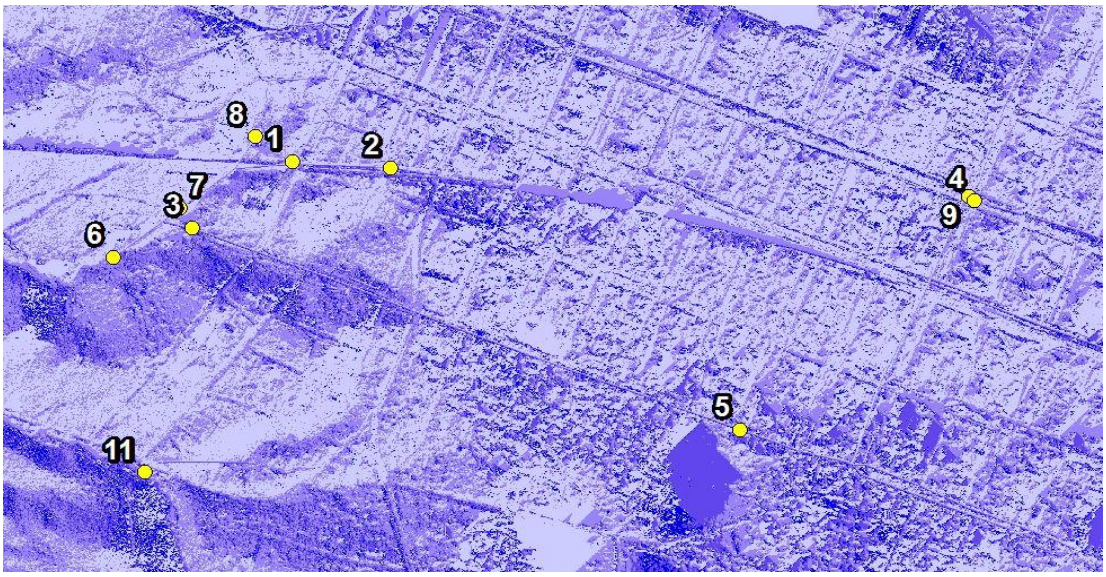

Figure 3.8: Flow Direction grid derived from the steepest slope of the surrounding cell grid to demonstrate the route of flow with darker blue areas indicating the path of flow following the burned in Stormline

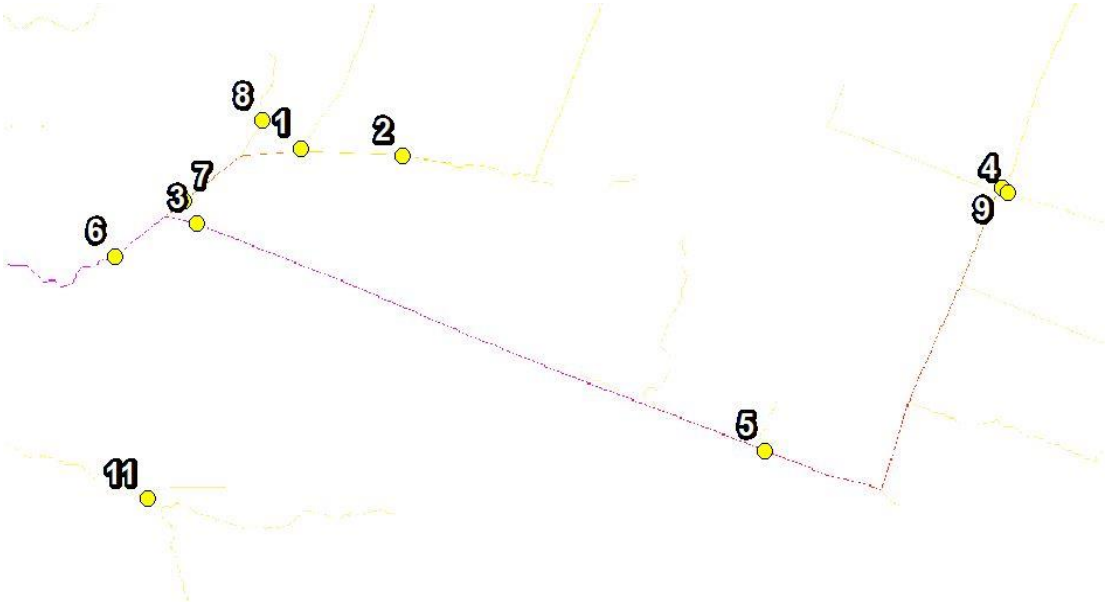

Figure 3.9: Flow Accumulation grid derived from the surrounding cell grid with the most flow with the darker colors indicating more accumulated flows following the hypothesized outlet order of flow

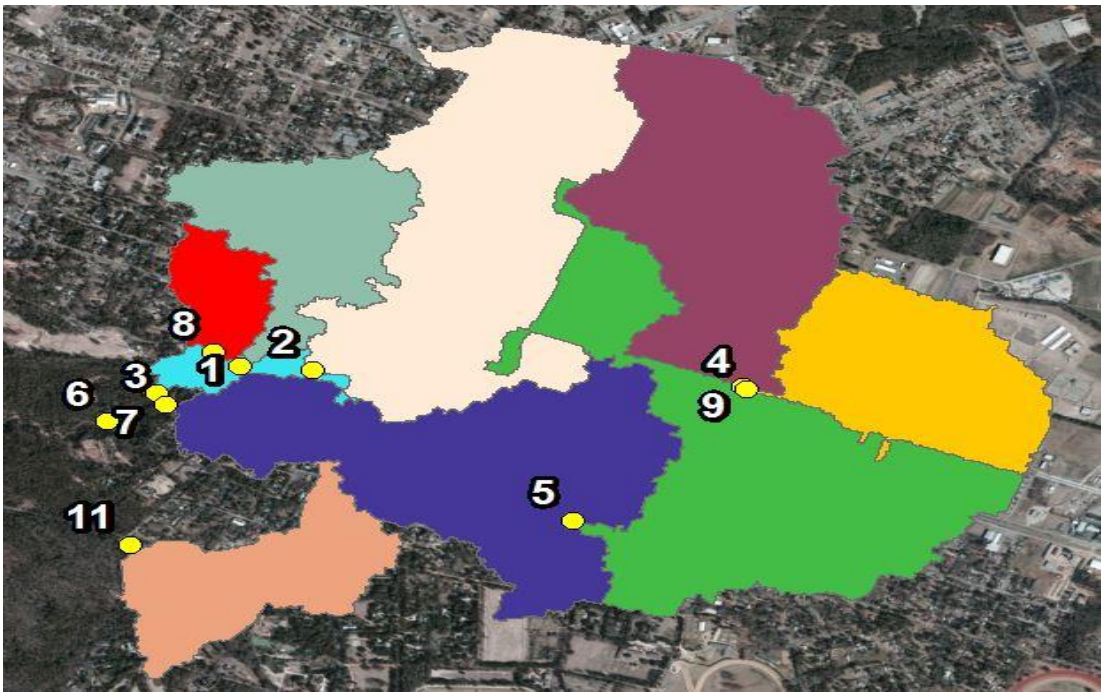

Figure 3.10: Subwatershed delineation output for all monitoring locations used as snap pour points

Figure 3.11: Subwatershed delineation output demonstrating the stormline included in each subwatershed

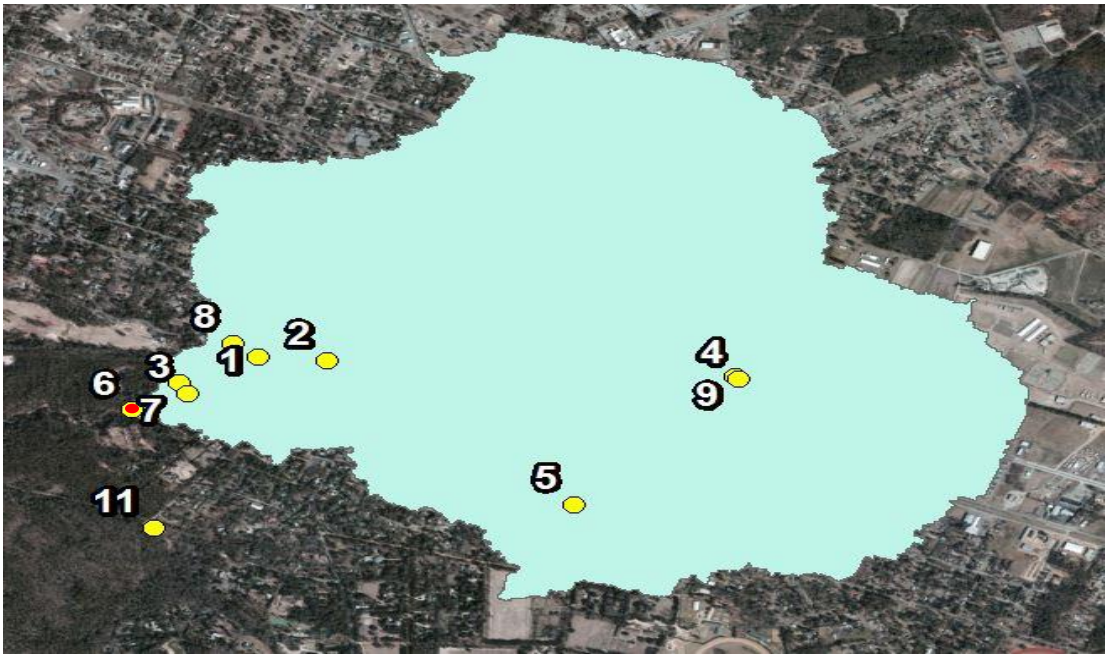

Figure 3.12: Watershed delineation output for the 10 foot pipe, indicated in red, being used as the only snap pour point

Table 3.1: Subwatershed output lengths, measure of longest length from one end of the subwatershed to the other, and areas

Subwatershed	Length (ft)	Area (ft^2)	Area (acres)
1	19,450	3,734,750	86
2	32,690	9,677,100	222
3	29,190	8,621,875	198
4	16,720	4,797,300	110
5	38,600	9,965,250	229
7	9,740	644,475	15
8	8,620	1,303,700	30
9	22,160	7,864,225	180
11	16,240	3,570,475	82

Table 3.2: Total outlet watershed output length and area compared to summed Subwatershed output length and area

Watershed	Length (ft)	Area (ft^2)	Area (acres)
6	52,490	47,027,550	1079
Contributing Subwatershed Total	177,170	46,608,675	1070

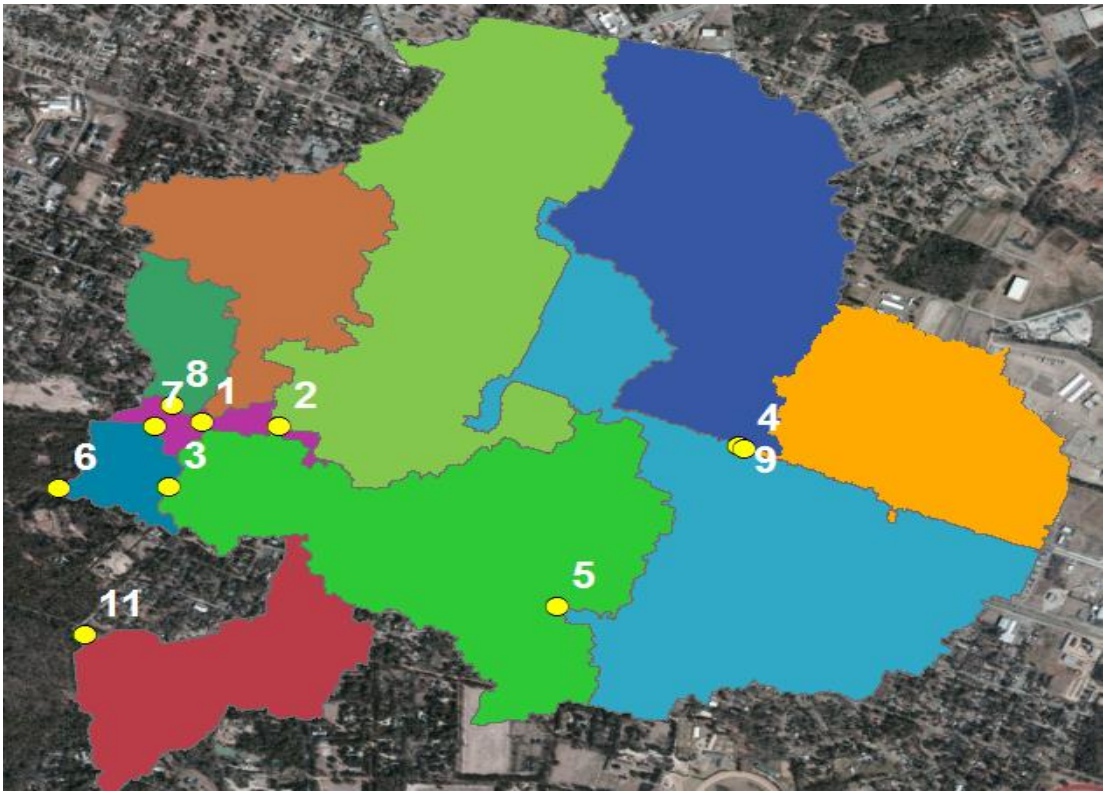

Figure 3.13: Subwatershed delineation outputs for the original locations of monitoring location 3

Table 3.3: Subwatershed lengths and areas at the original Subwatershed 3 location

Subwatershed	Length (ft)	Area (ft^2)	Area (acres)
1	19,450	3,734,750	86
2	32,690	9,677,100	222
3	28,000	8,348,300	192
4	15,980	4,732,425	109
5	37,850	10,030,075	230
7	9,740	644,475	15
8	8,620	1,303,700	30
9	22,160	7,864,225	180
11	16,240	3,570,475	82

3.3.2 WATERSHED ANALYSIS

After the subwatersheds were delineated, analysis was performed in ArcMap 10.1 to assure that all subwatersheds flowed into outlet points 7 and 3 before flowing into the total watershed outlet. Analysis was completed by only selecting certain monitoring locations to turn into snap pour points, which were then used as the outlet points for subwatershed delineation. Monitoring points 6, 7, and 3 were first chosen to prove that all other subwatersheds flowed into outlets 3 and 7 before entering the total watershed outlet. Outputs were established by following all of the same steps listed above using the "snap pour point", "watershed", and "raster to polygon" tools. Output watersheds in fact showed that this flow routing hypothesis was true (Figure 3.22). Monitoring points 6, 7, 3, 5, 4, and 9, were used to prove that Subwatersheds 8, 1, and 2 all flowed into Subwatershed 7 before reaching the outlet (Figure 3.23). Output polygons showed positive results as well proving the flow order to match the

theory. Monitoring locations 6, 7, 3, 8, 1, and 2 were used as the snap pour points to show that Subwatersheds 5, 4, and 9 flowed into Subwatershed 3 before reaching the outlet (Figure 3.24). Just as the others, the output polygons proved the order of flow to be accurate. Model Builder made altering the pour points and rerunning the ArcHydro tools less time consuming and more efficient. All subwatersheds followed the expected flow order before entering the total watershed outlet confirming the original flow direction predictions by the City of Aiken Public Works Department and as demonstrated in the flow chart (Figure 3.25).

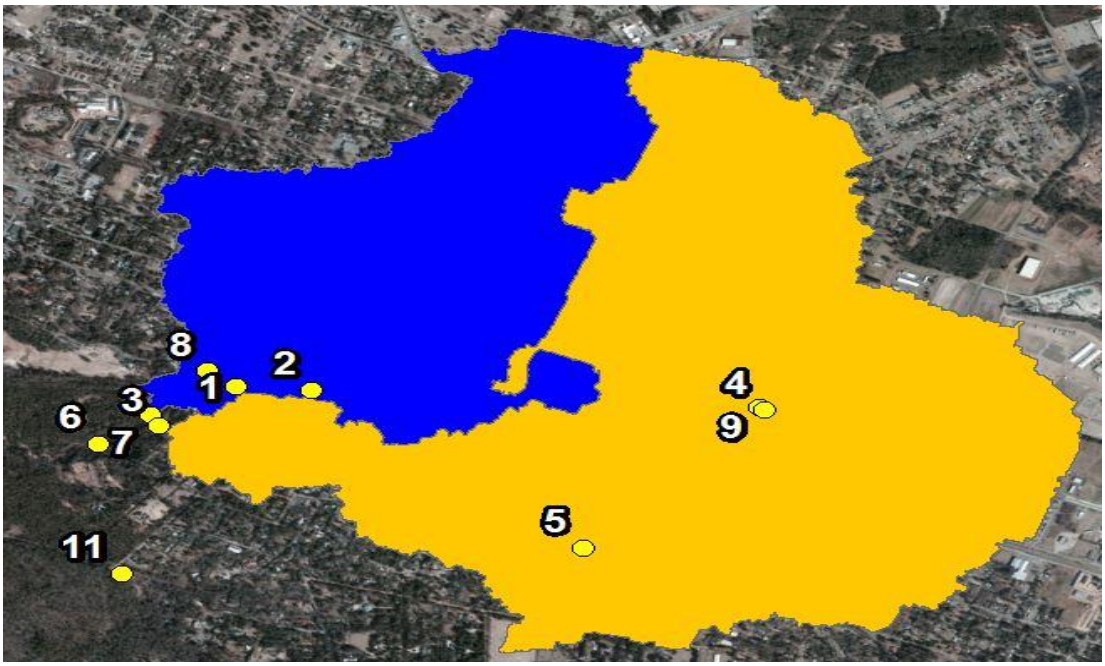

Figure 3.22: Watershed analysis output using monitoring points 6, 7, and 3 as snap pour points

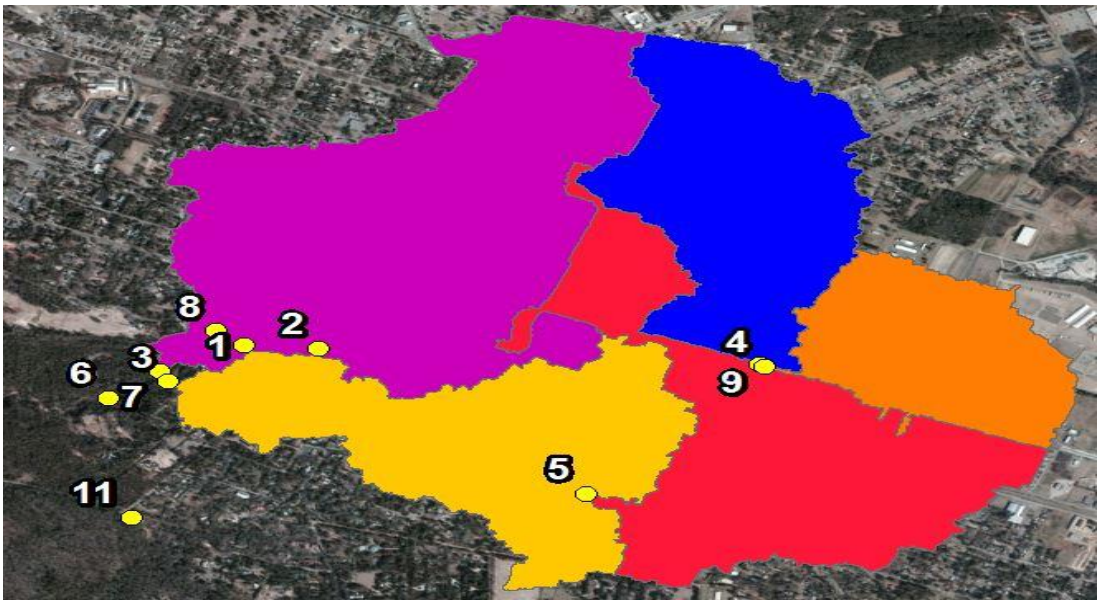

Figure 3.23: Watershed analysis output for monitoring points 6, 7, 3, 5, 4, and 9 used as snap pour points

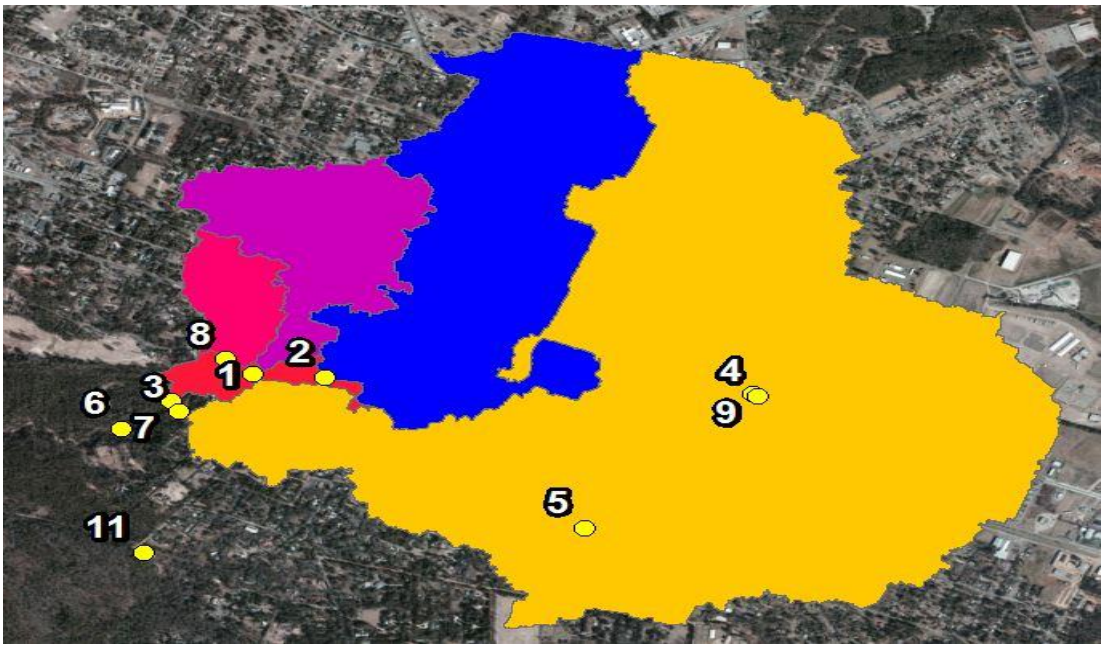

Figure 3.24: Watershed analysis output for monitoring points 6, 7, 3, 8, 1, and 2 used as snap pour points

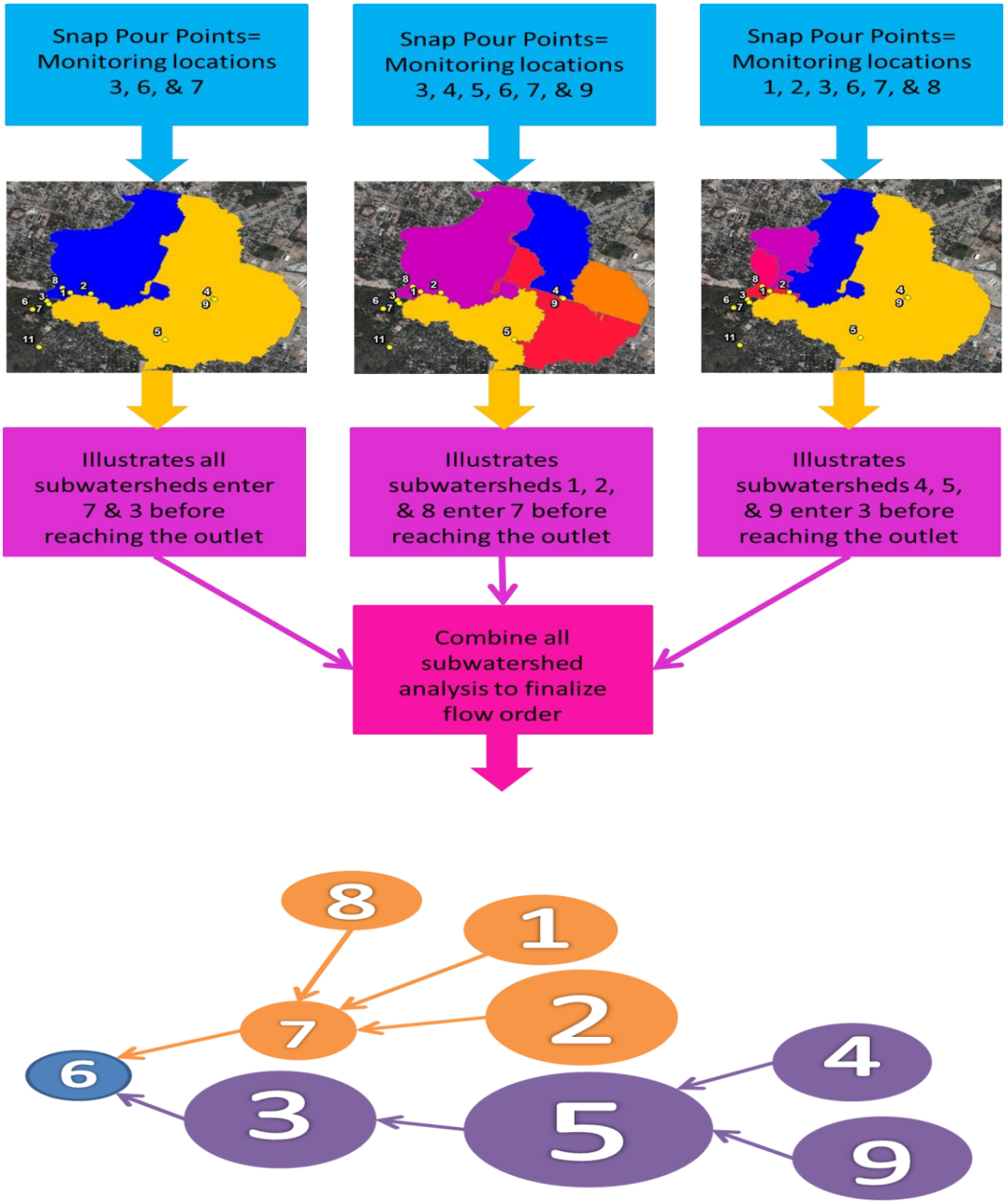

Figure 3.25: Flow chart indicating snap pour points for tool use and resulting flow order analysis results; in the finalized flow order bubbles are sized according to individual area and colored based on their contributing area division

Another watershed analysis was performed using the ArcHydro "catchment" and "adjoint catchment" tools. If the stormline is burned into the DEM correctly, and the stormline is accepted as the natural streams of the area, the watershed and the adjoint catchment should adhere to the exact same boundaries anywhere upstream of the outlet point. Downstream of the outlet point, the adjoint catchment adhered to the natural DEM stream flow and the watershed stopped at the watershed outlet location based on the extent of the stormwater piping. The Flow Accumulation (Figure 3.9) previously calculated was used along with the "stream definition" tool to define all flow segments larger than 5000 cells accumulated as streams, or a 1 on the stream grid, and all non-stream segments as 0. This raster was then used, along with the previously created Flow Direction raster (Figure 3.8), to calculate the Stream Link using the "stream segmentation" tool. Once the Stream Link was created, the Drainage Line (Figure 3.14) and the Catchment grid were created using the "drainage line processing" tool and the "catchment grid delineation" tool. A Catchment polygon (Figure 3.15) was created using the "catchment grid" and the "catchment polygon processing" tool. The output Catchment polygon and the Drainage Line were inputted into the "adjoint catchment processing" tool and used to create the Adjoint Catchment polygon (Figure 3.16) combining all catchments aggregated to the same drainage line. As stated above, the adjoint catchment and the watershed should extend to the same boundaries if the stormline was burned in correctly, and this was demonstrated in the output polygons of Figure 3.16.

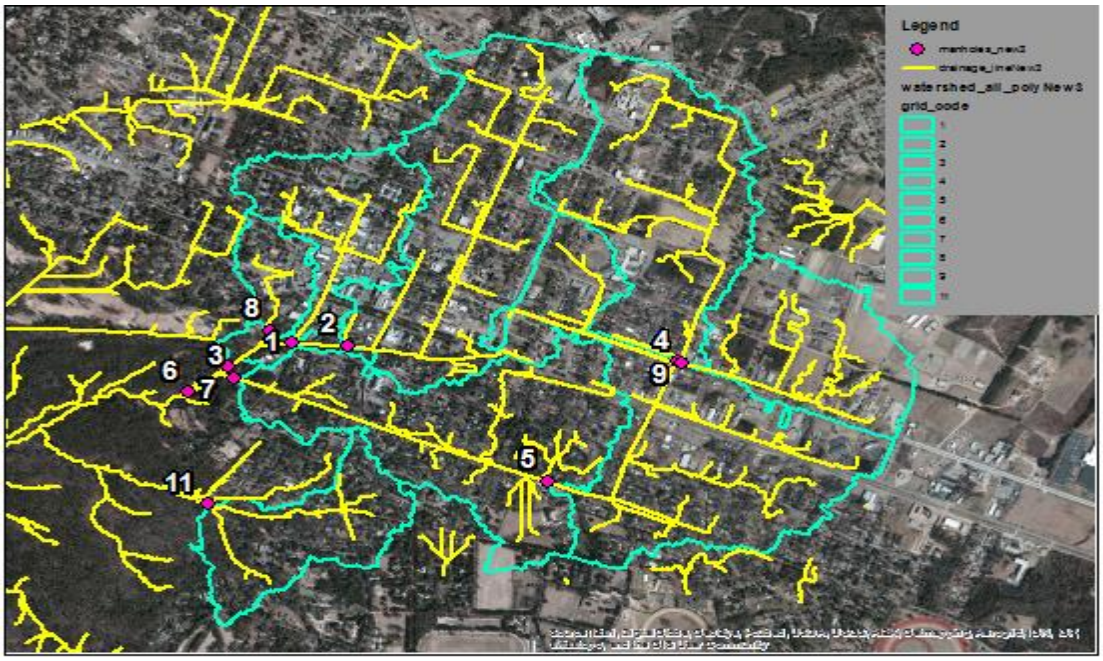

Figure 3.14: Drainage Line created from the Burned DEM showing stormline added to the natural streams

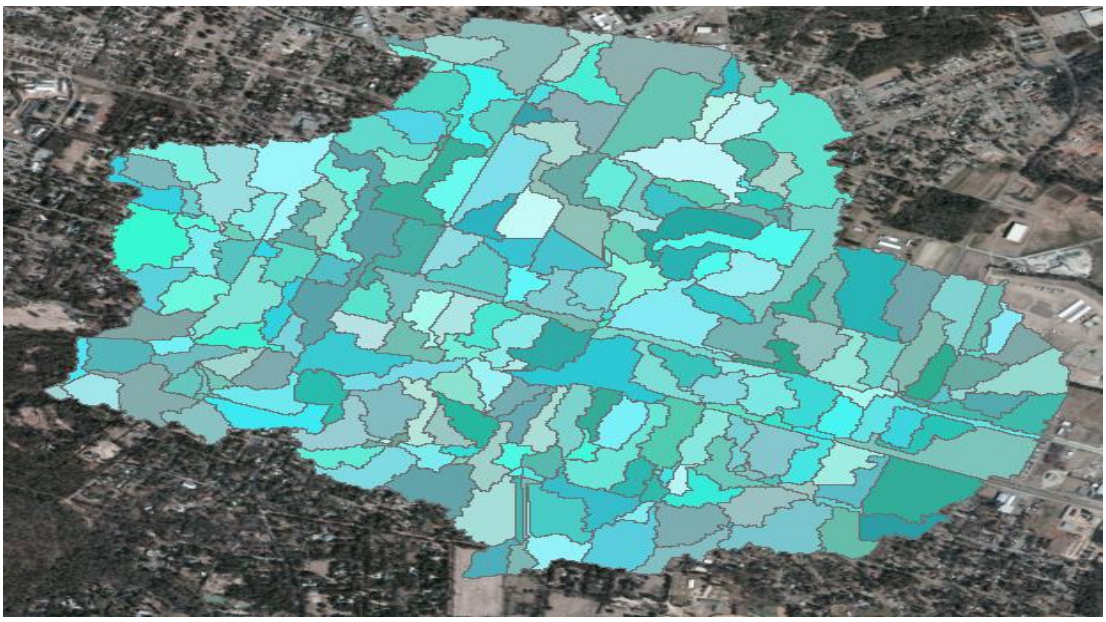

Figure 3.15: Catchment polygon derived from the Stream Link and Flow Direction grids for the 10 foot pipe outlet

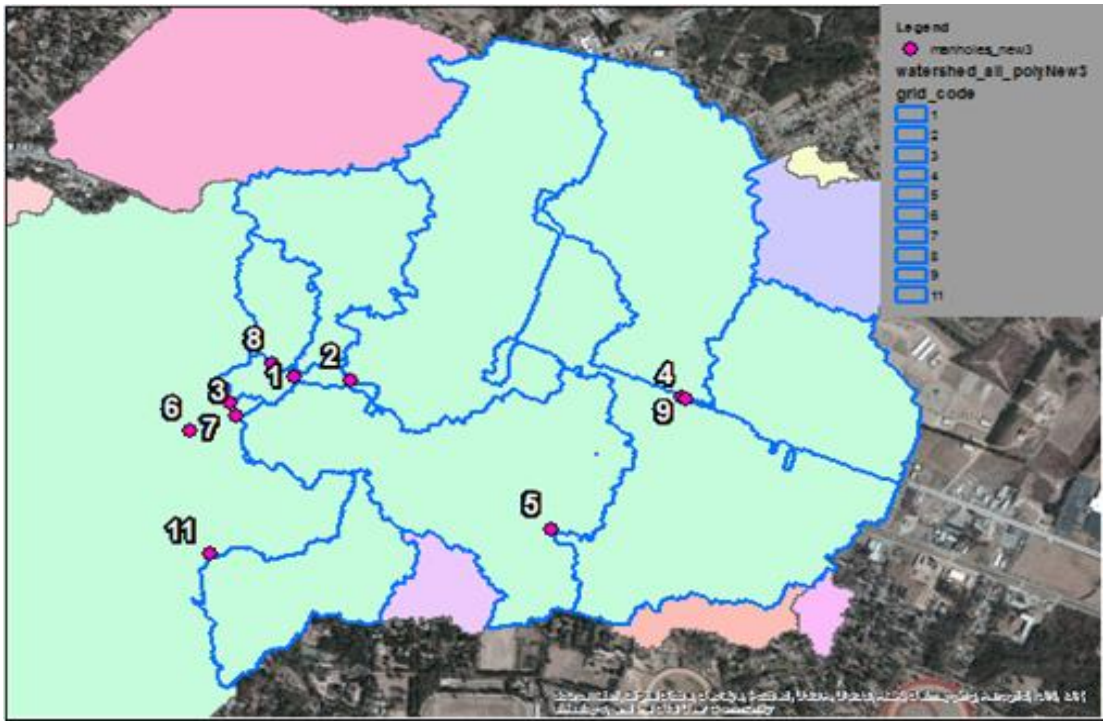

Figure 3.16: Adjoint Catchment polygon derived from the Catchment polygon and the Drainage Line showing all catchments aggregated that contribute to the flow out of the 10 foot pipe. The Subwatershed layer is turned on to show that the Adjoint Catchment boundary is exactly the same as the Subwatershed boundary indicating that the stormline was burned into the DEM correctly and accepted as the natural stream element

3.3.3 CURVE NUMBER LOOKUP TABLE

A curve number (CN) lookup table (Table 3.5) was created to be applied in future flow simulations using HEC-GeoHMS. The required datasets for CN lookup table creation (Merwade, 2012) include: the DEM for the area of interest, the NLCD 2011

land use grid from USGS (Jin et al., 2011), and SSURGO soil data (Soil Survey Staff, 2014. When the land use grid was downloaded from NLCD and added to ArcMap 10.1 at a spatial resolution of 30 meters, it included 15 land classifications: open water, woody wetlands, emergent herbaceous wetlands, developed open space, developed low intensity, developed medium intensity, developed high intensity, deciduous forest, evergreen forest, mixed forest, barren land, shrub/scub, herbaceous/grassland, pasture/hay, and cultivated crops (Merwade, 2012). These classifications were simplified to make the grid easier to use and demonstrate spatially. The "spatial analyst" extension in ArcMap 10.1 along with the "reclassify" tool was used to turn the 15 classifications above into 4 simple categories, as demonstrated in Table 3.4, including: water, medium residential, forest, and agriculture (Merwade, 2012). The output raster was then assigned a value of 1 through 4 depending on the land use classification of the cell. This new reclassified grid was added to the map and converted into a polygon feature class (Figure 3.17). The "Field" in the tool was defined as "Value", used to classify the new layer, to assure that the reclassified land use values were transferred to the new polygon.

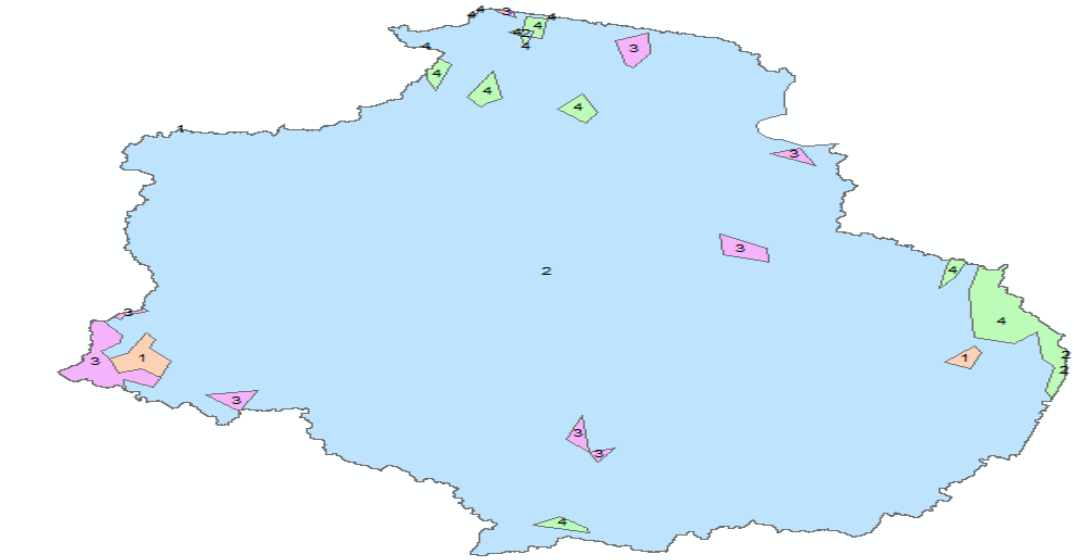

Figure 3.17: NLCD land use data, reclassified based on Table 3.4, converted into a polygon feature class and clipped to the study area

Table 3.4: NLCD land cover reclassification table to create a CN grid (Merwade, 2012)

Original NLCD	classification	Revised NLCD	classifiction
Number	Description	Number	Description
11	Open water	1	Water
90	Woody wetlands	1	Water
95	Emergent herbaceous wetlands	1	Water
21	Developed, open space	2	Medium residential
22	Developed, low intensity	2	Medium residential
23	Developed, medium intensity	2	Medium residential
24	Developed, high intensity	2	Medium residential
41	Deciduous forest	3	Forest
42	Evergreen forest	3	Forest
43	Mixed forest	3	Forest
31	Barren land	4	Agriculture
52	Shrub/scub	4	Agriculture
71	Grassland/herbaceous	4	Agriculture
81	Pasture/hay	4	Agriculture
81	Cultivated crops	4	Agriculture

Next, the SSURGO soil data from NRCS were prepared to use for the CN lookup table. Soil data were downloaded and converted into a readable file type in ArcMap 10.1 through the MS Access file downloaded with each SSURGO soil dataset. The tabular data from the download dataset were imported by placing the path to where the data was saved in the import form accessible upon opening MS Access. This tabular data then populated the corresponding tables in the database from the downloaded dataset to be read in ArcMap 10.1 (Merwade, 2012). The SSURGO spatial data map was added to ArcMap 10.1 along with the "component" and "map unit" tables from the MS Access population. The soil map was then clipped to the area of study and a "SoilCode" field was added to the SSURGO attribute table for storing soil group information. The data needed for soil group was in the "component" table, so the "component" table and the SSURGO attribute tables were "joined". The "Mapunit Key" field from the SSURGO layer was joined by the "mukey" field derived from the column in the "component" table directly related to the "soil identification number" in the SSURGO attribute table. All of the fields from the "component" table were available in the SSURGO soil attribute table as well. The newly created "SoilCode" field was populated with the "component.hydgrp" field using the "field calculator" tool. The SSURGO soil polygon layer is demonstrated in Figure 3.18 and labeled by hydrologic soil group. Four new fields were created in SSURGO attribute table and named "PctA", "PctB", "PctC", and "PctD" and populated according to their hydrologic soil group. For example, if the hydrologic soil group was A, then "PctA" received a 100 and the rest received 0s, but if the soil

group was A/D then “PctA” and “PctD” received 50s and “PctB” and “PctC” received 0s. To fill all of these values, the layer was edited and the percent of each soil group was entered manually for all four columns.

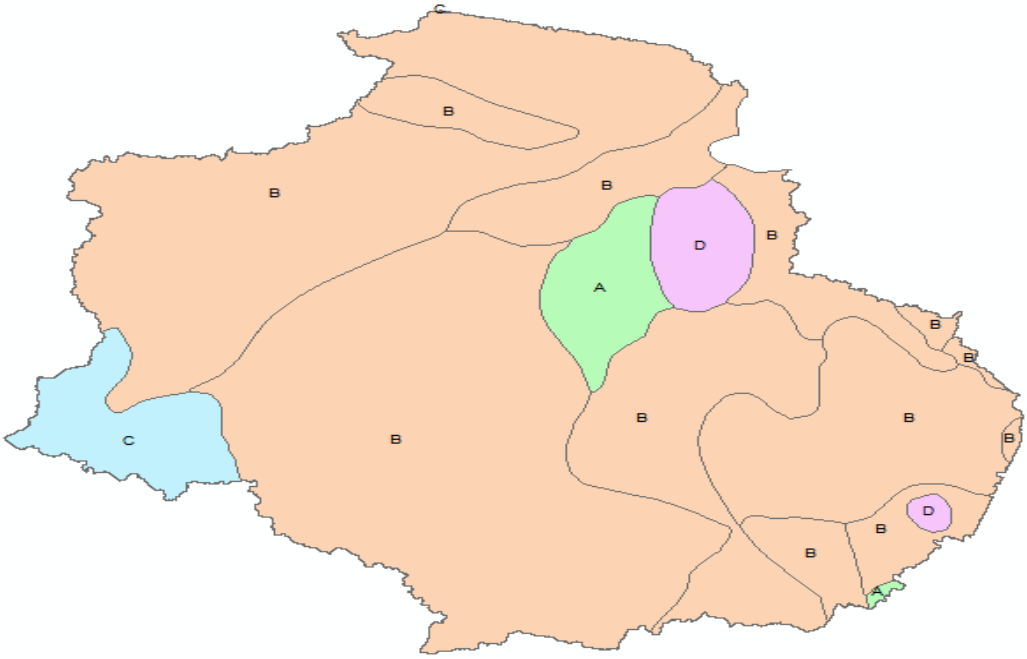

Figure 3.18: SSURGO soil data (Soil Survey Staff, 2014) clipped to study area and classified by hydrologic soil group (NRCS, 2007)

Once soil and land use data were ready for use in ArcMap 10.1, they were combined for the CN lookup table using the “union” tool. A table was created called CNLookUp (Table 3.5) using the “create table” tool and fields LUValue, A, B, C, and D were created, all being “short integer” fields, while description was a “text” field. The table was populated manually using “edit features” as described above using SCS TR55 curve numbers for water, medium residential, forest, and agriculture depending

on their soil group. The LUValue field was filled with number 1 through 4 according to the numbering of each land use classification as reclassified in the land use table (Table 3.4). Once the CN lookup table (Table 3.5) was created, it was ready for future flow simulations in HEC-GeoHMS for creation of the CN grid needed to lump basin parameters in HEC-HMS and a CN polygon was created (Figure 3.19). The NLCD 2011 impervious surface grid (Xian et al., 2011) was used for later analyses in HEC-GeoHMS and added to ArcMap 10.1 and clipped to the watershed area (Figure 3.20) using the "extract by mask" tool. The NLCD data was simply downloaded from the NLCD 2011 website and imported into ArcMap for land use analysis within Aiken, SC. The NLCD legend used to read the NLCD percent impervious surface grid, also simply downloaded from the NLCD 2011 website, is demonstrated where 0 percent impervious surface can be seen in black, while 100 percent impervious surface can be seen in purple. All of these layers were saved to ArcMap 10.1 for future use with HEC-GeoHMS.

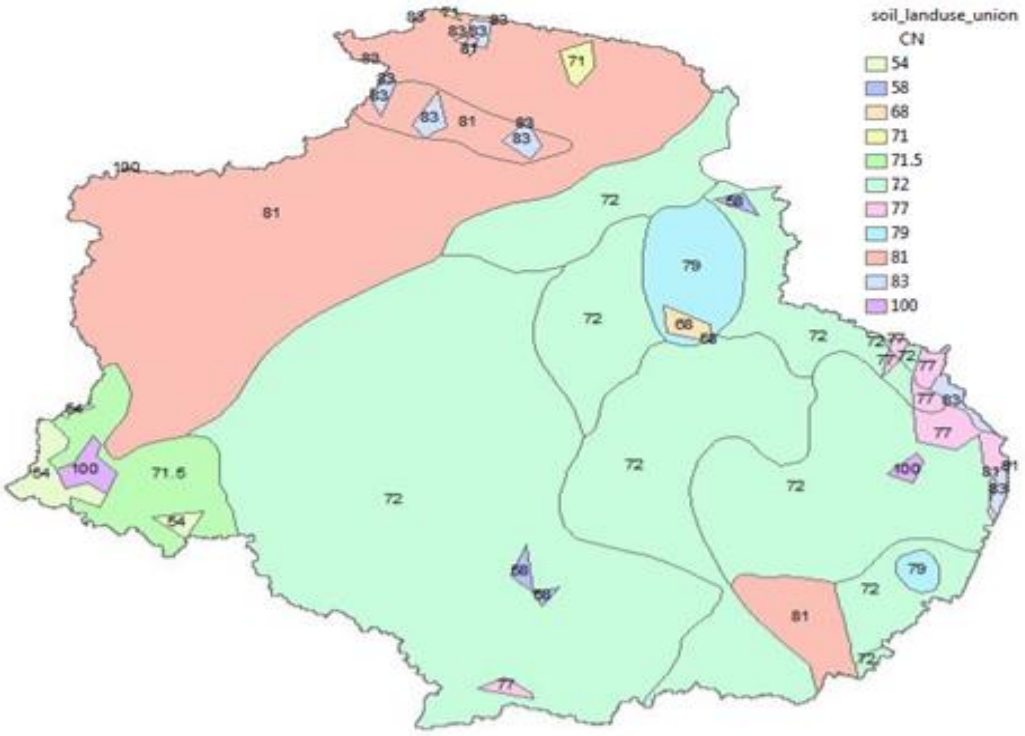

Figure 3.19: Soil and land use data combined and classified by SCS CN according to the CN lookup Table 3.5

Table 3.5: "CN Look-up table" used to calculate CN grid and polygon layer demonstrated in figure 3.22 above (Merwade, 2012)

LUValue	Desciption	A	B	C	D
1	Water	100	100	100	100
2	Medium residential	57	72	81	86
3	Forest	30	58	71	78
4	agriculture	67	77	83	87

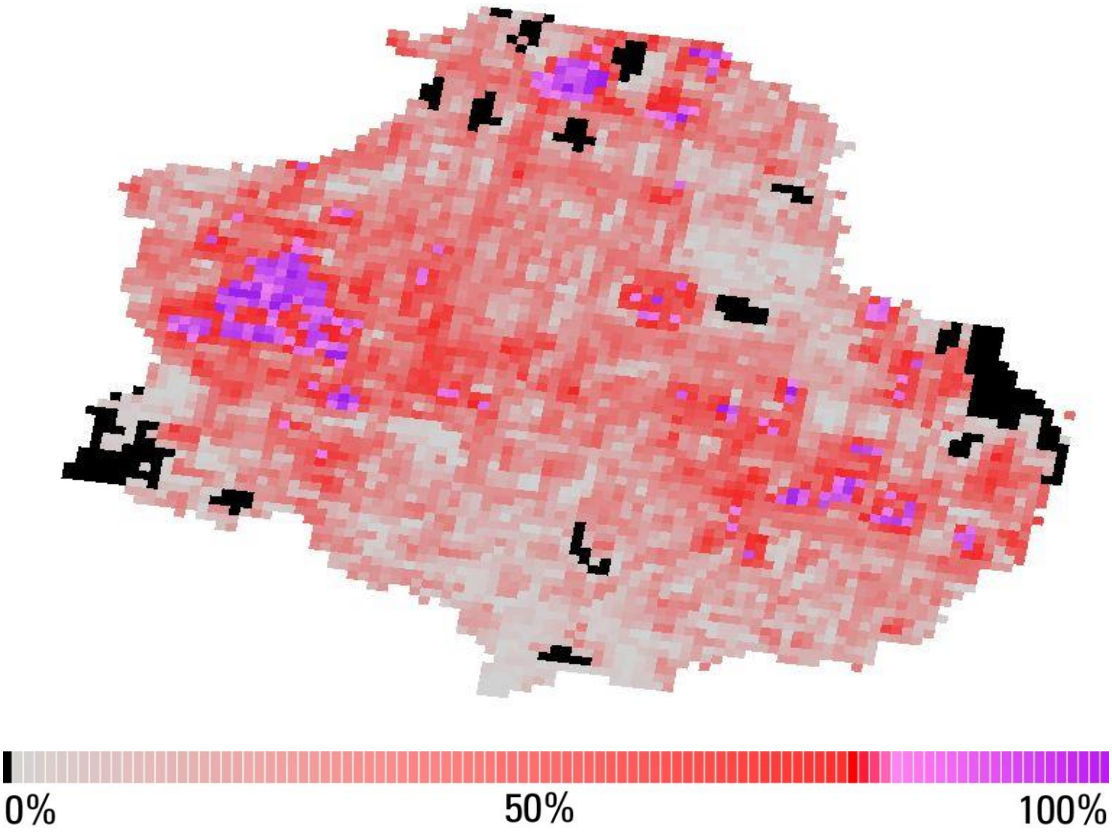

Figure 3.20: NLCD 2011 percent impervious grid (Xian et al., 2011) clipped to the study area

3.4 RESULTS

Original DEM creation from the LiDAR data (Figure 3.5) demonstrated a range of elevations from 566.08 to 219.33 feet. The DEM after it had been clipped to the area of interest (Figure 3.6) and all sinks and depressions had been filled showed that the area had elevation values of 259.18 feet to the highest elevation of 553.15 feet. It was discovered that the "burn stream slope" tool was not functioning properly and the "DEM reconditioning" tool was used to achieve the burning at an artificial elevation

below that of any surface of the original DEM and reasonable output elevations. Upon completing all watershed delineation, the DEM was clipped to only the total watershed, and the raster demonstrated elevations ranging from 551.15 to 364.27 feet with an elevation difference of 187 feet. The Flow Direction grid (Figure 3.8) established values from 1 to 128 routing the direction of flow following the higher values of the underground stormwater system. The Flow Accumulation grid (Figure 3.9) ranged from 0 to 4,295,880 cells accumulating downstream of the outlet also following the routing of the underground stormwater system. Subwatershed delineation established eight watersheds within the total outlet watershed with the smallest being Subwatershed 7 at 15 acres and the largest being Subwatershed 5 at 229 acres. Delineation also established a subwatershed outside of the total watershed, number 11, which did not contribute to the flow at the outlet with an area of 82 acres. The total area of the subwatersheds combined, excluding Subwatershed 11, equaled 1,070 acres, and the total outlet watershed gave an output of 1,079 acres. The excluded 9 acres define the area after Subwatersheds 7 and 3 before reaching the outlet. This flow is not received by any outlet other than the total watershed outlet, and was therefore not delineated in any of the other previous subwatersheds.

The Drainage Line was derived from the Stream Link grid and the Flow Direction grid to produce Figure 3.14 including the burned in stormline. The Catchment polygon layer (Figure 3.15) derived from the Flow Direction and Stream Link grids as well demonstrated 248 separate catchments flowing into the outlet, with 14 derived for Subwatershed 11. The Adjoint Catchment layer (Figure 3.16) derived 313

catchments, demonstrating the major adjoint catchment to match the boundary of the total outlet watershed. The NLCD reclassified land use polygon (Figure 3.17) demonstrated, as was expected, that the overwhelming majority of the City of Aiken is highly developed as demonstrated by the polygons labeled 2 for developed open space, developed low intensity, developed medium intensity, and developed high intensity (Table 3.4) (Jin et al., 2011). SSURGO soil data (Soil Survey Staff, 2014) established the hydrologic soil group polygon (Figure 3.18) and illustrated an overwhelming majority of hydrologic soil group B, with much smaller portions representing groups A, C, and D. Joining the hydrologic soil group and land use polygons, the CN polygon (Figure 3.19) was created and provided a range of CNs from 54 to 100. The majority of the polygon demonstrated CNs 72 and 81 representing impervious surfaces and developed areas with lower CNs surrounding the outlet due to evergreen forests, deciduous forests, and mixed forests. These CNs were defined by the lookup values in Table 3.5 (Merwade, 2012). The impervious percentage grid (Xian et al., 2011) from NLCD (Figure 3.20) demonstrated values from 100 percent impervious, dark purple, to 0 percent impervious, or black. The majority of the city of Aiken is covered in light purple to dark and light red indicating 50 to 100 percent impervious surface (Xian et al., 2011).

All ArcMap volume outputs are shown in Table 3.6, and detailed individual storm information is found in Appendix A. Each figure demonstrates the ArcMap volumes for each subwatershed calculated by multiplying the area of each subwatershed by the amount of inches of the corresponding storm event and converting acre-in to gallons.

GIS volumes summed means that after ArcMap delineated each area, each subwatershed area was summed according to whether it was a first order or second order subwatershed; whether or not it had an additional subwatershed contributing to it before reaching the total watershed outlet. These outputs are shown in column seven of all output tables in Mgal. The volume column, or column six in all output tables, is the individual subwatershed volumes delineated without being summed according to flow order. The largest volume over all storm events was seen at Subwatershed 6 with the highest runoff generated resulting from an event on May 15, 2014 to May 16, 2014 as being 68 million gallons of stormwater volume generated from a rainfall depth of 2.32 inches, the largest storm event recorded over the study period. The smallest volume per storm is always observed at Subwatershed 8, with the least amount of total runoff recorded being 0.3 million gallons on the storm event on July 22, 2014 derived from 0.01 inches of rainfall, which was the smallest storm event recorded. Figure 3.21 and Table 3.6 demonstrate all storm events, their rainfall depths (inches), and the ArcMap derived volumes summed per storm (Mgal). The trend line for the rainfall versus GIS volumes summed graph was linear, with a slope of 29.3 and an R squared value of 1, as expected due to the GIS volumes being directly calculated by the rainfall amount per storm event. Unfortunately, NEXRAD gridded rainfall data was unavailable for Aiken, SC and was collected from two weather stations along with a rain gage when neither station was available for data collection for model calibration. Weather station data is preferred due to the ability to

gather incremental rainfall data for per storm calculations versus a total depth for the entire day with the rain gage only allowing calculations per day.

Table 3.6: All selected storm events for study and their date renumbering, rainfall (inches), and GIS total volume at the 10 foot pipe outlet (mega gallons)

Run/Storm	Date & # of Storm	Rainfall (in)	Total GIS Volume (Mgal)
1	12/22/13	0.77	22.6
2	12/23/13	0.82	24.0
3	2/21/14	0.34	10.0
4	2/26/14	1.28	37.5
5	3/6/14-3/7/14	0.77	22.6
6	3/16/14-3/17/14 (1)	1.27	37.2
7	3/17/14 (2)-3/18/14	0.20	5.9
8	3/28/14-3/29/14	0.50	14.7
9	4/7/14-4/8/14	1.31	38.4
10	4/14/14-4/15/14 (1)	1.36	39.9
11	4/15/14 (2)	0.26	7.6
12	4/18/14-4/19/14	1.54	45.1
13	4/22/14-4/23/14	0.16	4.7
14	5/15/14-5/16/14	2.32	68.0
15	5/25/14	0.15	4.4
16	5/27/14-5/28/14	0.54	15.8
17	5/29/14-5/30/14	1.59	46.6
18	6/7/14-6/8/14	0.31	9.1
19	6/11/14 (1)	0.70	20.5
20	6/11/14 (2)-6/12/14	0.10	2.9
21	6/13/14-6/14/14	0.13	3.8
22	6/24/14-6/25/14	0.71	20.8
23	7/15/14	0.38	11.1
24	7/19/14	0.51	15.0
25	7/20/14	0.15	4.4
26	7/21/14 (1)	0.63	18.5
27	7/21/14 (2)-7/22/14 (1)	0.49	14.3
28	7/22/14 (2)	0.01	0.3
29	7/22/14 (3)-7/23/14	0.06	1.8
30	8/2/14	0.58	17.0
31	8/8/14-8/9/14 (1)	0.60	17.6
32	8/9/14 (2)	0.05	1.5
33	8/10/14-8/11/14	0.97	28.4
34	8/12/14	0.09	2.6
35	8/18/14-8/19/14	0.06	1.8
36	8/31/14	0.24	7.0
37	9/2/14-9/3/14	0.06	1.8
38	9/4/14	1.61	47.2
39	9/5/14	0.05	1.5
40	9/13/14 (1)	0.06	1.8
41	9/13/14 (2)	0.08	2.4
42	9/14/14 (1)	0.36	10.6
43	9/14/14 (2)-9/15/14 (1)	0.22	6.5
44	9/15/14 (2)	0.12	3.5
45	9/15/14 (3)-9/16/14 (1)	0.01	0.3
46	9/16/14 (2)	0.11	3.2
47	9/16/14 (3)-9/17/14 (1)	0.19	5.6
48	9/17/14 (2)-9/18/14 (1)	1.05	30.8
49	9/18/14 (2)-9/19/14 (1)	0.41	12.0
50	9/19/14 (2)-9/20/14	0.02	0.6
51	9/24/14	0.15	4.4

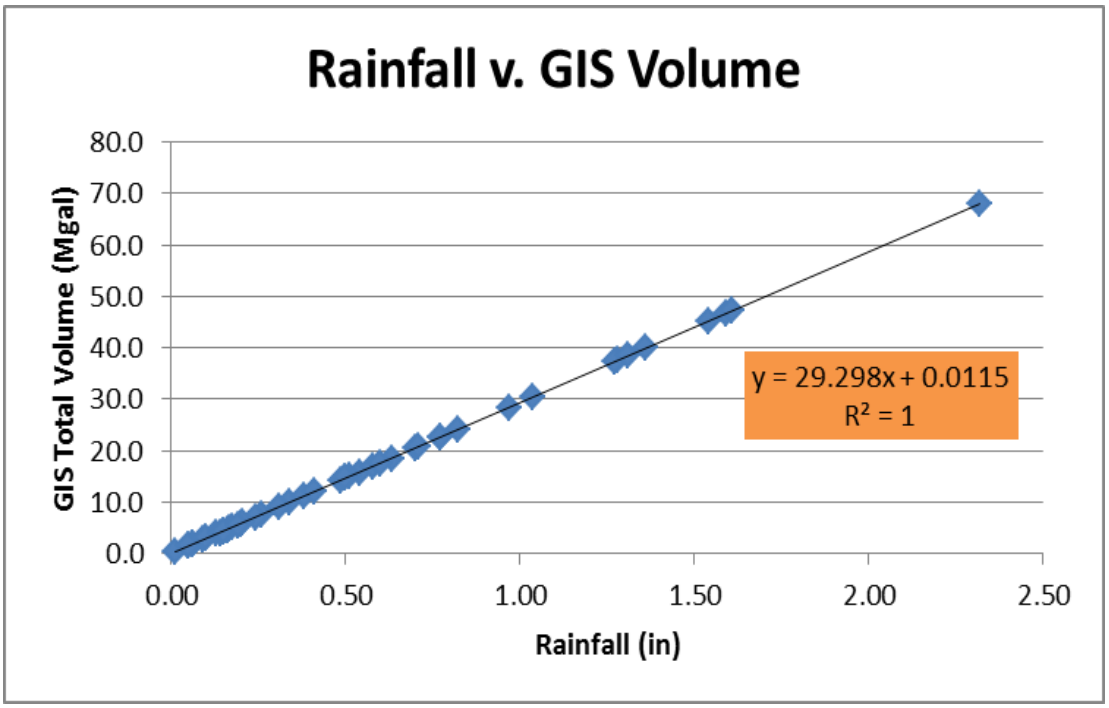

Figure 3.21: Rainfall (inches) versus GIS total volume at the 10 foot pipe outlet (mega gallons) for all selected storm events with R^2 of 1 indicating a direct fit expected due to direct multiplication

3.5 DISCUSSION

Finalized stormlines and sensor locations were based on City Engineer and project team discussions, previous maps of the stormline system, and field studies. DEM creation from LiDAR data was completed and the stormline was successfully burned into the DEM at an artificial elevation lower than that of any natural DEM surface as demonstrated in Figure 3.7. Watershed delineation illustrated that eight of the subwatersheds combined to contribute to the total outlet watershed, while

Subwatershed 11 flowed downstream to another branch of the natural DEM stream network. Delineated subwatersheds all adhered to the same boundary as the total outlet watershed polygon, excluding Subwatershed 11, leading to the conclusion that the subwatersheds were delineated correctly and water from all subwatersheds routed to the same exit conduit at the total watershed outlet as predicted. Watershed analysis (Figures 3.23 to 3.26) showed that the hypothesized flow order from each inlet to the next; and then subsequent flow to the outlet based on information from the City of Aiken Public Works staff was correct for the existing stormline system. Selecting certain pour points for watershed delineation proved that Subwatersheds 4 and 9 flowed to Subwatershed 5, which then conjoins with Subwatershed 3 before flowing to the exit conduit. It also demonstrated that flows from Subwatersheds 8, 1, and 2 conveyed to Subwatershed 7 before reaching the overall watershed outlet. The results then demonstrate that Subwatersheds 3 and 7 combined before being routed to the final total watershed outlet, which was also confirmed in the field. This flow succession established that the volumes flowing through monitoring points 3 and 7 should be the greatest of the subwatersheds based on the overall combined land area derived from this succession. All land area contributing flow to Subwatershed 7 equaled 353 acres, or 33.5 percent, and all land area contributing flow to Subwatershed 3 equaled 717 acres, or 66.5 percent. This area accumulation indicated that the most effective placement of additional green infrastructure would be within Subwatersheds 3, 4, 5, or 9 based on the direct relationship between rainfall and runoff demonstrating the subwatersheds with the largest areas contribute the largest

volumes of runoff to the stormwater system. The Flow Accumulation grid also showed that as the stormline flow reached each outlet in succession, the flow gradually accumulated until all flow congregated at the total watershed outlet (Figure 3.9).

Another definitive success was defined by the fact that the Adjoint Catchment boundary adhered identically to the total outlet watershed boundary upstream of the outlet point. The corresponding boundaries of the adjoint catchment and the subwatersheds are demonstrated in Figure 3.16 and the reason that the subwatershed layer is also turned on in this figure. These results indicated that the stormline was correctly burned into the DEM and accepted as the natural stream element of the DEM and drainage line. As also seen in Figure 3.14, the stormline is clearly visible throughout the drainage line layer again indicating acceptance of the stormwater pipe system as part of the natural layer and the artificial burn of a lower elevation than the natural terrain was successful. The Adjoint Catchment layer derived more individual catchments than the Catchment polygon due to the difference in clip area. The Catchment polygon was clipped specifically to the outlet watershed and Subwatershed 11. The Adjoint Catchment layer remained clipped to the area of interest drawn before subwatershed delineation, as opposed to the watershed delineated area of the outlet, to demonstrate the matching boundaries of the total watershed and the largest adjoint catchment proving flow accumulation and direction along with acceptance of the stormline.

NLCD land use (Jin et al., 2011), SSURGO soil data (Soil Survey Staff, 2014), and CN polygons all showed reasonable and expected values for the urban watershed comprised by the City of Aiken. The NLCD land use grid was reclassified for better visual interpretation and ease of CN derivation, and the raster was reclassified into water, medium residential, forest, and agriculture (Merwade, 2012). As expected the majority of the area illustrated medium residential due to the high amounts of impervious surface in the City, because-as shown in Table 3.4- medium residential was derived from all developed categories. A large area of developed land within the watershed was also demonstrated by the impervious percentage grid illustrated in Figure 3.20. As seen in Figure 3.21, the majority of area in Aiken is 50 to 100 percent impervious indicated by the darker purple and darker red stormlines. As for hydrologic soil group, SSURGO soil data demonstrated in Figure 3.18 illustrated an overwhelming majority of soil group B. Group B soils typically have between 10 percent and 20 percent clay and 50 percent to 90 percent sand and have loamy sand or sandy loam textures (NRCS, 2007). Aiken is known for its majority of sandy soils demonstrated by its erosion problems throughout the hydrologic system, specifically at the outlet; therefore, this majority hydrologic soil grouping was also predicted.

The CN parameter is highly influential throughout runoff simulations, allowing for subwatershed lag time calculations and infiltration method selection; therefore the soil and land use polygons were combined to determine a CN polygon (Figure 3.19) based on the CN lookup Table 3.5. CN is also important for additional green infrastructure placement, as high CNs indicate areas where runoff generation is

probable and low CNs indicate areas where runoff generation is less likely. CN can also demonstrate infiltration capabilities of the surrounding soil, with high CNs establishing low soil permeability as indicated by the CN of water at 100 and the CN of impervious pavement at 98 (USDA, 1986). As projected due to high impervious surface, the majority of CN values were higher ranging from 71 to 100, while smaller percentages of land area included lower values from 54 to 58. CN figures were expected to be high within the City of Aiken due to the high percent of fully developed surface, and lower towards the total watershed outlet due to the more natural settings of the surrounding area including deciduous forests, mixed forests, and evergreen forests. As demonstrated in Figure 3.19, the CN polygon does indeed follow this trend towards the outlet aside from the small area of CN 100 which indicates open water or wetlands as also expected near the outlet. Land use, soil group, and percent impervious surface layers were used for later modeling in HEC-GeoHMS and HEC-HMS in the next chapter.

Once the SSURGO soil data, NLCD percent impverious grid, and NLCD land cover grid were downloaded and converted into usable formats within ArcMap 10.1, they could be used to demonstrate a total representative scale of subwatershed suitability for future green infrastructure installation. Each layer, along with other layers such as land area, municipality layers, distance from impervious surface, connected versus disconnected impervious surfaces, etc. could be utilized and given a weight of importance by city officials to demonstrate importance related to installation. Within ArcMap there are several tools, such as “raster calculator” or

"kriging", that can be used for layer weighting and most effective placement for green infrastructure. These tools create a scale based on the various weighted layers and generate a grid of best suited locations for the specified outcome based on the weighted rasters. Not only would this give the best suited subwatershed for installation, but it would also give specific locations within each subwatershed for the most effective placement for installation. More data layers and increased interaction with city officials for weighting of importance per layer would be necessary for this suitability scale creation; however, this suitability scale would be extremely helpful in future applications of this project, in Aiken or other urban watersheds, to determine a more specific placement for additional green infrastructure installation and generation of a scale for all subwatersheds.

GIS volumes demonstrated a linear relationship with rainfall amounts (Figure 3.21) illustrating a higher volume the more rainfall is received with a slope of 29.3 and an R^2 value of 1 indicating a direct fit expected due to direct multiplication of rainfall and ArcMap derived areas to calculate runoff volume. The highest volume recorded at the total watershed outlet derived from runoff generation over all storms was 68 Mgal from the rainfall event on May 15, 2014 and May 16, 2014 from a depth of 2.32 inches. The lowest volume recorded at the total watershed outlet derived from generation over all storms occurred on July 22, 2014 with a value of 0.3 Mgal from a rainfall of 0.01 inches. Throughout the detailed individual storm data (Appendix A), flow prediction results indicated that even small storms in this area of high impervious surfaces had high runoff volumes and potential long-term adverse impacts

on the stream stability and downstream water quality. All GIS volumes (Table 3.6) were calculated by multiplying the GIS delineated subwatershed areas by a rainfall amount allowing for no infiltration into the soil and translating all rainfall directly into runoff volumes. Although this method was not completely accurate, for the extremely high amount of impervious surface in the City of Aiken the direct multiplication of rainfall and delineated watershed areas was a feasible method for runoff volume calculations.

Runoff volumes were summed according to the flow paths established and proven accurate based on the City of Aiken Public Works flow order hypothesis demonstrating that Subwatersheds 1, 2, and 8 flowed into Subwatershed 7 before reaching the outlet and Subwatersheds 4, 5, and 9 flowed into Subwatershed 3 before reaching the outlet. ArcMap volumes, summed according to the established flow order of subwatersheds, were used as the output volume for each subwatershed accordingly, and the total watershed outlet volume was calculated by summing all subwatersheds excluding 11. The total watershed area could be used and multiplied by the rainfall amount instead of summing all individual subwatersheds, but the use of each individual subwatershed for the calculation allows for a double check on the accuracy of the model, as well proving the summed subwatershed area equaled the total outlet watershed area.

DEM reconditioning and watershed delineation in ArcMap 10.1 allowed for valuable modeling and runoff volume derivation for the urban stormwater system in Aiken, SC. ArcMap outputs were compared with previous subwatershed delineations

derived from HEC-1 and were determined to be more detailed and more accurate than previous models obtaining more precise stormwater piping analysis and development and a more comprehensive subwatershed delineation within the total outlet watershed. More accurately delineated subwatershed areas can allow for more accurate runoff predictions, which in turn derive a more efficient location for the installation of additional green infrastructure due to increased spatial analysis of land surface impacts on flow and volume accumulations. Increased spatial analysis can allow for a higher understanding of the land use, percent impervious surface, CN, and flow routing which allows placement of additional green infrastructure to capture and treat the largest volume of runoff possible to have the most advantageous effect on the stormwater system. The outputs from the ArcMap 10.1 model and the runoff calculations can provide the City of Aiken, SC a method to predict the effect of future storm events on the stormwater system and allow for the most effective choice in placement for green infrastructure.

3.6 CONCLUSION

The City of Aiken, SC, specifically the Sand River Headwaters watershed has had complications with severe erosion, downstream sediment deposition, and subsequent water quality impairments due to improper stormwater management that includes extreme stormwater discharge at the urban watershed outlet. In January 2012, Phase 1 of this project was completed including install and efficiency analysis of green infrastructure including bioretention cells, permeable pavement, and a cistern. Phase

2 of the project was initiated with the goal to quantify volumes and peak flow rates at 10 monitoring locations including the overall urban watershed outlet and also to establish a stormwater model using GIS technology to predict flow generation from given rainfall depths. Ultimately, the goal was to determine the most effective placement for the installment of additional green infrastructure to continue the effort to decrease runoff and peak flow rate at the outlet. Utilizing the increased spatial and temporal analysis GIS technology can provide a greater understanding of the relationship between land surface flow and the underground stormwater system was developed to determine the land areas where installation of additional green infrastructure would capture and treat the largest amounts of runoff for maximum volume and flow rate reduction downstream. The results from this project demonstrated that urban watersheds and their stormwater systems can be modeled and analyzed effectively through the use of GIS technology, specifically ArcMap 10.1 and the ArcHydro toolbox.

3.7 REFERENCES

Boucher, M. "Re: Unable to Recondition or Burn Stream into Raster." Web log comment. *ArcHydro Solutions*. ESRI, 30 Jan. 2013. Web. 30 Aug. 2014.

"CoCoRaHS - Community Collaborative Rain, Hail & Snow Network." CoCoRaHS - Community Collaborative Rain, Hail & Snow Network. Colorado Climate Center, 1998-2014. Web. 09 Oct. 2014.

Crawford, Clayton. "Lidar Solutions in ArcGIS_part2: Creating Raster DEMs and DSMs from Large Lidar Point Collections." Web log post. *ArcGIS Resources*. ESRI, 15 Dec. 2008. Web. 26 Sept. 2013.

De Loza, Victor, and Nahm H. Lee. "Urban Hydrology Modeling Using GIS." Web log post. *ArcGIS Resources*. ESRI, 26 Aug. 2013. Web. 26 Sept. 2013.

Eidson, Gene, Victoria Chanse, Calvin Sawyer, and Erin Cooke. Sand River Ecological Restoration Preferred Alternative. Rep. no. 2096199. Clemson: Clemson U Center for Watershed Excellence, 2009. Print.

Gironás, Jorge, Jeffrey D. Niemann, Larry A. Roesner, Fabrice Rodriguez, and Hervé Andrieu. "Evaluation of Methods for Representing Urban Terrain in Storm-Water Modeling." *Journal of Hydrologic Engineering* 15.1 (2010): 1. Web.

Institute of Applied Ecology/Center for Watershed Excellence. Sand River Headwaters Green Infrastructure Project. Rep. Clemson: n.p., 2013. Print.

Jin, S., Yang, L., Danielson, P., Homer, C., Fry, J., and Xian, G. 2011. A comprehensive change detection method for updating the National Land Cover Database to circa 2011. Remote Sensing of Environment, 132: 159 – 175.

Maidment, David R. *Arc Hydro: GIS for Water Resources*. Redlands, CA: ESRI, 2002. Print.

Meadows, Michael E., Katalin B. Morris, and William E. Spearman. Stormwater Management Study for the City of Aiken: Sand River Drainage Basin. Rep. Columbia: Department of Civil Engineering at U of South Carolina, South Carolina Land Resources Conservation Commission, 1992. Print.

Merwade, Venkatesh. "Creating SCS Curve Number Grid Using HEC-GeoHMS." *Purdue University* (2012): n. pag. Web.

Merwade, Venkatesh. "Downloading SSURGO Soil Data from Internet." *Purdue University* (2012): n. pag. Web.

NRCS. "Chapter 7 Hydrologic Soil Groups." Hydrology National Engineering Handbook. N.p.: United State Department of Agriculture, 2007. N. pag. Print. Part 630.

Soil Survey Staff, Natural Resources Conservation Service, United States Department of Agriculture. Soil Survey Geographic (SSURGO) Database for [Aiken, SC].Available online at http://www.arcgis.com/apps/OnePane/basicviewer/index.html?appid=a23eb436f6ec4ad6982000dbaddea5ea. Accessed [August, 2014].

United States Department of Agriculture (1986). Urban hydrology for small watersheds. Technical Release 55 (TR-55) (Second Edition ed.). Natural Resources Conservation Service, Conservation Engineering Division.

"Weather Station History." Aiken Standard. The Weather Underground, Inc., 2014. Web. 09 Oct. 2014.

Woolpert. Sand River Watershed Study. Rep. Aiken: n.p., 2003. Print.

Xian, G., Homer, C., Dewitz, J., Fry, J., Hossain, N., and Wickham, J., 2011. The change of impervious surface area between 2001 and 2006 in the conterminous United States. Photogrammetric Engineering and Remote Sensing, Vol. 77(8): 758-762.

CHAPTER 4: AN APPLICATION OF HEC-GEOHMS AND HEC-HMS FOR SITING FEASIBILITY OF URBAN STORMWATER REDUCTION USING GREEN INFRASTRUCTURE

4.1 ABSTRACT

Urban watershed hydrology is often difficult to evaluate due to variable land uses, modified soils and topography, and subsurface stormwater infrastructure with complex connections and routing. The City of Aiken, SC is highly urbanized with downstream adverse erosion impacts due to high energy stormwater discharges from the Sand River Headwaters watershed. The objective of the study was to quantify runoff volumes and peak flow rates at the subwatershed scale to establish the most effective placement of additional green infrastructure in the larger urban Aiken watershed to reduce stormwater flows. Toward this aim, ten subwatersheds and the total watershed area were delineated from a Digital Elevation Model (DEM) created from Light Detecting and Ranging (LiDAR) data and the ArcHydro toolbox in ArcMap 10.1. A unique technique called "burning" was used to implant the underground stormwater system and allow ArcMap 10.1 to interpret the piping as the natural stream element and then delineate subwatersheds based on this new routing structure. The total watershed area was derived along with ten subwatershed areas and combined with rainfall data to develop runoff volumes. This model was then converted for input into HEC-HMS through its preprocessor HEC-GeoHMS to achieve peak flow rates and additional runoff volumes.

The terrain preprocessing steps used through ArcHydro produce the output shapefiles and rasters needed to create the HEC-HMS inputs through HEC-GeoHMS. The Burned DEM, Drainage Line, and Catchment layers from ArcMap 10.1 created from a finalized stormline were used to generate River and Subbasin layers in HEC-GeoHMS. A slope grid based on the Burned DEM was also created, and the percent impervious grid (Xian et al., 2011) along with the Soil Survey Geological data (Soil Survey Staff, 2014) and NLCD land use (Jin et al., 2011) merged Soil Land Use layer and the CN lookup table were also input into HEC-GeoHMS. Utilizing these input files allows the preprocessor to determine slope, average CN, percent impervious surface, and lag time per subbasin. This finalized basin model, along with a meteorological model and time series data, were input into HEC-HMS to produce peak flow rates and flow volumes per storm event. The highest runoff volume and peak flow rate generated at the outlet over all storms from HEC-HMS was 30.9 million gallons and 7.2 cubic meters per second from a storm event of 2.32 inches on May 15, 2014 to May 16, 214. The smallest runoff volume and peak flow rate generated over all storms was 0.08 million gallons and 0.0 cubic meters per second from a storm event of 0.01 inches on July 22, 2014. The highest runoff volume and peak flow rate generated at the outlet over all storms from the sensor monitoring data were 69.35 million gallons from a storm event on March 6 to March 7, 2014 and 15.6 cubic meters per second on June 11, 2014. The lowest runoff volume and peak flow rate generated over all storms from the sensor monitoring data were 0.16 million

gallons on September 5, 2014 and 0.0 meters cubed per second on the same storm event.

4.2 BACKGROUND

In Aiken (Figure 1.1), the 1,080 acre watershed has an extensive stormwater pipe system that drains to a single 10 foot pipe outlet. It is a highly connected system in which runoff flows immediately from rooftops to parking lots or driveways to gutters and then to pipes resulting in extremely "flashy" hydrographs during and after a storm event; flow in the system rapidly peaks and then recedes (Woolpert, 2003). The stormwater outflow from the urbanized Aiken watershed drains to the headwaters of the Sand River, and then flows to Horse Creek and eventually into the Middle Savannah River. The erosion at this outlet is so extensive, that the resulting canyon that has formed has depths measuring up to 70 feet in some locations. Upon reaching the outlet, upper reaches are experiencing the greatest erosion, while there is only minor erosion along the middle reaches with considerable sediment transport from upstream sources, and sediment is being deposited in the main channel and in flood plains along the lower reaches (Meadows et al., 1992). With the majority of soils in the Sand River watershed being of sandy texture, the banks and stream beds have no protection from erosion and subsequent sediment transport and downstream loading which can lead to water quality impairments.

Several previous studies have been performed on the Sand River Headwaters to quantify stormwater flows and enhance the knowledge of the urban stormwater system in Aiken, SC. In 1992, Meadows et al performed a study (Stormwater Management Study for the City of Aiken: Sand River Drainage Basin) to determine the capacity of drainage networks in the Wise Hollow and Sand River basins to investigate ways to mitigate current and forecasted stormwater problems. They proposed to extend the storm sewer well downstream of the current outfall into an area where the channel is less erodible and/or a regional detention pond could be constructed. Woolpert completed a study in 2003 (Sand River Watershed Study) to examine the pollutant trends in each of these watersheds and assess potential erosion sites along tributaries within Hitchcock woods. The company proposed increased public involvement, a series of detention ponds on roadway medians in the downtown area, extending the gabion structures to protect susceptible areas further downstream, and diversion piping. In 2009, Eidson et. al. performed research (Sand River Ecological Restoration Preferred Alternative) to provide a "blue print" for the remediation of the stormwater canyon and restoration of natural communities and ecosystem processes within the greater Sand River watershed and to implement a long-term strategy to protect and maintain the restored sites. They proposed a combination of the following: upstream filtration and detention options, earthen dam, pond, wetland remediation, Sand River dual pipe system, wetlands, energy dissipation area, and tributary stabilization. Clemson University completed a study in 2013 (Sand River Headwaters Green Infrastructure Project) to summarize research associated

with the Sand River Headwaters Green Infrastructure project, conducted in partnership with the City and Woolpert Inc., which incorporated sustainable development practices to capture and treat stormwater within downtown watersheds, including the use of bioswales and bioretention, multiple applications of pervious pavement, and a cistern. They determined from analysis of green infrastructure installation and efficiency studies and analysis of storm events at monitoring stations including the 10 foot pipe outlet that the current green infrastructure installations were not making a significant impact on stormwater quantity and water quality downstream at the outlet. Phase 2 of the Aiken Project began in December, 2013 to continue these efforts to enhance understanding of the urban stormwater system and assess the most effective placement for additional green infrastructure within the subwatershed(s) to decrease stormwater volume quantity and flow rates downstream.

A Clemson University research team was asked to design a solution to the degradation problem incorporating green infrastructure. In 2009, the resulting project plan finalized by Clemson University's Center for Watershed Excellence incorporated bioretention cells, bioswales, permeable pavement, and a cistern in its green infrastructure solution and the effectiveness of these management practices to capture, store, infiltrate, and treat downtown stormwater (Clemson University, 2013). In January 2012, Phase 1 of the project was completed and on April 1, 2013 Phase 2 of the project began set to conclude on March 31, 2015. The objectives of Phase 2 include:

1. Quantify hydrologic flows during storm events draining to and within the downtown Aiken stormwater sewer system that constitutes Sand River headwaters.
2. Based on storm event flows, evaluate and optimize potential locations for further green infrastructure (GI) installation including analysis for hydrology and cost-effectiveness.
3. Enhance site-level remote data acquisition capabilities throughout the Sand River watershed and integrate associated collection, transmission, display, and archival facilities into the *Intelligent River*® network.

There were four main steps to completing these objectives. The first was to gain a better understanding of the existing stormwater network within the watershed and its drainage boundaries. The second step required quantification of volume and routing, with tasks that included: review of existing survey information of the water network, trunk line instrumentation with level and/or flow sensors in which ten monitoring locations were selected, and watershed scale modeling to effectively examine the overall efficiency of existing or future green infrastructure installation. Third, spatial analyses using Geographic Information Systems (GIS) were utilized to delineate watersheds and derive characteristics such as impervious surface and curve number (CN) per watershed. Lastly, an optimal location for future green infrastructure installation would be determined based on steps two and three, along with a cost benefit analyses and a decision matrix based on existing infrastructure, contributing area to stormflow and discharge, water volume availability, and proximity. Once all

of these steps have been completed and all the parameters determined, the subwatershed(s) that may be significantly contributing to high stormwater flows and subsequently to downstream erosion can be identified. If this is determined, then additional green infrastructure can be installed within these subwatershed(s) to effectively and efficiently decrease runoff and peak flow rate at the Sand River headwaters. This research approach and modeling methodology can then be used as a tool in other urban or developing areas.

4.3 METHODS

4.3.1 DATA MANAGEMENT

ArcMap 10.1 was used to produce the following layers from a LiDAR generated DEM and ArcHydro toolbox: Burned DEM, DEM Fill, Flow Direction grid, Flow Accumulation grid, Stream grid, Stream Link grid, Catchment grid, Catchment polygons, Drainage Line layer, and Adjoint Catchment polygons. For the purpose of utilizing the stormwater system as the natural stream element, the Stormline shapefile (Figure 4.1) was accepted into the Drainage Line layer (Figure 4.2). Due to HEC-HMS river connectivity limits, an edited stormline (Figure 4.3) had to be utilized for smooth execution and rerun through all of the previous ArcHydro steps in Chapter 3. All layers were input into the "data management" menu and the map was saved. A Slope grid (Figure 4.4) was also created using the reconditioned DEM to represent the slopes after the stormline was burned utilizing the "slope tool". A new project is created by selecting "start new project" under the "project setup" menu creating

Project Point and Project Area layers added to ArcMap. The default "original stream definition" and outside "MainView Geodatabase" for Project Data Location was chosen (Merwade, 2012). A project outlet was selected using the "add project points" button on the HEC-GeoHMS toolbar, and the outlet was chosen slightly farther down the drainage line layer, beyond the stormline extension. This selection allowed for the entire 10 foot pipe watershed to be chosen, as opposed to selecting the outlet on the end of the stormline layer only selecting part of the watersheds pipe system and not the entire drainage line incorporating the pipe system as a whole. "Generate project" was selected under the "project setup" menu, and subsequently HEC-GeoHMS created a mesh that extends to the boundary of the basin delineated based on outlet location (Figure 4.5). Basin boundary was determined to be correctly defined based on the watershed boundary delineated in ArcMap 10.1 using ArcHydro toolbox. The default layer names, Subbasin, Project Point, and BasinHeader were chosen and the project was generated and the following output layers were added to the geodatabase generated for the project based on the data management input layers: MainViewDEM (created by HEC-GeoHMS), the RAW DEM (Burned DEM), the Hydro DEM as "Fil" (filled DEM), the Flow Direction grid as "Fdr", the Flow Accumulation grid as "Fac", the Stream grid as "Str", the Stream Link grid as "StrLnk", and the Catchment grid as "Cat". HEC-GeoHMS also subsequently created a Subbasin, ProjectPoint, and River layer.

Figure 4.1: Finalized Stormline based on city official drawings and field studies utilized in ArcMap 10.1 and HEC-GeoHMS

Figure 4.2: Drainage Line demonstrating the incorporation of the Stormline into the natural streams

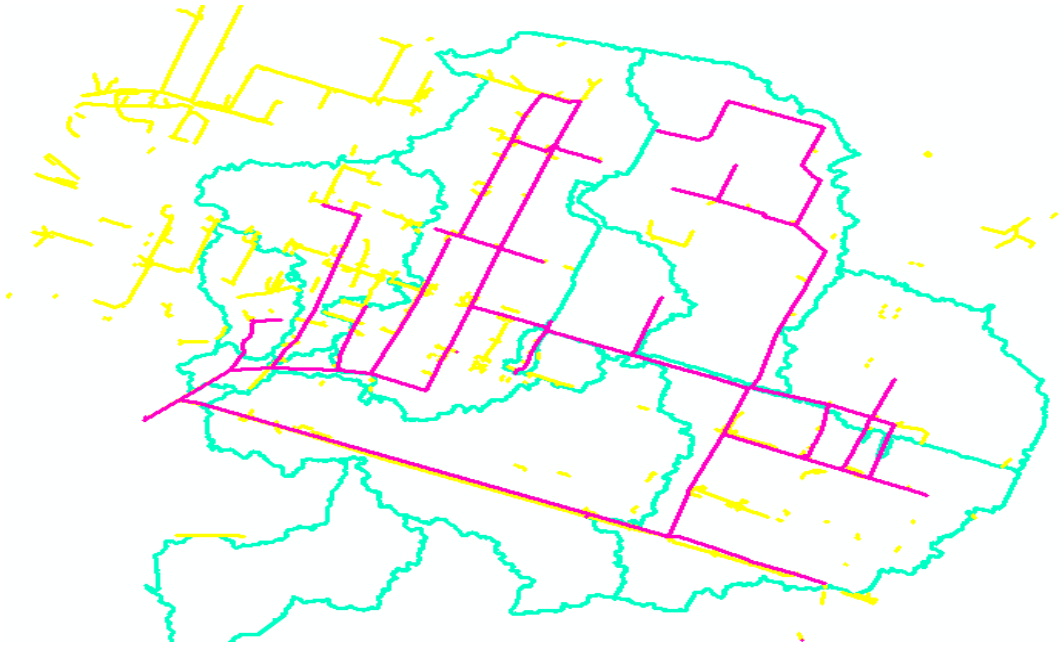

Figure 4.3: Altered Stormline layer for HEC-HMS river connectivity purposes

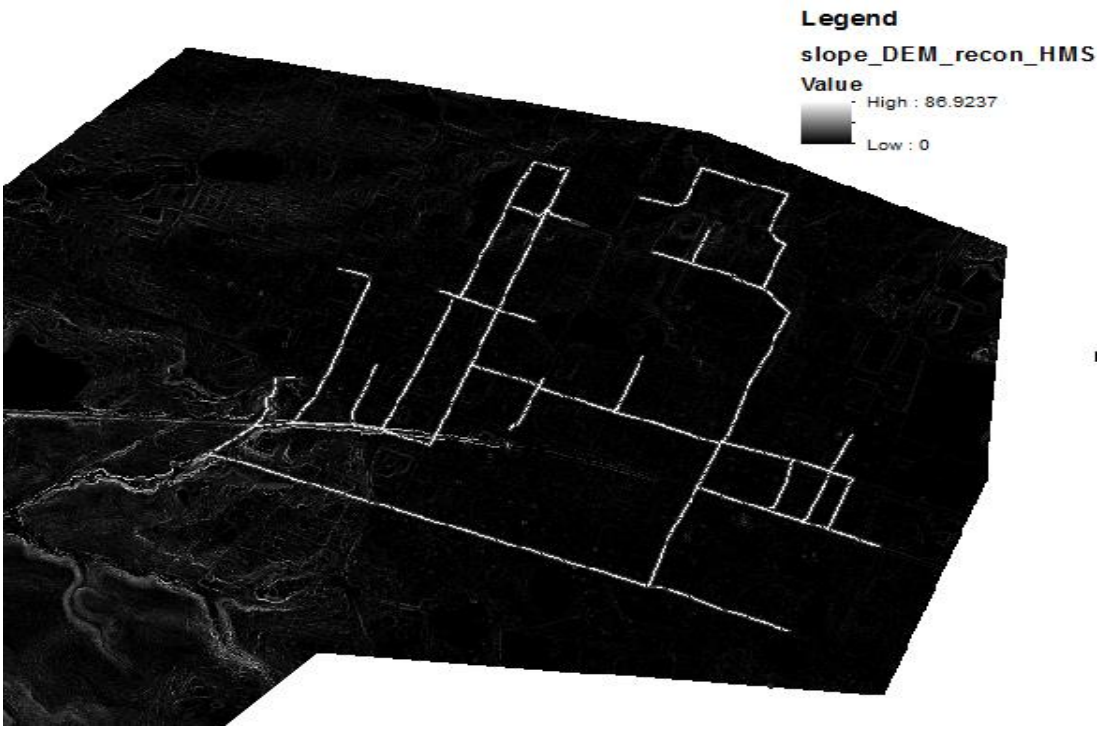

Figure 4.4: Slope grid created from Burned DEM demonstrating slopes up to 87ft/ft

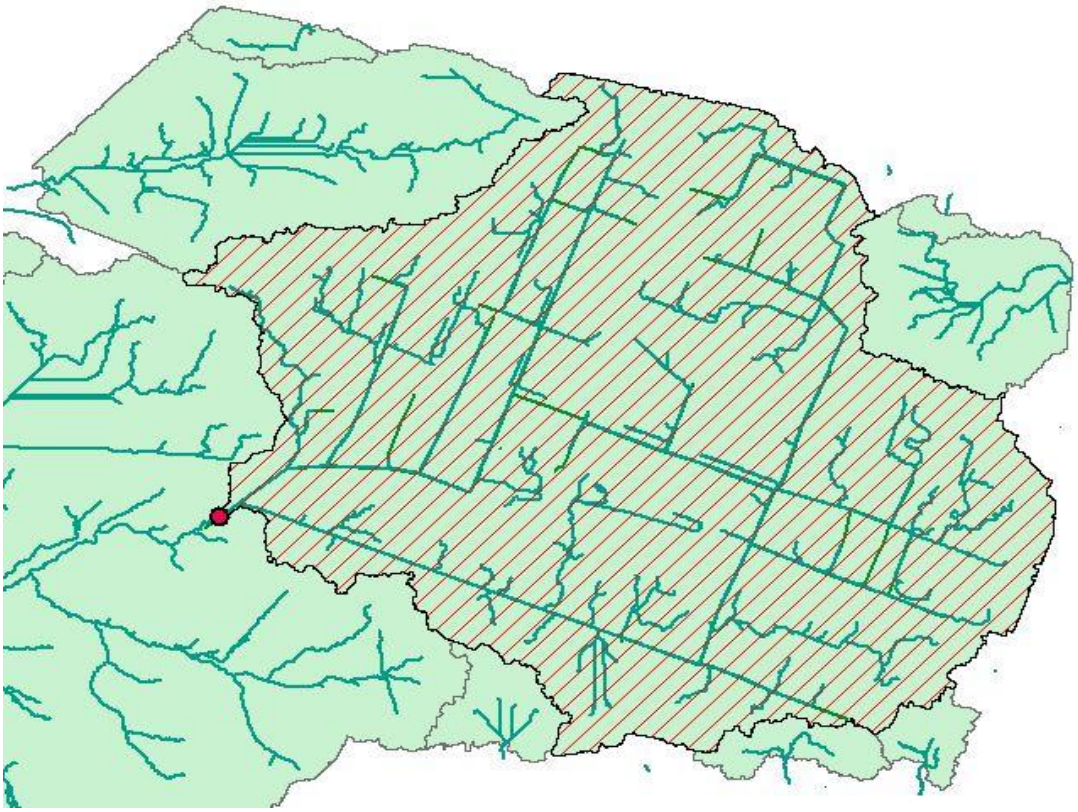

Figure 4.5: Mesh produced from HEC-GeoHMS “project generation” tool for acceptance or relocation of outlet

4.3.2 BASIN PROCESSING

Once all the data management layers were inputted and the output Subbasin and River layers were created the development of basin processing was initiated under the “basin processing” menu. In order to create the subbasins to match the subwatersheds previously generated in ArcMap 10.1, the Subwatershed layer was added to the map. The “basin merge tool” under the “basin processing” menu in HEC-GeoHMS was

used to merge all subbasins to closely match the Subwatershed layer, with caution to only select subbasins with adjacent streams. After merging was completed the Subwatershed were then referred to as Subbasins and Subbasin was used in this study from this point on. Once the Subbasin layer matched the Subwatershed layer as closely as possible, the River layer was required to match the Stormline layer. The River layer is defined as a product of the Drainage Line layer and the Stream Link layer; therefore, it includes the stormline and some segments of the natural stream layer. When segments of the River layer were deleted to completely match the Stormline layer, further analysis on the layer was unsuccessful due to null values in the attribute table after deletion. However, the River layer was very similar to the Stormline layer with few extra segments from the Stream Link layer, and therefore remained intact but was later simplified by HEC-GeoHMS to more closely resemble the Stormline layer.

Once the Subbasin and the River layers were finalized (Figure 4.6), the extraction of basin characteristics was executed. “River length” and “river slope” were obtained from the River layer, and the resulting outputs were added to the attribute table. “Basin slope” was executed on the Basin layer and added to its attribute table. The “longest flow path” tool was executed (Figure 4.7) using the Raw DEM, Flow Direction, and Subbasin layers as inputs. “Basin centroid” was run (Figure 4.8) selecting the “center of gravity” method and the Subbasin layer. The “center of gravity” method, as opposed to the longest flow path or fifty percent area methods, computed the centroid as the center of gravity of the subbasin when the centroid was

located within the subbasin, and if the centroid was located outside of the subbasin it was snapped to the closest subbasin boundary (Merwade, 2012). The “basin centroid elevation” was then calculated using the Raw DEM and Centroid layer, and “centroidal longest flow path” (Figure 4.9) was calculated using Subbasin, Centroid, and Longest Flow Path to derive the length of the longest flow path from the centroid of the subbasin to the outlet, or monitoring location, of the subbasin following the stormline system after exiting that subbasin outlet. The “longest flow path” is used to determine the hydraulic length of the subbasin to derive subbasin lag time, in hours, along with subbasin slope and average CN per subbasin.

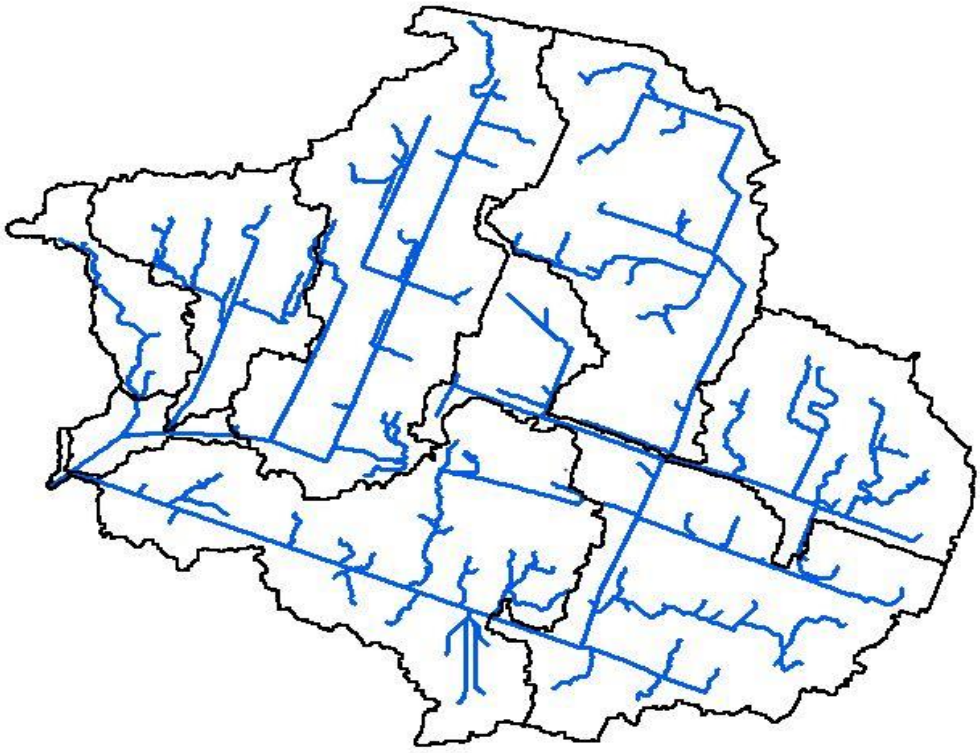

Figure 4.6: Subbasin and River layers after subbasins were merged to match the subwatersheds delineated as closely as possible due to catchment limitations

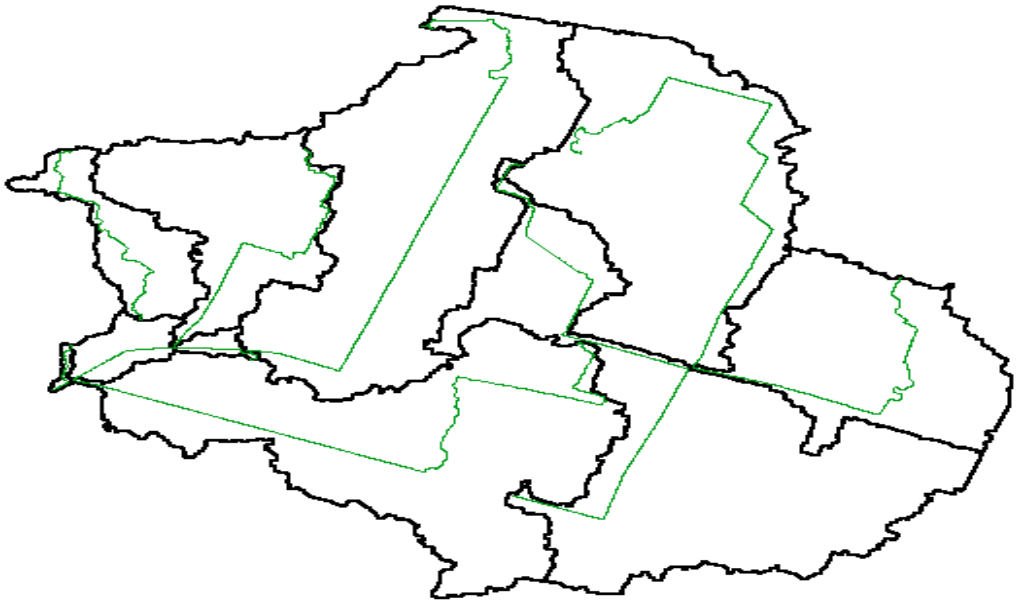

Figure 4.7: Longest Flow Path generated from the Raw DEM, Flow Direction grid, and Subbasin layers used for lag time per subbasin calculations

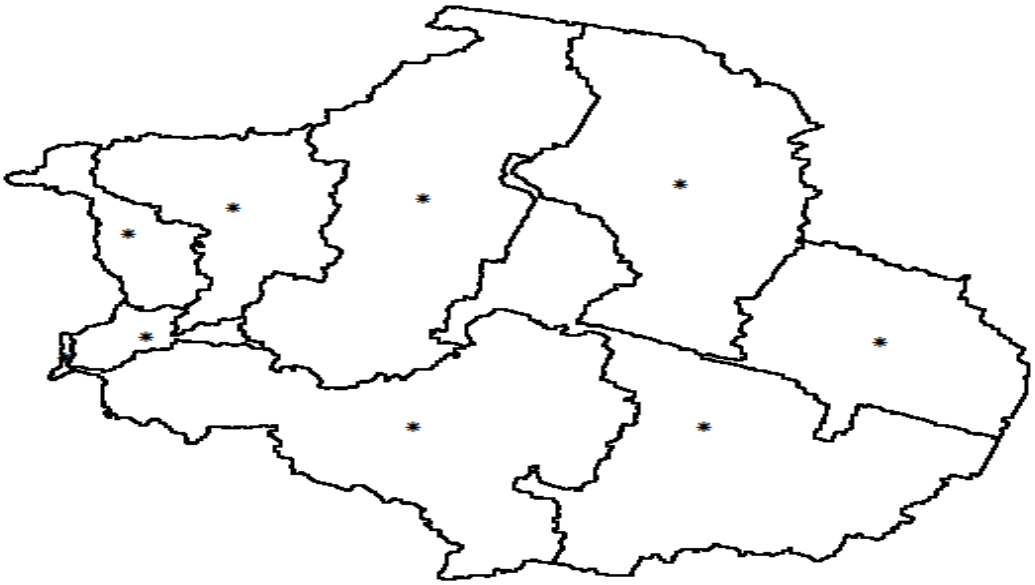

Figure 4.8: Basin Centroid generated by “center of gravity” method utilizing the Subbasin layer as input

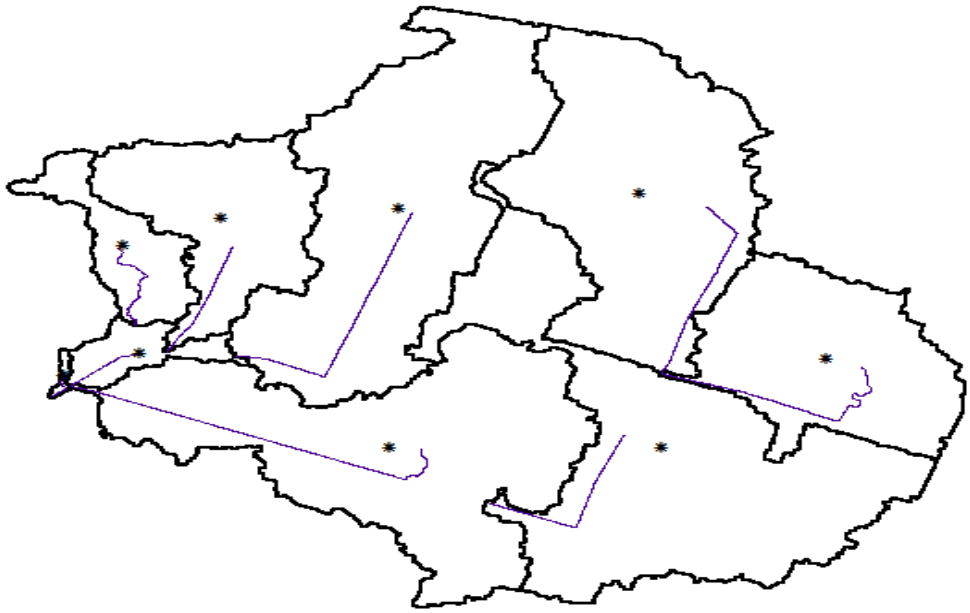

4.9: Centroidal Longest Flow Path generated by Basin Centroid and Longest Flow Path layers demonstrating the longest flow path from centroid to outlet

4.3.3 PARAMETERS AND HMS CREATION

Hydrological parameters selection was required for completion of the HEC-HMS model setup. All processes were edited or changed in HEC-HMS once the model was created. The SCS CN method is the most widely used technique to determine storm runoff volumes and peak discharges (Eli and Lamont, 2010) and was selected for the loss method and transform method. Due to averaging of prior baseflow data available, baseflow was selected as "constant monthly" and "lag" was chosen as the route method due to ease of use and access to all necessary data requirements for the stormwater conduits. These methods were added to the attribute tables of Subbasin and River respectively for use after import into HEC-HMS.

Next, tools were executed including “river auto name” and “basin auto name” and added to the attribute tables and used for numbering purposes in HEC-HMS. Subbasin parameters were also calculated including average CN and percent impervious surface. The percent impervious grid (Xian et al., 2011), directly downloaded from the NLCD website and imported into ArcMap, was clipped to the area of study (Figure 4.10) and the soil (Soil Survey Staff, 2014) and land use data (Jin et al., 2011), also directly downloaded from the NLCD website, were merged to create a CN lookup table. The CN lookup table was used, along with the Hydro DEM, and the soil land use polygon layer to calculate the CN grid (Figure 4.11) using the “generate CN grid” tool in HEC-GeoHMS. The “subbasin parameters from raster” tool was chosen and the percent impervious grid was inputted into the input percent impervious grid slot, while the CN grid was inputted into the input CN grid slot. A field for CN per subbasin (Figure 4.12) and percent impervious surface per subbasin (Figure 4.13) was added to the Subbasin layer attribute table. CN lag (hours) was computed using the “CN lag” tool and subsequently also added to the Subbasin layer attribute table. All of these outputs, along with subbasin area and basin slope as calculated by HEC-GeoHMS, are demonstrated in Table 4.1.

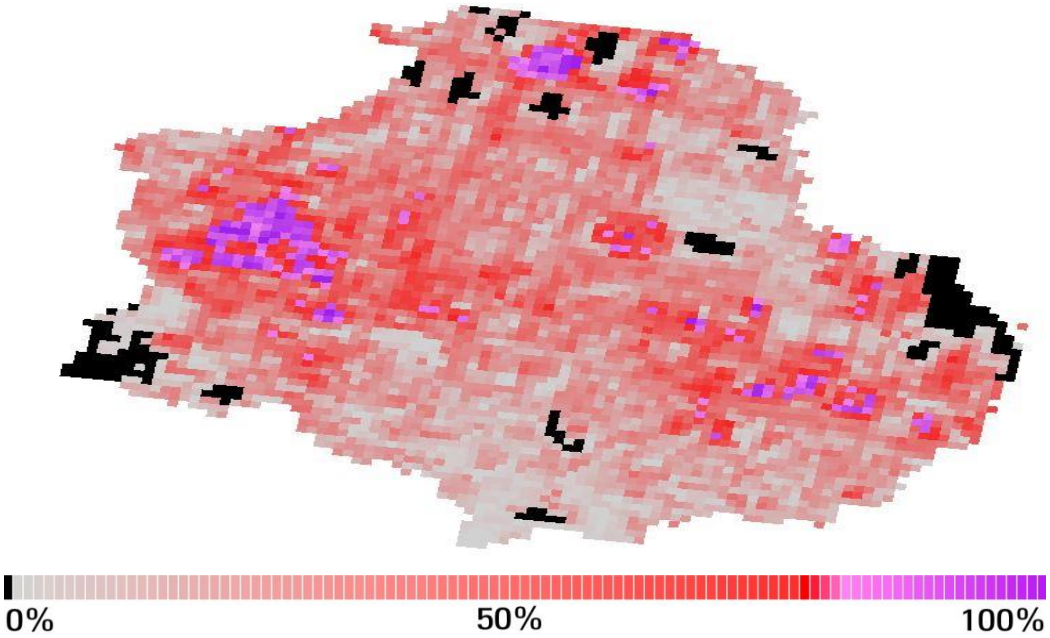

Figure 4.10: NLCD impervious percentage grid (Xian et al., 2011) clipped to study area

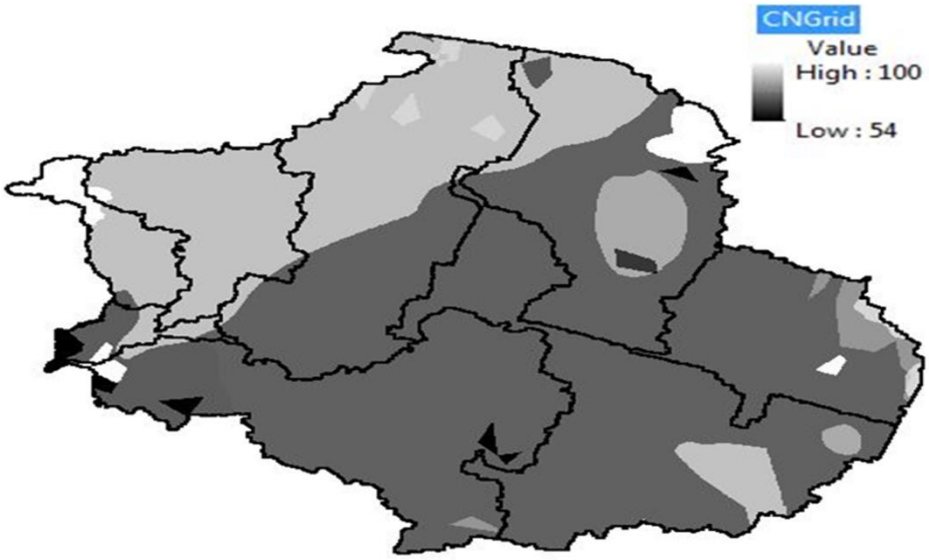

Figure 4.11: CN grid created from the CN lookup table generated in ArcMap 10.1 by the merging of soil (Soil Survey Staff, 2014) and land use data (Jin et. al., 2011)

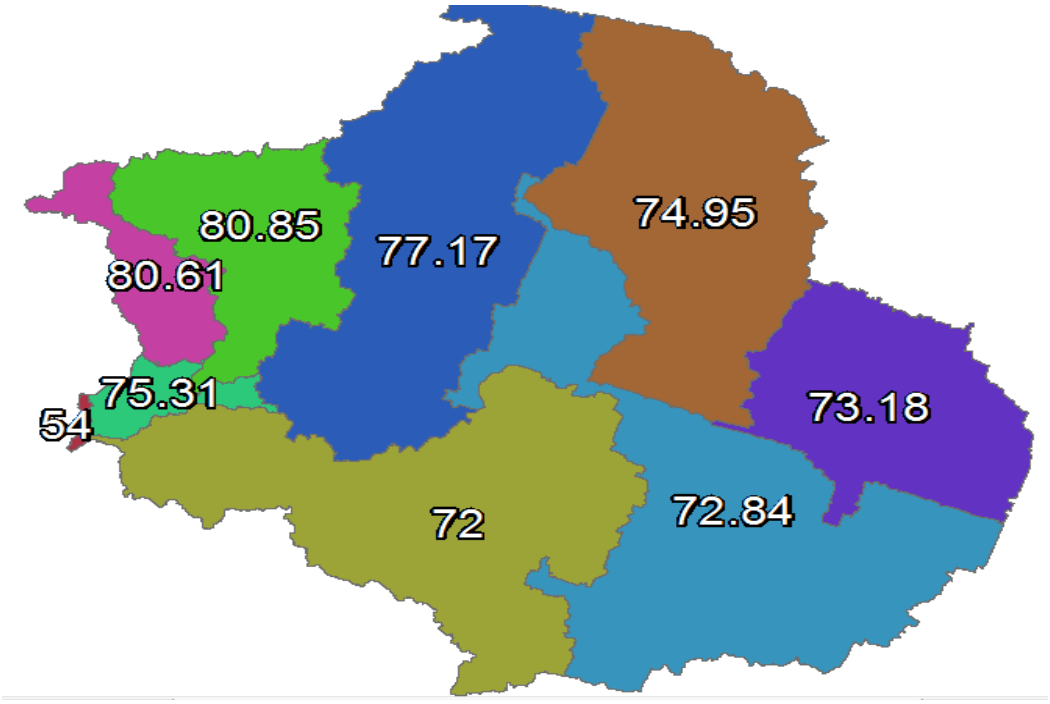

Figure 4.12: Average CN per subbasin as calculated in HEC-GeoHMS

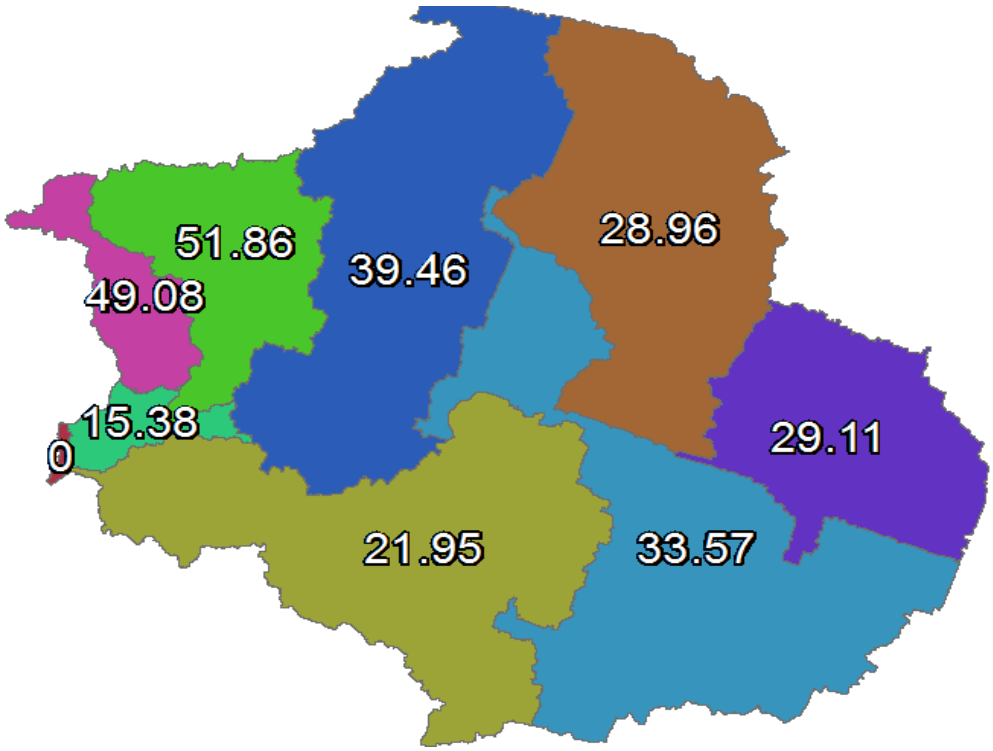

Figure 4.13: Percent impervious surface calculated per subbasin in HEC-GeoHMS

Table 4.1: Subbasin area, average CN, percent impervious surface, and lag time (hours) based on CN lag, percent impervious grid, and CN grid

Subbasin	Area (acres)	Average CN	Percent Impervious	Lag Time (hours)	Basin Slope
1	86.0	81	51.9	0.55	3.74
2	205.3	77	39.5	0.74	5.75
3	205.9	72	22.0	1.17	3.54
4	113.3	73	29.1	0.86	2.59
5	230.0	73	33.6	1.03	4.19
6	1.5	54	00.0	0.16	14.23
7	18.4	75	15.4	0.17	14.51
8	36.8	81	49.1	0.49	3.25
9	180.4	75	29.0	0.90	4.39

Lastly, the model was prepared for export from ArcMap 10.1 and import into HEC-HMS. The “Map to HMS Units” tool was executed under the “HMS” menu using the Raw DEM, Subbasin, Longest Flow Path, Centroidal Longest Flow Path, River, and Centroid layers. The units needed for export are chosen in the next window as SI and fields are added to River and Subbasin layers ending in HMS. Execution of the “Map to HMS Units” tool was unsuccessful due to a failed attempt to locate the BasinHeader file. The BasinHeader file was then copied from the geodatabase created when the model was first opened in ArcMap 10.1 to the

geodatabase automatically produced when the project was established in HEC-GeoHMS (ESRI, 2012). The “Map to HMS Units” tool was then rerun and completed without any errors upon location of the BasinHeader file. The “check data” tool was executed under the “HMS” menu to detect unique names, river containment, center containment, river connectivity, and VIP relevance. The tool “HMS schematic” under the “HMS” menu was then executed to create HMS nodes and HMS links (Figure 4.14) in ArcMap 10.1 including input layers Project Point, Centroid, River, and Subbasin, and the default names are used for layers HMSLink and HMSNode. The HMSNode layer differentiates between watershed nodes, junction nodes, and all other nodes illustrating how the model will look in HEC-HMS. The HMSLink layer also differentiates its links in the same way and once imported into HEC-HMS the links became the reaches in the finalized HEC-HMS model. All watershed nodes demonstrated as “subbasin” tools within HEC-HMS and all junction nodes demonstrated as HEC-HMS “junction” tools (Figure 4.15). Coordinates were then added using the “add coordinates” tool under the “HMS” menu utilizing The Raw DEM, HMSLink, and HMSNode as input layers.

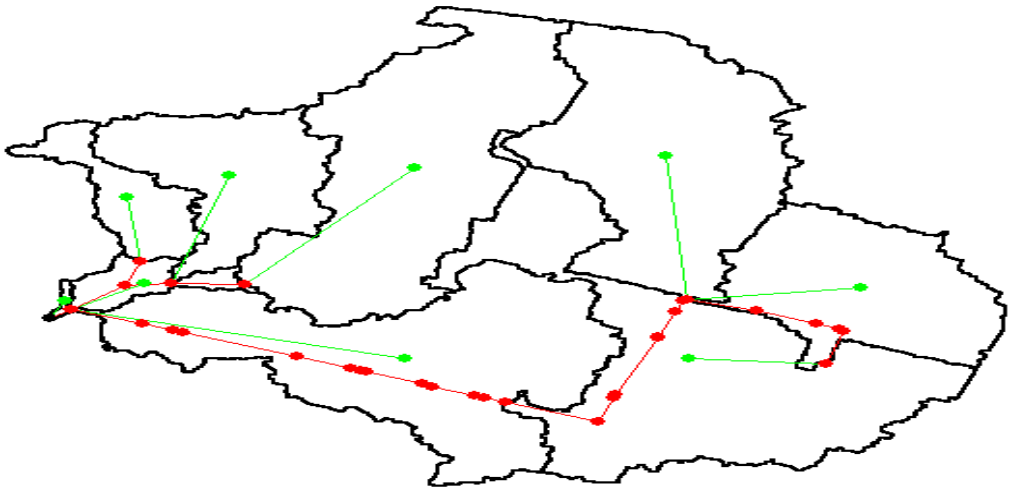

Figure 4.14: HMS links and nodes created by the HMS schematic tool with green representing watershed nodes and links, red representing junction nodes and length, and the entire watershed outlet is shown in black

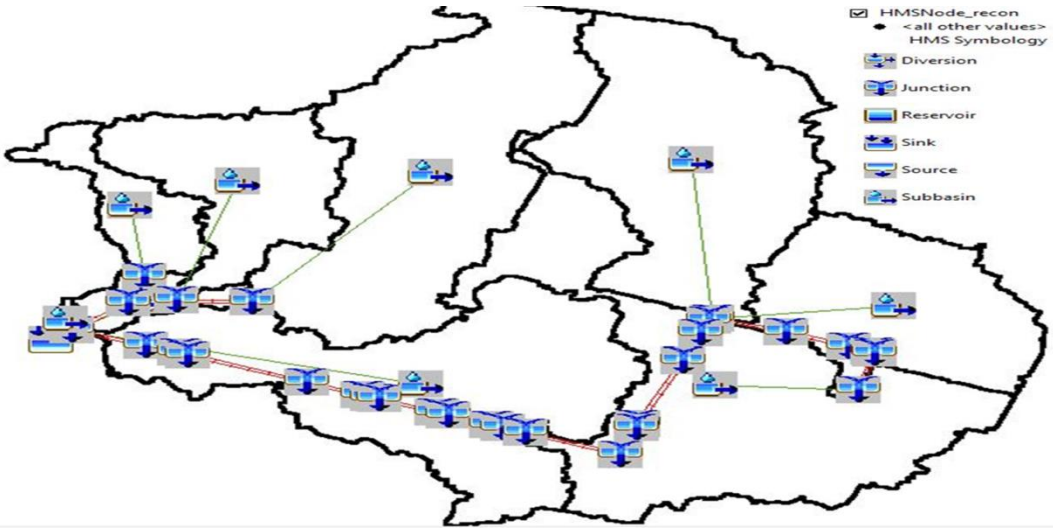

Figure 4.15: HMS mapping demonstration generated by “HMS toggle legend” tool to simulate how the model will be illustrated after import into HEC-HMS with green links representing basin connectors and red links representing reaches

The ArcMap 10.1 model was then prepared for export using the "prepare data for model export" tool and inputting the Subbasin and River layers. A background shapefile was also created by selecting "background shapefile" and a River shapefile and a Subbasin shapefile were added to a folder for illustrative use upon import into HEC-HMS. The "basin model file" tool was then executed to create the Basin file, and the Met Model file selecting the specified hyetograph meteorological method (Merwade, 2012) was used to create the meteorological file for HEC-HMS. In future routine flow simulation runs, the specified hyetograph method was changed in HEC-HMS to the SCS storm method due to the available precipitation data (inches) collected from local weather stations and thus directly inputted into HEC-HMS. The last step was to execute the "create HMS project" tool by selecting an output project location, the Basin file, the Met file, and the Gage file previously created when running the Met Model file. An HMS "run name" was created and the default start date, end date, and time interval were chosen and later changed in HEC-HMS. A log file was created showing that all files had successfully copied, and if there were any errors they were corrected and then exported again. Once completed the model was opened in HEC-HMS along with the background files for Subbasin and River (Figure 4.16), where the only input not calculated was lag time per reach (minutes). Lag time per reach was calculated in Excel using ArcMap 10.1 to extract upstream and downstream elevations per pipe and lengths as well. Slope was calculated and input into Equation 1 (hours):

$$T_{lag} = \frac{\left(L*3.28*10^{3}\right)^{0.8}\left(\frac{1000}{CN}-9\right)^{0.7}}{1900Y^{0.5}}$$

(Costache, 2014). Length (L) and Slope (Y) in percent were extracted from ArcMap 10.1 and calculated in Excel (Table 4.2). CN was assumed to be 98 for all pipes, allowing no infiltration throughout the stormwater system.

When calculating certain slopes, the elevations for both nodes of a pipe segment were the same establishing no change in elevation and consequently no slope. For these reaches, highlighted in yellow in Table 4.2, a very small slope of 0.0001 was assumed for calculation of lag time and modeling purposes. “Create compute” was chosen and “simulation run” was selected, along with the Basin model, the Meteorological model, and control specifications. The results tab created a global summary along with a hydrograph, summary table, time series table, and other various summary graphs (outflow, precipitation, cumulative precipitation, soil infiltration, excess precipitation, cumulative excess precipitation, precipitation loss, cumulative precipitation loss, direct runoff, and baseflow) per watershed. Outputs also included a hydrograph, summary table, time series table, outflow graph, and combined inflow graph per junction and reach. Toward achieving the objectives of this hydrological project, the primary model outputs of interest were volumes and peak flows generated from each subwatershed as well as those generated at the outlet of the entire watershed. Total watershed outlet hydrographs are demonstrated in Figures 4.17 to 4.19 illustrating peak flow rate versus time for a small storm of 0.06 inches and 0.14 cubic meters per second, a medium storm of 0.58 inches and 1.30 cubic meters per second, and a large storm of 2.32 inches and 7.20 cubic meters per second respectively.

Figure 4.16: HEC-HMS model after export from HEC-GeoHMS and import into HEC-HMS and background shapefile added for illustration purposes

Table 4.2: Calculated lag times per reach based on Time lag Equation 1 (Costache, 2014) with zero elevation change highlighted and 0.0001 slopes given to those selected

Reach	FromElev	ToElev	Elev Diff (ft)	Length (ft)	Length (km)	Slope	Slope (%)	CN	Lag (hr)	Lag (min)
1	-544	-525	19	696	0.21	0.03	2.73	98	0.07	4.09
2	-543	-568	25	427	0.13	0.06	5.85	98	0.03	1.89
3	-568	-544	24	442	0.13	0.05	5.43	98	0.03	2.02
4	-507	-506	1	39	0.01	0.03	2.56	98	0.01	0.42
5	-601	-568	33	662	0.20	0.05	4.98	98	0.05	2.91
6	-506	-506	0	699	0.21	0.00	0.01	98	1.13	67.84
7	-507	-507	0	204	0.06	0.00	0.01	98	0.42	25.35
8	-632	-601	31	246	0.07	0.13	12.62	98	0.01	0.83
9	-601	-565	36	718	0.22	0.05	5.02	98	0.05	3.09
10	-506	-508	2	611	0.19	0.00	0.33	98	0.18	10.64
11	-508	-509	1	236	0.07	0.00	0.42	98	0.07	4.37
12	-565	-555	10	321	0.10	0.03	3.11	98	0.03	2.06
13	-509	-509	0	39	0.01	0.00	0.01	98	0.11	6.75
14	-555	-548	7	92	0.03	0.08	7.62	98	0.01	0.48
15	-508	-507	1	451	0.14	0.00	0.22	98	0.17	10.15
16	-508	-508	0	16	0.00	0.00	0.01	98	0.05	3.27
17	-548	-506	42	1166	0.36	0.04	3.60	98	0.09	5.38
18	-509	-502	7	571	0.17	0.01	1.23	98	0.09	5.22
19	-506	-511	5	541	0.17	0.01	0.92	98	0.10	5.75
20	-511	-512	1	103	0.03	0.01	0.97	98	0.02	1.49
21	-512	-512	0	63	0.02	0.00	0.01	98	0.17	9.92
22	-512	-513	1	562	0.17	0.00	0.18	98	0.22	13.50
23	-513	-513	0	114	0.03	0.00	0.01	98	0.27	15.92
24	-514	-508	6	1035	0.32	0.01	0.58	98	0.20	12.19
25	-513	-513	0	416	0.13	0.00	0.01	98	0.75	44.78
26	-513	-513	0	114	0.03	0.00	0.01	98	0.27	15.92
27	-514	-514	0	62	0.02	0.00	0.01	98	0.16	9.75
28	-513	-513	0	218	0.07	0.00	0.01	98	0.45	26.73
29	-513	-512	1	937	0.29	0.00	0.11	98	0.44	26.24
30	-512	-514	2	433	0.13	0.00	0.46	98	0.11	6.81

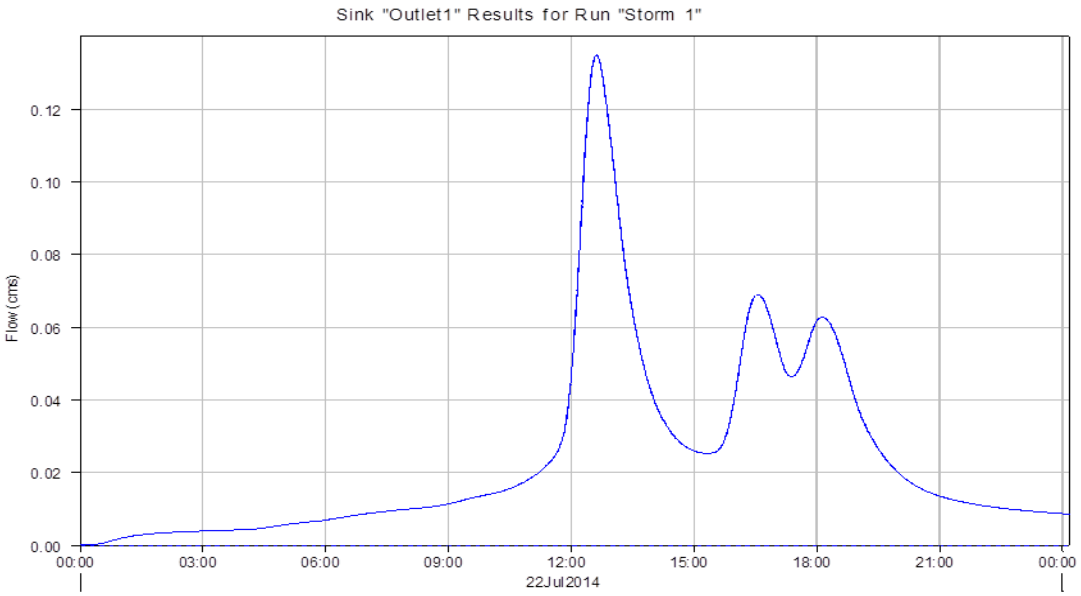

Figure 4.17: HEC-HMS flow rate hydrograph for a storm event on July 22-23rd, 2014 of 0.06 inches demonstrating a small storm event

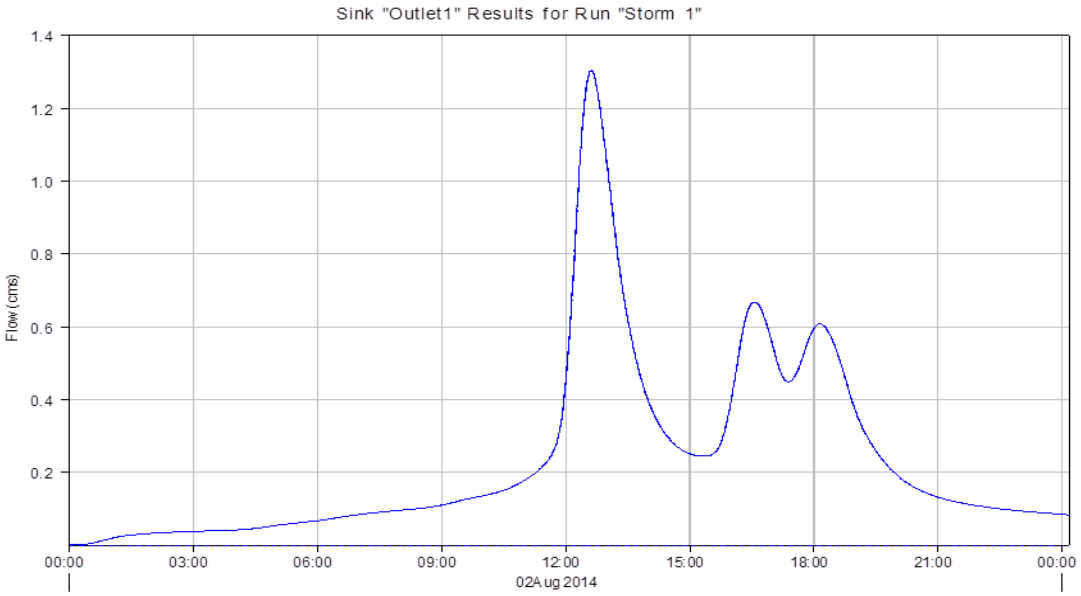

Figure 4.18: HEC-HMS flow rate hydrograph for a storm event on August 8, 2014 of 0.58 inches demonstrating a medium storm event

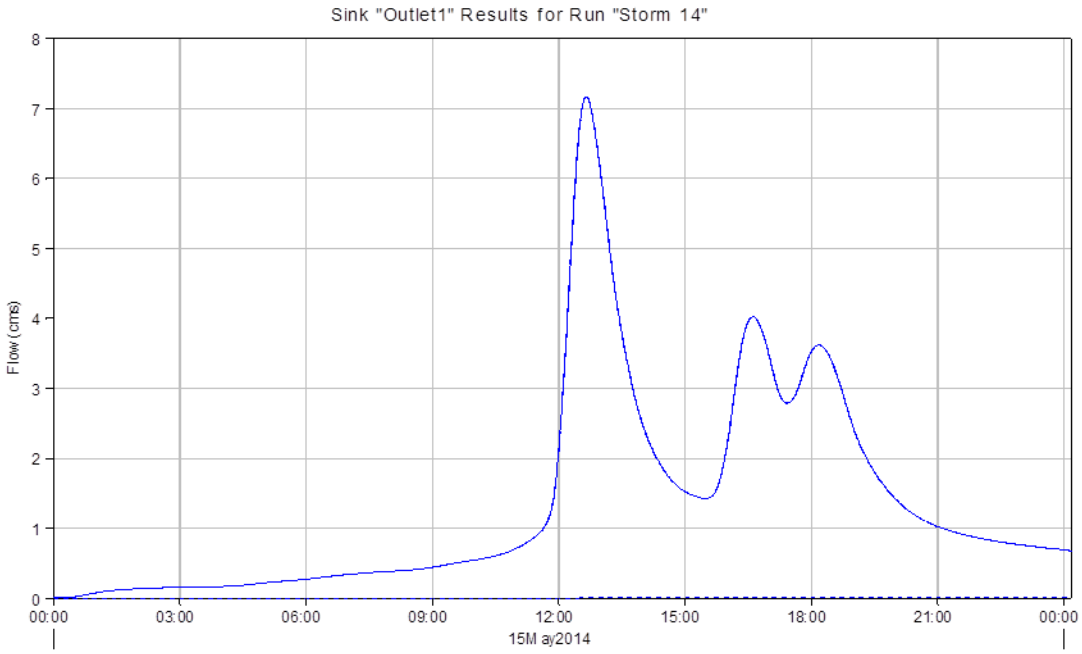

Figure 4.19: HEC-HMS flow rate hydrograph for a storm event on May 15-16th, 2014 of 2.32 inches demonstrating a large storm event

4.3.4 STORMWATER PIPE MONITORING AND FLOW CALCULATIONS

For model calibration and validation, acoustic Doppler profiling sensors capable of measuring stage and velocity were deployed in stormwater pipes throughout the Sand River Headwaters watershed, and specifically throughout the urban Aiken watershed. Monitoring locations were based on historical stormwater pipe infrastructure and expected routing (City of Aiken Public Works) and assumed corrections and routing based on field investigations. SonTek™-IQ Pipe® sensors (Figure 4.20) were typically mounted on scissor rings adjusted to the diameter of each stormwater pipe during installation (Figure 4.21). The SonTek™-IQ Pipe® sensor is

a multi-beam acoustic flow meter with five 3.0 MHz transducers measuring water level, flow, velocity, and temperature, along with calculating flow rates and total volume flow internally based on the channel shape and instrument location set by the user (Xylem Inc., 2012). The scissor ring mount allowed the sensor to be paced at the bottom center of the pipe, unless evidence of sediment was present and thus the sensor was installed at a known offset from the pipe center. Sensors were installed 10 feet downstream of flow entrance to ensure placement in critical flow not turbulent. All monitoring sensor locations, diameters, sampling times, slopes, materials, and Manning's n (Chow, 1959) are summarized in Table 4.3. Stage data were used to calculate velocity, flow rate, and volume based on the following calculations (r=radius [m], d=stage depth [m], D=diameter [m], S=slope, n=Manning's n (Chow, 1959)):

(1) Calculation(C): $2arctan\sqrt{r^2 - \frac{(r-d)^2}{r-d}}$

(2) Theta (θ): If d<r →C, If d>r →C+2Π

(3) Area(A): $\frac{D^2}{8}(1 - \frac{\sin(\theta)}{\theta})$

(4) Calculated Radius (R) [m]: $\frac{D^2}{4}(1 - \frac{\sin(\theta)}{\theta})$

(5) Calculated Velocity (v) [mps]: $\frac{1}{n} * R^{\frac{2}{3}} * S^{.5}$

(6) Calculated Flow (F) [cms]: V*A

(7) Calculated Volume (V) [m^3]: F*300seconds

(600 seconds for sensors 3 & 5 operating at 10 minute intervals)

(8) Volume If Statement: If A=0→0, If not→V

(9) Flow If Statement: If A=0→0, If not→F

HEC-HMS and sensor volumes were then compared with ArcMap volumes and demonstrated in Figures 4.26 to 4.28 for a small storm event of 0.06 inches, a medium storm event of 0.58 inches, and a large storm event of 2.32 inches. Once the flow rate for both the HEC-HMS model and the monitoring location data is calculated, the Nash-Sutcliffe efficiency was calculated to measure the goodness of fit of the HEC-HMS hydrologic model (McCuen et al., 2006). The relative root mean squared error (RRMSE) as a measure of model fit for both prediction models of volume was also calculated (Gepsoft Ltd, 2014).

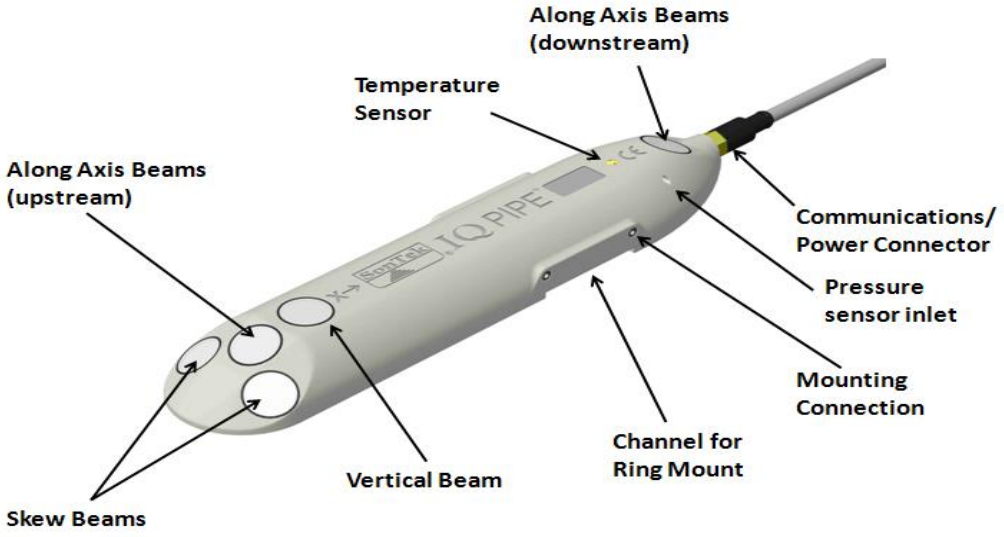

Figure 4.20: SonTek™ IQ-Pipe® attributes (Xylem Inc., 2012)

Figure 4.21: SonTek™ Ring mount installed in a pipe with the SonTek™ IQ-Pipe® system (Xylem Inc., 2012)

Table 4.3: Monitoring sensor locations and detailed information specific to each monitoring location for runoff volume and flow rate calculations

Sensor	Location	Sample Time (mins)	Diameter (ft)	Slope	Manning's n	Material
1	Laurens at RR	5	3.00	0.178	0.022	80% CMP w/ 20% concrete
2	Newberry at RR	5	3.00	0.017	0.022	80% CMP w/ 20% concrete
3	S Boundary at Laurens	10	3.00	0.026	0.015	RCP
4	Williamsburg at Richland	5	3.00	0.005	0.015	RCP
5	S Boundary at Horry	10	4.25	0.002	0.015	RCP
6	10 foot pipe	5	10.00	0.073	0.024	CMP
7	Woods between RR & S Boundary	5	7.00	0.069	0.024	95% CMP w/ 5% concrete
8	Behind #10 Downing	5	3.00	0.071	0.024	CMP
9	Williamsburg at Richland	5	3.50	0.006	0.024	CMP
11	Coker Springs at Newberry	5	4.00	0.007	0.015	RCP
New 3	South Boundary Extension	10	4.00	0.037	0.015	RCP

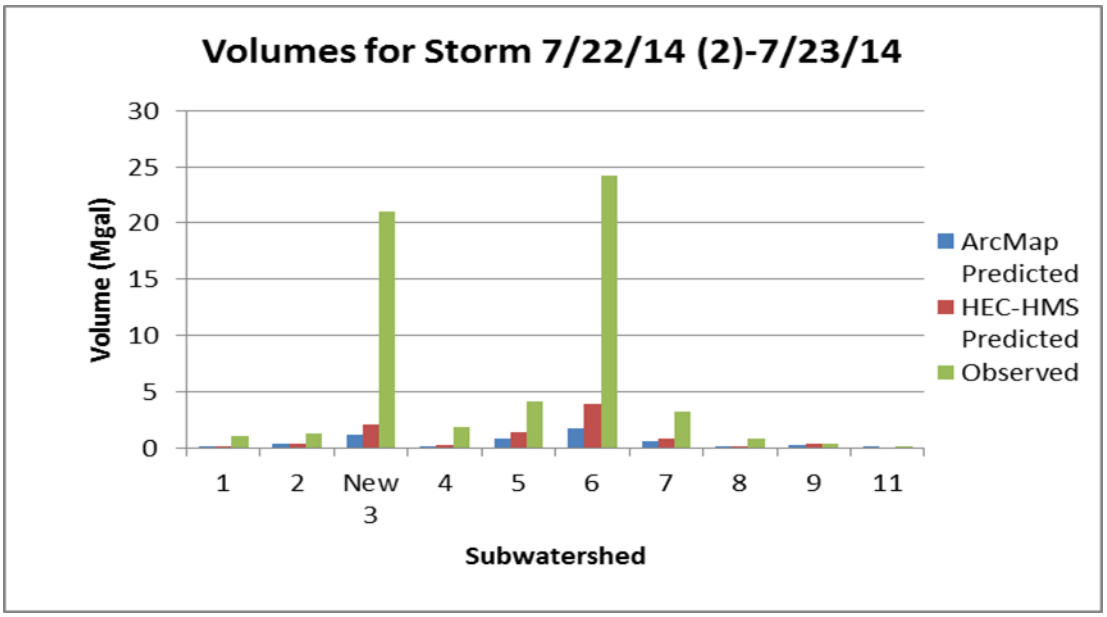

Figure 4.26: Volume comparison graph for a storm event on July 22-23rd, 2014 of 0.06 inches demonstrating a small storm event

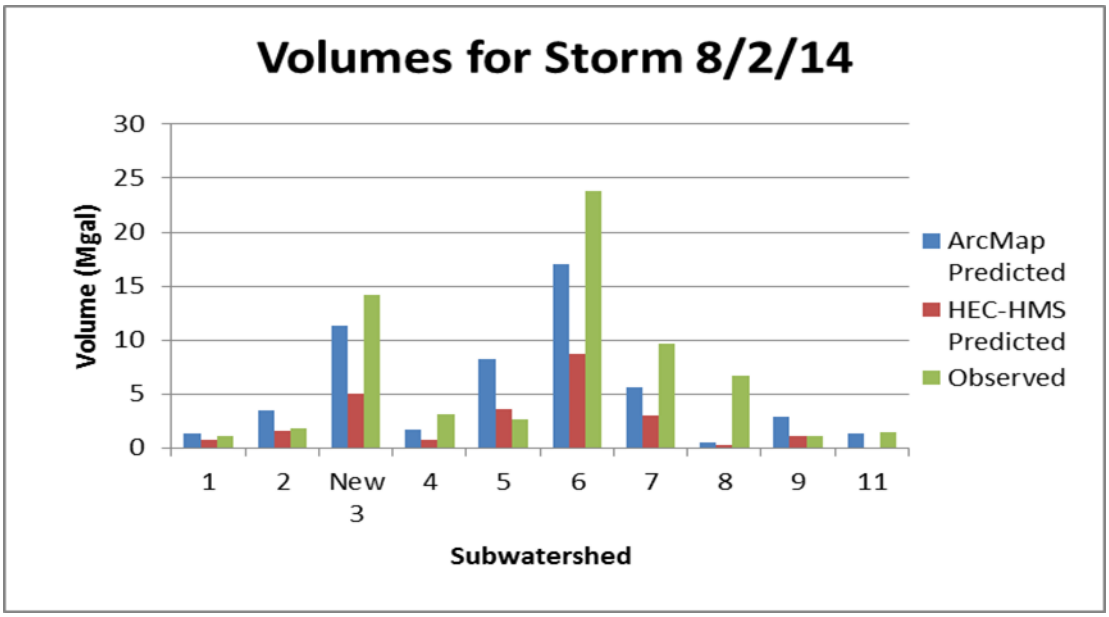

Figure 4.27: Volume comparison graph for a storm event on August 2, 2014 of 0.58 inches demonstrating a medium storm event

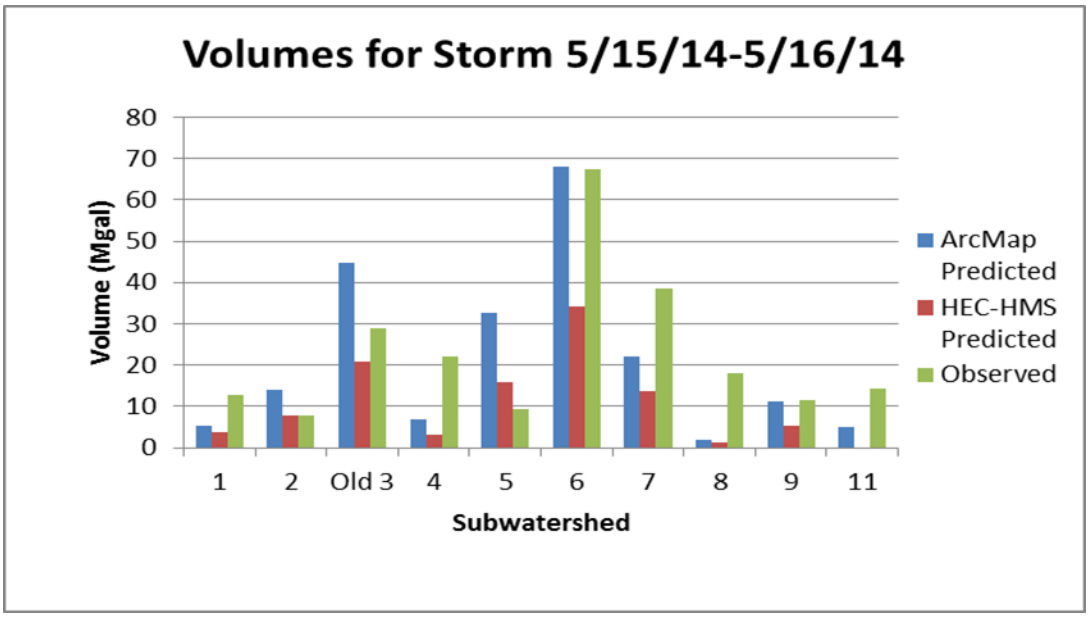

Figure 4.28: Volume comparison graph for a storm event on May 15-16th, 2014 of 2.32 inches demonstrating a large storm event

4.4 RESULTS

Due to river connectivity issues with HEC-HMS, the finalized stormline (Figure 4.1) was altered to include only segments that were directly connected to the main branch of the stormline (Figure 4.3). A slope grid was also necessary to develop the CN lag times per subbasin (Figure 4.4) developing slopes ranging from 86.9ft/ft to 0ft/ft. The Subbasin and River layers (Figure 4.6) were created from the Drainage layer (Figure 4.2) and the Catchment layer. The subbasins were then merged to match the areas of the subwatersheds as closely as possible, with the most noticeable differences in Subbasins 2 and 3. The smallest was Subbasin 6 with an area of 2 acres and the largest was Subbasin 5 with 230 acres (Table 4.1).

The most applicable results from HEC-GeoHMS were percent impervious surface per subbasin (Figure 4.13), average CN per subbasin (Figure 4.14), and lag time per subbasin. As demonstrated in Table 4.1, the percent impervious surface ranged from 0 in Subbasin 6 to 51.9 in Subbasin 1. Subbasins 8 and 1 had the highest average CN at 81 and Subbasin 6 had the lowest at 54. Lag time, in hours, ranged from 0.16 hours at Subbasin 6 to 1.17 hours at Subbasin 3. The final HEC-HMS model imported into the program is demonstrated in Figure 4.17.

Once imported, the only factor not automatically calculated was lag time per reach or river segment. All slopes and reach lengths were derived in ArcMap 10.1 using the "measure" and "information" tools on the Burned DEM (Table 4.2). The longest lag time was derived to be 1.13 hours or 67.8 minutes and the shortest lag time derived was 0.007 hours or 0.43 minutes using Equation 1. Once these lag times were added to HEC-HMS, individual storms were entered (in inches) and output volumes and flow rates were generated. All storm events were graphed versus the outlet, or total watershed, HEC-HMS volumes in Figure 4.23 demonstrating a non-linear relationship with a trend line equation of $y = 2.60x^2 + 7.04x + 0.27$ and an R^2=0.9995. HEC-HMS hydrographs produced at the total watershed outlet are demonstrated in Figures 4.17 to 4.19 indicating a small storm event of 0.06 inches and a peak flow rate of 0.14 cubic meters per second, a medium storm event of 0.58 inches and a peak flow rate of 1.30 cubic meters per second, and a large storm event of 2.32 inches and a peak flow rate of 7.20 cubic meters per second.

Stage data were downloaded remotely (Figure 4.22) and used to calculate peak flow rate and total volume data per monitoring location for validation and calibration of the ArcMap 10.1 and HEC-HMS prediction models. Table 4.3 summarizes all locations, diameters, Manning's n, slopes, and materials for each stormwater pipe with a monitoring sensor installed. All storm events, sensor peak flow rates, and HEC-HMS peak flow rates (cms) are summarized in Table 4.4. Table 4.5 summarizes all storm events, their rainfall depth in inches, and the sensor volumes, ArcMap 10.1 output volumes, and the HEC-HMS output volumes and peak flow rates. Detailed individual storm data can be found in Appendix A for all sensor data, ArcMap 10.1 output volumes, and HEC-HMS output volume and peak flow rates per subbasin and for the total watershed. Examples of volume comparison graphs for a small storm event, a medium storm event, and a large storm event are demonstrated in Figures 4.26 to 4.28 respectively. Figure 4.23 illustrates the HEC-HMS outlet volume graphed against rainfall data, while Figure 4.24 demonstrates sensor outlet volume graphed against rainfall data. Figure 4.25 also demonstrates HEC-HMS and sensor peak flow rates graphed against rainfall data to show their correlation. The Nash Sutcliffe efficiency derived for the HEC-HMS prediction model and the monitoring location flow rate calculations was -12.74. Relative root mean squared error (RRMSE) was also calculated for ArcMap and HEC-HMS volumes versus stage data calculated volumes at the total watershed outlet over all storm events and determined to be 3.25 and 3.49 respectively.

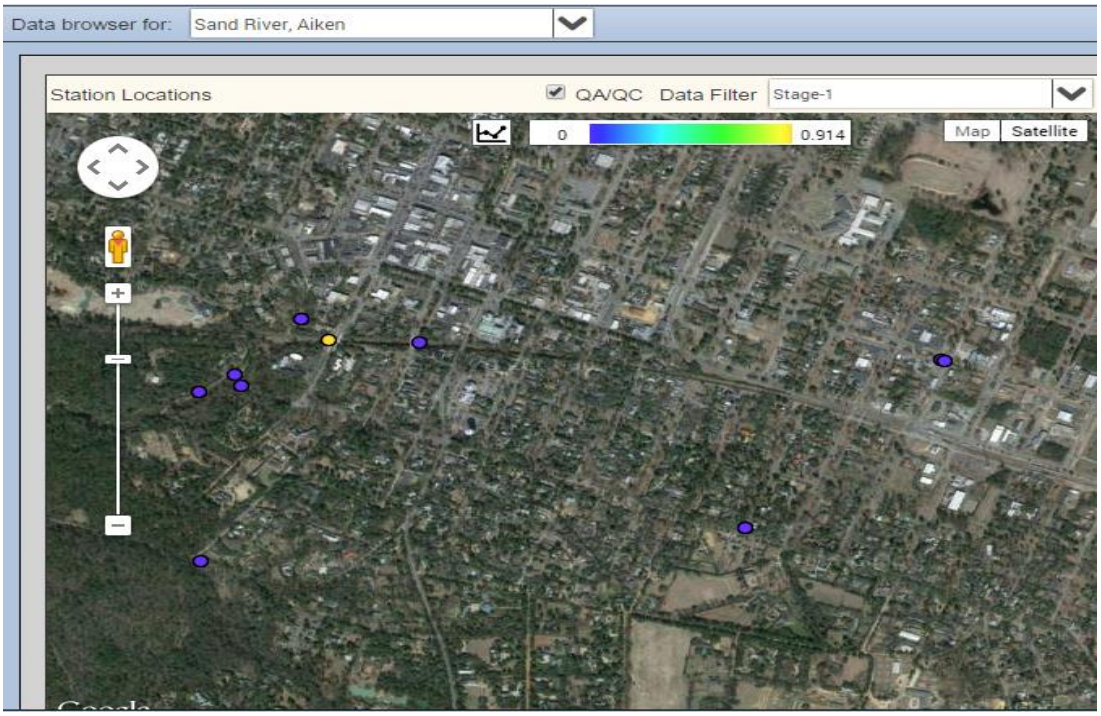

Figure 4.22: Clemson University's Intelligent River Web Portal used for remote downloading access of stage data per monitoring location for volume and flow rate calculations used for model validation and calibration (Clemson University, 2013-2014)

Table 4.4: Sensor peak flow rates and HEC-HMS peak flow rates along with rainfall in inches

Date & # of Storm	Rainfall (in)	HEC-HMS Peak Flow Rate (cms)	Sensor Peak Flow Rate (cms)
12/22/13	0.77	1.9	4.7
12/23/13	0.82	2.0	5.0
2/21/14	0.34	0.9	13.5
2/26/14	1.28	3.3	13.8
3/6/14-3/7/14	0.77	1.9	14.2
3/16/14-3/17/14 (1)	1.27	3.2	13.8
3/17/14 (2)-3/18/14	0.20	0.6	14.1
3/28/14-3/29/14	0.50	1.3	14.0
4/7/14-4/8/14	1.31	3.4	14.3
4/14/14-4/15/14 (1)	1.36	3.5	13.9
4/15/14 (2)	0.26	0.7	14.0
4/18/14-4/19/14	1.54	4.1	14.0
4/22/14-4/23/14	0.16	0.5	13.4
5/15/14-5/16/14	2.32	7.3	13.8
5/25/14	0.15	0.5	12.6
5/27/14-5/28/14	0.54	1.4	11.8
5/29/14-5/30/14	1.59	4.3	14.1
6/7/14-6/8/14	0.31	0.8	14.3
6/11/14 (1)	0.70	1.7	13.7
6/11/14 (2)-6/12/14	0.10	0.4	15.6
6/13/14-6/14/14	0.13	0.4	13.4
6/24/14-6/25/14	0.71	1.7	12.7
7/15/14	0.38	1.0	13.4
7/19/14	0.51	1.3	10.5
7/20/14	0.15	0.5	11.0
7/21/14 (1)	0.63	1.6	9.9
7/21/14 (2)-7/22/14 (1)	0.49	1.2	12.5
7/22/14 (2)	0.01	0.2	12.4
7/22/14 (3)-7/23/14	0.06	0.3	12.6
8/2/14	0.58	1.5	8.6
8/8/14-8/9/14 (1)	0.60	1.5	7.9
8/9/14 (2)	0.05	0.3	9.5
8/10/14-8/11/14	0.97	2.4	10.0
8/12/14	0.09	0.3	8.6
8/18/14-8/19/14	0.06	0.3	8.9
8/31/14	0.24	0.7	9.5
9/2/14-9/3/14	0.06	0.3	13.8
9/4/14	1.61	4.4	8.7
9/5/14	0.05	0.3	0.0
9/13/14 (1)	0.06	0.3	9.9
9/13/14 (2)	0.08	0.3	10.8
9/14/14 (1)	0.36	1.0	11.1
9/14/14 (2)-9/15/14 (1)	0.22	0.6	11.3
9/15/14 (2)	0.12	0.4	11.1
9/15/14 (3)-9/16/14 (1)	0.01	0.2	10.3
9/16/14 (2)	0.11	0.4	11.6
9/16/14 (3)-9/17/14 (1)	0.19	0.6	11.4
9/17/14 (2)-9/18/14 (1)	1.05	2.6	12.9
9/18/14 (2)-9/19/14 (1)	0.41	1.1	13.8
9/19/14 (2)-9/20/14	0.02	0.2	13.6
9/24/14	0.15	0.5	12.9

Table 4.5: Summary of all storm events, their rainfall in inches, and sensor volumes, ArcMap 10.1 output volumes, and HEC-HMS output volumes

Run/Storm	Date & # of Storm	Rainfall (in)	ArcMap Outlet Volume (Mgal)	HEC-HMS Outlet Volume (Mgal)	Sensor Outlet Volume (Mgal)
1	12/22/13	0.77	22.6	10.57	16.26
2	12/23/13	0.82	24.0	11.07	50.00
3	2/21/14	0.34	10.0	6.50	22.76
4	2/26/14	1.28	37.5	16.75	16.43
5	3/6/14-3/7/14	0.77	22.6	10.57	69.35
6	3/16/14-3/17/14 (1)	1.27	37.2	16.62	41.41
7	3/17/14 (2)-3/18/14	0.20	5.9	5.20	33.47
8	3/28/14-3/29/14	0.50	14.7	7.98	17.31
9	4/7/14-4/8/14	1.31	38.4	17.17	14.64
10	4/14/14-4/15/14 (1)	1.36	39.9	17.88	16.39
11	4/15/14 (2)	0.26	7.6	5.76	27.83
12	4/18/14-4/19/14	1.54	45.1	20.61	64.35
13	4/22/14-4/23/14	0.16	4.7	4.83	11.11
14	5/15/14-5/16/14	2.32	68.0	34.26	67.42
15	5/25/14	0.15	4.4	4.76	12.33
16	5/27/14-5/28/14	0.54	15.8	8.35	6.77
17	5/29/14-5/30/14	1.59	46.6	21.40	37.09
18	6/7/14-6/8/14	0.31	9.1	6.23	19.23
19	6/11/14 (1)	0.70	20.5	9.88	18.70
20	6/11/14 (2)-6/12/14	0.10	2.9	4.28	30.27
21	6/13/14-6/14/14	0.13	3.8	4.57	14.63
22	6/24/14-6/25/14	0.71	20.8	9.96	8.18
23	7/15/14	0.38	11.1	6.87	17.82
24	7/19/14	0.51	15.0	8.08	21.87
25	7/20/14	0.15	4.4	4.76	10.37
26	7/21/14 (1)	0.63	18.5	9.19	24.16
27	7/21/14 (2)-7/22/14 (1)	0.49	14.3	7.90	30.39
28	7/22/14 (2)	0.01	0.3	3.46	27.97
29	7/22/14 (3)-7/23/14	0.06	1.8	3.91	24.17
30	8/2/14	0.58	17.0	8.72	23.86
31	8/8/14-8/9/14 (1)	0.60	17.6	8.90	29.63
32	8/9/14 (2)	0.05	1.5	3.83	19.83
33	8/10/14-8/11/14	0.97	28.4	12.73	1.29
34	8/12/14	0.09	2.6	4.20	20.74
35	8/18/14-8/19/14	0.06	1.8	3.91	1.35
36	8/31/14	0.24	7.0	5.57	18.53
37	9/2/14-9/3/14	0.06	1.8	3.91	7.84
38	9/4/14	1.61	47.2	21.71	32.02
39	9/5/14	0.05	1.5	3.83	0.16
40	9/13/14 (1)	0.06	1.8	3.91	19.35
41	9/13/14 (2)	0.08	2.4	4.09	12.77
42	9/14/14 (1)	0.36	10.6	6.68	28.91
43	9/14/14 (2)-9/15/14 (1)	0.22	6.5	5.39	25.93
44	9/15/14 (2)	0.12	3.5	4.46	13.28
45	9/15/14 (3)-9/16/14 (1)	0.01	0.3	3.46	34.49
46	9/16/14 (2)	0.11	3.2	4.39	20.05
47	9/16/14 (3)-9/17/14 (1)	0.19	5.6	5.12	32.55
48	9/17/14 (2)-9/18/14 (1)	1.05	30.8	13.68	20.96
49	9/18/14 (2)-9/19/14 (1)	0.41	12.0	7.16	31.42
50	9/19/14 (2)-9/20/14	0.02	0.6	3.54	23.94
51	9/24/14	0.15	4.4	4.76	16.28

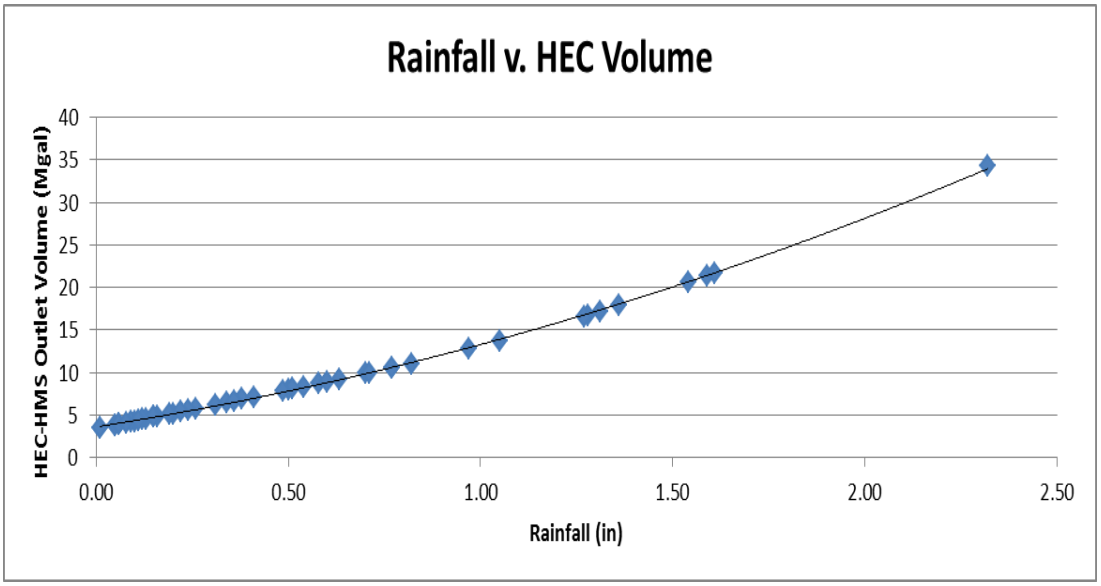

Figure 4.23: Rainfall versus total volume from HEC-HMS at the outlet for all storm events

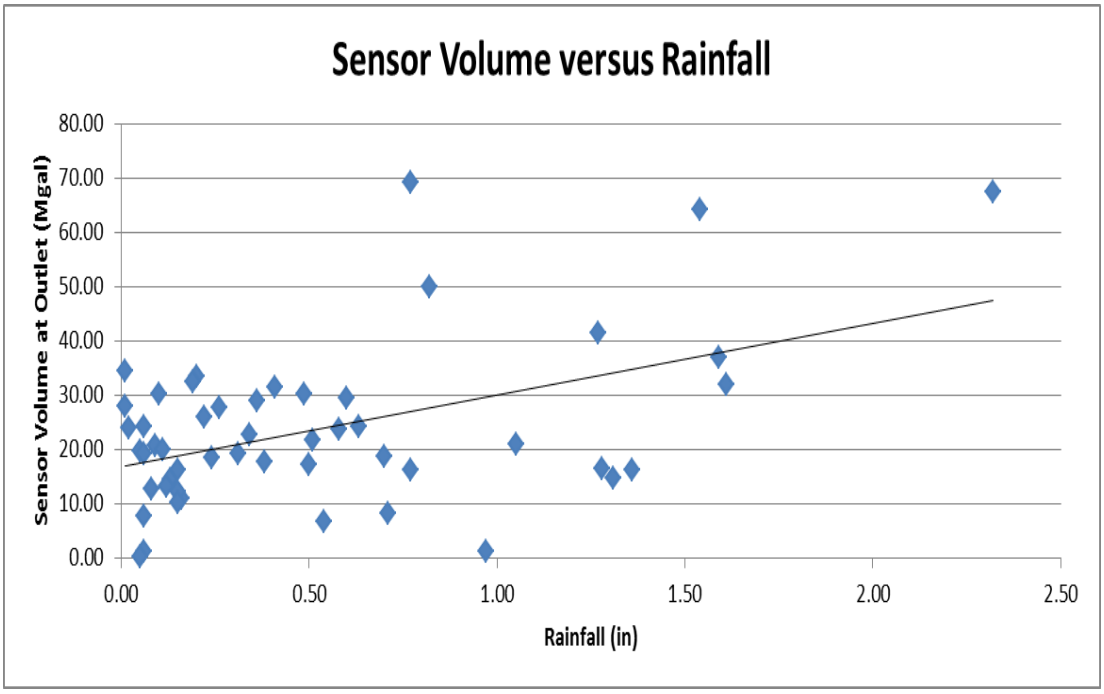

Figure 4.24: Sensor outlet volume versus rainfall (inches)

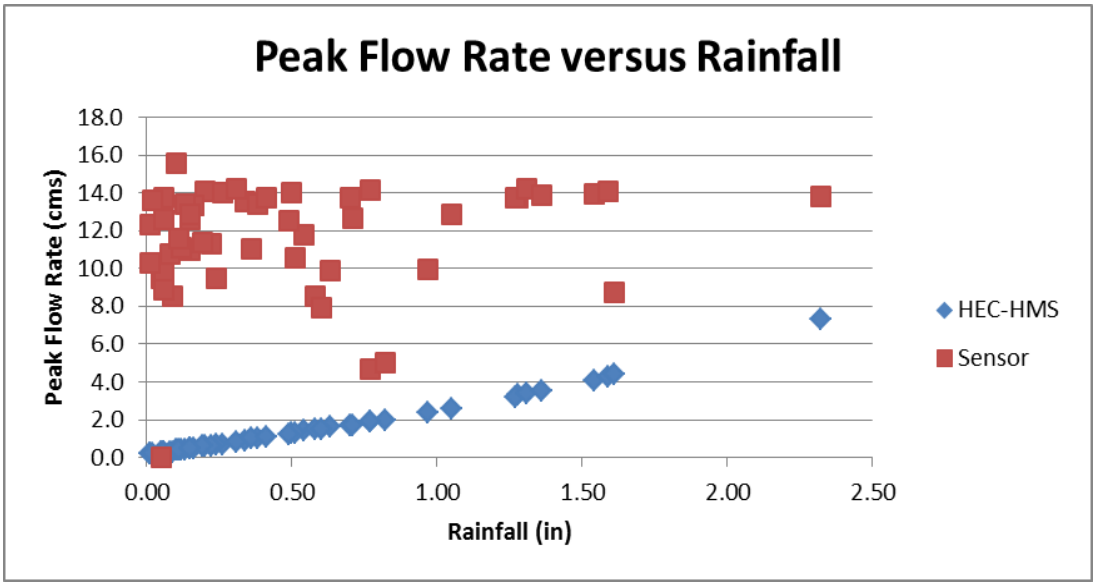

Figure 4.25: HEC-HMS (blue) and sensor (red) peak flow rates versus rainfall (inches)

Some modifications in monitoring protocol were made during the course of the study. Monitoring location 3 was relocated on July 10, 2014, to capture a larger drainage area and improve discharge measurements, resulting in the need to modify pipe diameters and materials in the calculations Also during the project, it was discovered that Sensors 6 and 7 were not reporting accurately; new SonTek™ documentation released during the study specified that the IQ-pipe® was not accurate for pipe diameters>72 in. Therefore, sums of calculated flows from Sensors 1, 2, and 8 were used for the flow volume at Sensor 7, while sums of calculated flows from Sensors 1, 2, 8, and 3 were used for the flow volume at Sensor 6 (outlet of the entire watershed) as confirmed through ArcMap 10.1 watershed delineation analysis. Overflow from larger pipes flowing into smaller pipes and backing up stormwater

accumulation required adjustment and occurred in sensor monitoring location 3. Overflow was accounted for by summing the volumes in location 3 after location 6 had stopped reporting during a storm and adding them to the total volume of location 6. The largest storm occurred on May 15 and 16, 2014 with a rainfall of 2.32 inches and a sensor volume of 67.4 Mgal, an ArcMap 10.1 total volume of 68 Mgal, and a HEC-HMS outlet volume of 34.26 Mgal. The smallest storm occurred on July 22, 2014 with a rainfall of 0.01 inches and a sensor volume of 28.0 Mgal, an ArcMap 10.1 volume of 0.3 Mgal, and a HEC-HMS outlet volume of 3.46 Mgal. The highest peak flow rate for the total watershed outlet over all storm events was derived from the HEC-HMS prediction model as 7.3 cubic meters per second on the May 15-16th storm event and 15.6 cubic meters per second from sensor data on the June 11-12th storm event. The lowest peak flow rate for the total watershed outlet over all storm events was derived from the HEC-HMS prediction model as 0.2 cubic meters per second on several storm events and 0.0 cubic meters per second from sensor data on the September 5th storm event. Table 4.5 summarizes the rainfall for each storm, total volumes from the sensor calculations, the ArcMap 10.1 outlet volume summed for the 10 foot pipe, and the total outlet volumes from HEC-HMS per storm.

4.5 DISCUSSION

Subbasin and subwatershed layers varied slightly in area due to the edited stormline layer for river connectivity purposes in HEC-HMS and upon completion of

the Subbasin layer, subwatersheds were then referred to as subbasins. In large combined-and storm-sewer systems it is impractical to account for every pipe, manhole, and component of the system for flow simulations (Cantone and Schmidt, 2009). The most noticeable differences were in Subbasins 2 and 3 with area differences of 17 acres and 8 acres respectively. The subbasins were merged based on the catchment layer, which was slightly different for the original finalized stormline and the altered stormline for HEC-HMS. With different areas, the derived volumes were slightly different, but with the highest percent difference at only 8 percent, the difference in the total watershed(s) areas was not significant.

Another issue with the HEC-HMS model occurred when merging the subbasins to match the areas of the subwatersheds or subcatchment aggregation. When applying this method one must also consider with parameterization, which involves the determination of input parameters (e.g. subcatchment slope, % impervious, flow length, etc.) for the larger subcatchments that represent the physical processes of the combined smaller subcatchments (Cantone and Schmidt, 2009). Subcatchment aggregation can result in underestimation of the peak flow for all degrees of simplification (Cantone and Schmidt, 2009); however, for this project, in order to achieve the volumes per subwatershed accumulation, needed for the calibration using the sensor locations and subwatershed accumulation the merging of the subbasins was necessary for model validation.

The average CN, percent impervious, and lag time were calculated within HEC-GeoHMS per subbasin using the CN grid from land use (Jin et al., 2011) and SSURGO soil data (Soil Survey Staff, 2014), basin slope, and percent impervious grid (Xian et al., 2011). These factors are critical to determining the most effective place to install structural stormwater control measures on the land surface or hardscape surfaces (i.e. roofs, parking lots, etc.). Due to 32 percent of the total watershed area established from Subbasins 1, 2, 7, and 8 with all subbasins flowing into Subbasin 7 before exiting at the entire watershed outlet, and 68 percent of the total watershed area established from Subbasins 3, 4, 5, and 9 with all subbasins flowing into Subbasin 9 before the outlet, the most effective placement for additional green infrastructure would be in Subbasins 3, 4, 5, or 9. The largest areas occurred in Subbasins 2, 3, and 5 making these three subbasins the most effective placement for runoff catchment and treatment. The lowest percent impervious surface areas were Subbasins 3, 6, and 7 allowing for larger total areas of green infrastructure installation upon the landscape. The highest percent impervious surface areas were Subbasins 1, 2, and 8 allowing for larger total areas of green infrastructure installation upon hardscapes. The curve numbers ranged from 54 to 81 with the lowest being Subbasin 6 and the highest being Subbasins 1 and 8. From these outputs, the most effective placement for additional green infrastructure was within Subbasins 3 and 9 with the largest amount of runoff flow and least amount of percent impervious surface out of the four subbasins contributing to the 68 percent area of the total watershed. With Subwatershed 2 also having one of the largest individual contributing areas and a

high amount of impervious surface, it is an effective subwatershed to install green infrastructure on the subwatershed's hardscapes. An additional space for green infrastructure installations may also exist within Subbasins 6 and 7 closer to the natural areas near the watershed outlet with very low percent impervious surface, but significantly smaller area for placement.

Green infrastructure can be installed on various surfaces as needed including landscapes (i.e. grass, soil, land surface) or hardscapes (i.e. roofing, pavement, etc.). Structural green infrastructure such as green roofing is effective for hard scape installation or areas with impervious surface, and bioretention cells are effective for landscape installation or areas with pervious surface. A small green roof (200 feet squared) can retain a volume of 374 gallons utilizing the equation $V = 0.33 * A_s * D_m$ where A_s is the surface area and D_m is the media depth (MPCA, 2014). A small bioretention cell (200 feet squared) can store a volume of 1,496 gallons above ground utilizing the simplified equation $V = A_s * D_s$ where A_s is the device area and D_s is the soil depth (LIDC, 2007). Green roofing would be an effective installation within Subwatershed 2, because it has one of the largest individual contributing areas and has a high percent impervious surface, or higher areas of hardscapes. With an area of 9,677,100 feet squared and 39.5 percent impervious surface and assuming 50 percent of that impervious surface is roofing, Subwatershed 2 has area for 9,556 (200 feet squared) greenroof installations capturing 3,573,944 gallons. Even in a Subwatershed with low percent impervious surface such as Subwatershed 3 with an area of 8,621,875 feet squared and a percent impervious surface of 22, an area is available for

4,742 green roofs capturing an area of 1,773,508 gallons. Bioretention cells would be an effective insallation within Subwatershed 3, because it has one of the largest individual contributing areas as well and a low percent impervious surface, or higher areas of landscapes. Subwatershed 3 has area for 33,625 (200 feet squared) bioretention cells capturing a volume of 50,303,000 gallons. Even in a subwatershed with high amounts of impervious surface such as Subwatershed 2, there is area for 29,273 bioretention cells capturing a volume of 43,792,408 gallons. With the largest volume at the total watershed outlet over all storm events being 68 million gallons, the green roofing and bioretention cell installs would have a major impact on the discharge volume of any storm event at the total watershed outlet improving erosion impacts and water quality downstream.

There were no errors with river connectivity or model parameters when the model check was executed within HEC-GeoHMS. River and Subbasin layers were exported out of HEC-GeoHMS and imported into HEC-HMS with lag reach parameters remaining to be calculated. HEC-HMS model analysis was performed by calculating the rainfall runoff ratio with current percent impervious surface and average CN versus maximized percent impervious surface at 100 and average CN per subbasin at 98. The rainfall runoff ratio did not have a significant change in number, indicating that the model effectively captured all rainfall and modeled the runoff correctly. When reach elevations and lengths were determined from ArcMap 10.1, several reaches (highlighted in yellow in Table 4.2) had an elevation change of 0 feet, and required slope assumptions for calculation purposes within HEC-HMS. These reaches

were given a very low slope percent to account for calculation completion, but as to not disrupt the final outlet volumes and flow rates. The final outlet volumes and peak flow rates are summarized in Table 4.4 and Table 4.5 and demonstrated smaller values than predicted. HEC-HMS outlet volumes were always less than those of ArcMap 10.1, because ArcMap directly correlated all rainfall to runoff with a linear relationship and HEC-HMS took into account other factors such as basin lag time, infiltration, CN, and percent impervious surface.

Underestimation of predicted flows could be accounted for by subcatchment aggregation or conduit skeletonization, which is the omission of conduits in a combined sewer system to reduce model complexity (Cantone and Schmidt, 2009). It is possible to simulate storm event-based flows with impervious and pervious surfaces on separate planes using a two-plane kinematic wave approach according to Cantone and Schmidt (2009), and this approach could be used to further model accuracy and increase output flows. Another improvement-with the addition of available pipe data for every conduit within the stormwater system- would be to use the Green-Ampt method for infiltration. The CN method consistently resulted in under-prediction of runoff discharge peaks as compared to the Green-Ampt method (Eli and Lamont, 2010). However, for ease of use and lack of conduit data, the CN method was used for the infiltration method. Also, the greatest difference in infiltration loss rates occur at low CN values, with less difference at high CN values (Brevnova, 2001). As all average CN per subbasin, except for Subbasin 6, are over 72, the CN method was used as an acceptable infiltration method for HEC-HMS.

One limitation, however, was the lack of spatially representative rainfall data within each subbasin to more accurately simulate flow generation with higher spatial resolution and to reduce spatial and temporal variability over the larger watershed. All rainfall data were collected at one location, five miles away, and then used as inputs for all subbasin flow simulations. Highly isolated storm events are typical phenomenon in the urban Aiken watershed, with the potential for heavy rain events in one part of the watershed and no rainfall in another. This high spatial variability leads to potential over-prediction and under-prediction of runoff volumes over the different subbasins in some cases. To account for rainfall variability, additional monitoring stations should be deployed and distributed throughout the larger watershed for more spatially representative input data for simulated flow predictions. Another factor contributing to runoff volumes in HEC-HMS is the base flow contribution, of which there was no current available data and an average from previous total watershed outlet data was used as a constant monthly average. This average at the total watershed outlet was then scaled to the other subwatersheds based on their contributing areas in relation to the total contributing areas. Assuming baseflow within simulations could allow for over prediction or under prediction of runoff volumes produced from HEC-HMS subbasin, and any available base flow data -if available- could be subtracted from observed flow and volume calculations to demonstrate a more accurate comparison between observed and predicted flow.

The output volumes and flow rates, summarized in Table 4.4 and Table 4.5, predicted the highest runoff generation over all storm events at the HEC_HMS outlet

on May 15 and 16, 2014 to be 30,881,707 gallons after 2.32 inches of rainfall and the lowest runoff generation over all storm events at the HEC-HMS outlet on July 22, 2014 to be 79,252 gallons from 0.01 inches of rainfall. The peak flow rates at the watershed outlet, respectively, were 7.3 cubic meters per second and 0.0 cubic meters per second with a Nash Sutcliffe efficiency over all storm events of -12.74 when compared with stage data calculated flow rates at the total watershed outlet. Runoff coefficients were also calculated per subbasin and demonstrated in Appendix A per storm event. Although many runoff coefficients were greater than 1, discharge equivalent depth can never be greater than rainfall depth. This could be due to the lack of spatially representative rainfall data at each subbasin location or to the sensor malfunction within the larger pipes or malfunction in general due to debris interruption or sensor misfiring. As demonstrated in Figures 4.26 to 4.28, ArcMap 10.1 volumes were generally less than observed at the outlet for small and medium storms while HEC-HMS underestimated outlet volume, and as events increased in intensity ArcMap 10.1 tended to overestimate total watershed outlet volume for the larger storms and HEC-HMS tended to continue to underestimate for all storm events. Although ArcMap should always over predict runoff volumes, the lack of spatially representative rainfall data impacted the output due to the direct multiplication of subwatershed area and rainfall depth. Relative root mean squared error (RRMSE) was also calculated for ArcMap and HEC-HMS volumes versus stage data calculated volumes at the total watershed oulet over all storm events and determined to be 3.25 and 3.49 respectively. If the model fits the observed data perfectly the RRMSE is 0

ranging from 0 to infinity following model deviation from the observed (Gepsoft Ltd., 2014). Detailed individual storm data is available in Appendix A with volume and flow rates per subbasin and hydrographs per storm event for the outlet.

4.6 CONCLUSION

Overall, both prediction models, ArcMap 10.1 and HEC-HMS underestimated volume and peak flow rates for smaller storms and ArcMap 10.1 overestimated volumes for larger storms; however, both provide spatial demonstration and analyses to provide accurate and efficient placement of additional green infrastructure installation in the urban Sand River Headwaters watershed in Aiken, SC. Both prediction models demonstrated that 32-33 percent of the total watershed area was established from Subbasins 1, 2, 7, and 8 with all subbasins flowing into 7 before exiting the watershed at the 10 foot pipe, and 67-68 percent of the total watershed area was established from Subbasins 3, 4, 5, and 9 with all subbasins flowing into 9 before the outlet, establishing the most effective placement for additional green infrastructure in Subbasins 3, 4, 5, or 9. The largest areas were determined to be Subbasins 5, 3, and 2 and these three Subbasins would be the best location for effective placement for runoff catchment and treatment. The lowest percent impervious surface areas are Subbasins 3, 6, and 7 allowing for larger total areas of green infrastructure installation on landscapes in these subbasins. Subbasins 1, 2, and 8 had the highest percent impervious surface areas allowing or larger total areas of

green infrastructure installation on hardscapes in these subbasins. The curve numbers range from 54 to 81 with the lowest being Subbasin 6 and the highest being Subbasins 1 and 8. From these outputs, it can be determined that the most effective placement for additional green infrastructure would be within Subbasins 3 and 9 with the largest amount of runoff flow and least amount of percent impervious surface from the watersheds contributing 67-68 percent of the total outlet watershed area. There is also additional space for landscape installation within Subbasins 6 and 7 closer to the natural areas near the outlet with very low percent impervious surface, but significantly smaller area for placement.

This project could be improved by several factors including but not limited to: limitation of subcatchment aggregation and conduit skeletonization (Cantone and Schmidt, 2009), utilization of the Green-Ampt infiltration method as opposed to the CN method (Eli and Lamont, 2010), modeling impervious and pervious surfaces on separate layers using a two-plane kinematic wave approach (Cantone and Schmidt, 2009), and the installation of weather stations at all monitoring locations relating to subbasin delineation to acquire spatially representative rainfall data throughout the watershed and within each subwatershed. Further analysis and data is needed for more accurate validation and calibration of the prediction models ArcMap 10.1 and HEC-HMS; however, both can successfully provide spatial analysis and demonstration of effective installation of additional green infrastructure for the urban city of Aiken, SC.

4.7 REFERENCES

Brevnova, E.V., 2001, "Green-Ampt Infiltration Model Parameter Determination using SCS Curve Number (CN) and Soil Texture Class, and Application to the SCS Runoff Model", Master's Thesis, Department of Civil and Environmental Engineering, West Virginia University, Morgantown, WV.

"Calculating Credits for Green Roofs." - *Minnesota Stormwater Manual*. Minnesota Pollution Control Agency, 2014. Web. 17 Nov. 2014.

Cantone, Joshua P., and Arthur R. Schmidt. "Potential Dangers of Simplifying Combined Sewer Hydrologic/Hydraulic Models." Journal of Hydrologic Engineering 14.6 (2009): 596. Web.

Chow, V.T., 1959, Open-channel hydraulics: New York, McGraw-Hill, 680 p.

Clemson University Institute of Computational Ecology. Stage data downloaded remotely. 2013-2014. Raw data. South Carolina, Aiken.

Costache, Romulus. "Using Gis Techniques For Assessing Lag Time And Concentration Time In Small River Basins. Case Study: Pecineaga River Basin, Romania." *Geographia Technica 9.1* (2014): 31-38. Web.

Eidson, Gene, Victoria Chanse, Calvin Sawyer, and Erin Cooke. Sand River Ecological Restoration Preferred Alternative. Rep. no. 2096199. Clemson: Clemson U Center for Watershed Excellence, 2009. Print.

Eli, Robert N., and Samuel J. Lamont. "Curve Numbers and Urban Runoff Modeling-Application Limitations." Low Impact Development (2010): 405-18. Web.

Institute of Applied Ecology/Center for Watershed Excellence. Sand River Headwaters Green Infrastructure Project. Rep. Clemson: n.p., 2013. Print.

Jin, S., Yang, L., Danielson, P., Homer, C., Fry, J., and Xian, G. 2013. A comprehensive change detection method for updating the National Land Cover Database to circa 2011. Remote Sensing of Environment, 132: 159 – 175.

"LID Urban Design Tools - Green Roofs." *LID Urban Design Tools - Green Roofs*. Low Impact Development Center, 2007. Web. 17 Nov. 2014.

Mccuen, Richard H., Zachary Knight, and A. Gillian Cutter. "Evaluation of the Nash–Sutcliffe Efficiency Index." *Journal of Hydrologic Engineering* 11.6 (2006): 597. Web.

Meadows, Michael E., Katalin B. Morris, and William E. Spearman. Stormwater Management Study for the City of Aiken: Sand River Drainage Basin. Rep. Columbia: Department of Civil Engineering at U of South Carolina, South Carolina Land Resources Conservation Commission, 1992. Print.

Merwade, Venkatesh. "Creating SCS Curve Number Grid Using HEC-GeoHMS." *Purdue University* (2012): n. pag. Web.

Merwade, Venkatesh. "Terrain Processing and HMS-Model Development Using GeoHMS." *Purdue University* (2012): n. pag. Web.

"Re: HEC-GeoHMS BasinHeader Table Missing." Web log comment. *GeoNet: The ESRI Community*. ESRI, 31 July 2012. Web.

"Root Mean Squared Error." *GeneXProTools*. Gepsoft Ltd., 2000-2014. Web. 17 Nov. 2014.

Soil Survey Staff, Natural Resources Conservation Service, United States Department of Agriculture. Soil Survey Geographic (SSURGO) Database for [Aiken, SC].Available online at http://www.arcgis.com/apps/OnePane/basicviewer/index.html?appid=a23eb436f6ec4ad6982000dbaddea5ea. Accessed [August, 2014].

"SonTek - A Xylem Brand." SonTek-IQ Series Intelligent Flow User's Manual. Xylem Inc., Oct. 2012. Print. 20 Oct. 2014.

Woolpert. Sand River Watershed Study. Rep. Aiken: n.p., 2003. Print.

Xian, G., Homer, C., Dewitz, J., Fry, J., Hossain, N., and Wickham, J., 2011. The change of impervious surface area between 2001 and 2006 in the conterminous United States. Photogrammetric Engineering and Remote Sensing, Vol. 77(8): 758-762.

CHAPTER 5: CONCLUSIONS

In this study, hydrologic modeling, specifically utilizing ArcMap 10.1, HEC-GeoHMS, and HEC-HMS, was used to prioritize the installation of additional green infrastructure within the urban Sand River Headwaters watershed of Aiken, SC. Higher accuracy LiDAR data was used to create a higher resolution DEM to delineate nine subwatersheds and a total outlet watershed based on the "burning in" of the current underground stormwater piping system at an artificial elevation below that of the natural DEM. HEC-GeoHMS, HEC-HMS's preprocessor, was then used to transfer the ArcMap outputs into acceptable HEC-HMS formats for input into the prediction model. Volumes, derived from rainfall and subwatershed delineation areas, were calculated from ArcMap along with volumes and flow rates per subbasin from HEC-HMS. Ten monitoring locations were chosen, and stage data was calculated from each subwatershed/subbasin to use for calibration and validation of both the ArcMap and HEC-HMS prediction models. These volumes and peak flow rates, along with spatial representation of land cover and average CN, were then used to determine the most efficient placement for additional green infrastructure installation.

Watershed delineation demonstrated a total watershed area of 1,080 acres draining to the outlet leading to the Sand River with an area of nine acres separating the last monitoring points and the total watershed outlet not delineated into a subbasin. Subbasin flow routing analysis demonstrated that Subbasins 4, 5, and 9 all flowed into Subbasin 3 before reaching the total watershed outlet accounting for 66.5 percent of the total watershed area, and Subbasins 1, 2, and 8 all flowed into Subbasin

7 before entering the outlet accounting for 33.5 percent of the total watershed area. Of the four subbasins contributing to 66.5 percent of the total watershed area, Subbasins 3 and 5 had the largest runoff volumes generated from ArcMap and rainfall depth. Of the four subbasins contributing to 33.5 percent of the total watershed area, Subbasin 2 had the largest runoff volume generated from ArcMap and rainfall depth determining the most potential for runoff capture within Subbasins 2, 3, and 5. These subbasins should be targeted for additional green infrastructure installation and low impact development (LID) practices.

Urban watersheds, such as the 1,080 Sand River Headwaters watershed, produce larger quantities of runoff at higher velocities and flow rates requiring the optimization of effective land use strategies due to limited space for installation. Urban hydrology requires a balance between ecology and engineering to try and return areas with high land use and land cover change to their previous hydrologic state. Low impact development seeks to reduce these runoff quantities and flow rates by mimicking the natural hydrologic features by increasing infiltration and evapotranspiration. LID now includes water quality and quantity approaches to not only focus on one or the other, but to attempt to improve both within the same system. LID has also shifted to more of a holistic approach to include the entire watershed as a whole when considering efficiency of green infrastructure/LID installation versus individual BMP efficiency. LID can improve the urban watershed of Aiken, SC by reducing impervious percentage areas and returning the hydrology to that of the natural terrain, reducing the direct connectivity of impervious surfaces, and

improving the landscape of the watershed while also improving water quality and erosion control downstream. Structural and nonstructural practices can be installed within the watershed to have an overall positive effect downstream impacting the Sand River, Horse Creek, and eventually Middle Savannah River.

Of the subbasins contributing 66.5 percent to the total watershed area, Subbasins 3 and 9 had the lowest percent impervious cover deriving more space for additional green infrastructure installation upon landscapes. Subbasin 7 and the nine acres directly before the total watershed outlet also had very low percent impervious surface and additional space for green infrastructure at a much smaller scale. Although Subbasin 5 had a slightly higher CN than Subbasin 3 indicating potential for more assistance from the green infrastructure installation, it also had a much higher percent impervious illustrating less area for landscape installation. Subbasin 2 also had a significantly higher percent impervious surface, demonstrating more room for installation of green infrastructure upon hardscapes as well as having one of the highest individual contributing volumes making installation more effective within this subbasin. These outputs indicate that the most effective placement for additional green infrastructure upon landscapes was within Subbasins 3 and 9 with the largest amount of runoff flow and least amount of percent impervious surface out of the four subbasins contributing to the 67 percent area of the total watershed. These outputs also indicate that the most effective placement for additional green infrastructure upon hardscapes was within Subbasin 2 with the largest amount of runoff flow and highest amount of impervious surface within the subbasins with the largest amount of

individual volume contribution. An additional space for green infrastructure installations upon landscapes may also exist within Subbasins 6 and 7 closer to the natural areas near the watershed outlet with very low percent impervious surface, but significantly smaller area for placement.

There are various green infrastructure installation options that could be implemented within various subbasins of the Sand River Headwaters watershed. With a high percent impervious surface over the majority of the watershed, a large area is available for structural installation upon hardscapes such as roofing and paved areas; however, there are still large areas of pervious surface within certain subbasins that are available for structural installation upon natural landscaping as well. Subbasins 1, 2, and 8 have the largest areas for hardscape installation and Subbasins 3, 4, and 9 have the largest areas for natural landscape installation. It is recommended that on every roof available for loading and install, green roofing be implemented for as large of an area as can be applied within structural constraints. A relatively small green roof of 200 square feet has the potential to capture 374 gallons of stormwater allowing for the detention of approximately 3.5 million gallons of stormwater just within Subbasin 2 at 39.5 percent impervious assuming 50 percent is roofing. These green roofs should be routed to rain barrels or other LID practices such as vertical farming or irrigation usages to refrain from direct connection of impervious surfaces. Permeable pavement should be installed wherever possible, to add another LID practice upon hardscape surfaces with limited sizing capabilities available. All permeable pavement areas should be routed to bioretention cells or bioswales within

natural landscaping to increase storage and improve water quality. A relatively small bioretention cell of 200 square feet can capture 1,496 gallons allowing for the detention of approximately 50 million gallons of stormwater just within Subbasin 3. It is recommended to combine all of these practices and to implement as many as possible to have the greatest impact on stormwater reduction at the total watershed outlet and the improvement of water quality downstream. Installing these LID practices within various subbasins will significantly reduce stormwater runoff volumes and flow rates.

The urban stormwater piping system was successfully imported into HEC-HMS without any issues and runoff volumes and flow hydrographs were created per storm event. These volumes and peak flow rates were then used to compare to the ArcMap runoff volumes and the monitoring location volume and peak flow rates derived from stage depth using SonTek™IQ-Pipe® acoustic Doppler sensors. During the project, it was discovered that Sensors 6 and 7 were not reporting accurately; new SonTek™ documentation released during the study specified that the IQ-pipe® was not accurate for pipe diameters>72 in. Therefore, sums of calculated flows at Subbasin outlets 1, 2, and 8 were used for the flow volume at Subbasin 7, while sums of calculated flows at Subbasin outlets 1, 2, 8, and 3 were used for the flow volume at Subbasin 6 (outlet of the entire watershed) as confirmed through ArcMap 10.1 watershed delineation analysis.

When comparing the output volumes generated from ArcMap, monitoring location stage data volumes, and HEC-HMS output volumes, both ArcMap and HEC-HMS directly correlated with rainfall depth while sensor volume calculations were scattered with much less correlation. When comparing peak flow rates generated from HEC-HMS outputs and sensor stage data calculations, HEC-HMS peak flow rates directly correlated with rainfall depth; however, sensor peak flow rates derived from stage data demonstrated a maximum peak flow regardless of rainfall depth at approximately 14 cubic meters per second. If this project were replicated, a more accurate stage depth would need to be determined at the total watershed outlet to derive more comparable peak flow rates and total watershed runoff volume generations.

HEC-HMS outputs underestimated runoff generation and peak flow rates over all storm events while ArcMap output volumes showed underestimation for smaller storm events but overestimation for larger storms. One reason for this overestimation and underestimation could be accounted for by the lack of spatially representative rainfall data throughout the entire watershed and respective to individual subbasins. All rainfall data were collected at one location and then used as inputs for all subbasin flow simulations. Highly isolated storm events are typical phenomenon in the urban Aiken watershed, with the potential for heavy rain events in one part of the watershed and no rainfall in another. For future studies, it is recommended to install rain gages to account for variability between monitored subbasins to improve flow predictions throughout the larger watershed.

This project could be improved various ways including (1) enhanced local rainfall data, (2) more extensive stormwater piping knowledge to decrease connectivity issues for HEC-HMS, (3) alternate stage depth sensors at monitoring locations 6 and 7, (4) utilizing the two plane kinematic approach for impervious/pervious surfaces within HEC-HMS, (5) selection of the Green-Ampt infiltration method within HEC-HMS, and (6) inclusion of current baseflow data specific to every subbasin within HEC-HMS. The Green-Ampt method and the two plane kinematic approach would both require more extensive stormwater piping knowledge as well. ArcMap 10.1, HEC-GeoHMS, and HEC-HMS were successfully used to effectively model an urban underground stormwater system specific to Aiken, SC. Subbasin and total watershed delineation allowed for runoff volume generation and peak flow rate measurements that can be calibrated based on local rainfall depths per storm event. This volume generation data can then be used along with percent impervious surface and CN data within an urban watershed to determine the most effective placement of green infrastructure installation within the subbasin(s).

Future direction of this project should strive to create an effective weighting or scale that all subbasins can be defined upon to determine a much more specific location within each subbasin for additional green infrastructure install. Increased interaction with city officials and project managers would be necessary to aquire additional information or data layers such as: municipalities, land areas with approval for install of green infrastructure, public acceptance areas, public versus private land areas, utility piping, etc. These layers, along with impervious surface, soil, land use,

CN, directly connected versus not directly connected impervious surface, storage volume potential, etc. derived within ArcMap would then need to be given a weight or importance factor derived by city officials to utilize calculation tools within ArcMap to derive a raster output demonstrating the highest scoring cell areas within the subbasins. The highest scoring cell areas would indicate the most efficient placement for additional green infrastructure on a much more specific location basis and a generic scale ranking all land areas within the total watershed. The City of Aiken should then take the highest scoring land areas and implement previous LID and green infrastructure consulting recommendations including but not limited to: green roofing, rain barrels, vertical farming, permeable pavement, and bioretention cells. Combining these practices as frequently and efficiently as possible will significantly reduce stormwater runoff volumes and peak flow rates in turn improving erosion control and water quality downstream of the total watershed outlet.

APPENDIX A

A.1 VOLUME AND PEAK FLOW COMPARISON

Legend:

	Sensor continued reading before/after storm event
	Sensor value was used as opposed to estimation
	Sensor was not functioning properly
	Sensor was offline

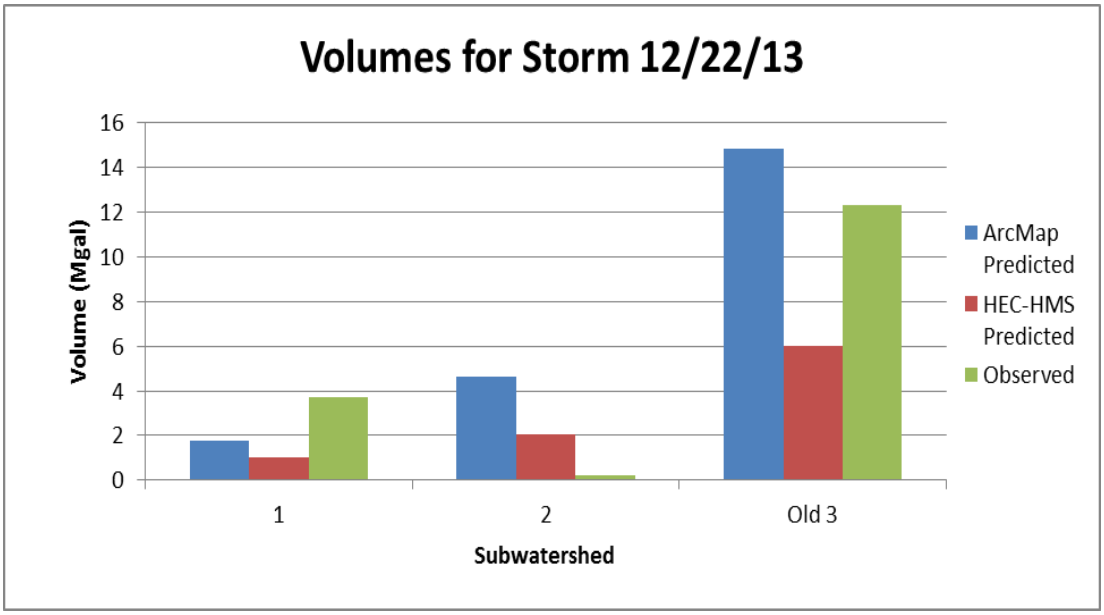

Figure A.1: Volume comparison graph for storm event 12/22/13 of 0.77 inches

Table A.1: Volume and flow rate comparison table for storm event 12/22/13 of 0.77 inches with rainfall runoff ratios calculated

Subwatershed	GIS Volume Summed (Mgal)	HEC-HMS Volume Summed (Mgal)	Sensor Volume (Mgal)	Runoff (ft)	Ratio	Sensor Peak Flow (cms)	HEC-HMS Peak Flow (cms)
1	1.79	1.03	3.69	0.13	2.06	4.66	0.50
2	4.65	2.06	0.23	0.00	0.05	1.44	0.80
Old 3	14.87	6.02	12.34	0.20	3.09	2.74	0.30

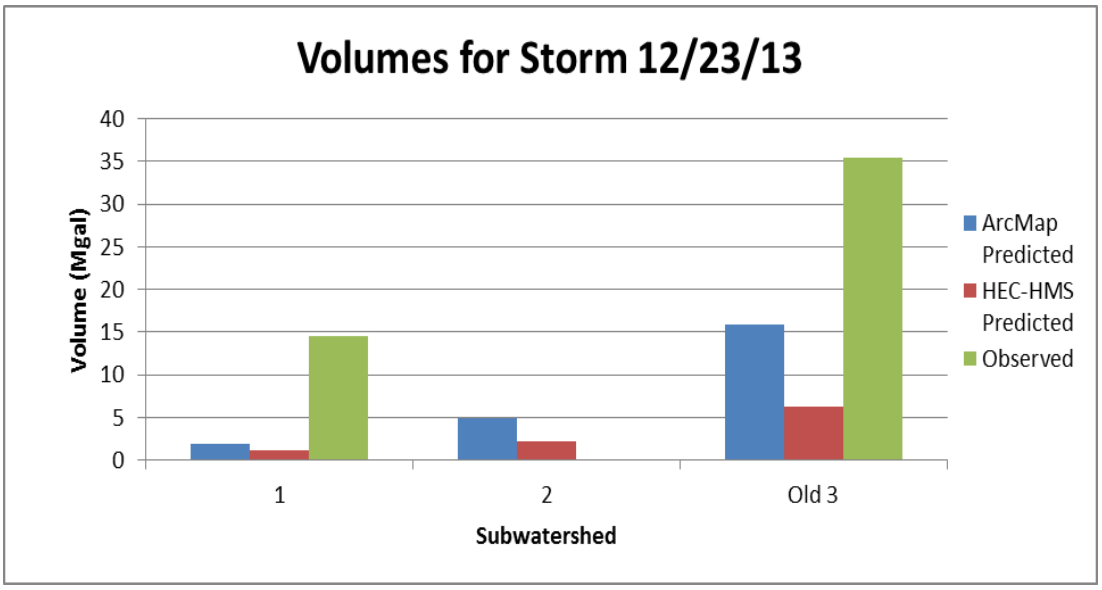

Figure A.2: Volume comparison graph for storm event 12/23/13 of 0.82 inches

Table A.2: Volume and flow rate comparison table for storm event 12/23/13 of 0.82 inches with rainfall runoff ratios calculated

Subwatershed	GIS Volume Summed (Mgal)	HEC-HMS Volume Summed (Mgal)	Sensor Volume (Mgal)	Runoff (ft)	Ratio	Sensor Peak Flow (cms)	HEC-HMS Peak Flow (cms)
1	1.91	1.11	14.54	0.52	7.65	5.01	0.60
2	4.95	2.19	0.00	0.00	0.00	0.00	0.90
Old 3	15.83	6.31	35.46	0.57	8.35	2.74	0.30

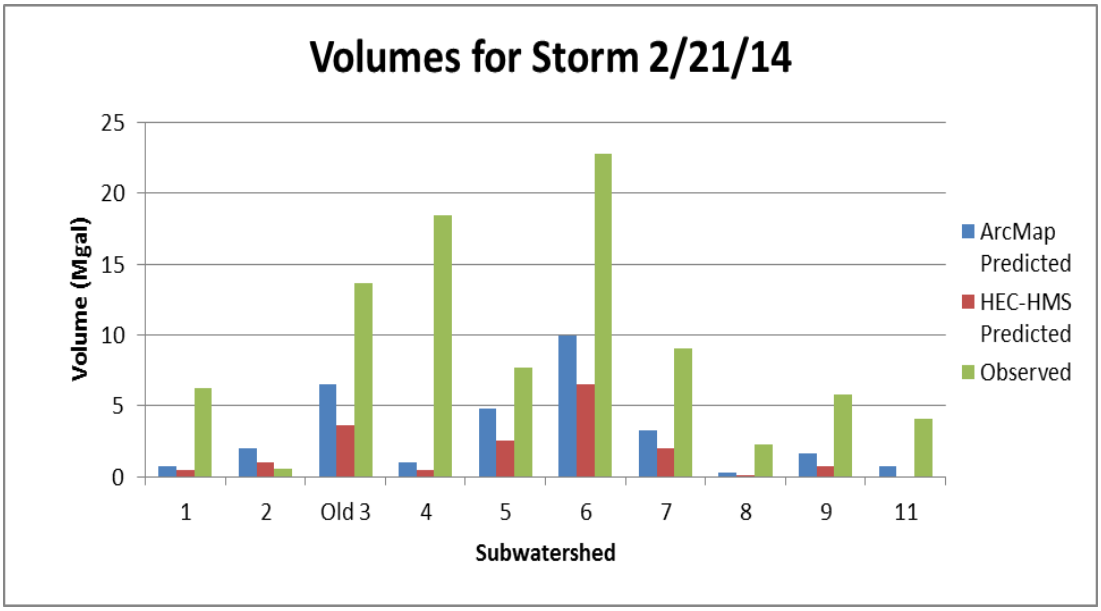

Figure A.3: Volume comparison graph for storm event 2/21/14 of 0.34 inches

Table A.3: Volume and flow rate comparison table for storm event 2/21/14 of 0.34 inches with rainfall runoff ratios calculated

Subwatershed	GIS Volume Summed (Mgal)	HEC-HMS Volume Summed (Mgal)	Sensor Volume (Mgal)	Runoff (ft)	Ratio	Sensor Peak Flow (cms)	HEC-HMS Peak Flow (cms)
1	0.79	0.48	6.24	0.22	7.88	5.00	0.20
2	2.05	1.00	0.58	0.01	0.28	1.55	0.40
Old 3	6.56	3.65	13.69	0.06	2.08	2.74	0.20
4	1.00	0.53	18.42	0.52	18.36	1.81	0.10
5	4.80	2.59	7.68	0.05	1.60	1.59	0.30
6	9.97	6.50	22.76	0.06	2.28	13.52	0.90
7	3.26	1.98	9.07	0.08	2.79	0.93	0.00
8	0.28	0.16	2.25	0.23	8.16	2.90	0.10
9	1.67	0.71	5.77	0.10	3.46	1.31	0.20
11	0.76		4.08	0.15	5.39	2.45	

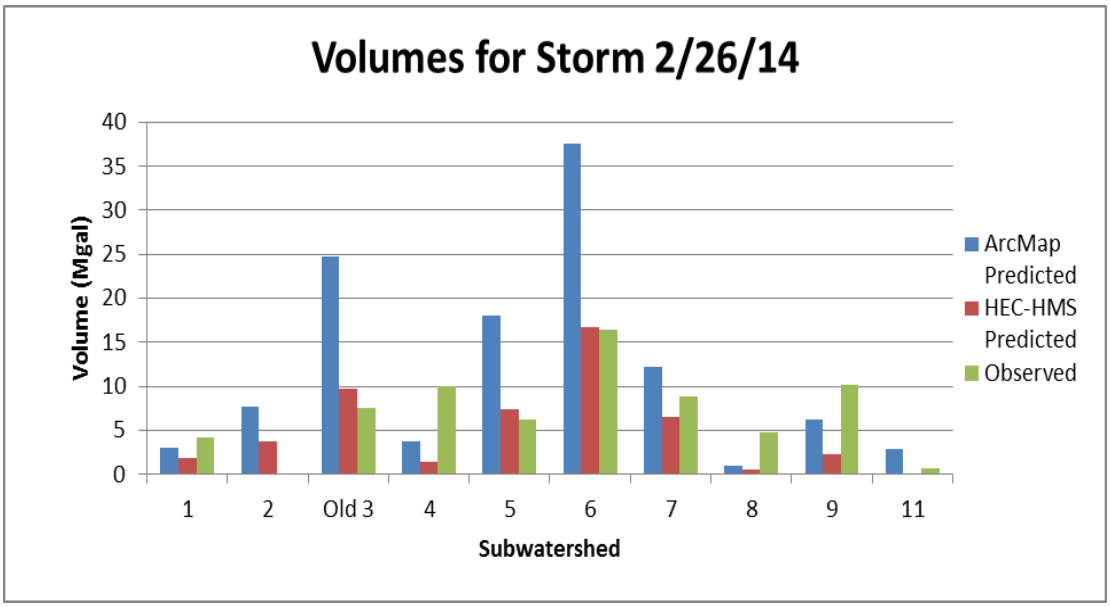

Figure A.4: Volume comparison graph for storm event 2/26/14 of 1.28 inches

Table A.4: Volume and flow rate comparison table for storm event 2/26/14 of 1.28 inches with rainfall runoff ratios calculated

Subwatershed	GIS Volume Summed (Mgal)	HEC-HMS Volume Summed (Mgal)	Sensor Volume (Mgal)	Runoff (ft)	Ratio	Sensor Peak Flow (cms)	HEC-HMS Peak Flow (cms)
1	2.98	1.82	4.17	0.15	1.40	4.23	1.00
2	7.72	3.70	0.00	0.00	0.00	0.00	1.50
Old 3	24.71	9.75	7.53	0.03	0.30	2.74	0.50
4	3.78	1.48	9.95	0.28	2.64	1.75	0.50
5	18.05	7.37	6.29	0.04	0.35	1.58	1.00
6	37.52	16.75	16.43	0.05	0.44	13.78	3.30
7	12.26	6.55	8.90	0.08	0.73	6.43	0.10
8	1.04	0.61	4.73	0.48	4.55	2.94	0.30
9	6.27	2.35	10.23	0.17	1.63	1.31	0.80
11	2.85		0.74	0.03	0.26	2.67	

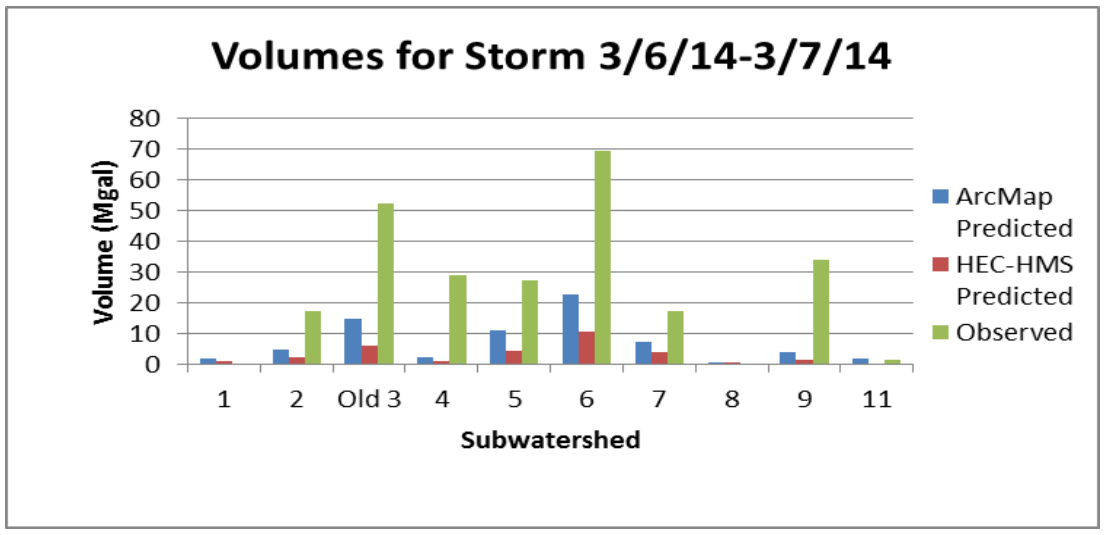

Figure A.5: Volume comparison graph for storm event 3/6/14-3/7/14 of 0.77 inches

Table A.5: Volume and flow rate comparison table for storm event 3/6/14-3/7/14 of 0.77 inches with rainfall runoff ratios calculated

Subwatershed	GIS Volume Summed (Mgal)	HEC-HMS Volume Summed (Mgal)	Sensor Volume (Mgal)	Runoff (ft)	Ratio	Sensor Peak Flow (cms)	HEC-HMS Peak Flow (cms)
1	1.79	1.03	0.00	0.00	0.00	0.00	0.50
2	4.64	2.06	17.38	0.24	3.74	1.55	0.80
Old 3	14.87	6.02	51.98	0.22	3.49	2.74	0.30
4	2.27	0.90	28.82	0.81	12.68	1.71	0.30
5	10.86	4.46	27.36	0.16	2.52	1.64	0.60
6	22.57	10.57	69.35	0.20	3.07	14.17	1.90
7	7.37	3.80	17.38	0.15	2.36	3.28	0.10
8	0.63	0.34	0.00	0.00	0.00	0.00	0.20
9	3.77	1.32	33.75	0.57	8.94	1.31	0.40
11	1.71		1.17	0.04	0.68	2.04	

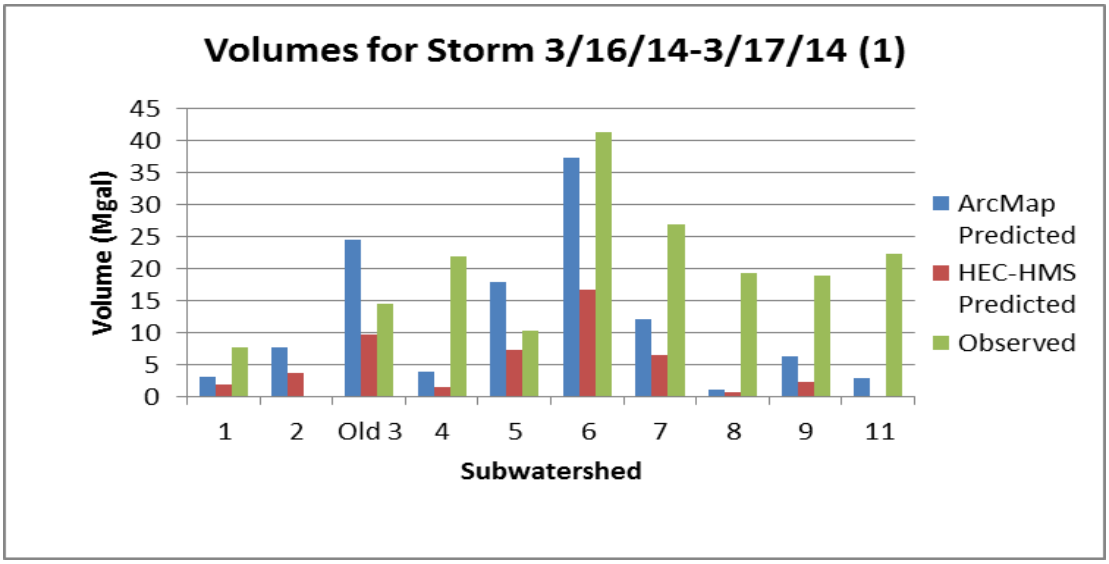

Figure A.6: Volume comparison graph for storm event 3/16/14-3/17/14 of 1.27 inches

Table A.6: Volume and flow rate comparison table for storm event 3/16/14-3/17/14 of 1.27 inches with rainfall runoff ratios calculated

Subwatershed	GIS Volume Summed (Mgal)	HEC-HMS Volume Summed (Mgal)	Sensor Volume (Mgal)	Runoff (ft)	Ratio	Sensor Peak Flow (cms)	HEC-HMS Peak Flow (cms)
1	2.96	1.82	7.61	0.27	2.57	5.00	0.90
2	7.66	3.65	0.00	0.00	0.00	0.00	1.50
Old 3	24.52	9.64	14.48	0.06	0.59	2.74	0.50
4	3.75	1.45	21.93	0.62	5.85	1.81	0.50
5	17.91	7.29	10.26	0.06	0.57	1.55	1.00
6	37.23	16.62	41.41	0.12	1.11	13.78	3.20
7	12.16	6.50	26.93	0.23	2.21	12.06	0.10
8	1.03	0.61	19.32	1.98	18.72	2.94	0.30
9	6.23	2.32	18.91	0.32	3.04	1.31	0.80
11	2.83		22.35	0.84	7.91	3.05	

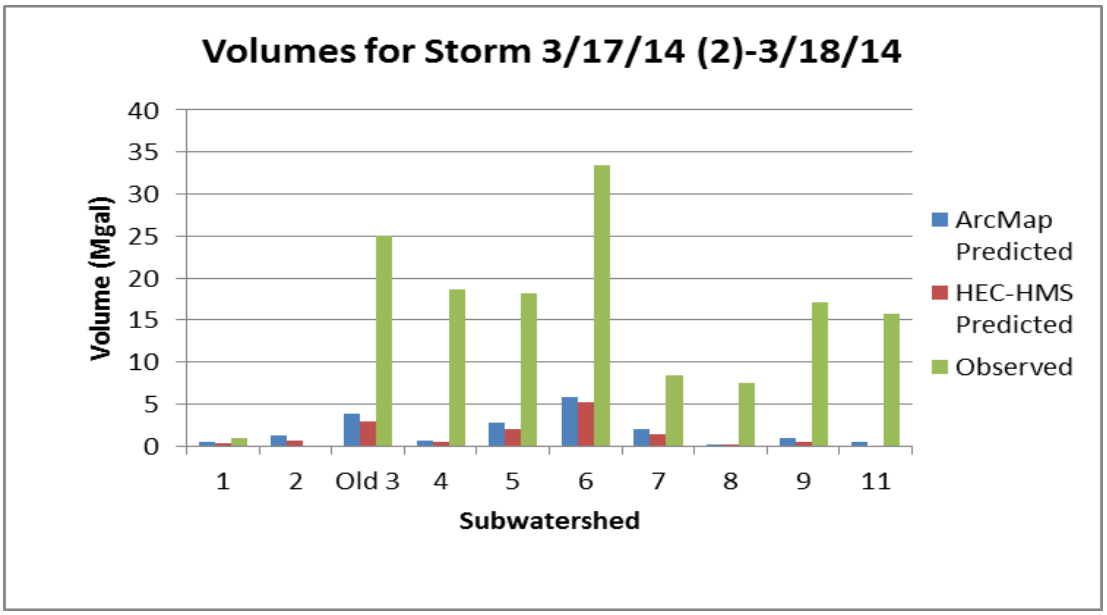

Figure A.7: Volume comparison graph for storm event 3/17/14-3/18/14 of 0.20 inches

Table A.7: Volume and flow rate comparison table for storm event 3/17/14-3/18/14 of 0.20 inches with rainfall runoff ratios calculated

Subwatershed	GIS Volume Summed (Mgal)	HEC-HMS Volume Summed (Mgal)	Sensor Volume (Mgal)	Runoff (ft)	Ratio	Sensor Peak Flow (cms)	HEC-HMS Peak Flow (cms)
1	0.47	0.32	0.98	0.03	2.10	2.50	0.10
2	1.21	0.69	0.00	0.00	0.00	0.00	0.20
Old 3	3.86	2.85	25.02	0.11	6.48	2.74	0.10
4	0.59	0.40	18.65	0.53	31.60	1.59	0.10
5	2.82	1.95	18.15	0.11	6.43	1.61	0.20
6	5.86	5.20	33.47	0.10	5.71	14.06	0.60
7	1.91	1.45	8.44	0.07	4.41	0.00	0.00
8	0.16	0.11	7.47	0.77	45.94	2.90	0.00
9	0.98	0.50	17.05	0.29	17.39	1.31	0.10
11	0.45		15.78	0.59	35.44	3.06	

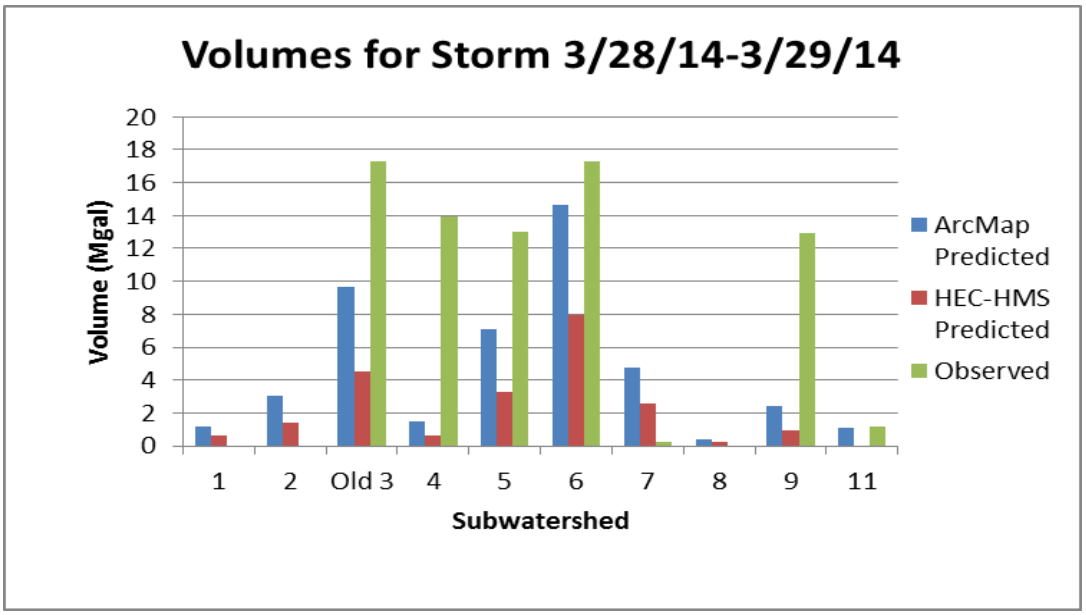

Figure A.8: Volume comparison graph for storm event 3/28/14-3/29/14 of 0.50 inches

Table A.8: Volume and flow rate comparison table for storm event 3/28/14-3/29/14 of 0.50 inches with rainfall runoff ratios calculated

Subwatershed	GIS Volume Summed (Mgal)	HEC-HMS Volume Summed (Mgal)	Sensor Volume (Mgal)	Runoff (ft)	Ratio	Sensor Peak Flow (cms)	HEC-HMS Peak Flow (cms)
1	1.16	0.66	0.00	0.00	0.00	0.00	0.30
2	3.02	1.37	0.00	0.00	0.00	0.00	0.50
Old 3	9.65	4.52	17.31	0.07	1.79	2.25	0.20
4	1.47	0.66	13.93	0.39	9.44	1.48	0.20
5	7.05	3.28	12.97	0.08	1.84	1.64	0.40
6	14.66	7.98	17.31	0.05	1.18	13.99	1.30
7	4.79	2.59	0.23	0.00	0.05	2.74	0.00
8	0.41	0.21	0.00	0.00	0.00	0.00	0.10
9	2.45	0.92	12.92	0.22	5.27	1.31	0.30
11	1.11		1.17	0.04	1.05	2.81	

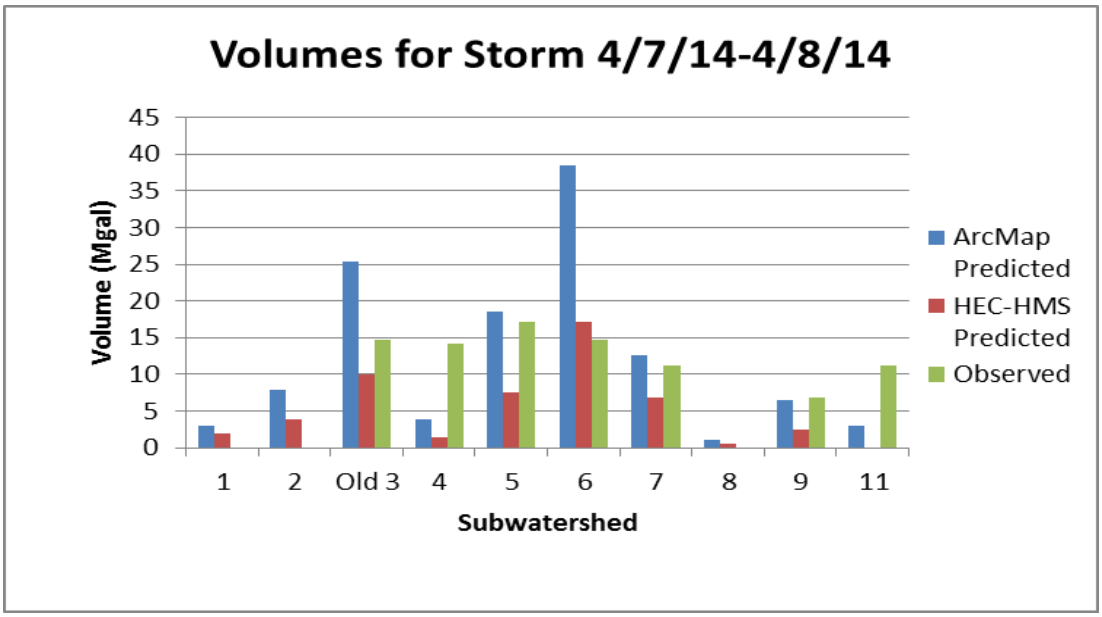

Figure A.9: Volume comparison graph for storm event 4/7/14-4/8/14 of 1.31 inches

Table A.9: Volume and flow rate comparison table for storm event 4/7/14-4/8/14 of 1.31 inches with rainfall runoff ratios calculated

Subwatershed	GIS Volume Summed (Mgal)	HEC-HMS Volume Summed (Mgal)	Sensor Volume (Mgal)	Runoff (ft)	Ratio	Sensor Peak Flow (cms)	HEC-HMS Peak Flow (cms)
1	3.05	1.88	0.00	0.00	0.00	0.00	1.00
2	7.90	3.80	0.00	0.00	0.00	0.00	1.50
Old 3	25.29	9.99	14.64	0.06	0.58	2.74	0.50
4	3.86	1.51	14.22	0.40	3.68	1.81	0.50
5	18.48	7.56	17.19	0.10	0.93	1.62	1.00
6	38.40	17.17	14.64	0.04	0.38	14.25	3.40
7	12.54	6.76	11.20	0.10	0.89	4.23	0.10
8	1.06	0.63	0.00	0.00	0.00	0.00	0.40
9	6.42	2.40	6.89	0.12	1.07	1.30	0.80
11	2.92		11.21	0.42	3.84	3.05	

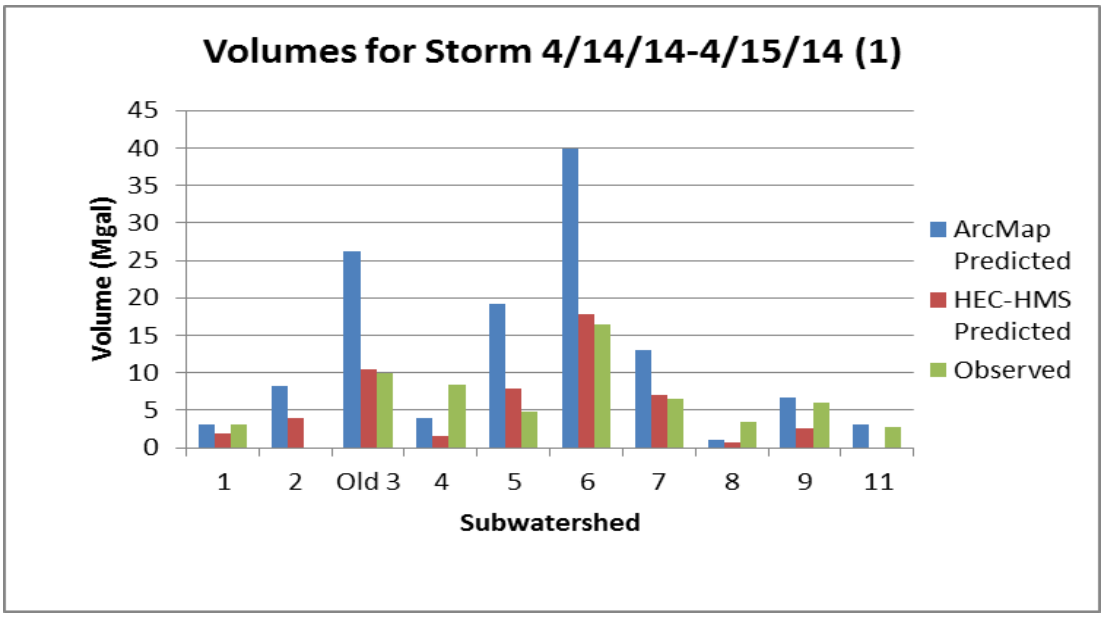

Figure A.10: Volume comparison graph for storm event 4/14/14-4/15/14 of 1.36 inches

Table A.10: Volume and flow rate comparison table for storm event 4/14/14-4/15/14 of 1.36 inches with rainfall runoff ratios calculated

Subwatershed	GIS Volume Summed (Mgal)	HEC-HMS Volume Summed (Mgal)	Sensor Volume (Mgal)	Runoff (ft)	Ratio	Sensor Peak Flow (cms)	HEC-HMS Peak Flow (cms)
1	3.17	1.95	3.07	0.11	0.97	4.90	1.00
2	8.20	3.99	0.00	0.00	0.00	0.00	1.60
Old 3	26.26	10.46	9.92	0.04	0.38	2.74	0.60
4	4.01	1.59	8.44	0.24	2.10	1.80	0.50
5	19.18	7.93	4.77	0.03	0.25	1.64	1.10
6	39.87	17.88	16.39	0.05	0.41	13.88	3.50
7	13.02	7.05	6.47	0.06	0.50	0.00	0.10
8	1.11	0.66	3.40	0.35	3.08	2.90	0.40
9	6.67	2.54	5.96	0.10	0.89	1.31	0.80
11	3.03		2.82	0.11	0.93	3.02	

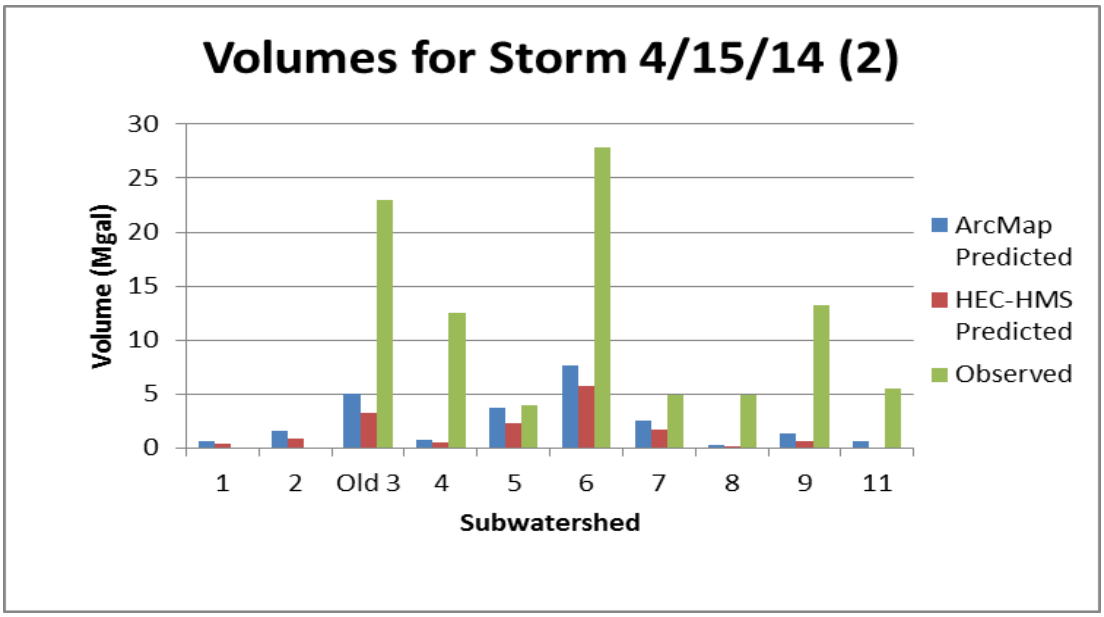

Figure A.11: Volume comparison graph for storm event 4/15/14 of 0.26 inches

Table A.11: Volume and flow rate comparison table for storm event 4/15/14 of 0.26 inches with rainfall runoff ratios calculated

Subwatershed	GIS Volume Summed (Mgal)	HEC-HMS Volume Summed (Mgal)	Sensor Volume (Mgal)	Runoff (ft)	Ratio	Sensor Peak Flow (cms)	HEC-HMS Peak Flow (cms)
1	0.61	0.37	0.00	0.00	0.00	0.00	0.20
2	1.57	0.82	0.00	0.00	0.00	0.00	0.30
Old 3	5.02	3.20	22.95	0.10	4.57	2.74	0.10
4	0.77	0.45	12.47	0.35	16.25	1.81	0.10
5	3.67	2.25	3.97	0.02	1.08	1.64	0.20
6	7.62	5.76	27.83	0.08	3.65	13.99	0.70
7	2.49	1.66	4.88	0.04	1.96	0.00	0.00
8	0.21	0.13	4.88	0.50	23.08	2.86	0.10
9	1.27	0.61	13.26	0.23	10.40	1.31	0.20
11	0.58		5.50	0.21	9.51	2.62	

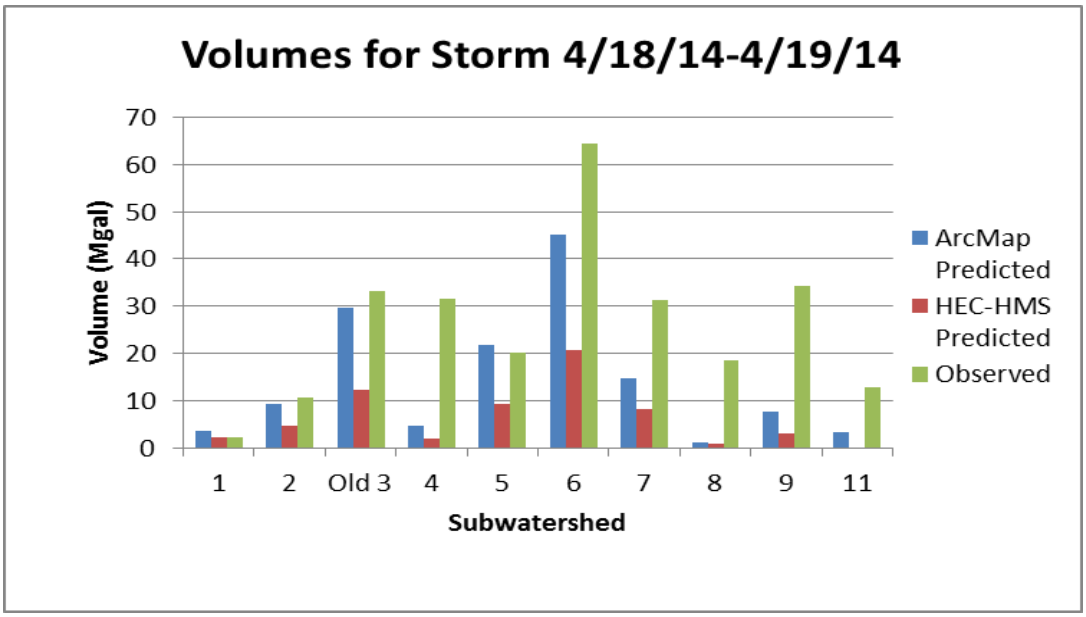

Figure A.12: Volume comparison graph for storm event 4/18/14-4/19/14 of 1.54 inches

Table A.12: Volume and flow rate comparison table for storm event 4/18/14-4/19/14 of 1.54 inches with rainfall runoff ratios calculated

Subwatershed	GIS Volume Summed (Mgal)	HEC-HMS Volume Summed (Mgal)	Sensor Volume (Mgal)	Runoff (ft)	Ratio	Sensor Peak Flow (cms)	HEC-HMS Peak Flow (cms)
1	3.59	2.27	2.13	0.08	0.59	4.55	1.20
2	9.29	4.65	10.57	0.15	1.14	1.55	1.90
Old 3	29.73	12.15	33.07	0.14	1.11	2.74	0.70
4	4.54	1.85	31.68	0.89	6.97	1.71	0.60
5	21.72	9.22	20.12	0.12	0.93	1.64	1.30
6	45.14	20.61	64.35	0.18	1.43	13.96	4.10
7	14.74	8.16	31.28	0.27	2.12	0.00	0.20
8	1.25	0.77	18.58	1.90	14.84	2.94	0.40
9	7.55	2.99	34.33	0.58	4.55	1.31	1.00
11	3.43		12.78	0.48	3.73	3.06	

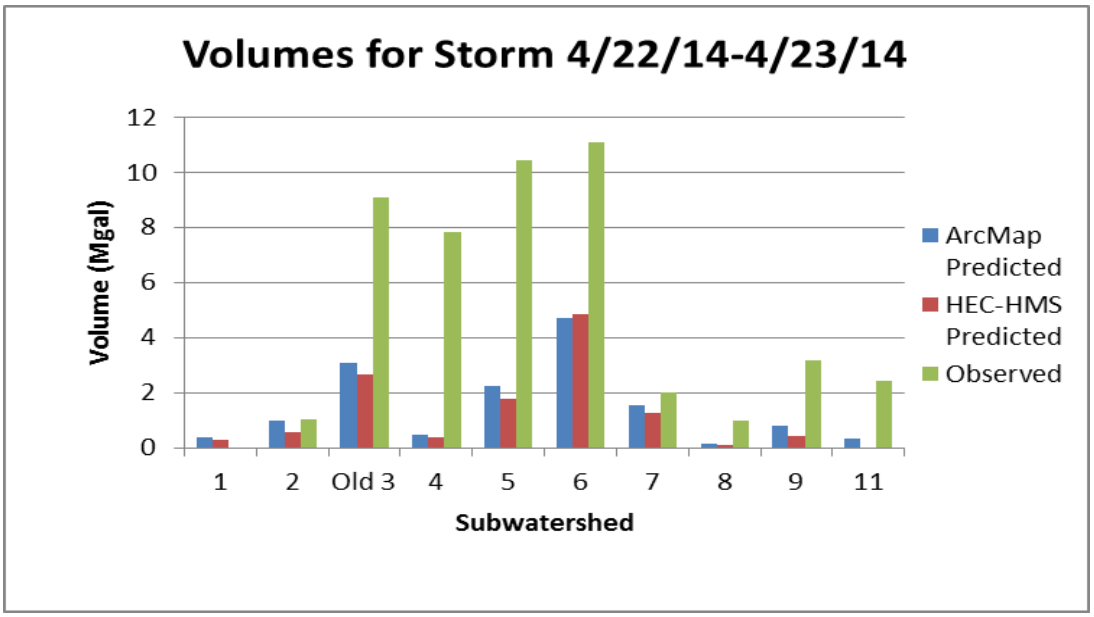

Figure A.13: Volume comparison graph for storm event 4/22/14-4/23/14 of 0.16 inches

Table A.13: Volume and flow rate comparison table for storm event 4/22/14-4/23/14 of 0.16 inches with rainfall runoff ratios calculated

Subwatershed	GIS Volume Summed (Mgal)	HEC-HMS Volume Summed (Mgal)	Sensor Volume (Mgal)	Runoff (ft)	Ratio	Sensor Peak Flow (cms)	HEC-HMS Peak Flow (cms)
1	0.37	0.26	0.00	0.00	0.00	0.00	0.10
2	0.97	0.58	1.05	0.01	1.08	1.48	0.20
Old 3	3.09	2.64	9.09	0.04	2.94	2.00	0.10
4	0.47	0.37	7.84	0.22	16.61	1.46	0.10
5	2.26	1.80	10.44	0.06	4.63	1.59	0.10
6	4.69	4.83	11.11	0.03	2.37	13.36	0.50
7	1.53	1.27	2.02	0.02	1.32	0.00	0.00
8	0.13	0.08	0.97	0.10	7.48	2.76	0.00
9	0.78	0.45	3.18	0.05	4.06	1.31	0.10
11	0.36		2.41	0.09	6.77	1.99	

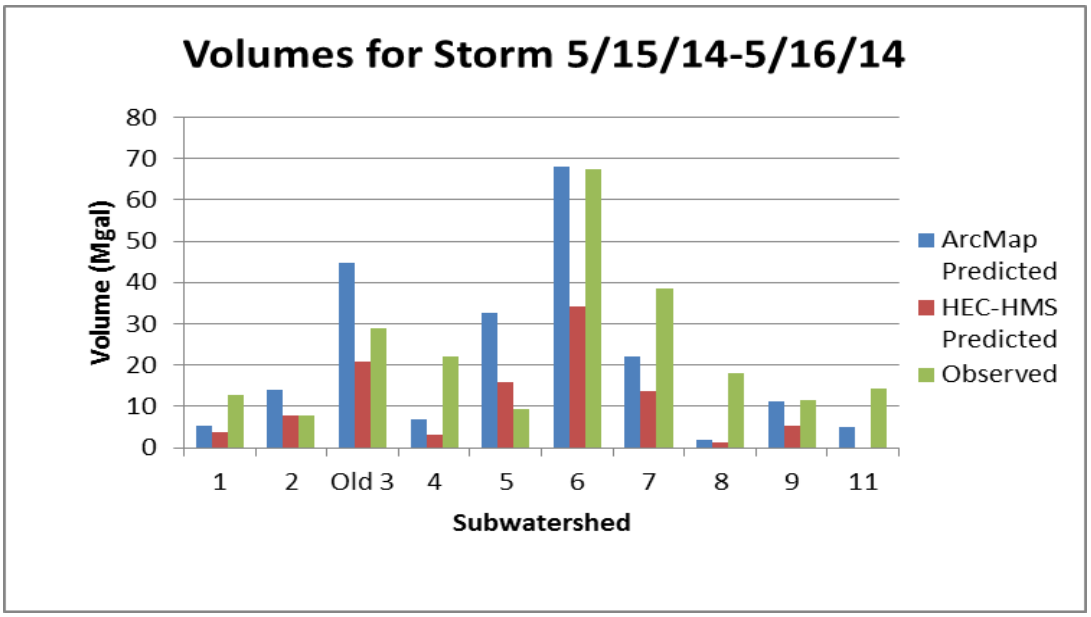

Figure A.14: Volume comparison graph for storm event 5/15/14-5/16/14 of 2.32 inches

Table A.14: Volume and flow rate comparison table for storm event 5/15/14-5/16/14 of 2.32 inches with rainfall runoff ratios calculated

Subwatershed	GIS Volume Summed (Mgal)	HEC-HMS Volume Summed (Mgal)	Sensor Volume (Mgal)	Runoff (ft)	Ratio	Sensor Peak Flow (cms)	HEC-HMS Peak Flow (cms)
1	5.40	3.75	12.70	0.45	2.35	5.01	2.10
2	13.99	7.95	7.69	0.11	0.55	1.55	3.50
Old 3	44.80	20.98	28.88	0.12	0.64	2.74	1.40
4	6.84	3.22	22.01	0.62	3.22	1.81	1.20
5	32.72	15.85	9.26	0.05	0.28	1.63	2.30
6	68.01	34.26	67.42	0.19	0.99	13.80	7.30
7	22.21	13.63	38.54	0.34	1.74	0.00	0.40
8	1.89	1.27	18.15	1.86	9.63	2.94	0.80
9	11.37	5.34	11.44	0.19	1.01	1.22	2.00
11	5.16		14.28	0.53	2.77	3.06	

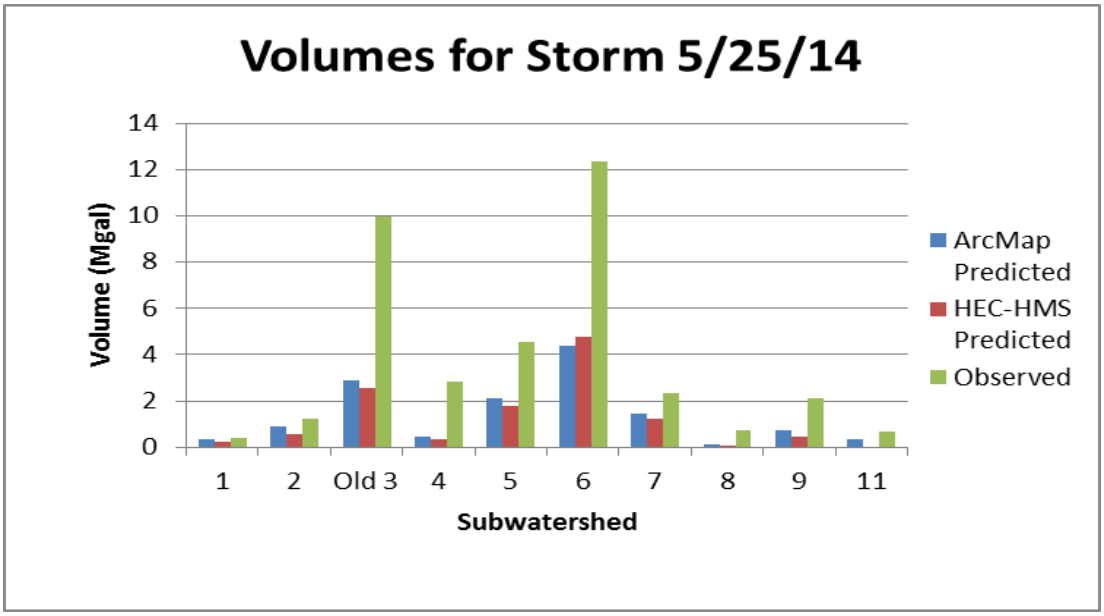

Figure A.15: Volume comparison graph for storm event 5/25/14 of 0.15 inches

Table A.15: Volume and flow rate comparison table for storm event 5/25/14 of 0.15 inches with rainfall runoff ratios calculated

Subwatershed	GIS Volume Summed (Mgal)	HEC-HMS Volume Summed (Mgal)	Sensor Volume (Mgal)	Runoff (ft)	Ratio	Sensor Peak Flow (cms)	HEC-HMS Peak Flow (cms)
1	0.35	0.24	0.42	0.02	1.21	4.00	0.10
2	0.90	0.55	1.22	0.02	1.35	1.55	0.20
Old 3	2.90	2.59	9.96	0.04	3.44	2.74	0.10
4	0.44	0.37	2.83	0.08	6.39	1.77	0.10
5	2.12	1.77	4.54	0.03	2.15	1.45	0.10
6	4.40	4.76	12.33	0.04	2.80	12.58	0.50
7	1.44	1.22	2.37	0.02	1.65	0.00	0.00
8	0.12	0.08	0.72	0.07	5.94	2.93	0.00
9	0.74	0.45	2.11	0.04	2.87	1.22	0.10
11	0.33		0.68	0.03	2.05	2.01	

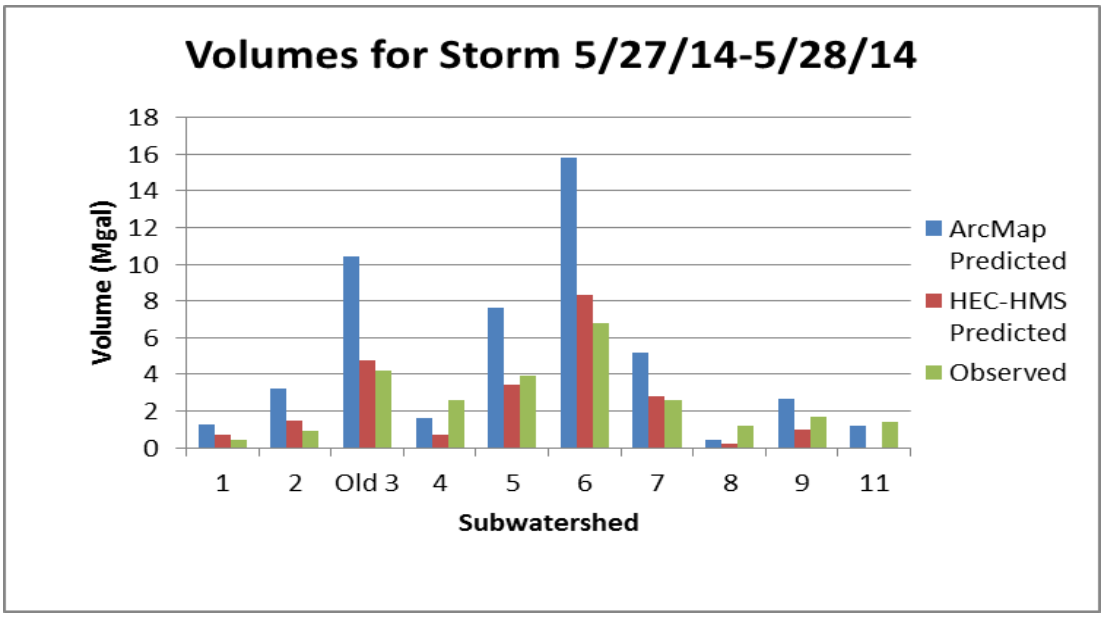

Figure A.16: Volume comparison graph for storm event 5/27/14-5/28/14 of 0.54 inches

Table A.16: Volume and flow rate comparison table for storm event 5/27/14-5/28/14 of 0.54 inches with rainfall runoff ratios calculated

Subwatershed	GIS Volume Summed (Mgal)	HEC-HMS Volume Summed (Mgal)	Sensor Volume (Mgal)	Runoff (ft)	Ratio	Sensor Peak Flow (cms)	HEC-HMS Peak Flow (cms)
1	1.26	0.71	0.46	0.02	0.36	3.21	0.40
2	3.26	1.48	0.91	0.01	0.28	1.54	0.60
Old 3	10.43	4.73	4.19	0.02	0.40	1.67	0.20
4	1.59	0.69	2.58	0.07	1.62	1.42	0.20
5	7.62	3.43	3.93	0.02	0.52	1.41	0.40
6	15.83	8.35	6.77	0.02	0.43	11.81	1.40
7	5.17	2.77	2.58	0.02	0.50	0.00	0.00
8	0.44	0.24	1.21	0.12	2.76	2.83	0.10
9	2.65	0.98	1.71	0.03	0.64	1.22	0.30
11	1.20		1.38	0.05	1.15	1.63	

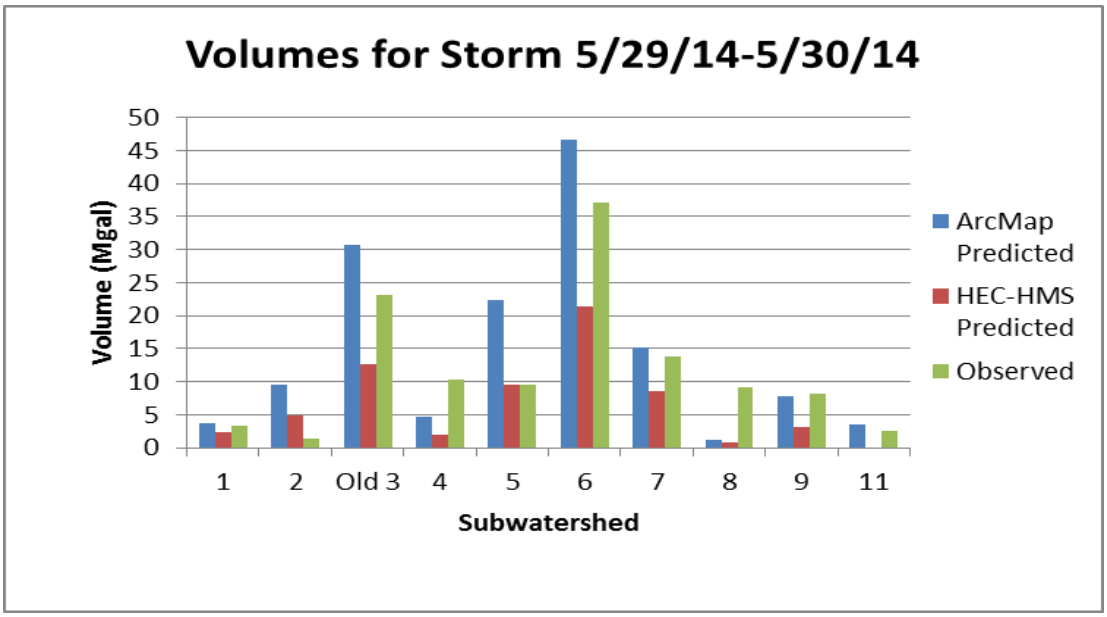

Figure A.17: Volume comparison graph for storm event 5/29/14-5/30/14 of 1.59 inches

Table A.17: Volume and flow rate comparison table for storm event 5/29/14-5/30/14 of 1.59 inches with rainfall runoff ratios calculated

Subwatershed	GIS Volume Summed (Mgal)	HEC-HMS Volume Summed (Mgal)	Sensor Volume (Mgal)	Runoff (ft)	Ratio	Sensor Peak Flow (cms)	HEC-HMS Peak Flow (cms)
1	3.70	2.38	3.41	0.12	0.92	5.01	1.30
2	9.59	4.86	1.30	0.02	0.14	1.44	2.00
Old 3	30.70	12.68	23.21	0.10	0.76	2.74	0.70
4	4.69	1.93	10.24	0.29	2.18	1.81	0.60
5	22.43	9.62	9.55	0.06	0.43	1.70	1.30
6	46.61	21.40	37.09	0.11	0.80	14.07	4.30
7	15.22	8.53	13.88	0.12	0.91	0.00	0.20
8	1.29	0.79	9.17	0.94	7.10	2.94	0.50
9	7.79	3.14	8.23	0.14	1.06	1.22	1.10
11	3.54		2.59	0.10	0.73	2.89	

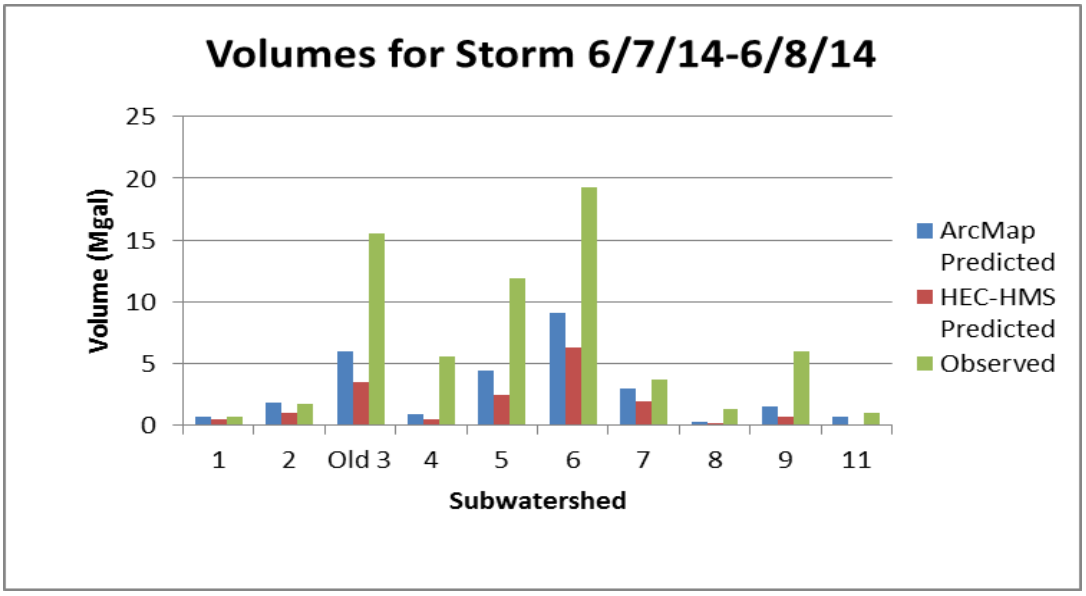

Figure A.18: Volume comparison graph for storm event 6/7/14-6/8/14 of 0.31 inches

Table A.18: Volume and flow rate comparison table for storm event 6/7/14-6/8/14 of 0.31 inches with rainfall runoff ratios calculated

Subwatershed	GIS Volume Summed (Mgal)	HEC-HMS Volume Summed (Mgal)	Sensor Volume (Mgal)	Runoff (ft)	Ratio	Sensor Peak Flow (cms)	HEC-HMS Peak Flow (cms)
1	0.72	0.45	0.69	0.02	0.96	4.99	0.20
2	1.87	0.95	1.68	0.02	0.90	1.55	0.30
Old 3	5.99	3.46	15.57	0.07	2.60	2.74	0.10
4	0.91	0.50	5.59	0.16	6.11	1.59	0.10
5	4.37	2.46	11.93	0.07	2.73	1.63	0.30
6	9.09	6.23	19.23	0.05	2.12	14.25	0.80
7	2.97	1.90	3.66	0.03	1.23	0.00	0.00
8	0.25	0.16	1.29	0.13	5.11	2.93	0.10
9	1.52	0.66	5.92	0.10	3.90	1.22	0.20
11	0.69		0.97	0.04	1.40	1.95	

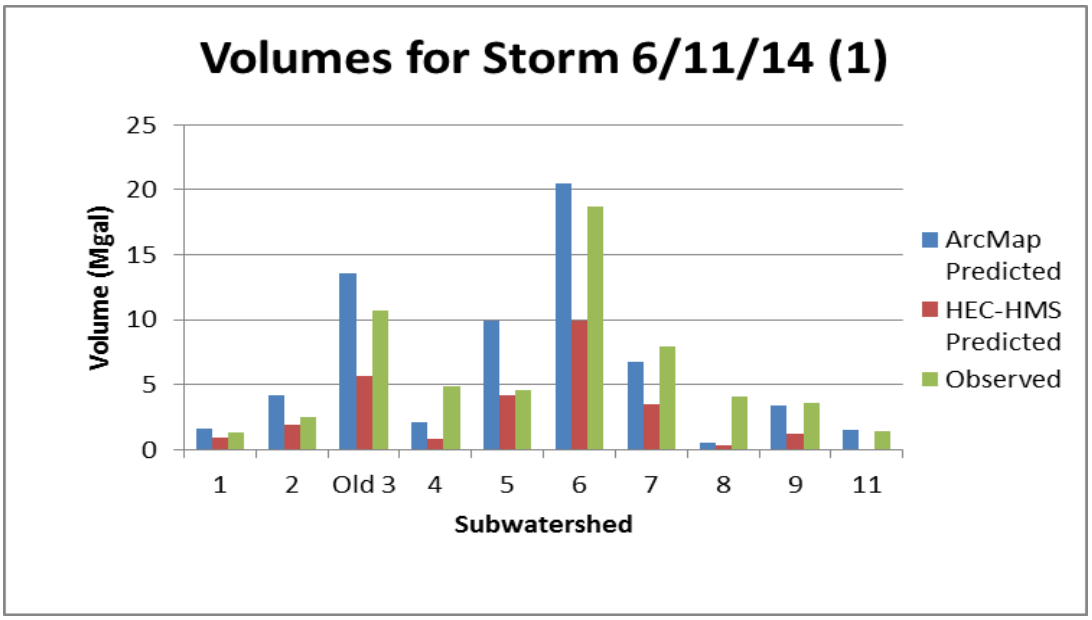

Figure A.19: Volume comparison graph for storm event 6/11/14 of 0.70 inches

Table A.19: Volume and flow rate comparison table for storm event 6/11/14 of 0.70 inches with rainfall runoff ratios calculated

Subwatershed	GIS Volume Summed (Mgal)	HEC-HMS Volume Summed (Mgal)	Sensor Volume (Mgal)	Runoff (ft)	Ratio	Sensor Peak Flow (cms)	HEC-HMS Peak Flow (cms)
1	1.63	0.92	1.34	0.05	0.82	5.01	0.50
2	4.22	1.88	2.53	0.03	0.60	1.55	0.80
Old 3	13.52	5.63	10.73	0.05	0.79	2.74	0.30
4	2.06	0.85	4.90	0.14	2.37	1.70	0.30
5	9.87	4.15	4.57	0.03	0.46	1.64	0.50
6	20.52	9.88	18.70	0.05	0.91	13.72	1.70
7	6.70	3.49	7.97	0.07	1.19	0.00	0.10
8	0.57	0.32	4.10	0.42	7.21	2.91	0.20
9	3.43	1.22	3.61	0.06	1.05	1.22	0.40
11	1.56		1.45	0.05	0.93	2.94	

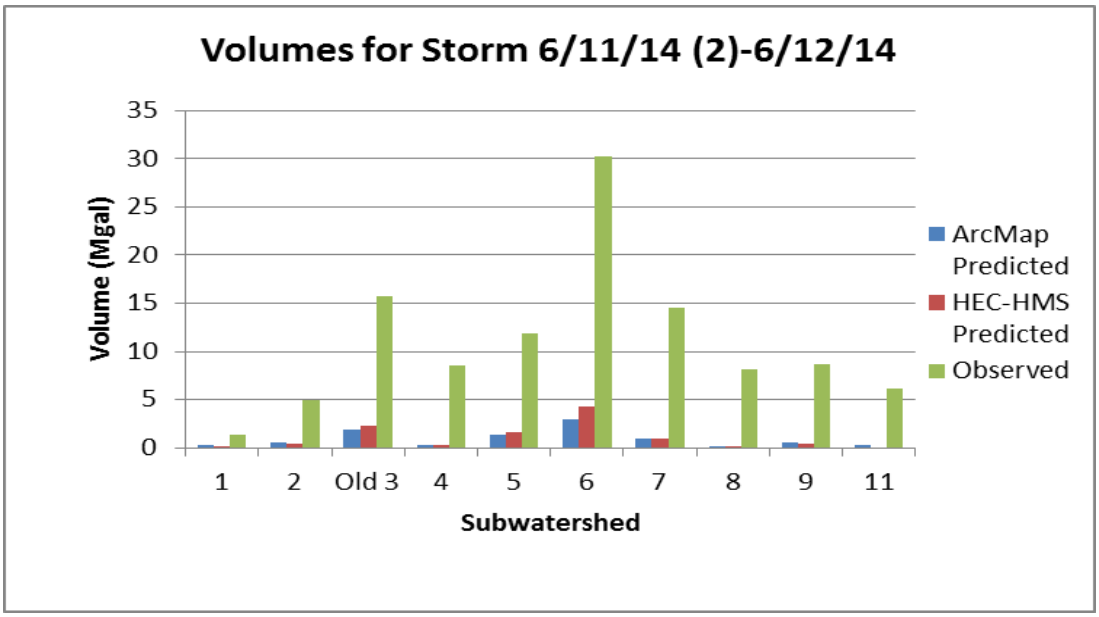

Figure A.20: Volume comparison graph for storm event 6/11/14-6/12/14 of 0.10 inches

Table A.20: Volume and flow rate comparison table for storm event 6/11/14-6/12/14 of 0.10 inches with rainfall runoff ratios calculated

Subwatershed	GIS Volume Summed (Mgal)	HEC-HMS Volume Summed (Mgal)	Sensor Volume (Mgal)	Runoff (ft)	Ratio	Sensor Peak Flow (cms)	HEC-HMS Peak Flow (cms)
1	0.23	0.18	1.36	0.05	5.86	5.01	0.10
2	0.60	0.45	4.98	0.07	8.26	1.55	0.10
Old 3	1.93	2.32	15.78	0.07	8.17	2.74	0.10
4	0.29	0.32	8.50	0.24	28.82	1.59	0.00
5	1.41	1.56	11.93	0.07	8.46	1.56	0.10
6	2.93	4.28	30.27	0.09	10.33	15.55	0.40
7	0.96	1.00	14.49	0.13	15.14	0.00	0.00
8	0.08	0.05	8.15	0.84	100.29	2.93	0.00
9	0.49	0.37	8.73	0.15	17.82	1.22	0.10
11	0.22		6.12	0.23	27.49	2.96	

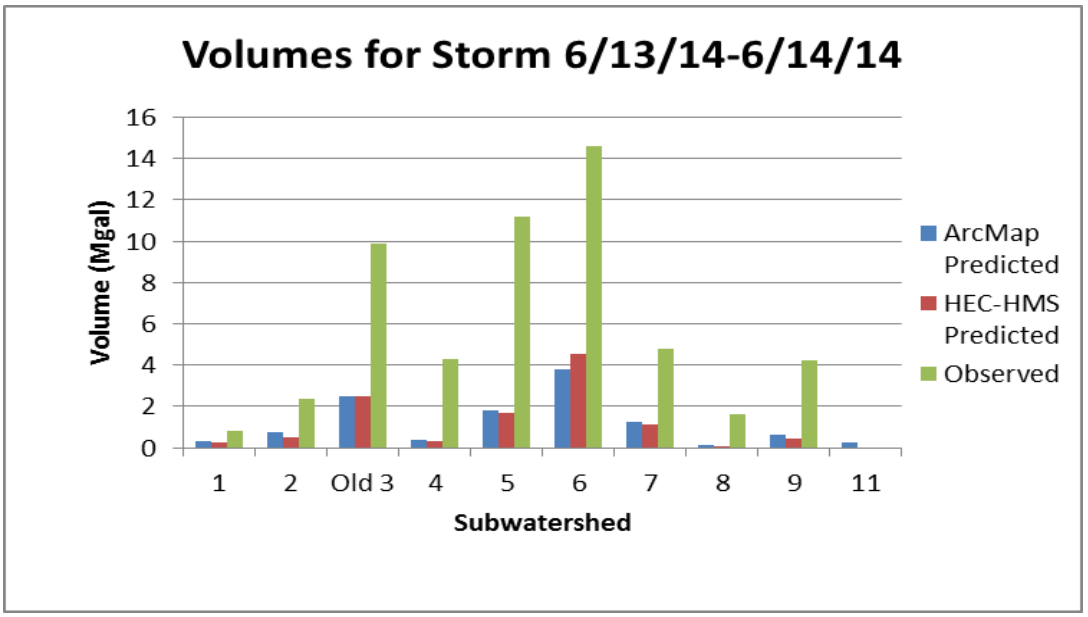

Figure A.21: Volume comparison graph for storm event 6/13/14-6/14/14 of 0.13 inches

Table A.21: Volume and flow rate comparison table for storm event 6/13/14-6/14/14 of 0.13 inches with rainfall runoff ratios calculated

Subwatershed	GIS Volume Summed (Mgal)	HEC-HMS Volume Summed (Mgal)	Sensor Volume (Mgal)	Runoff (ft)	Ratio	Sensor Peak Flow (cms)	HEC-HMS Peak Flow (cms)
1	0.30	0.24	0.81	0.03	2.68	4.66	0.10
2	0.78	0.50	2.34	0.03	2.99	1.55	0.10
Old 3	2.51	2.51	9.86	0.04	3.93	2.74	0.10
4	0.38	0.34	4.29	0.12	11.20	1.59	0.10
5	1.83	1.69	11.17	0.07	6.09	1.58	0.10
6	3.81	4.57	14.63	0.04	3.84	13.44	0.40
7	1.24	1.14	4.77	0.04	3.83	0.00	0.00
8	0.11	0.08	1.61	0.17	15.28	2.81	0.00
9	0.64	0.42	4.22	0.07	6.62	1.22	0.10
11	0.29		0.00	0.00	0.00	0.00	

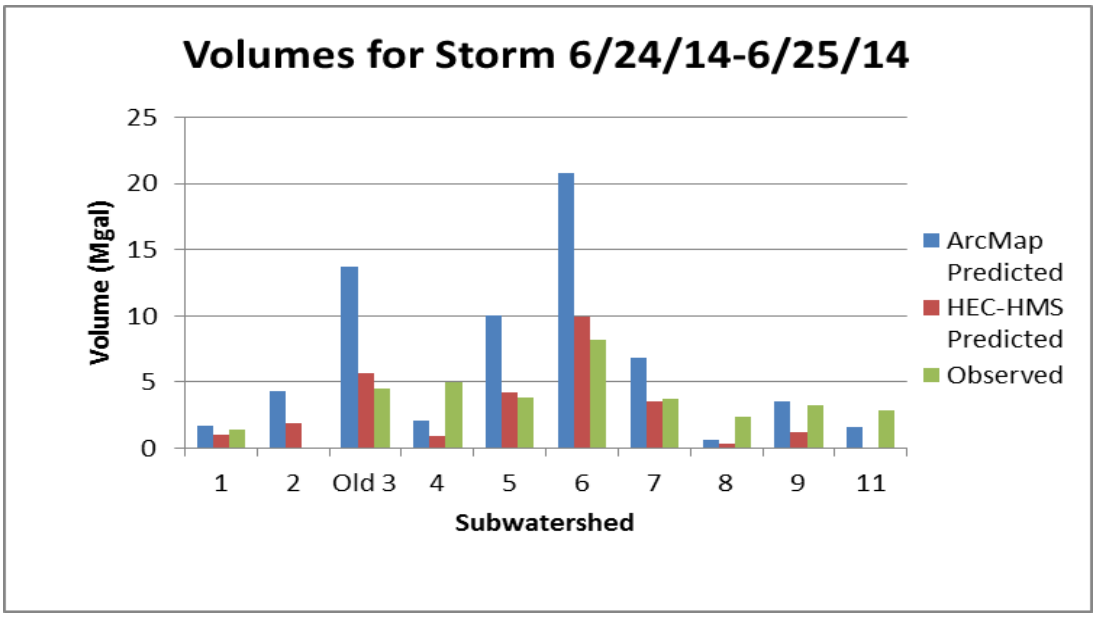

Figure A.22: Volume comparison graph for storm event 6/24/14-6/25/14 of 0.71 inches

Table A.22: Volume and flow rate comparison table for storm event 6/24/14-6/25/14 of 0.71 inches with rainfall runoff ratios calculated

Subwatershed	GIS Volume Summed (Mgal)	HEC-HMS Volume Summed (Mgal)	Sensor Volume (Mgal)	Runoff (ft)	Ratio	Sensor Peak Flow (cms)	HEC-HMS Peak Flow (cms)
1	1.65	0.95	1.33	0.05	0.81	5.01	0.50
2	4.28	1.90	0.00	0.00	0.00	0.00	0.80
Old 3	13.71	5.65	4.50	0.02	0.33	2.74	0.30
4	2.09	0.85	4.92	0.14	2.35	1.77	0.30
5	10.01	4.17	3.80	0.02	0.38	1.58	0.60
6	20.81	9.96	8.18	0.02	0.39	12.65	1.70
7	6.80	3.54	3.68	0.03	0.54	0.00	0.10
8	0.58	0.32	2.35	0.24	4.07	2.94	0.20
9	3.48	1.22	3.21	0.05	0.92	1.22	0.40
11	1.58		2.78	0.10	1.76	2.76	

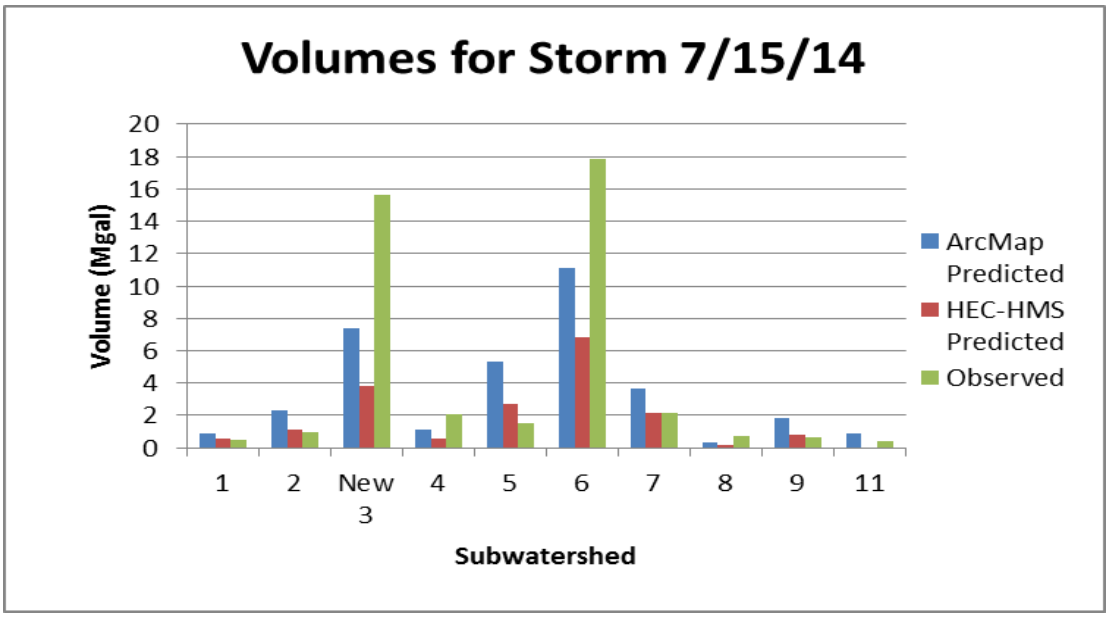

Figure A.23: Volume comparison graph for storm event 7/15/14 of 0.38 inches

Table A.23: Volume and flow rate comparison table for storm event 7/15/14 of 0.38 inches with rainfall runoff ratios calculated

Subwatershed	GIS Volume Summed (Mgal)	HEC-HMS Volume Summed (Mgal)	Sensor Volume (Mgal)	Runoff (ft)	Ratio	Sensor Peak Flow (cms)	HEC-HMS Peak Flow (cms)
1	0.88	0.53	0.52	0.02	0.59	5.00	0.30
2	2.29	1.11	0.92	0.01	0.40	1.54	0.40
New 3	7.40	3.86	15.64	0.07	2.13	4.93	0.20
4	1.14	0.55	2.08	0.06	1.85	1.78	0.10
5	5.36	2.75	1.49	0.01	0.28	1.41	0.30
6	11.14	6.87	17.82	0.05	1.60	13.41	1.00
7	3.64	2.17	2.17	0.02	0.60	4.38	0.00
8	0.31	0.18	0.73	0.07	2.36	2.94	0.10
9	1.86	0.77	0.68	0.01	0.37	0.98	0.20
11	0.85		0.45	0.02	0.53	2.45	

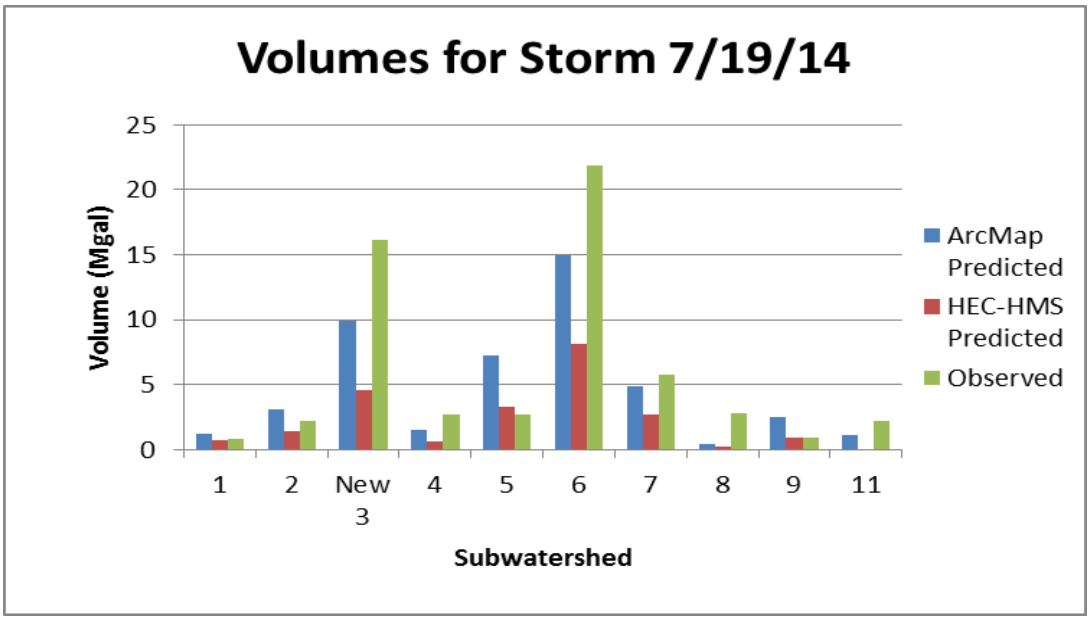

Figure A.24: Volume comparison graph for storm event 7/19/14 of 0.51 inches

Table A.24: Volume and flow rate comparison table for storm event 7/19/14 of 0.51 inches with rainfall runoff ratios calculated

Subwatershed	GIS Volume Summed (Mgal)	HEC-HMS Volume Summed (Mgal)	Sensor Volume (Mgal)	Runoff (ft)	Ratio	Sensor Peak Flow (cms)	HEC-HMS Peak Flow (cms)
1	1.19	0.69	0.79	0.03	0.67	4.77	0.30
2	3.08	1.40	2.16	0.03	0.70	1.55	0.60
New 3	9.93	4.57	16.15	0.07	1.64	5.12	0.20
4	1.53	0.66	2.69	0.08	1.79	1.28	0.20
5	7.19	3.33	2.65	0.02	0.37	1.59	0.40
6	14.96	8.08	21.87	0.06	1.46	10.54	1.30
7	4.88	2.67	5.72	0.05	1.17	10.18	0.00
8	0.41	0.24	2.77	0.28	6.68	2.91	0.10
9	2.50	0.95	0.96	0.02	0.39	0.68	0.30
11	1.14		2.21	0.08	1.95	3.04	

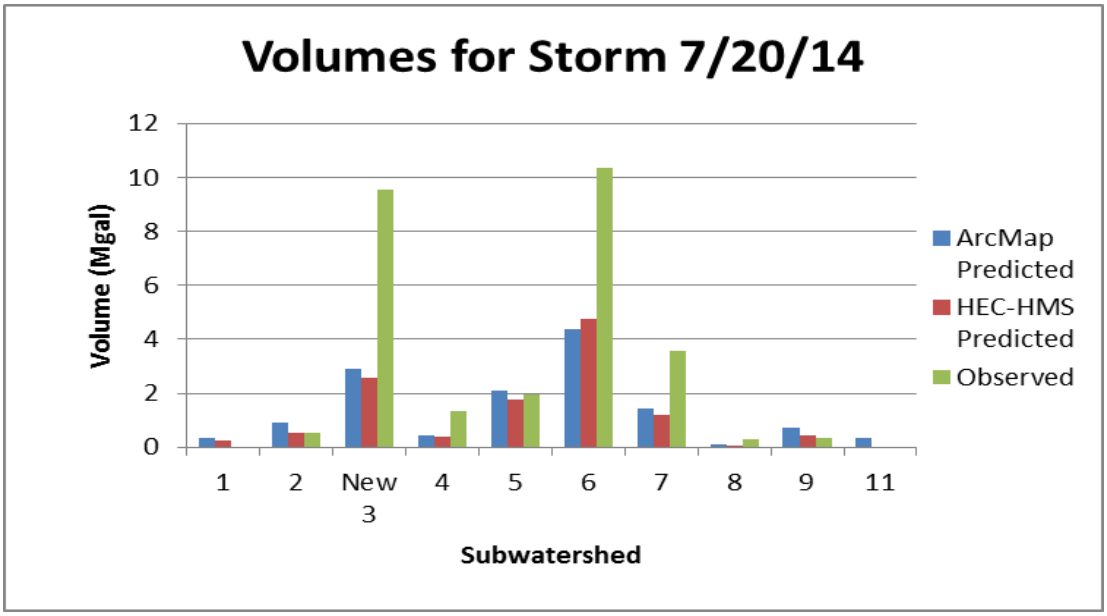

Figure A.25: Volume comparison graph for storm event 7/20/14 of 0.15 inches

Table A.25: Volume and flow rate comparison table for storm event 7/20/14 of 0.15 inches with rainfall runoff ratios calculated

Subwatershed	GIS Volume Summed (Mgal)	HEC-HMS Volume Summed (Mgal)	Sensor Volume (Mgal)	Runoff (ft)	Ratio	Sensor Peak Flow (cms)	HEC-HMS Peak Flow (cms
1	0.35	0.24	0.00	0.00	0.00	3.46	0.10
2	0.90	0.55	0.53	0.01	0.59	1.55	0.20
New 3	2.92	2.59	9.54	0.04	3.29	4.93	0.10
4	0.45	0.37	1.33	0.04	3.00	1.12	0.10
5	2.12	1.77	1.95	0.01	0.92	1.49	0.10
6	4.40	4.76	10.37	0.03	2.36	10.99	0.50
7	1.44	1.22	3.59	0.03	2.50	10.18	0.00
8	0.12	0.08	0.29	0.03	2.39	2.04	0.00
9	0.74	0.45	0.33	0.01	0.45	0.53	0.10
11	0.33		0.00	0.00	0.00	0.00	

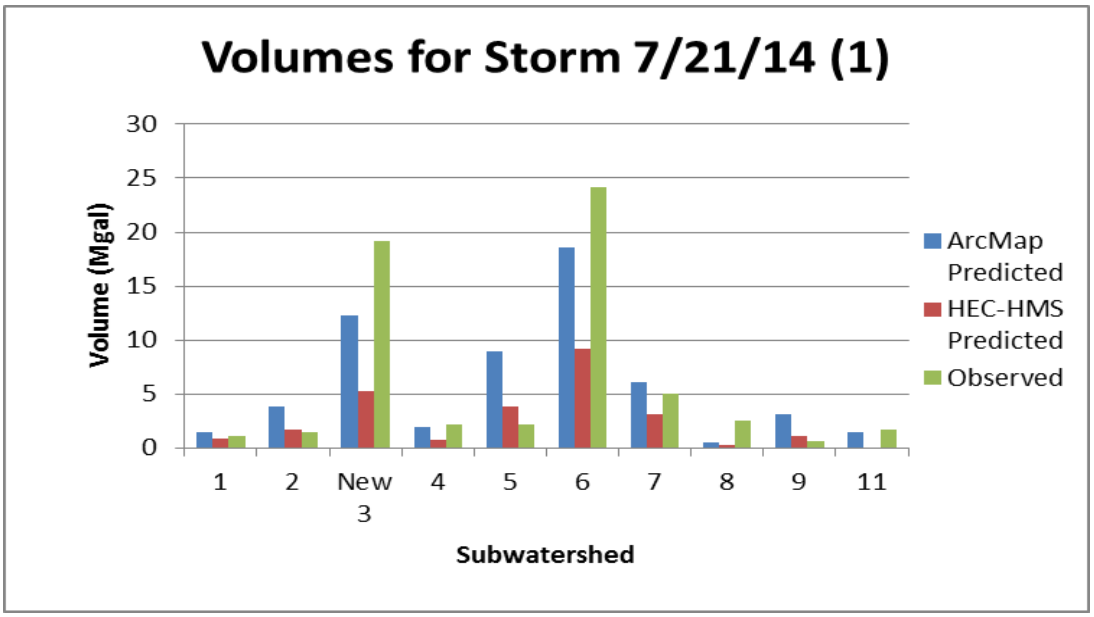

Figure A.26: Volume comparison graph for storm event 7/21/14 of 0.63 inches

Table A.26: Volume and flow rate comparison table for storm event 7/21/14 of 0.63 inches with rainfall runoff ratios calculated

Subwatershed	GIS Volume Summed (Mgal)	HEC-HMS Volume Summed (Mgal)	Sensor Volume (Mgal)	Runoff (ft)	Ratio	Sensor Peak Flow (cms)	HEC-HMS Peak Flow (cms
1	1.47	0.85	1.06	0.04	0.72	4.78	0.40
2	3.82	1.69	1.51	0.02	0.39	1.55	0.70
New 3	12.32	5.20	19.11	0.08	1.56	5.12	0.30
4	1.89	0.77	2.18	0.06	1.17	1.53	0.20
5	8.92	3.83	2.10	0.01	0.24	1.57	0.50
6	18.55	9.19	24.16	0.07	1.30	9.87	1.60
7	6.06	3.17	5.05	0.04	0.83	8.53	0.10
8	0.51	0.26	2.49	0.26	4.84	2.92	0.20
9	3.10	1.11	0.57	0.01	0.18	0.50	0.40
11	1.41		1.65	0.06	1.17	2.19	

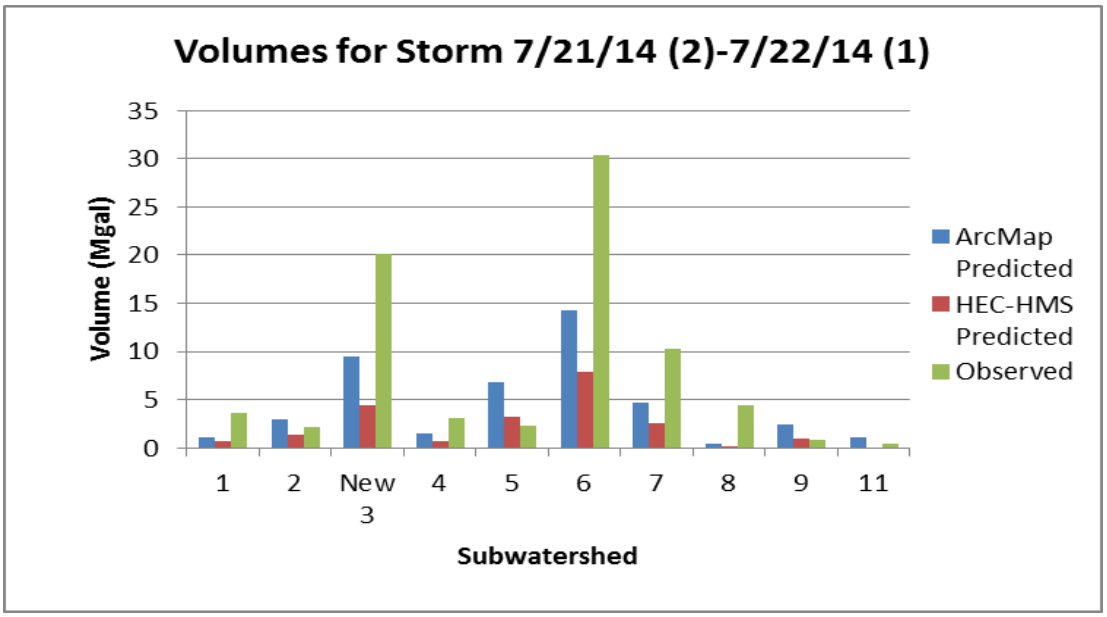

Figure A.27: Volume comparison graph for storm event 7/21/14-7/22/14 of 0.49 inches

Table A.27: Volume and flow rate comparison table for storm event 7/21/14-7/22/14 of 0.49 inches with rainfall runoff ratios calculated

Subwatershed	GIS Volume Summed (Mgal)	HEC-HMS Volume Summed (Mgal)	Sensor Volume (Mgal)	Runoff (ft)	Ratio	Sensor Peak Flow (cms)	HEC-HMS Peak Flow (cms
1	1.13	0.66	3.65	0.13	3.22	3.46	0.30
2	2.94	1.37	2.21	0.03	0.75	1.55	0.50
New 3	9.50	4.46	20.12	0.09	2.14	5.12	0.20
4	1.46	0.66	3.09	0.09	2.15	1.28	0.20
5	6.88	3.25	2.24	0.01	0.33	1.64	0.40
6	14.30	7.90	30.39	0.09	2.13	12.53	1.20
7	4.67	2.59	10.27	0.09	2.20	6.65	0.00
8	0.40	0.21	4.40	0.45	11.11	2.94	0.10
9	2.39	0.92	0.77	0.01	0.32	0.40	0.30
11	1.09		0.42	0.02	0.39	1.19	

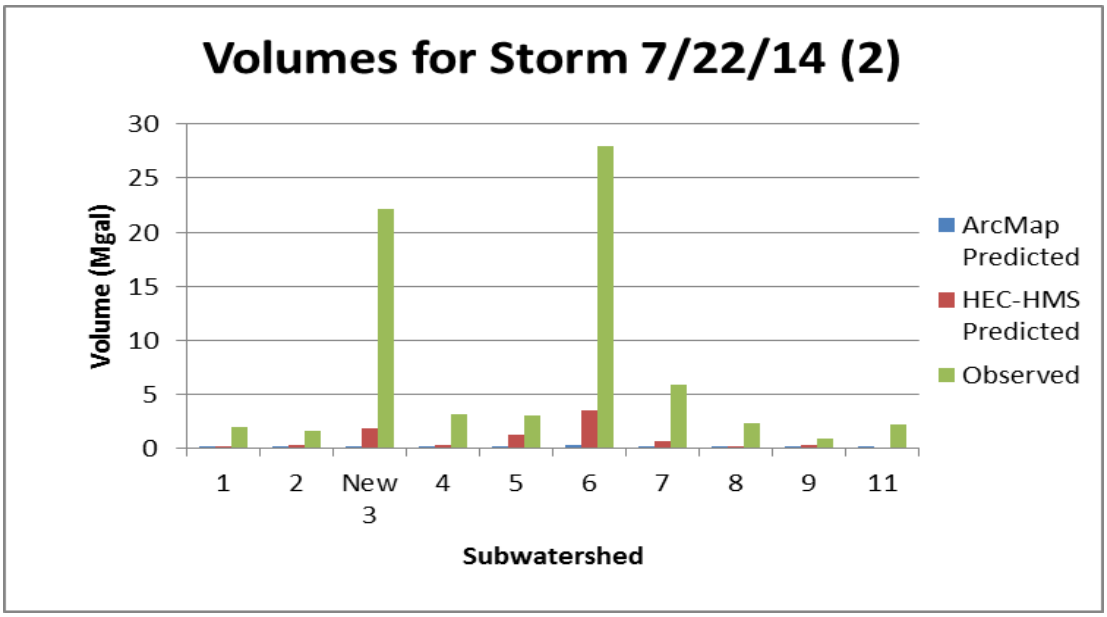

Figure A.28: Volume comparison graph for storm event 7/22/14 of 0.01 inches

Table A.28: Volume and flow rate comparison table for storm event 7/22/14 of 0.01 inches with rainfall runoff ratios calculated

Subwatershed	GIS Volume Summed (Mgal)	HEC-HMS Volume Summed (Mgal)	Sensor Volume (Mgal)	Runoff (ft)	Ratio	Sensor Peak Flow (cms)	HEC-HMS Peak Flow (cms
1	0.02	0.08	1.90	0.07	82.06	4.44	0.00
2	0.06	0.24	1.62	0.02	26.90	1.55	0.00
New 3	0.19	1.82	22.18	0.10	115.35	4.75	0.00
4	0.03	0.24	3.10	0.09	105.38	1.59	0.00
5	0.14	1.16	3.05	0.02	21.72	1.52	0.00
6	0.29	3.46	27.97	0.08	95.81	12.35	0.20
7	0.10	0.66	5.79	0.05	60.72	11.61	0.00
8	0.01	0.03	2.27	0.23	280.60	2.93	0.00
9	0.05	0.24	0.85	0.01	17.35	0.91	0.00
11	0.02		2.14	0.08	96.62	2.32	

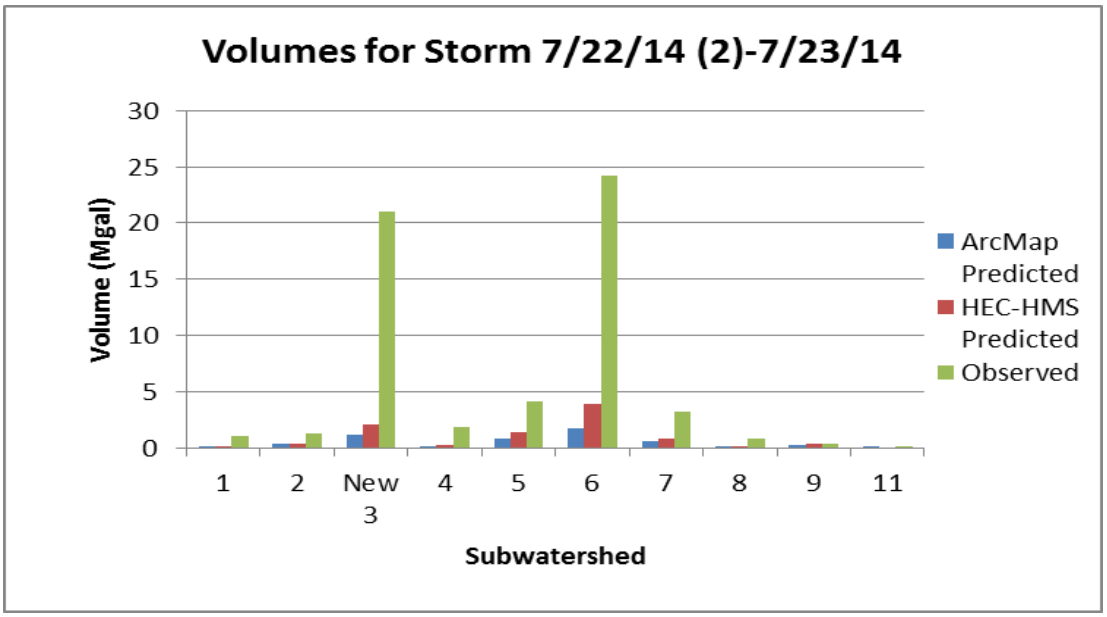

Figure A.29: Volume comparison graph for storm event 7/22/14-7/23/14 of 0.06 inches

Table A.29: Volume and flow rate comparison table for storm event 7/22/14-7/23/14 of 0.06 inches with rainfall runoff ratios calculated

Subwatershed	GIS Volume Summed (Mgal)	HEC-HMS Volume Summed (Mgal)	Sensor Volume (Mgal)	Runoff (ft)	Ratio	Sensor Peak Flow (cms)	HEC-HMS Peak Flow (cms)
1	0.14	0.13	1.04	0.04	7.45	4.66	0.00
2	0.36	0.34	1.32	0.02	3.65	1.55	0.10
New 3	1.17	2.09	20.99	0.09	18.12	4.80	0.10
4	0.18	0.29	1.79	0.05	10.10	1.25	0.00
5	0.85	1.37	4.18	0.02	4.94	1.45	0.10
6	1.76	3.91	24.17	0.07	13.74	12.63	0.30
7	0.57	0.85	3.18	0.03	5.54	10.50	0.00
8	0.05	0.05	0.82	0.08	16.81	2.93	0.00
9	0.29	0.32	0.31	0.01	1.06	1.13	0.00
11	0.13		0.14	0.01	1.02	0.82	

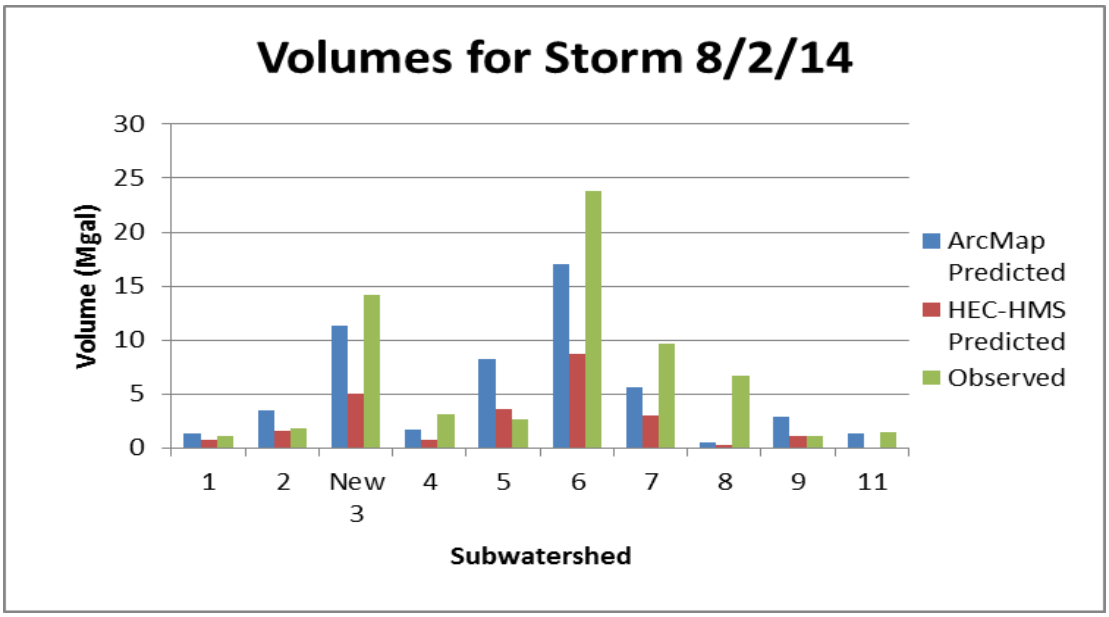

Figure A.30: Volume comparison graph for storm event 8/2/14 of 0.58 inches

Table A.30: Volume and flow rate comparison table for storm event 8/2/14 of 0.58 inches with rainfall runoff ratios calculated

Subwatershed	GIS Volume Summed (Mgal)	HEC-HMS Volume Summed (Mgal)	Sensor Volume (Mgal)	Runoff (ft)	Ratio	Sensor Peak Flow (cms)	HEC-HMS Peak Flow (cms)
1	1.35	0.77	1.11	0.04	0.82	2.67	0.40
2	3.50	1.59	1.83	0.03	0.52	1.55	0.60
New 3	11.30	4.97	14.21	0.06	1.27	5.12	0.20
4	1.73	0.74	3.10	0.09	1.81	1.18	0.20
5	8.18	3.65	2.63	0.02	0.32	1.58	0.50
6	17.01	8.72	23.86	0.07	1.40	8.57	1.50
7	5.55	2.99	9.65	0.08	1.74	11.88	0.10
8	0.47	0.26	6.71	0.69	14.24	2.94	0.10
9	2.84	1.06	1.04	0.02	0.36	0.48	0.30
11	1.29		1.42	0.05	1.10	1.51	

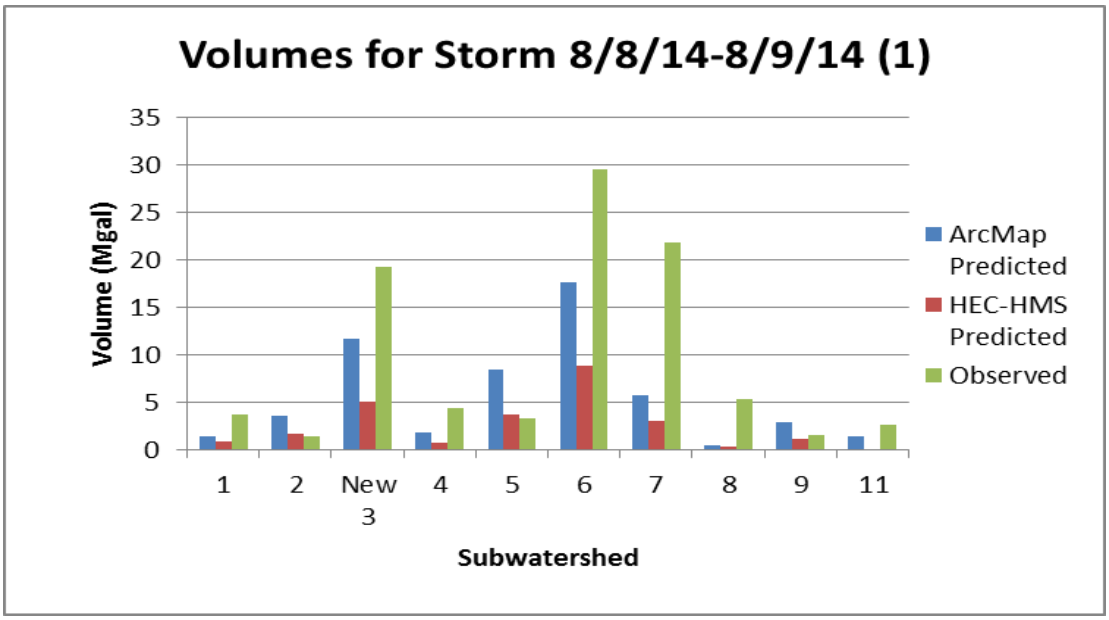

Figure A.31: Volume comparison graph for storm event 8/8/14-8/9/14 of 0.60 inches

Table A.31: Volume and flow rate comparison table for storm event 8/8/14-8/9/14 of 0.60 inches with rainfall runoff ratios calculated

Subwatershed	GIS Volume Summed (Mgal)	HEC-HMS Volume Summed (Mgal)	Sensor Volume (Mgal)	Runoff (ft)	Ratio	Sensor Peak Flow (cms)	HEC-HMS Peak Flow (cms)
1	1.40	0.79	3.67	0.13	2.63	4.99	0.40
2	3.62	1.61	1.38	0.02	0.38	1.51	0.70
New 3	11.69	5.07	19.27	0.08	1.66	5.09	0.30
4	1.79	0.74	4.43	0.13	2.50	1.69	0.20
5	8.46	3.72	3.29	0.02	0.39	1.60	0.50
6	17.60	8.90	29.63	0.08	1.68	7.90	1.50
7	5.74	3.04	21.80	0.19	3.79	8.15	0.10
8	0.49	0.26	5.31	0.54	10.89	2.94	0.10
9	2.94	1.08	1.60	0.03	0.54	1.10	0.30
11	1.34		2.68	0.10	2.00	3.03	

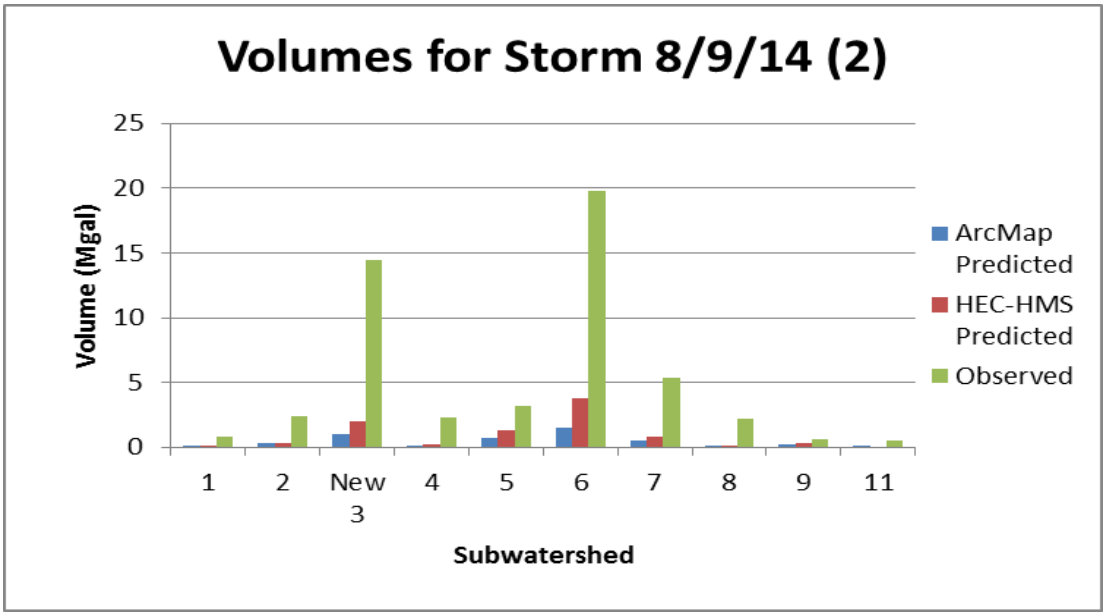

Figure A.32: Volume comparison graph for storm event 8/9/14 of 0.05 inches

Table A.32: Volume and flow rate comparison table for storm event 8/9/14 of 0.05 inches with rainfall runoff ratios calculated

Subwatershed	GIS Volume Summed (Mgal)	HEC-HMS Volume Summed (Mgal)	Sensor Volume (Mgal)	Runoff (ft)	Ratio	Sensor Peak Flow (cms)	HEC-HMS Peak Flow (cms)
1	0.12	0.13	0.80	0.03	6.90	4.25	0.00
2	0.30	0.32	2.41	0.03	7.99	1.55	0.10
New 3	0.97	2.03	14.43	0.06	14.93	5.12	0.00
4	0.15	0.26	2.26	0.06	15.31	1.24	0.00
5	0.71	1.32	3.16	0.02	4.48	1.49	0.10
6	1.47	3.83	19.83	0.06	13.52	9.51	0.30
7	0.48	0.82	5.40	0.05	11.27	9.87	0.00
8	0.04	0.05	2.18	0.22	53.65	2.90	0.00
9	0.25	0.29	0.66	0.01	2.68	1.18	0.00
11	0.11		0.54	0.02	4.80	1.57	

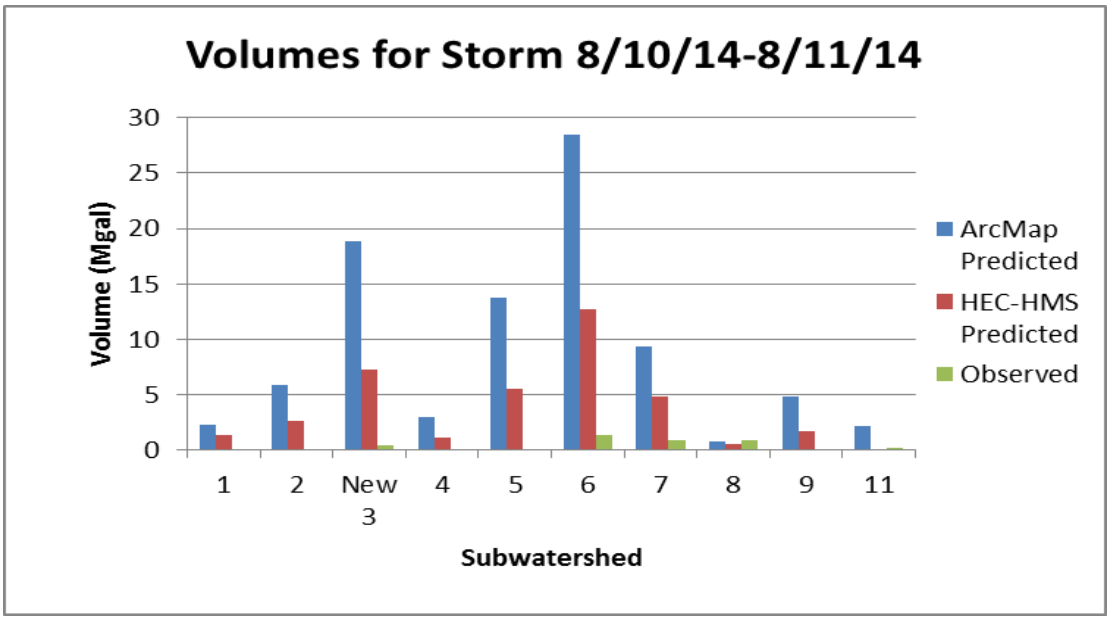

Figure A.33: Volume comparison graph for storm event 8/10/14-8/11/14 of 0.97 inches

Table A.33: Volume and flow rate comparison table for storm event 8/10/14-8/11/14 of 0.97 inches with rainfall runoff ratios calculated

Subwatershed	GIS Volume Summed (Mgal)	HEC-HMS Volume Summed (Mgal)	Sensor Volume (Mgal)	Runoff (ft)	Ratio	Sensor Peak Flow (cms)	HEC-HMS Peak Flow (cms)
1	2.26	1.32	0.00	0.00	0.00	0.00	0.70
2	5.85	2.64	0.00	0.00	0.00	0.00	1.10
New 3	18.89	7.26	0.44	0.00	0.02	2.75	0.40
4	2.90	1.08	0.00	0.00	0.00	0.00	0.40
5	13.68	5.44	0.00	0.00	0.00	0.00	0.70
6	28.45	12.73	1.29	0.00	0.05	9.99	2.40
7	9.29	4.81	0.85	0.01	0.09	0.00	0.10
8	0.79	0.45	0.85	0.09	1.08	1.96	0.20
9	4.76	1.66	0.00	0.00	0.00	0.00	0.50
11	2.16		0.19	0.01	0.09	1.27	

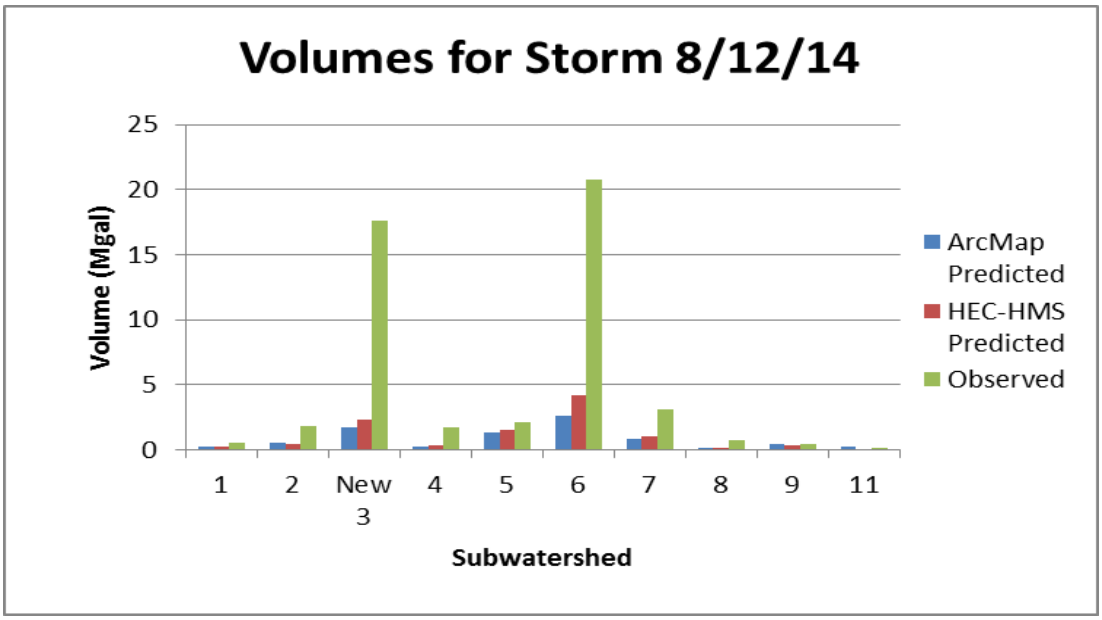

Figure A.34: Volume comparison graph for storm event 8/12/14 of 0.09 inches

Table A.34: Volume and flow rate comparison table for storm event 8/12/14 of 0.09 inches with rainfall runoff ratios calculated

Subwatershed	GIS Volume Summed (Mgal)	HEC-HMS Volume Summed (Mgal)	Sensor Volume (Mgal)	Runoff (ft)	Ratio	Sensor Peak Flow (cms)	HEC-HMS Peak Flow (cms)
1	0.21	0.18	0.57	0.02	2.70	4.64	0.10
2	0.54	0.42	1.84	0.03	3.40	1.55	0.10
New 3	1.75	2.27	17.66	0.08	10.16	5.06	0.10
4	0.27	0.32	1.70	0.05	6.41	1.31	0.00
5	1.27	1.51	2.10	0.01	1.65	1.52	0.10
6	2.64	4.20	20.74	0.06	7.86	8.57	0.30
7	0.86	0.98	3.08	0.03	3.58	8.38	0.00
8	0.07	0.05	0.68	0.07	9.24	2.92	0.00
9	0.44	0.34	0.46	0.01	1.04	0.78	0.10
11	0.20		0.01	0.00	0.04	0.09	

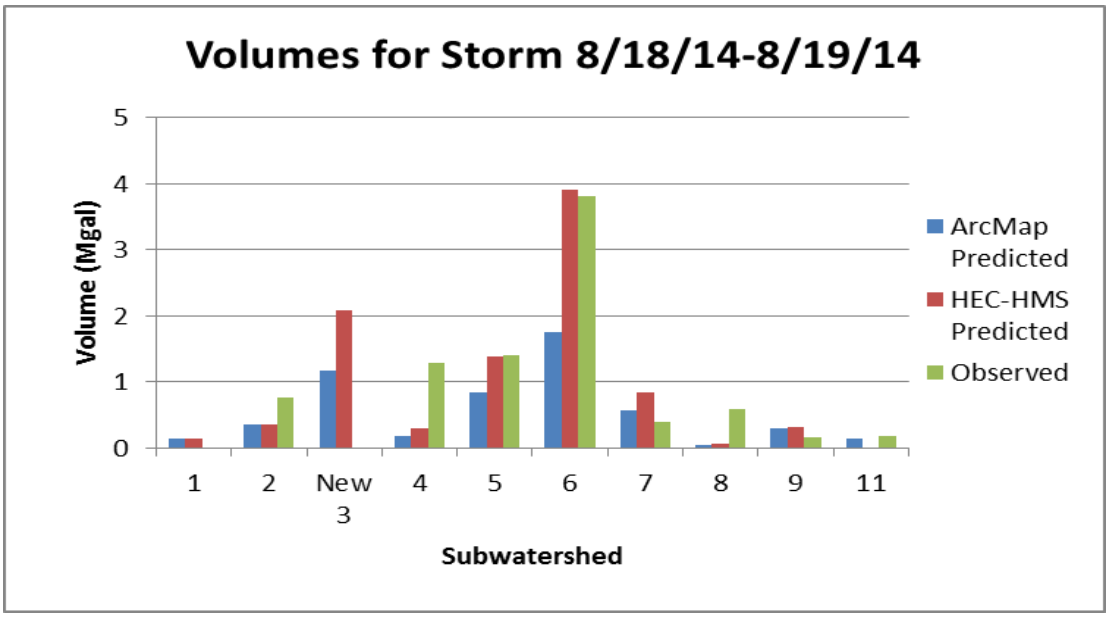

Figure A.35: Volume comparison graph for storm event 8/18/14-8/19/14 of 0.06 inches

Table A.35: Volume and flow rate comparison table for storm event 8/18/14-8/19/14 of 0.06 inches with rainfall runoff ratios calculated

Subwatershed	GIS Volume Summed (Mgal)	HEC-HMS Volume Summed (Mgal)	Sensor Volume (Mgal)	Runoff (ft)	Ratio	Sensor Peak Flow (cms)	HEC-HMS Peak Flow (cms)
1	0.14	0.13	0.00	0.00	0.00	0.00	0.00
2	0.36	0.34	0.76	0.01	2.10	1.44	0.10
New 3	1.17	2.09	0.00	0.00	0.00	0.00	0.10
4	0.18	0.29	1.28	0.04	7.22	1.47	0.00
5	0.85	1.37	1.39	0.01	1.64	1.34	0.10
6	1.76	3.91	3.80	0.01	2.16	8.90	0.30
7	0.57	0.85	0.39	0.00	0.68	4.96	0.00
8	0.05	0.05	0.59	0.06	12.15	2.73	0.00
9	0.29	0.32	0.16	0.00	0.56	0.39	0.00
11	0.13		0.17	0.01	1.29	1.23	

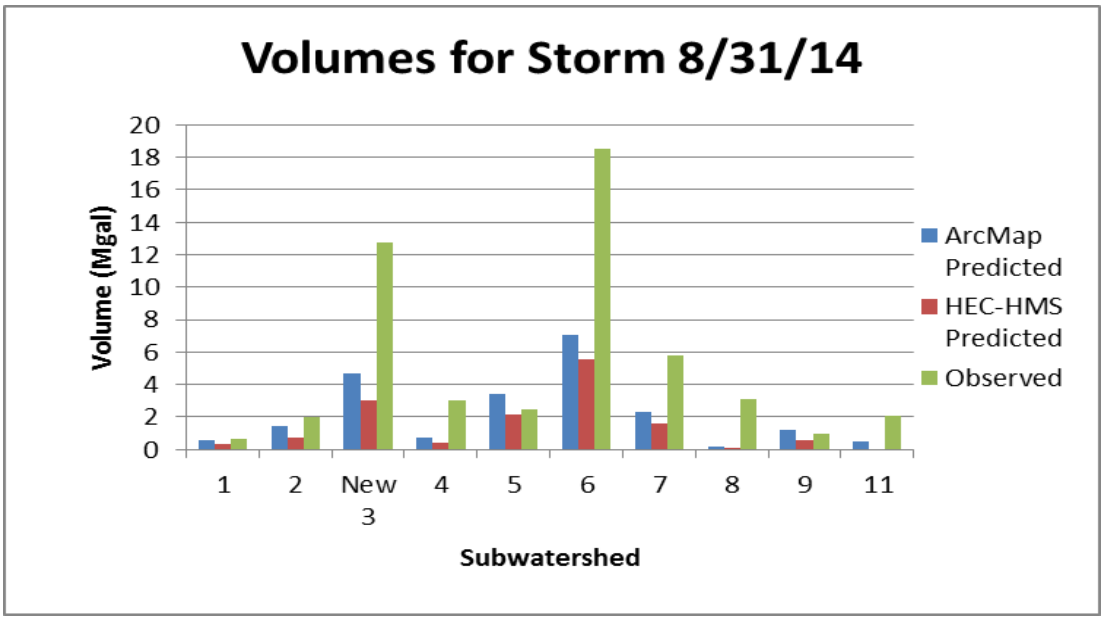

Figure A.36: Volume comparison graph for storm event 8/31/14 of 0.24 inches

Table A.36: Volume and flow rate comparison table for storm event 8/31/14 of 0.24 inches with rainfall runoff ratios calculated

Subwatershed	GIS Volume Summed (Mgal)	HEC-HMS Volume Summed (Mgal)	Sensor Volume (Mgal)	Runoff (ft)	Ratio	Sensor Peak Flow (cms)	HEC-HMS Peak Flow (cms)
1	0.56	0.37	0.67	0.02	1.20	4.68	0.20
2	1.45	0.77	2.02	0.03	1.40	1.55	0.30
New 3	4.67	3.06	12.77	0.06	2.76	5.12	0.10
4	0.72	0.45	3.03	0.09	4.28	1.81	0.10
5	3.39	2.14	2.46	0.01	0.73	1.60	0.20
6	7.04	5.57	18.53	0.05	2.63	9.47	0.70
7	2.30	1.59	5.76	0.05	2.51	5.96	0.00
8	0.20	0.11	3.07	0.31	15.74	2.93	0.10
9	1.18	0.55	1.01	0.02	0.86	1.02	0.10
11	0.53		2.04	0.08	3.82	2.37	

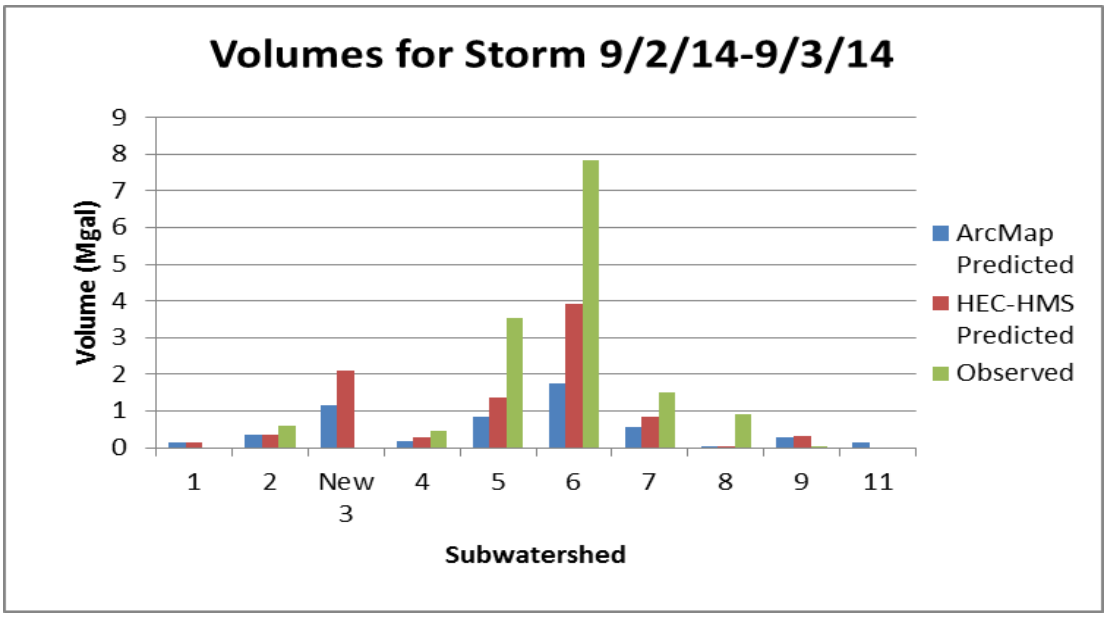

Figure A.37: Volume comparison graph for storm event 9/2/14-9/3/14 of 0.06 inches

Table A.37: Volume and flow rate comparison table for storm event 9/2/14-9/3/14 of 0.06 inches with rainfall runoff ratios calculated

Subwatershed	GIS Volume Summed (Mgal)	HEC-HMS Volume Summed (Mgal)	Sensor Volume (Mgal)	Runoff (ft)	Ratio	Sensor Peak Flow (cms)	HEC-HMS Peak Flow (cms)
1	0.14	0.13	0.00	0.00	0.00	0.00	0.00
2	0.36	0.34	0.60	0.01	1.66	1.50	0.10
New 3	1.17	2.09	0.00	0.00	0.00	0.00	0.10
4	0.18	0.29	0.45	0.01	2.56	0.75	0.00
5	0.85	1.37	3.52	0.02	4.16	1.33	0.10
6	1.76	3.91	7.84	0.02	4.46	13.78	0.30
7	0.57	0.85	1.50	0.01	2.61	2.76	0.00
8	0.05	0.05	0.90	0.09	18.45	2.78	0.00
9	0.29	0.32	0.01	0.00	0.04	0.07	0.00
11	0.13		0.00	0.00	0.00	0.00	

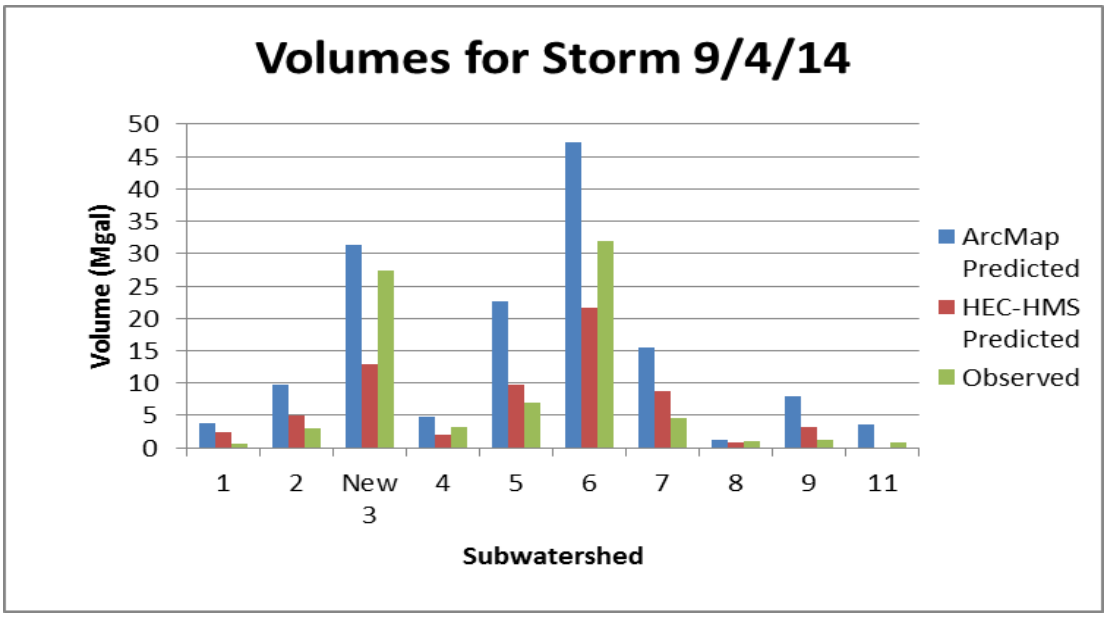

Figure A.38: Volume comparison graph for storm event 9/4/14 of 1.61 inches

Table A.38: Volume and flow rate comparison table for storm event 9/4/14 of 1.61 inches with rainfall runoff ratios calculated

Subwatershed	GIS Volume Summed (Mgal)	HEC-HMS Volume Summed (Mgal)	Sensor Volume (Mgal)	Runoff (ft)	Ratio	Sensor Peak Flow (cms)	HEC-HMS Peak Flow (cms)
1	3.75	2.40	0.68	0.02	0.18	4.52	1.30
2	9.71	4.94	2.93	0.04	0.30	1.54	2.00
New 3	31.36	12.87	27.47	0.12	0.88	5.12	0.70
4	4.81	1.95	3.20	0.09	0.67	1.80	0.70
5	22.71	9.75	7.00	0.04	0.31	1.63	1.40
6	47.21	21.71	32.02	0.09	0.68	8.74	4.40
7	15.42	8.66	4.55	0.04	0.29	10.58	0.20
8	1.31	0.82	0.93	0.10	0.71	2.94	0.50
9	7.89	3.20	1.32	0.02	0.17	1.31	1.10
11	3.58		0.87	0.03	0.24	2.43	

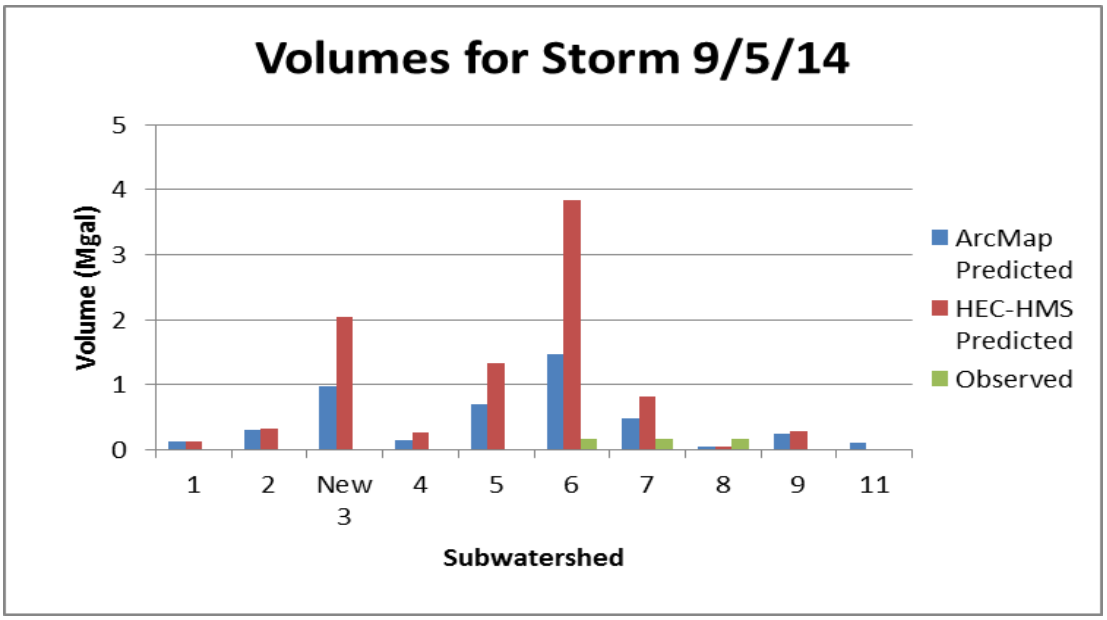

Figure A.39: Volume comparison graph for storm event 9/5/14 of 0.05 inches

Table A.39: Volume and flow rate comparison table for storm event 9/5/14 of 0.05 inches with rainfall runoff ratios calculated

Subwatershed	GIS Volume Summed (Mgal)	HEC-HMS Volume Summed (Mgal)	Sensor Volume (Mgal)	Runoff (ft)	Ratio	Sensor Peak Flow (cms)	HEC-HMS Peak Flow (cms)
1	0.12	0.13	0.00	0.00	0.00	0.00	0.00
2	0.30	0.32	0.00	0.00	0.00	0.00	0.10
New 3	0.97	2.03	0.00	0.00	0.00	0.00	0.00
4	0.15	0.26	0.00	0.00	0.00	0.00	0.00
5	0.71	1.32	0.00	0.00	0.00	0.00	0.10
6	1.47	3.83	0.16	0.00	0.11	0.00	0.30
7	0.48	0.82	0.16	0.00	0.33	0.00	0.00
8	0.04	0.05	0.16	0.02	3.94	2.04	0.00
9	0.25	0.29	0.00	0.00	0.00	0.00	0.00
11	0.11		0.00	0.00	0.00	0.00	

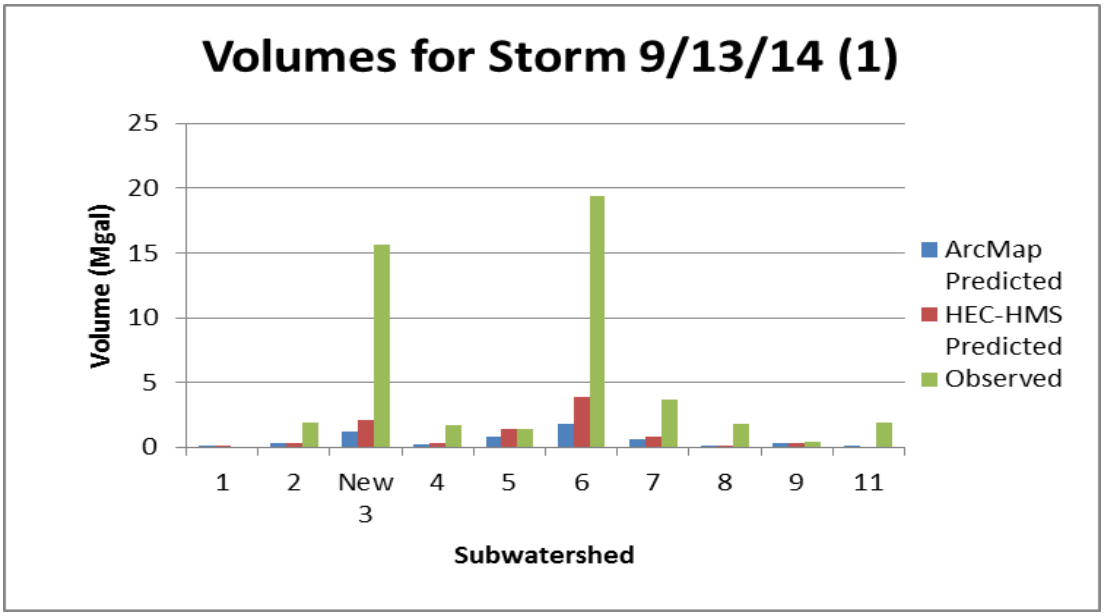

Figure A.40: Volume comparison graph for storm event 9/13/14 of 0.06 inches

Table A.40: Volume and flow rate comparison table for storm event 9/13/14 of 0.06 inches with rainfall runoff ratios calculated

Subwatershed	GIS Volume Summed (Mgal)	HEC-HMS Volume Summed (Mgal)	Sensor Volume (Mgal)	Runoff (ft)	Ratio	Sensor Peak Flow (cms)	HEC-HMS Peak Flow (cms)
1	0.14	0.13	0.00	0.00	0.00	0.00	0.00
2	0.36	0.34	1.93	0.03	5.32	1.54	0.10
New 3	1.17	2.09	15.65	0.07	13.51	5.12	0.10
4	0.18	0.29	1.71	0.05	9.68	1.31	0.00
5	0.85	1.37	1.37	0.01	1.62	1.55	0.10
6	1.76	3.91	19.35	0.06	11.00	9.90	0.30
7	0.57	0.85	3.70	0.03	6.45	6.59	0.00
8	0.05	0.05	1.78	0.18	36.44	2.93	0.00
9	0.29	0.32	0.40	0.01	1.37	1.03	0.00
11	0.13		1.90	0.07	14.21	2.01	

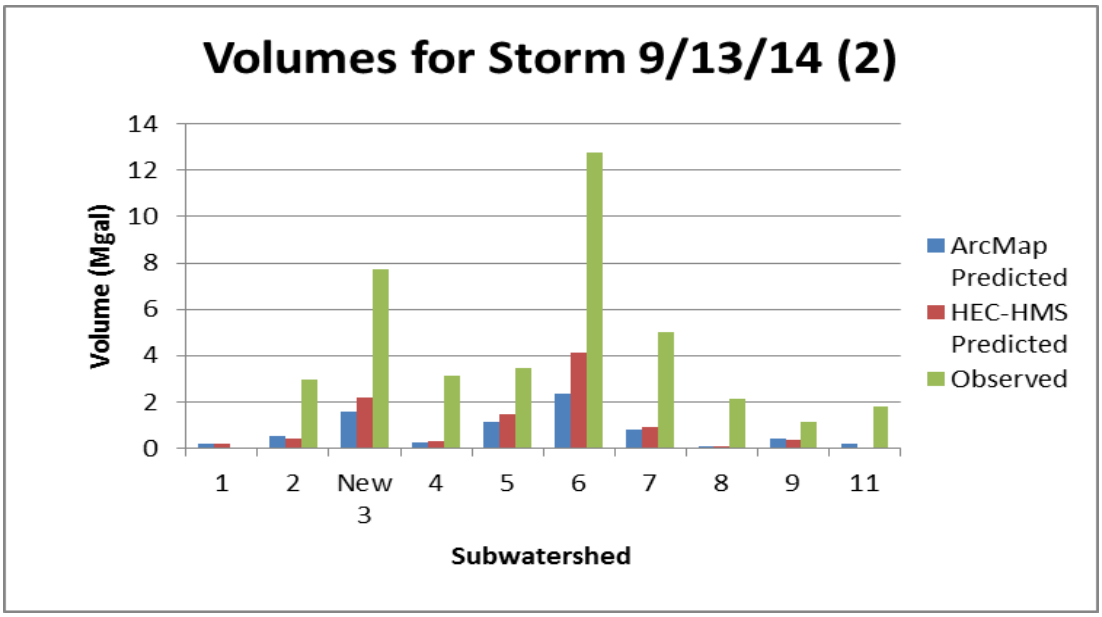

Figure A.41: Volume comparison graph for storm event 9/13/14 of 0.08 inches

Table A.41: Volume and flow rate comparison table for storm event 9/13/14 of 0.08 inches with rainfall runoff ratios calculated

Subwatershed	GIS Volume Summed (Mgal)	HEC-HMS Volume Summed (Mgal)	Sensor Volume (Mgal)	Runoff (ft)	Ratio	Sensor Peak Flow (cms)	HEC-HMS Peak Flow (cms
1	0.19	0.16	0.00	0.00	0.00	0.00	0.10
2	0.48	0.40	2.93	0.04	6.08	1.54	0.10
New 3	1.56	2.19	7.74	0.03	5.01	5.12	0.10
4	0.24	0.29	3.12	0.09	13.23	1.80	0.00
5	1.13	1.45	3.43	0.02	3.04	1.58	0.10
6	2.35	4.09	12.77	0.04	5.44	10.75	0.30
7	0.77	0.92	5.03	0.04	6.56	10.90	0.00
8	0.07	0.05	2.10	0.21	32.23	2.93	0.00
9	0.39	0.34	1.12	0.02	2.85	1.16	0.10
11	0.18		1.80	0.07	10.13	2.84	

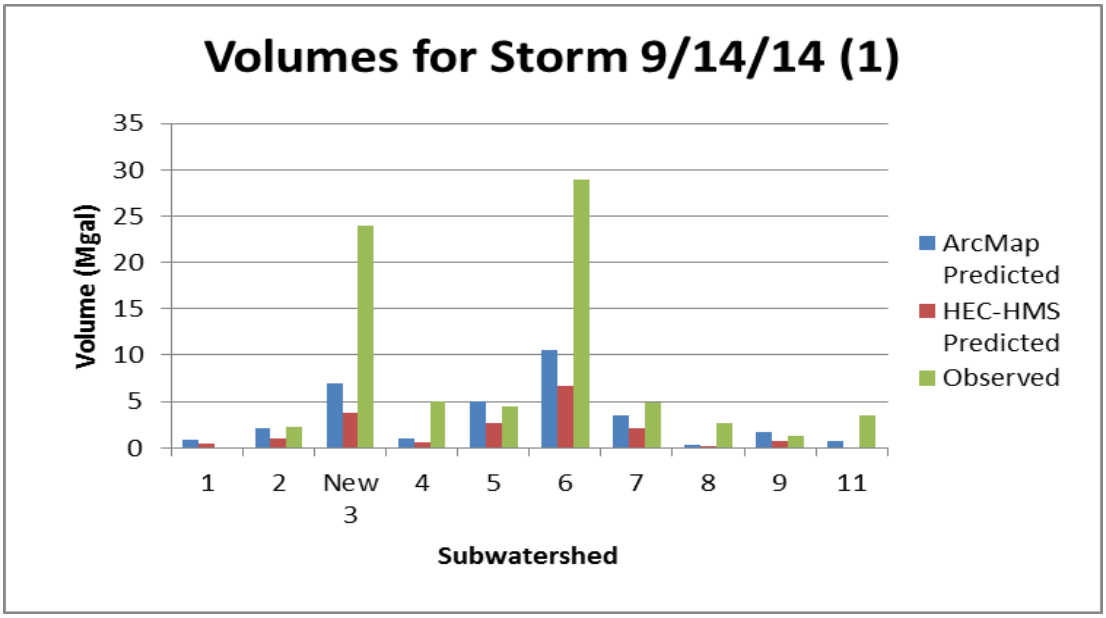

Figure A.42: Volume comparison graph for storm event 9/14/14 of 0.36 inches

Table A.42: Volume and flow rate comparison table for storm event 9/14/14 of 0.36 inches with rainfall runoff ratios calculated

Subwatershed	GIS Volume Summed (Mgal)	HEC-HMS Volume Summed (Mgal)	Sensor Volume (Mgal)	Runoff (ft)	Ratio	Sensor Peak Flow (cms)	HEC-HMS Peak Flow (cms
1	0.84	0.50	0.00	0.00	0.00	0.00	0.20
2	2.17	1.06	2.32	0.03	1.07	1.55	0.40
New 3	7.01	3.75	23.98	0.10	3.45	5.12	0.20
4	1.08	0.53	5.02	0.14	4.73	1.75	0.10
5	5.08	2.67	4.41	0.03	0.87	1.58	0.30
6	10.56	6.68	28.91	0.08	2.74	11.06	1.00
7	3.45	2.06	4.93	0.04	1.43	12.21	0.00
8	0.29	0.16	2.61	0.27	8.93	2.94	0.10
9	1.76	0.74	1.33	0.02	0.75	0.72	0.20
11	0.80		3.51	0.13	4.38	2.89	

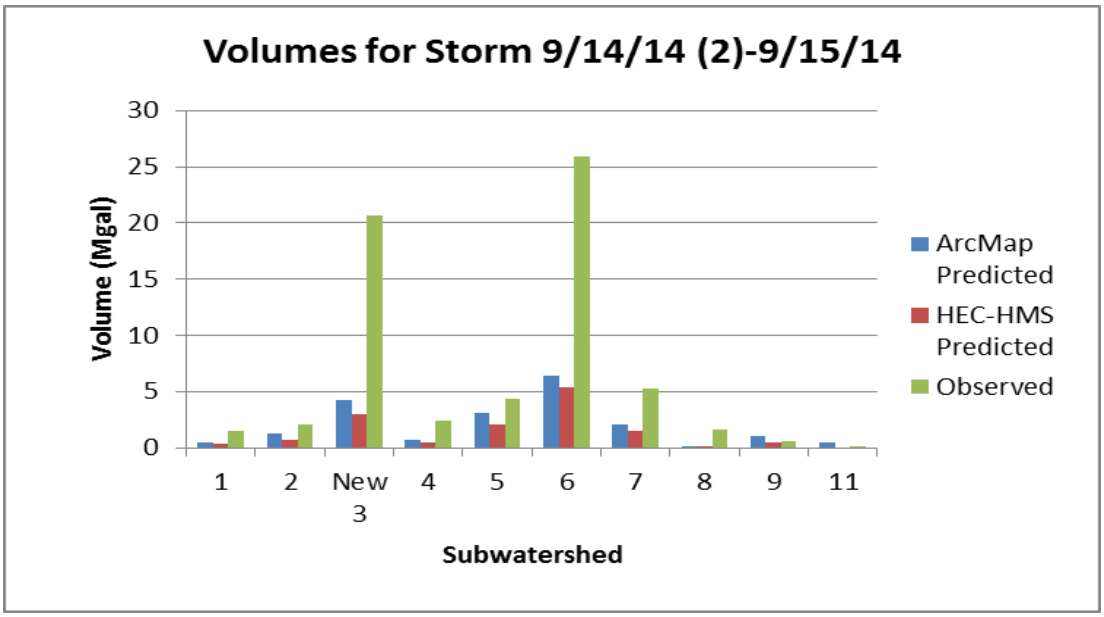

Figure A.43: Volume comparison graph for storm event 9/14/14-9/15/14 of 0.22 inches

Table A.43: Volume and flow rate comparison table for storm event 9/14/14-9/15/14 of 0.22 inches with rainfall runoff ratios calculated

Subwatershed	GIS Volume Summed (Mgal)	HEC-HMS Volume Summed (Mgal)	Sensor Volume (Mgal)	Runoff (ft)	Ratio	Sensor Peak Flow (cms)	HEC-HMS Peak Flow (cms
1	0.51	0.34	1.55	0.06	3.03	4.96	0.20
2	1.33	0.71	2.10	0.03	1.58	1.55	0.20
New 3	4.29	2.96	20.68	0.09	4.87	5.08	0.10
4	0.66	0.42	2.39	0.07	3.69	1.70	0.10
5	3.10	2.06	4.31	0.03	1.39	1.58	0.20
6	6.45	5.39	25.93	0.07	4.02	11.32	0.60
7	2.11	1.51	5.25	0.05	2.49	11.61	0.00
8	0.18	0.11	1.60	0.16	8.93	2.94	0.10
9	1.08	0.53	0.57	0.01	0.53	0.53	0.10
11	0.49		0.02	0.00	0.03	0.10	

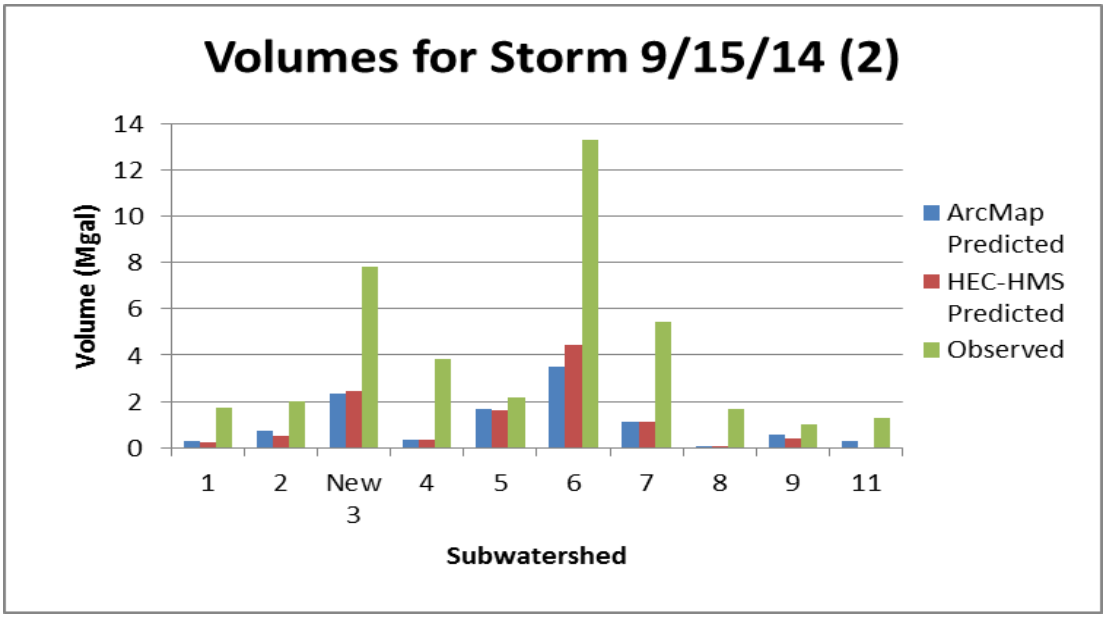

Figure A.44: Volume comparison graph for storm event 9/15/14 of 0.12 inches

Table A.44: Volume and flow rate comparison table for storm event 9/15/14 of 0.12 inches with rainfall runoff ratios calculated

Subwatershed	GIS Volume Summed (Mgal)	HEC-HMS Volume Summed (Mgal)	Sensor Volume (Mgal)	Runoff (ft)	Ratio	Sensor Peak Flow (cms)	HEC-HMS Peak Flow (cms
1	0.28	0.21	1.74	0.06	6.23	4.52	0.10
2	0.72	0.50	2.02	0.03	2.78	1.55	0.10
New 3	2.34	2.43	7.83	0.03	3.38	5.12	0.10
4	0.36	0.34	3.82	0.11	10.78	1.78	0.10
5	1.69	1.64	2.16	0.01	1.27	1.58	0.10
6	3.52	4.46	13.28	0.04	3.78	11.13	0.40
7	1.15	1.11	5.45	0.05	4.75	12.31	0.00
8	0.10	0.08	1.70	0.17	17.40	2.88	0.00
9	0.59	0.40	0.99	0.02	1.68	0.93	0.10
11	0.27		1.31	0.05	4.92	2.55	

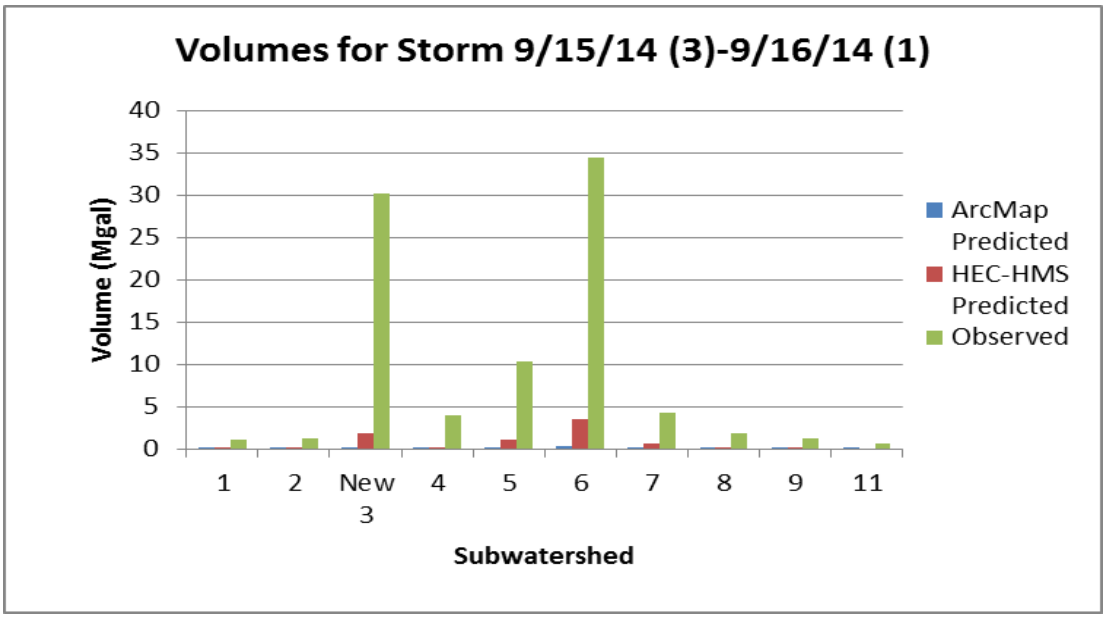

Figure A.45: Volume comparison graph for storm event 9/15/14-9/16/14 of 0.01 inches

Table A.45: Volume and flow rate comparison table for storm event 9/15/14-9/16/14 of 0.01 inches with rainfall runoff ratios calculated

Subwatershed	GIS Volume Summed (Mgal)	HEC-HMS Volume Summed (Mgal)	Sensor Volume (Mgal)	Runoff (ft)	Ratio	Sensor Peak Flow (cms)	HEC-HMS Peak Flow (cms
1	0.02	0.08	1.18	0.04	50.69	4.86	0.00
2	0.06	0.24	1.25	0.02	20.89	1.55	0.00
New 3	0.19	1.82	30.20	0.13	157.04	5.11	0.00
4	0.03	0.24	4.05	0.11	137.76	1.81	0.00
5	0.14	1.16	10.34	0.06	73.57	1.63	0.00
6	0.29	3.46	34.49	0.10	118.14	10.29	0.00
7	0.10	0.66	4.29	0.04	45.01	11.57	0.00
8	0.01	0.03	1.86	0.19	230.02	2.86	0.00
9	0.05	0.24	1.20	0.02	24.64	1.31	0.00
11	0.02		0.72	0.03	32.45	2.46	0.20

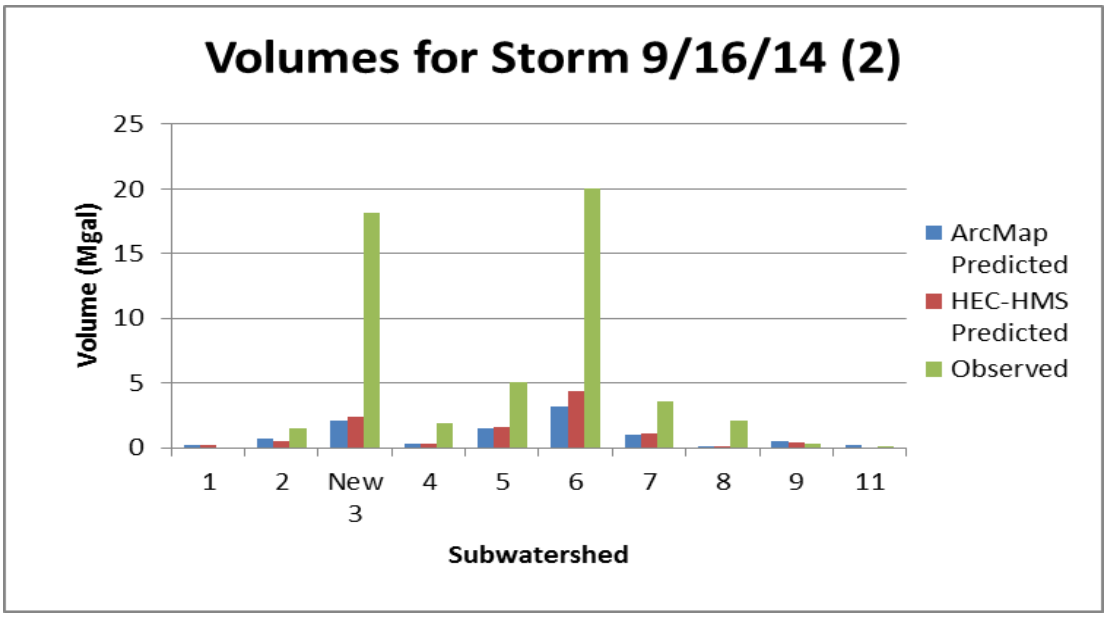

Figure A.46: Volume comparison graph for storm event 9/16/14 of 0.11 inches

Table A.46: Volume and flow rate comparison table for storm event 9/16/14 of 0.11 inches with rainfall runoff ratios calculated

Subwatershed	GIS Volume Summed (Mgal)	HEC-HMS Volume Summed (Mgal)	Sensor Volume (Mgal)	Runoff (ft)	Ratio	Sensor Peak Flow (cms)	HEC-HMS Peak Flow (cms
1	0.26	0.21	0.00	0.00	0.00	0.00	0.10
2	0.66	0.48	1.55	0.02	2.32	1.54	0.10
New 3	2.14	2.38	18.15	0.08	8.51	3.93	0.10
4	0.33	0.32	1.86	0.05	5.71	1.26	0.00
5	1.55	1.59	5.05	0.03	3.24	1.64	0.10
6	3.23	4.39	20.05	0.06	6.19	11.59	0.40
7	1.05	1.08	3.63	0.03	3.44	6.00	0.00
8	0.09	0.08	2.09	0.21	23.25	2.94	0.00
9	0.54	0.40	0.27	0.00	0.49	0.21	0.10
11	0.24		0.01	0.00	0.03	0.09	

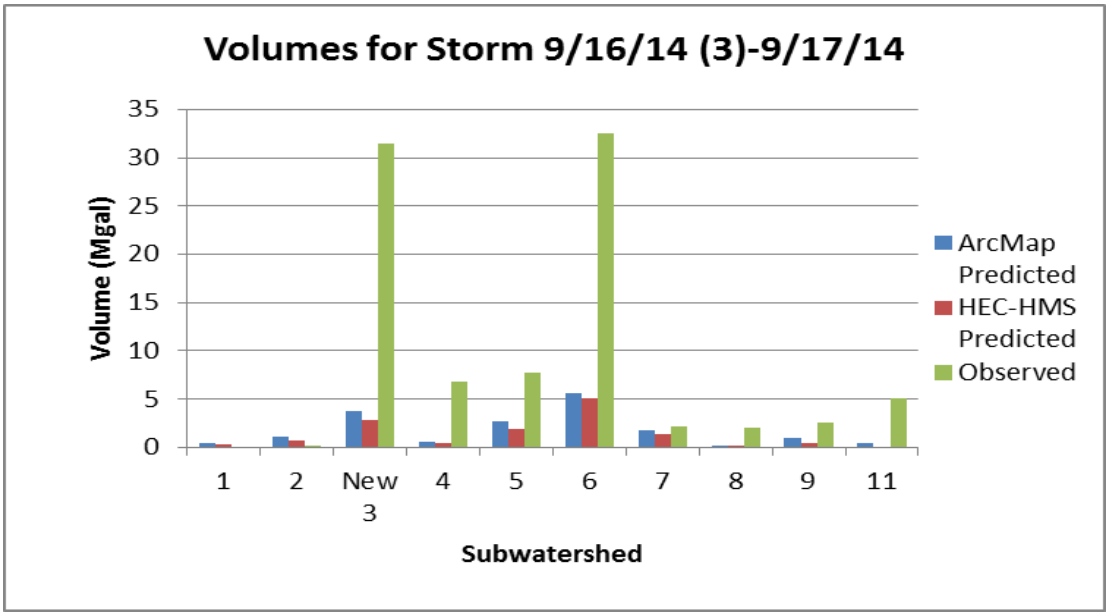

Figure A.47: Volume comparison graph for storm event 9/16/14-9/17/14 of 0.19 inches

Table A.47: Volume and flow rate comparison table for storm event 9/16/14-9/17/14 of 0.19 inches with rainfall runoff ratios calculated

Subwatershed	GIS Volume Summed (Mgal)	HEC-HMS Volume Summed (Mgal)	Sensor Volume (Mgal)	Runoff (ft)	Ratio	Sensor Peak Flow (cms)	HEC-HMS Peak Flow (cms
1	0.44	0.29	0.00	0.00	0.00	0.00	0.10
2	1.15	0.66	0.19	0.00	0.16	1.55	0.20
New 3	3.70	2.83	31.52	0.14	8.59	5.12	0.10
4	0.57	0.40	6.75	0.19	12.05	1.81	0.10
5	2.68	1.95	7.76	0.05	2.90	1.83	0.20
6	5.57	5.12	32.55	0.09	5.84	11.40	0.60
7	1.82	1.40	2.23	0.02	1.22	12.14	0.00
8	0.15	0.11	2.04	0.21	13.22	2.94	0.00
9	0.93	0.50	2.50	0.04	2.68	1.31	0.10
11	0.42		5.08	0.19	12.02	1.18	

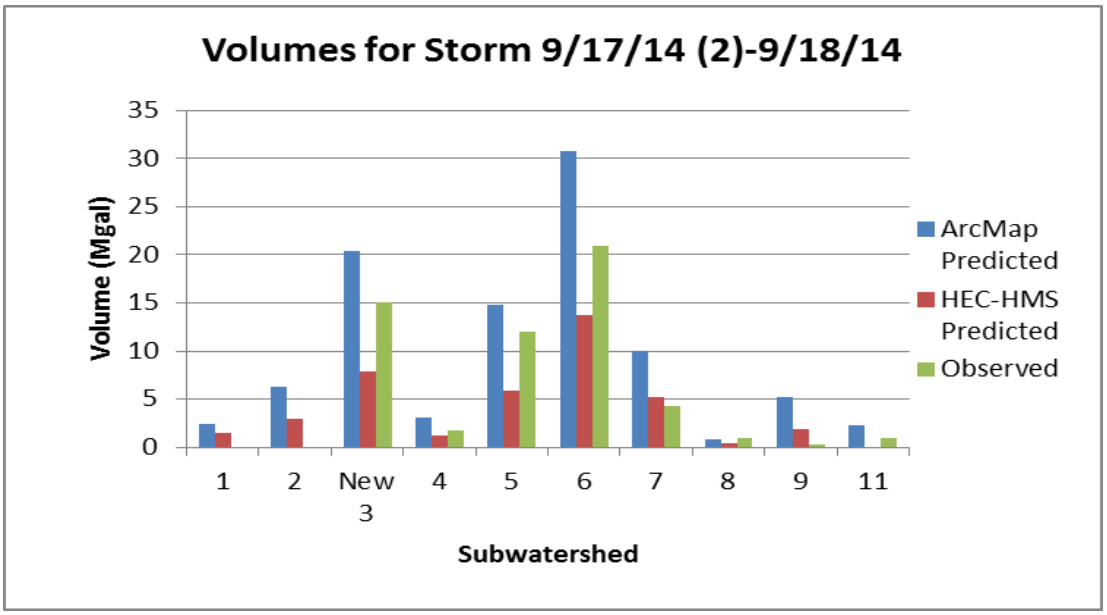

Figure A.48: Volume comparison graph for storm event 9/17/14-9/18/14 of 1.05 inches

Table A.48: Volume and flow rate comparison table for storm event 9/17/14-9/18/14 of 1.05 inches with rainfall runoff ratios calculated

Subwatershed	GIS Volume Summed (Mgal)	HEC-HMS Volume Summed (Mgal)	Sensor Volume (Mgal)	Runoff (ft)	Ratio	Sensor Peak Flow (cms)	HEC-HMS Peak Flow (cms
1	2.44	1.45	0.00	0.00	0.00	0.00	0.70
2	6.33	2.91	0.00	0.00	0.00	0.00	1.20
New 3	20.45	7.85	15.10	0.07	0.74	3.70	0.40
4	3.14	1.19	1.76	0.05	0.57	1.13	0.40
5	14.81	5.92	11.98	0.07	0.81	1.62	0.80
6	30.79	13.68	20.96	0.06	0.68	12.90	2.60
7	10.05	5.23	4.27	0.04	0.42	6.62	0.10
8	0.85	0.48	0.94	0.10	1.10	2.93	0.30
9	5.15	1.82	0.26	0.00	0.05	0.26	0.60
11	2.34		1.00	0.04	0.43	2.47	

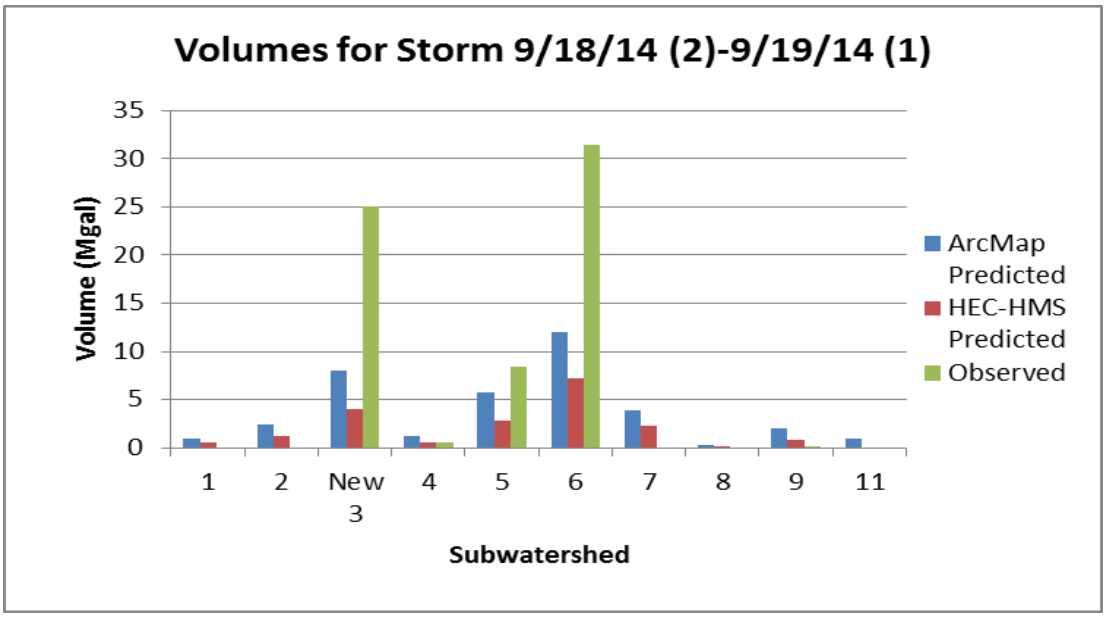

Figure A.49: Volume comparison graph for storm event 9/18/14-9/19/14 of 0.41 inches

Table A.49: Volume and flow rate comparison table for storm event 9/18/14-9/19/14 of 0.41 inches with rainfall runoff ratios calculated

Subwatershed	GIS Volume Summed (Mgal)	HEC-HMS Volume Summed (Mgal)	Sensor Volume (Mgal)	Runoff (ft)	Ratio	Sensor Peak Flow (cms)	HEC-HMS Peak Flow (cms)
1	0.95	0.55	0.00	0.00	0.00	0.00	0.30
2	2.47	1.16	0.00	0.00	0.00	0.00	0.40
New 3	7.99	4.02	25.05	0.11	3.16	3.85	0.20
4	1.23	0.58	0.56	0.02	0.47	0.75	0.20
5	5.78	2.88	8.39	0.05	1.45	1.57	0.30
6	12.02	7.16	31.42	0.09	2.61	13.75	1.10
7	3.93	2.25	0.00	0.00	0.00	0.00	0.00
8	0.33	0.18	0.00	0.00	0.00	0.00	0.10
9	2.01	0.79	0.04	0.00	0.02	0.15	0.20
11	0.91		0.00	0.00	0.00	0.00	

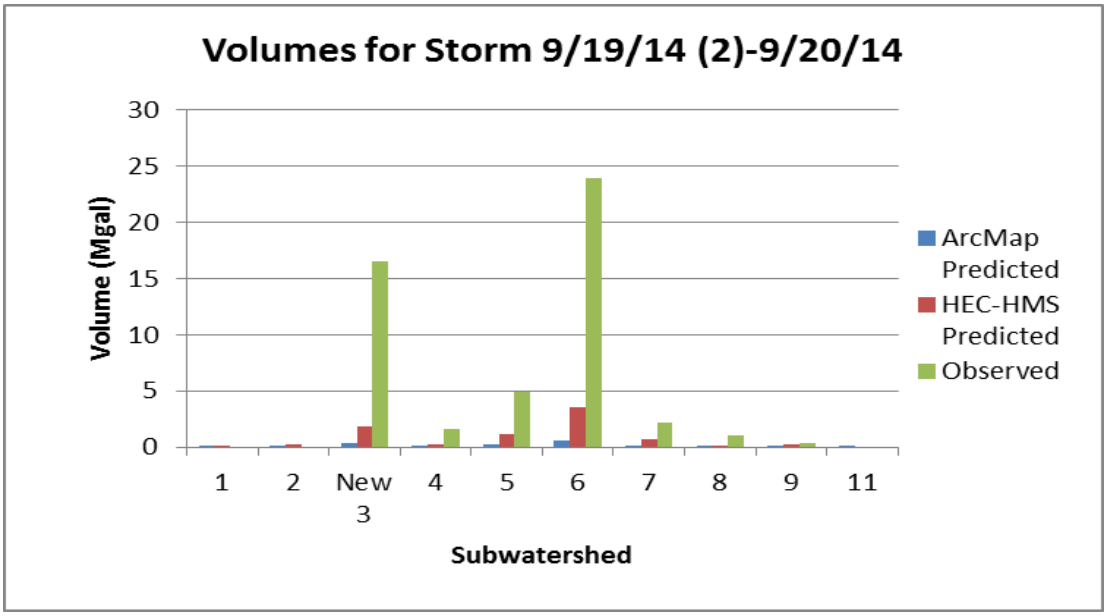

Figure A.50: Volume comparison graph for storm event 9/19/14-9/20/14 of 0.02 inches

Table A.50: Volume and flow rate comparison table for storm event 9/19/14-9/20/14 of 0.02 inches with rainfall runoff ratios calculated

Subwatershed	GIS Volume Summed (Mgal)	HEC-HMS Volume Summed (Mgal)	Sensor Volume (Mgal)	Runoff (ft)	Ratio	Sensor Peak Flow (cms)	HEC-HMS Peak Flow (cms)
1	0.05	0.11	0.00	0.00	0.00	0.00	0.00
2	0.12	0.26	0.00	0.00	0.00	0.00	0.00
New 3	0.39	1.88	16.54	0.07	42.73	3.91	0.00
4	0.06	0.24	1.60	0.05	27.03	1.09	0.00
5	0.28	1.19	4.92	0.03	17.42	1.62	0.00
6	0.59	3.54	23.94	0.07	40.75	13.60	0.20
7	0.19	0.71	2.15	0.02	11.20	5.27	0.00
8	0.02	0.03	1.02	0.10	62.59	2.83	0.00
9	0.10	0.26	0.37	0.01	3.74	0.37	0.00
11	0.04		0.00	0.00	0.00	0.00	

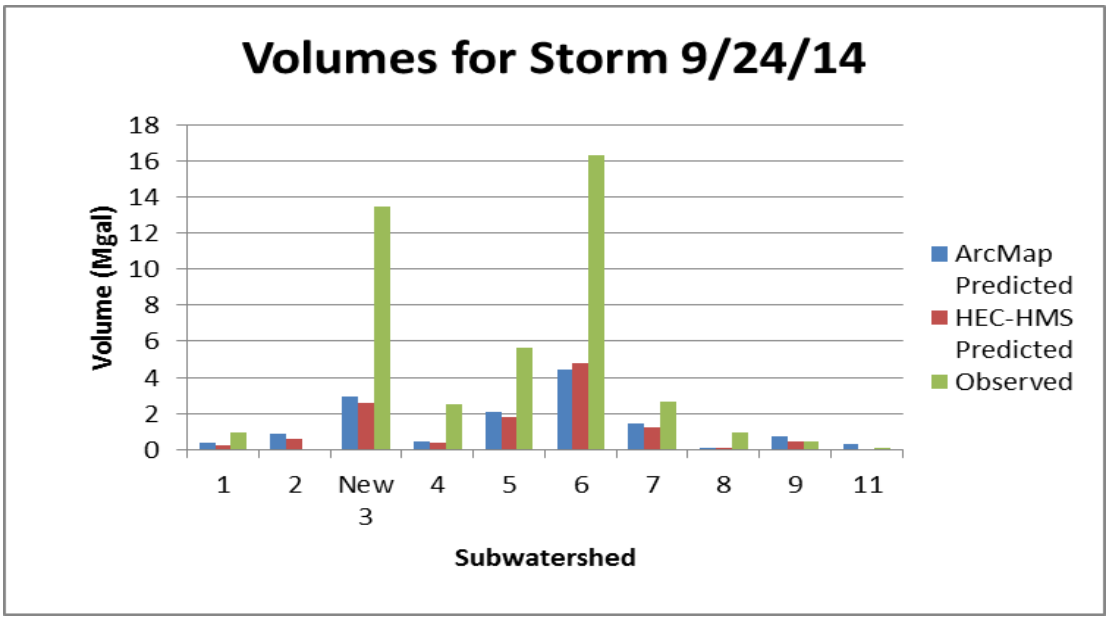

Figure A.51: Volume comparison graph for storm event 9/24/14 of 0.15 inches

Table A.51: Volume and flow rate comparison table for storm event 9/24/14 of 0.15 inches with rainfall runoff ratios calculated

Subwatershed	GIS Volume Summed (Mgal)	HEC-HMS Volume Summed (Mgal)	Sensor Volume (Mgal)	Runoff (ft)	Ratio	Sensor Peak Flow (cms)	HEC-HMS Peak Flow (cms)
1	0.35	0.24	0.94	0.03	2.68	3.51	0.10
2	0.90	0.55	0.00	0.00	0.00	0.00	0.20
New 3	2.92	2.59	13.45	0.06	4.64	4.36	0.10
4	0.45	0.37	2.48	0.07	5.60	1.51	0.10
5	2.12	1.77	5.61	0.03	2.65	1.59	0.10
6	4.40	4.76	16.28	0.05	3.70	12.88	0.50
7	1.44	1.22	2.67	0.02	1.86	5.67	0.00
8	0.12	0.08	0.93	0.10	7.61	2.94	0.00
9	0.74	0.45	0.44	0.01	0.60	0.65	0.10
11	0.33		0.01	0.00	0.02	0.09	

A.2 HEC-HMS HYDROGRAPHS

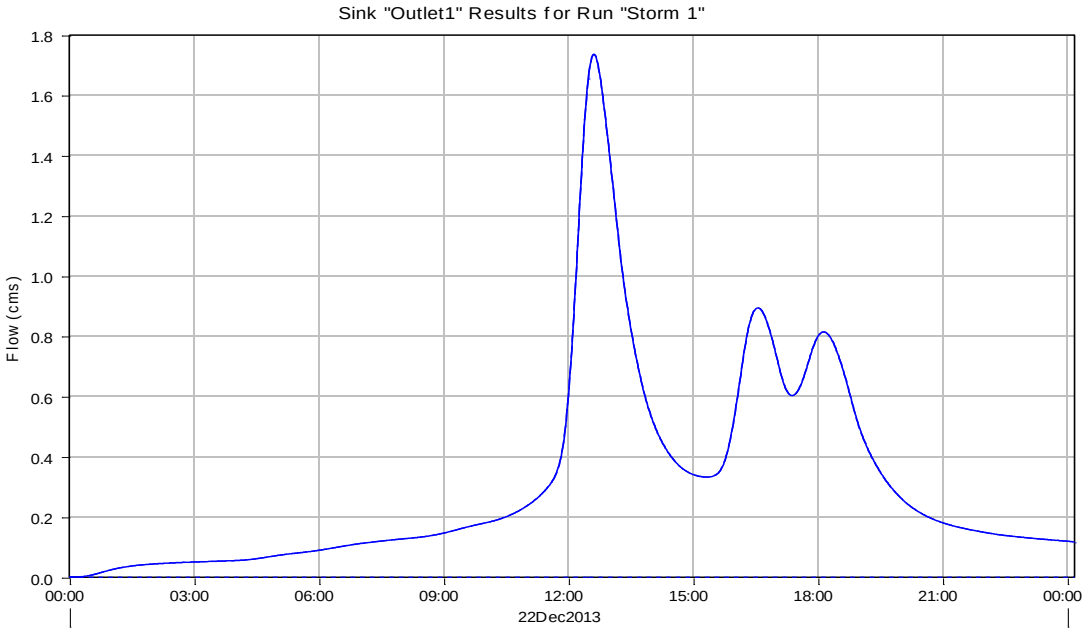

Figure A.52: HEC-HMS hydrograph at the total watershed outlet for storm event 12/22/13 of 0.77 inches

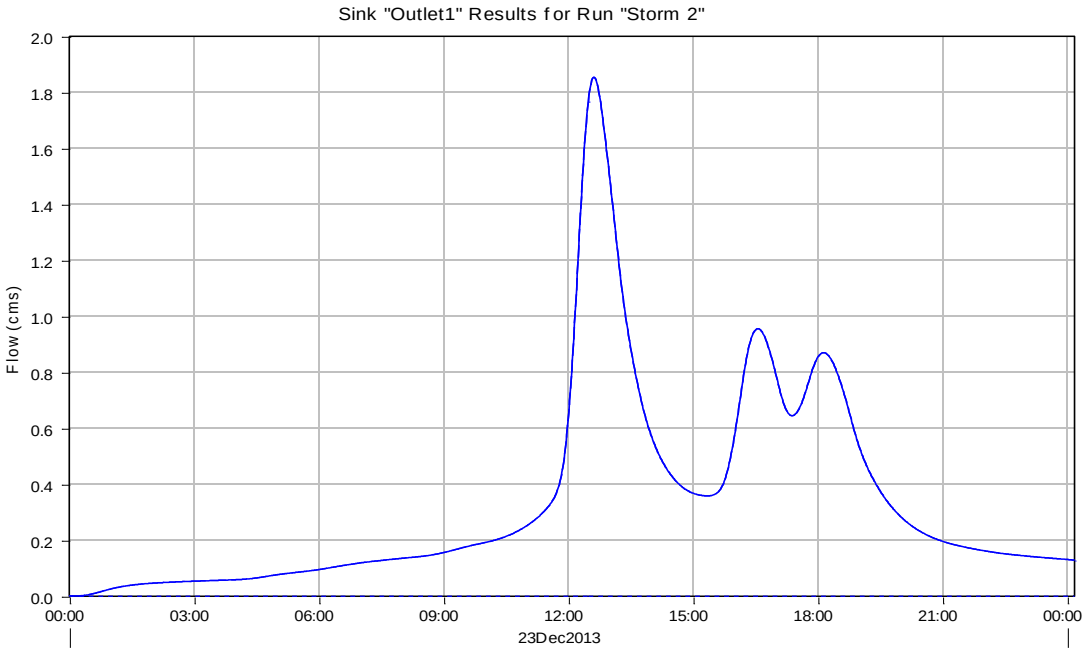

Figure A.53: HEC-HMS hydrograph at the total watershed outlet for storm event 12/23/13 of 0.82 inches

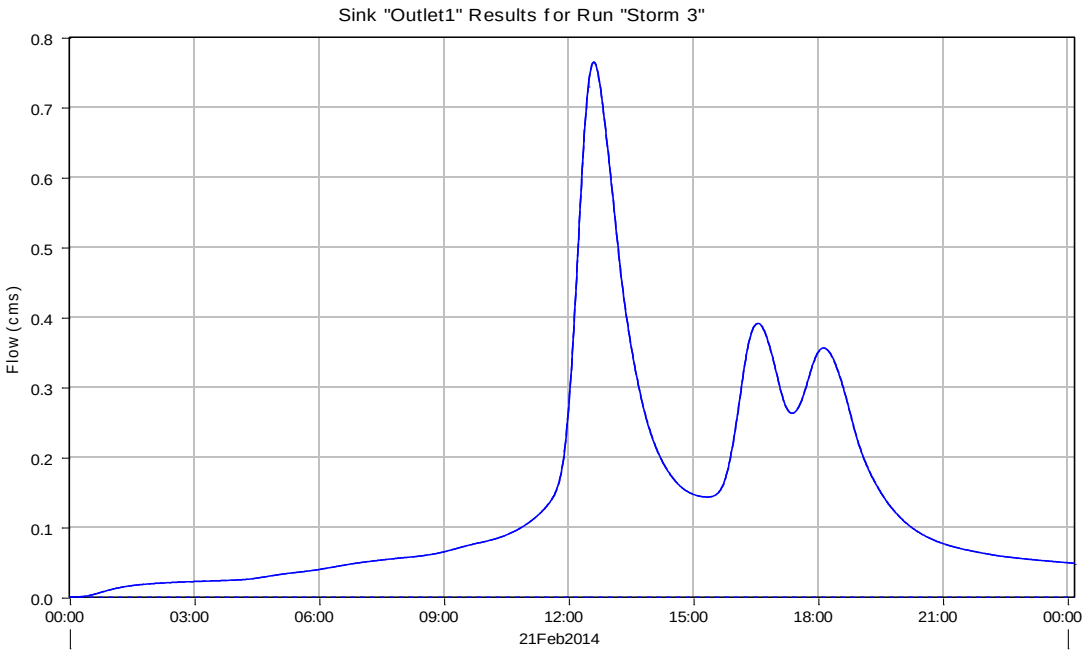

Figure A.54: HEC-HMS hydrograph at the total watershed outlet for storm event 2/21/14 of 0.34 inches

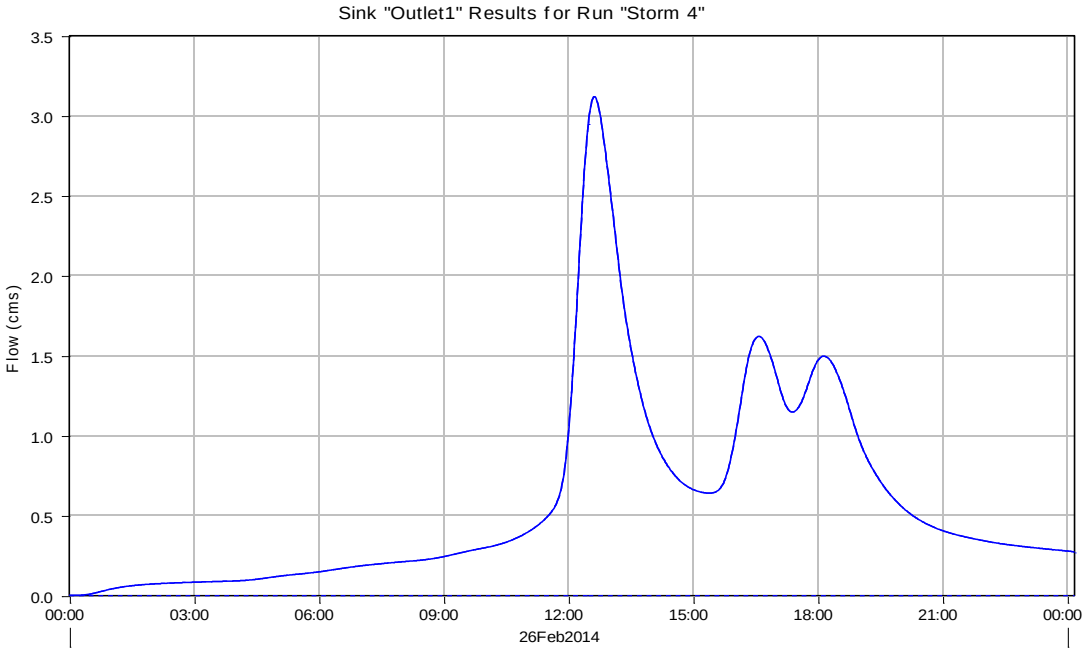

Figure A.55: HEC-HMS hydrograph at the total watershed outlet for storm event 2/26/14 of 1.28 inches

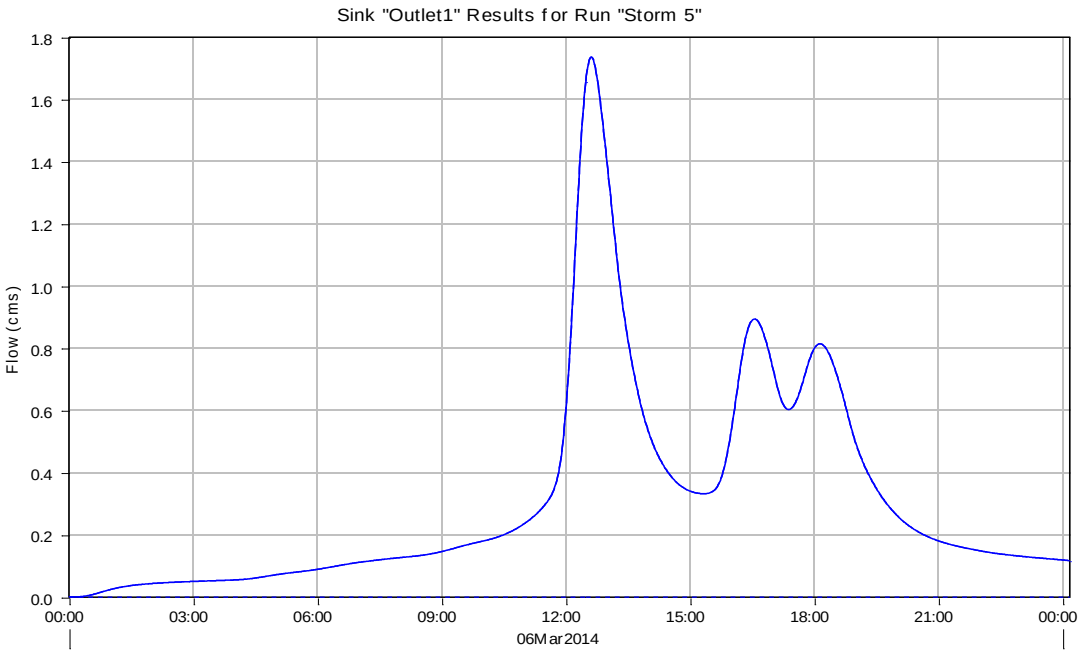

Figure A.56: HEC-HMS hydrograph at the total watershed outlet for storm event 3/6/14-3/7/14 of 0.77 inches

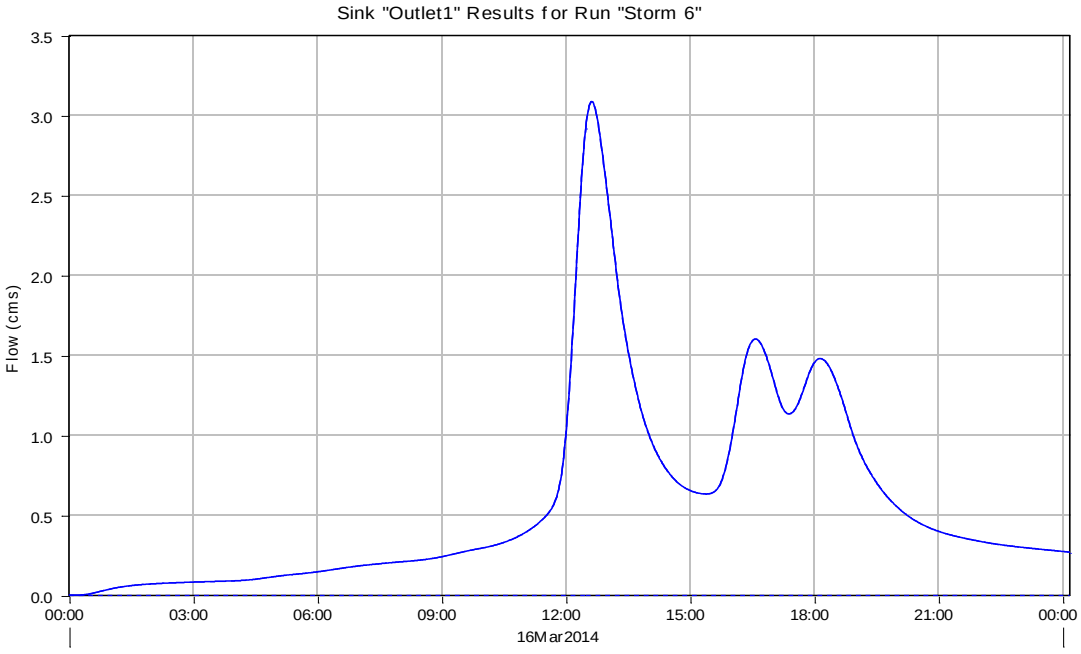

Figure A.57: HEC-HMS hydrograph at the total watershed outlet for storm event 3/16/14-3/17/14 of 1.27 inches

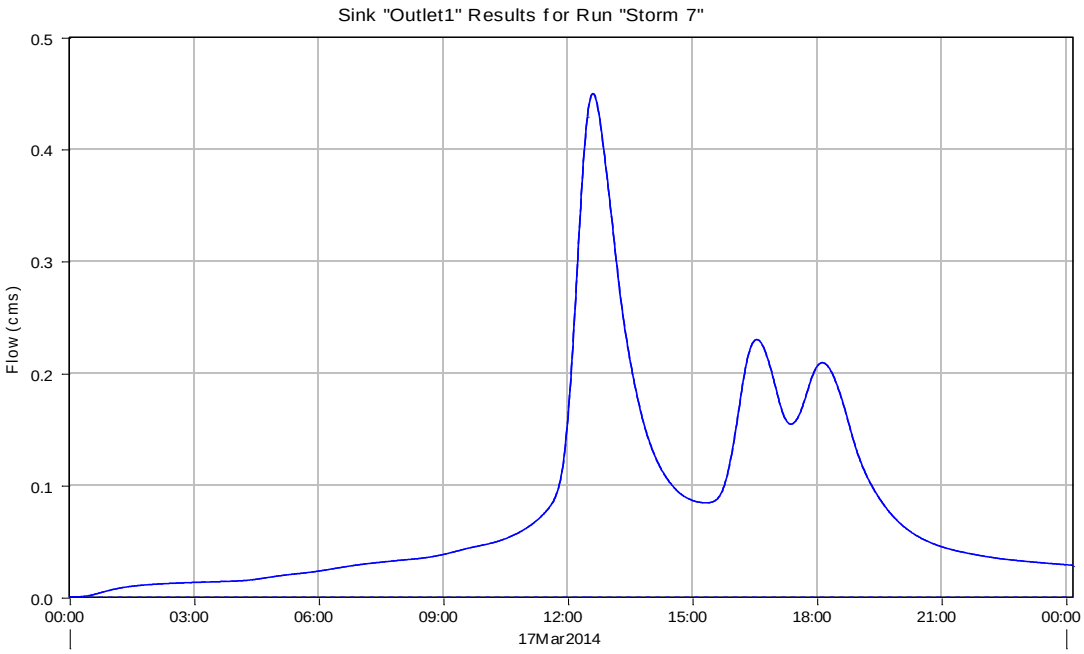

Figure A.58: HEC-HMS hydrograph at the total watershed outlet for storm event 3/17/14-3/18/14 of 0.20 inches

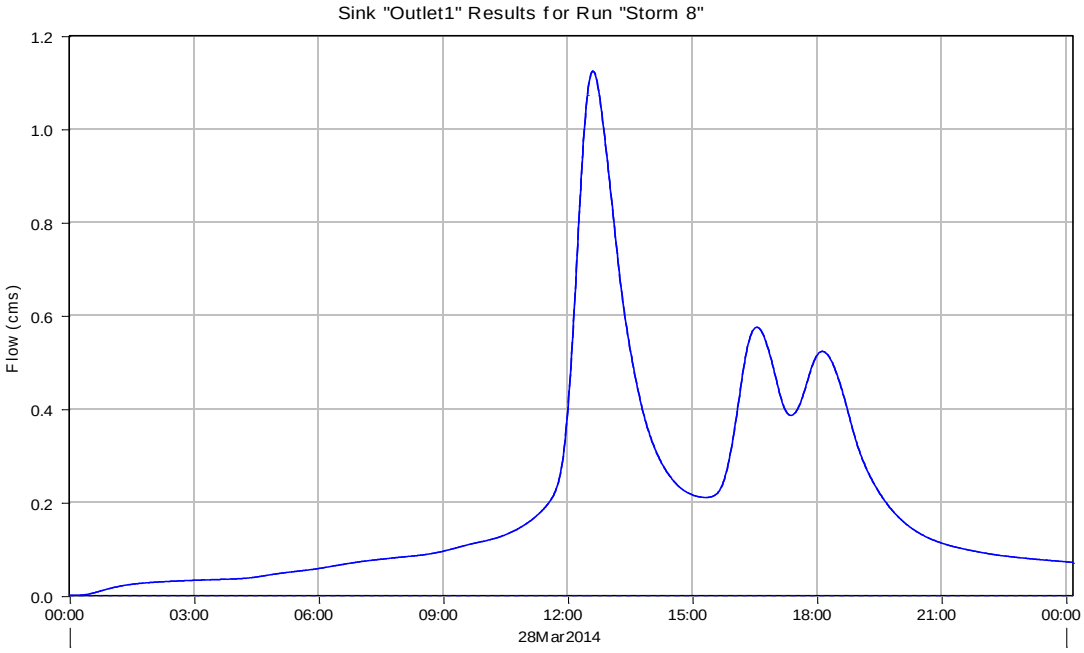

Figure A.59: HEC-HMS hydrograph at the total watershed outlet for storm event 3/28/14-3/29/14 of 0.50 inches

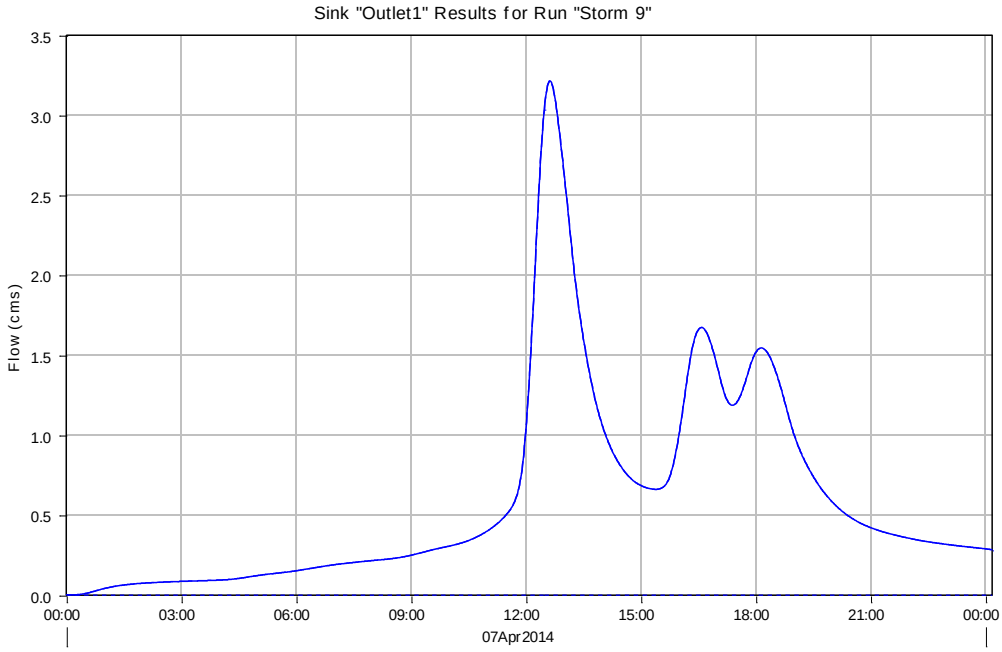

Figure A.60: HEC-HMS hydrograph at the total watershed outlet for storm event 4/7/14-4/8/14 of 1.31 inches

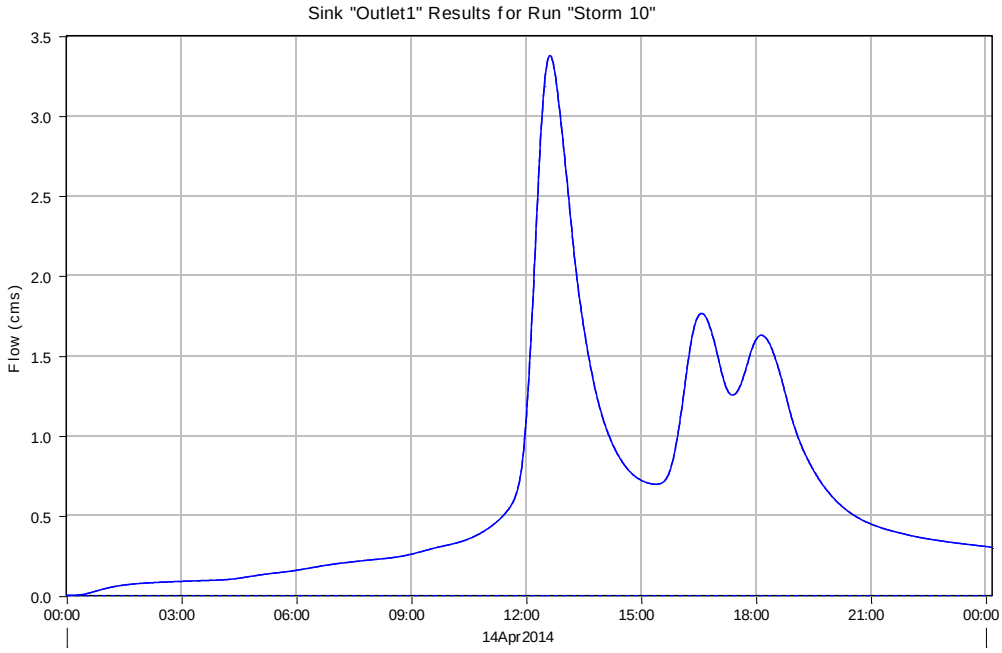

Figure A.61: HEC-HMS hydrograph at the total watershed outlet for storm event 4/14/14-4/15/14 of 1.36 inches

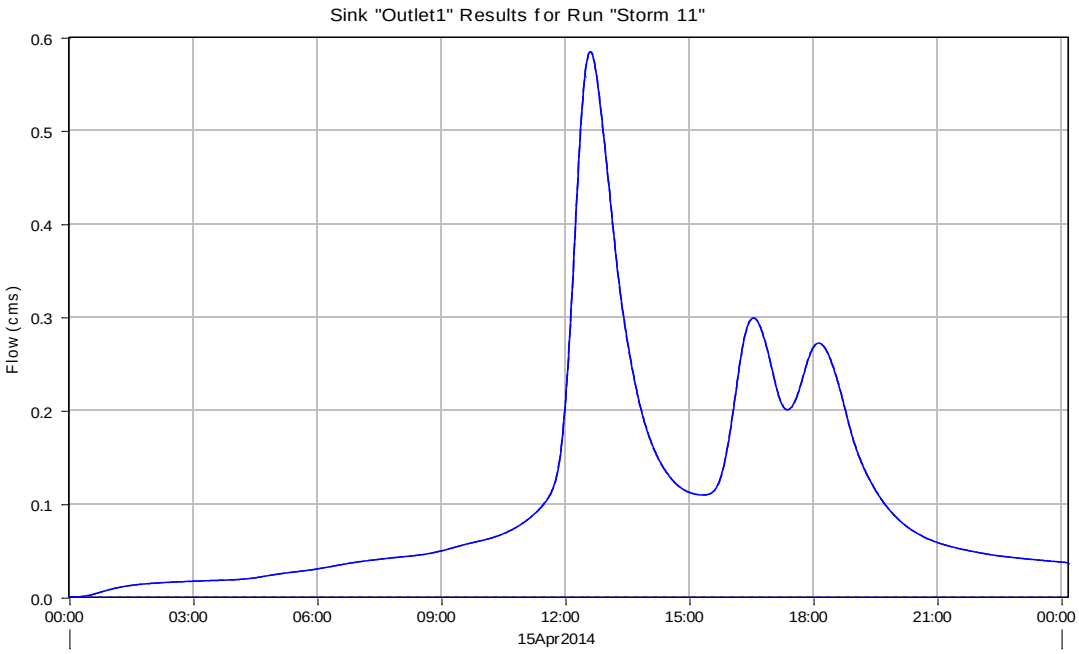

Figure A.62: HEC-HMS hydrograph at the total watershed outlet for storm event 4/15/14 of 0.26 inches

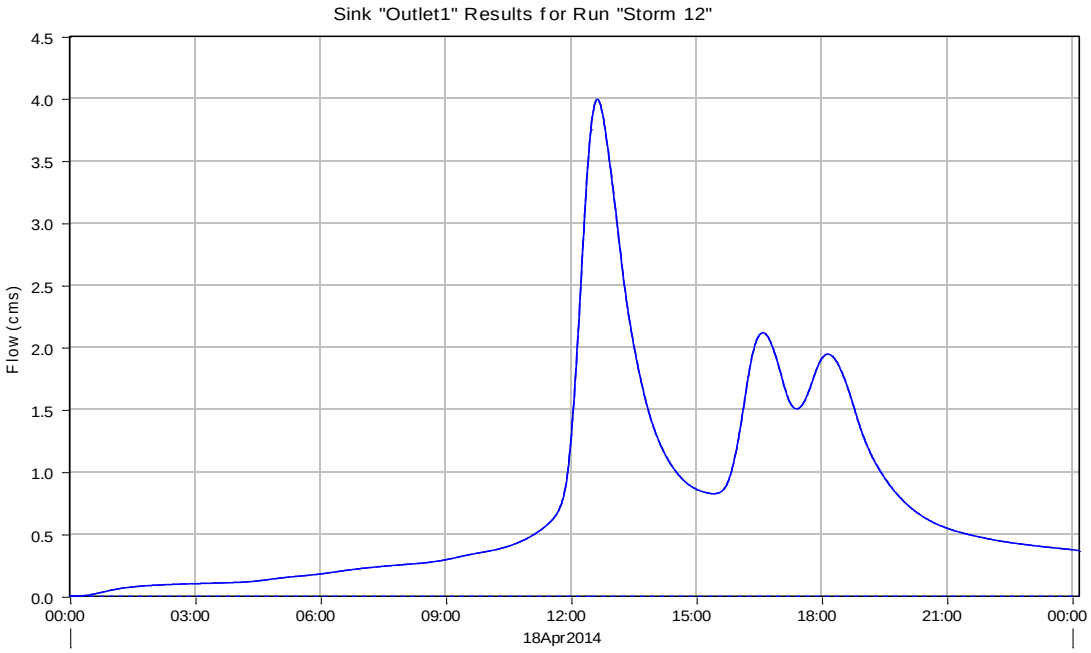

Figure A.63: HEC-HMS hydrograph at the total watershed outlet for storm event 4/18/14-4/19/14 of 1.54 inches

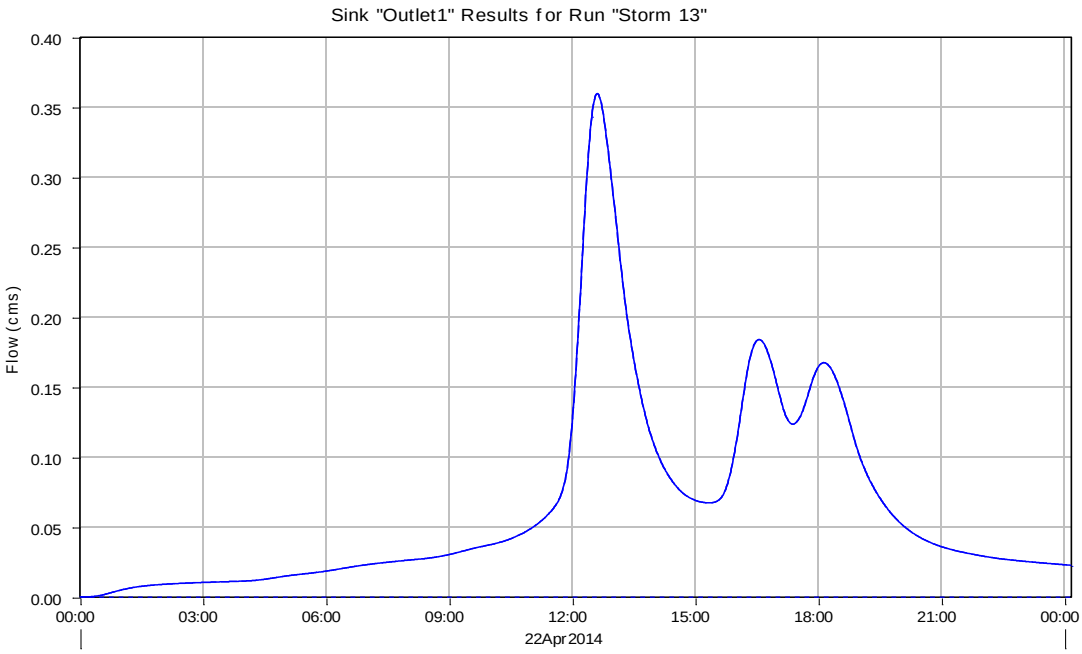

Figure A.64: HEC-HMS hydrograph at the total watershed outlet for storm event 4/22/14-4/23/14 of 0.16 inches

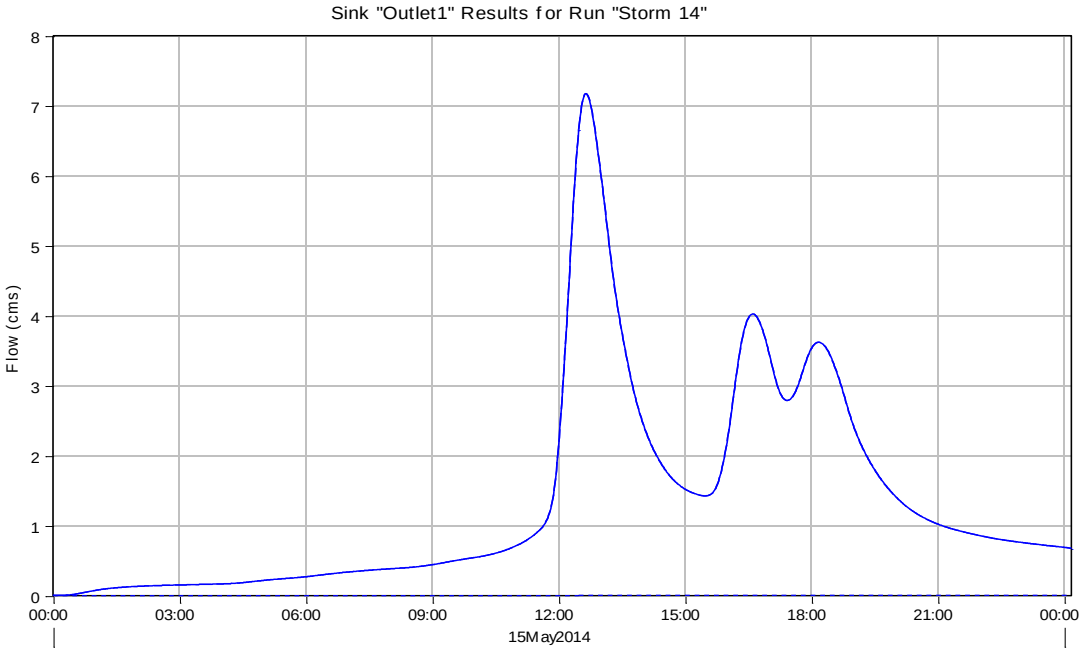

Figure A.65: HEC-HMS hydrograph at the total watershed outlet for storm event 5/15/14-5/16/14 of 2.32 inches

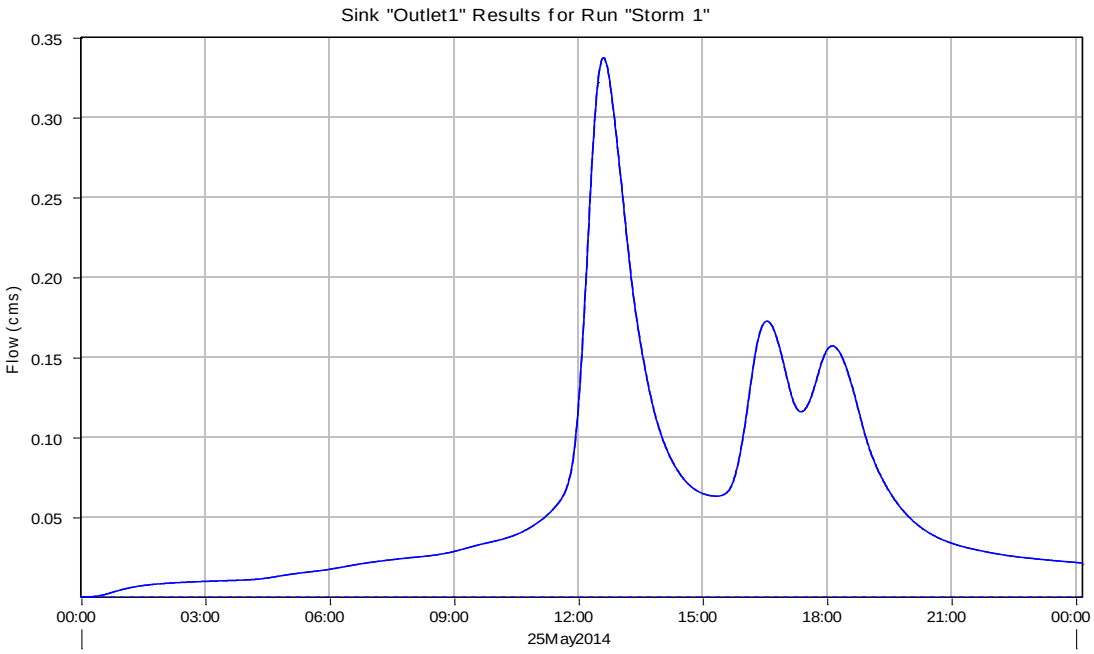

Figure A.66: HEC-HMS hydrograph at the total watershed outlet for storm event 5/25/14 of 0.15 inches

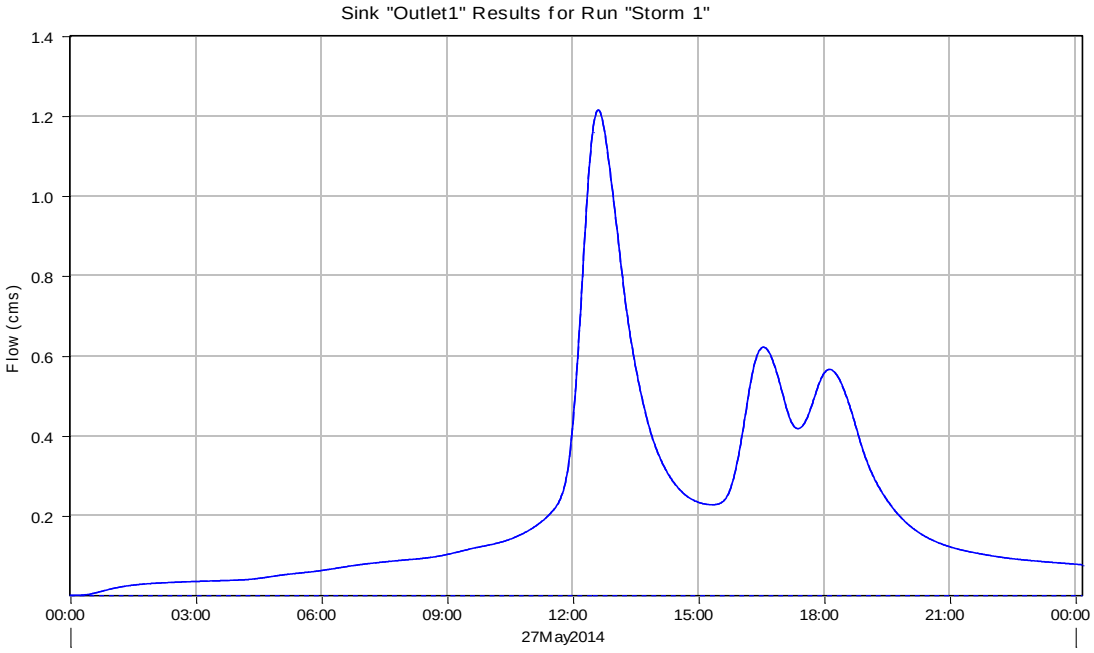

Figure A.67: HEC-HMS hydrograph at the total watershed outlet for storm event 5/27/14-5/28/14 of 0.54 inches

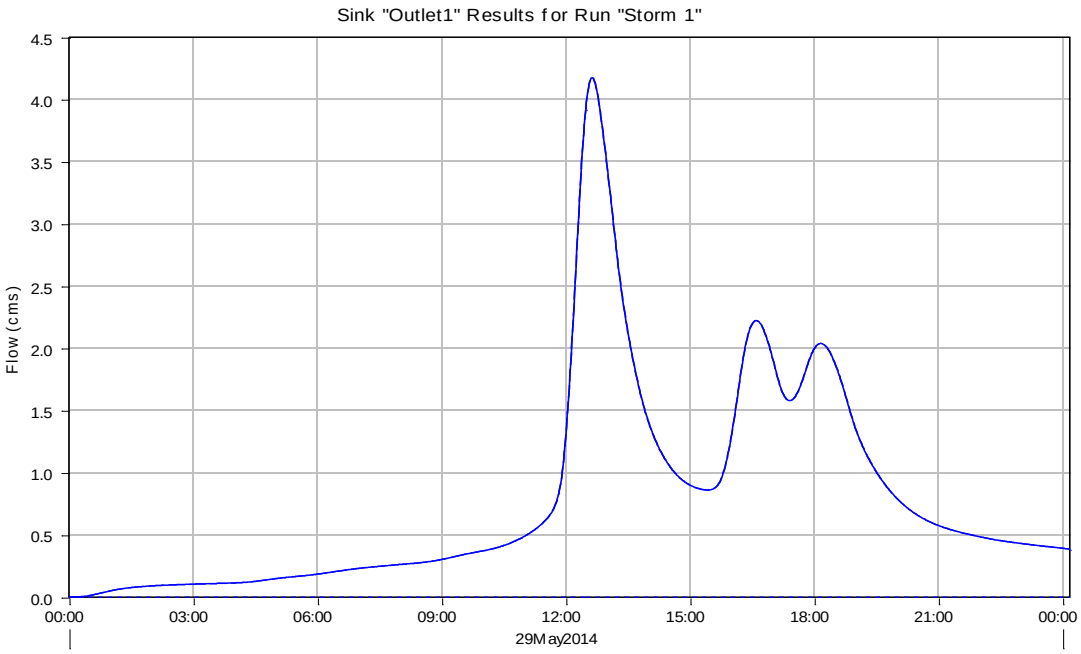

Figure A.68: HEC-HMS hydrograph at the total watershed outlet for storm event 5/29/14-5/30/14 of 1.59 inches

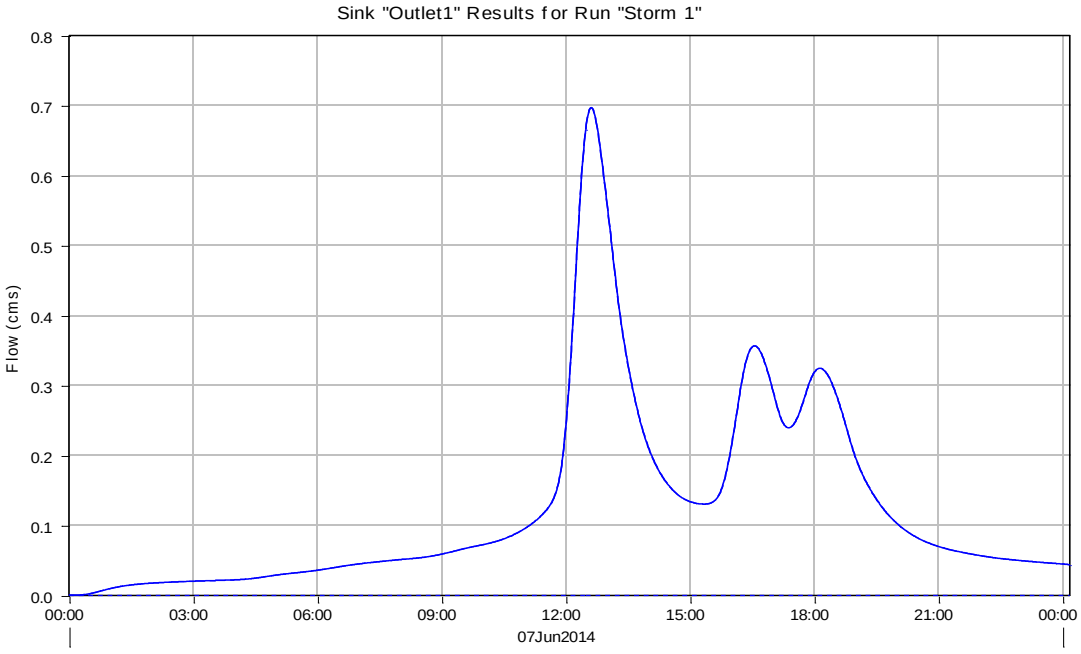

Figure A.69: HEC-HMS hydrograph at the total watershed outlet for storm event 6/7/14-6/8/14 of 0.31 inches

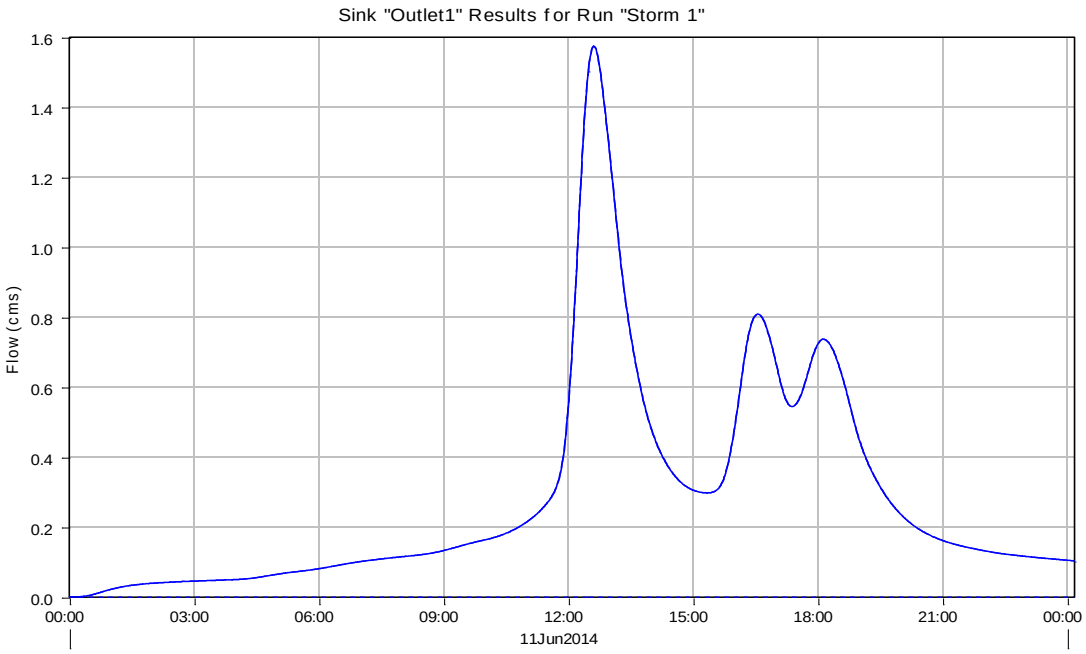

Figure A.70: HEC-HMS hydrograph at the total watershed outlet for storm event 6/11/14 of 0.70 inches

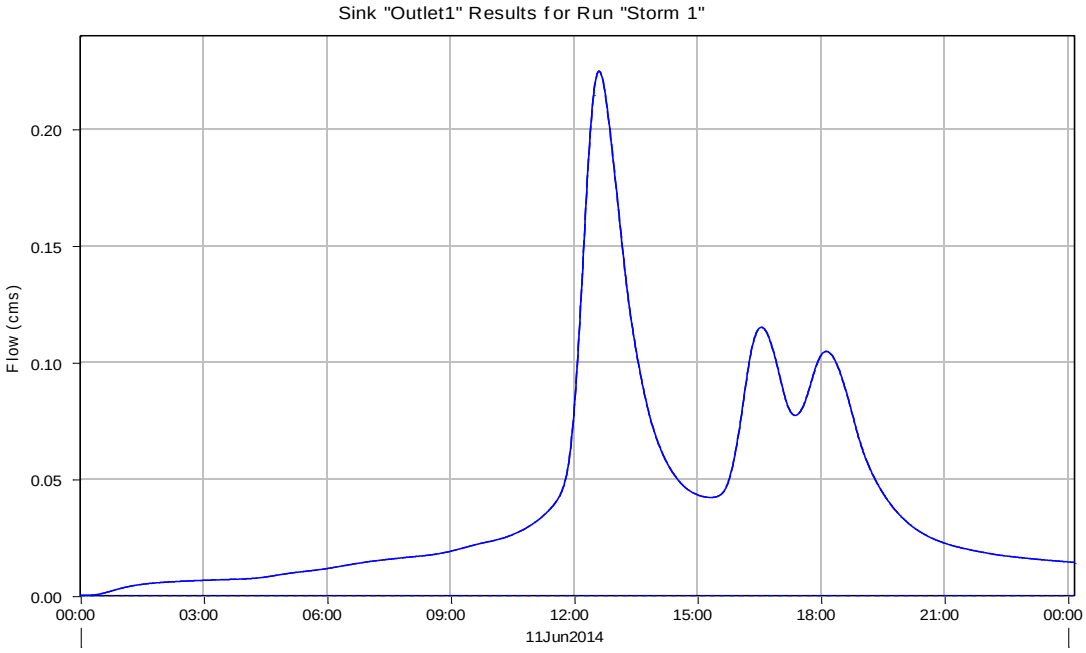

Figure A.71: HEC-HMS hydrograph at the total watershed outlet for storm event 6/11/14 of 0.10 inches

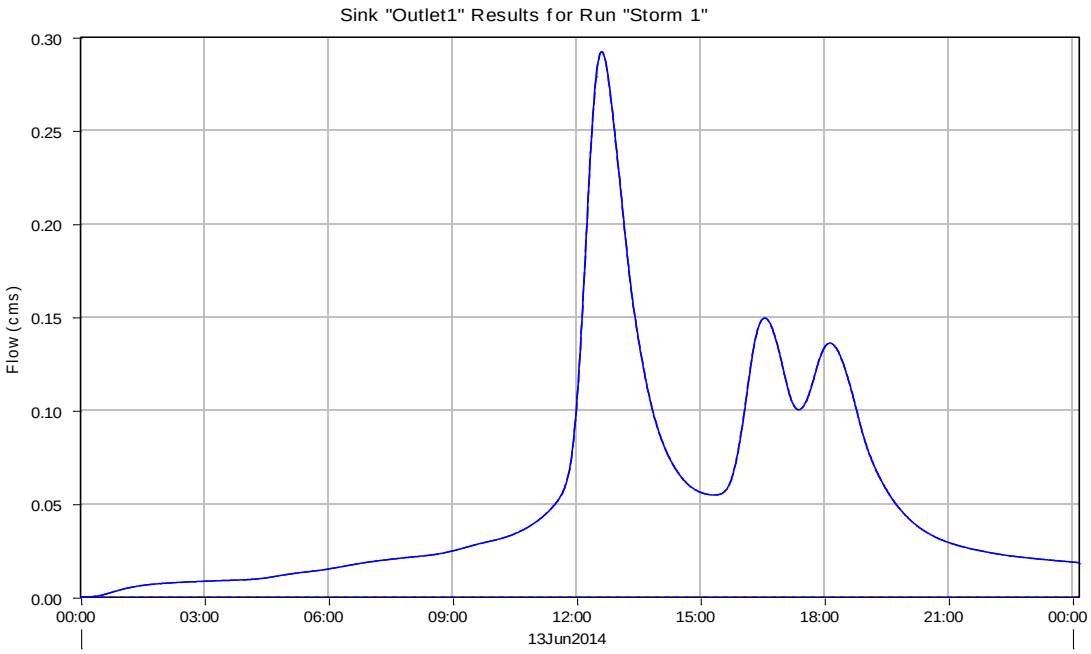

Figure A.72: HEC-HMS hydrograph at the total watershed outlet for storm event 6/13/14-6/14/14 of 0.13 inches

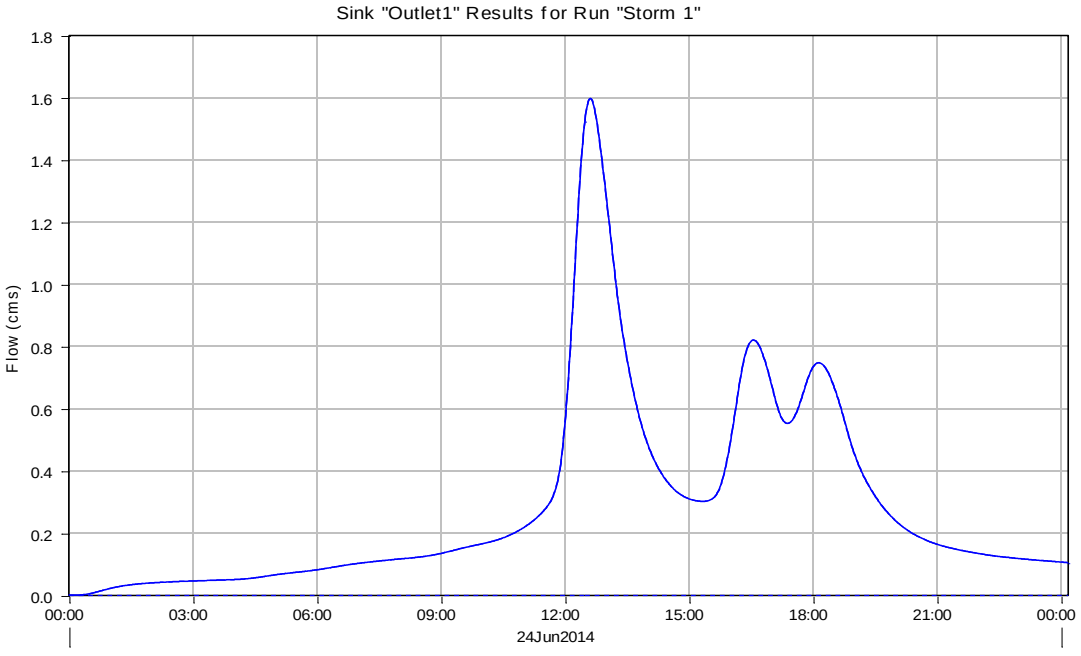

Figure A.73: HEC-HMS hydrograph at the total watershed outlet for storm event 6/24/14-6/25/14 of 0.71 inches

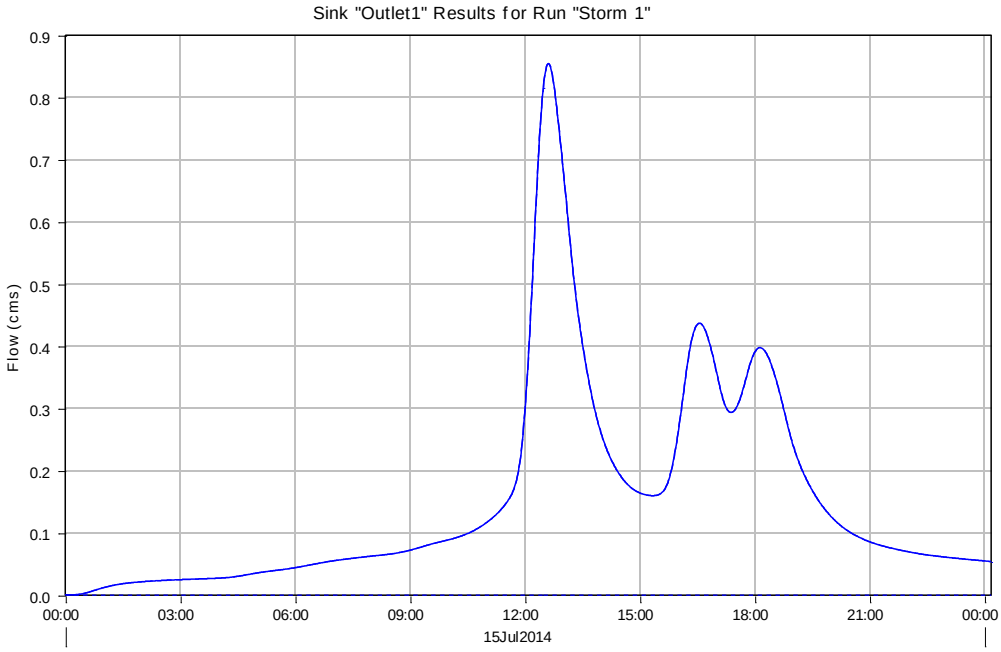

Figure A.74: HEC-HMS hydrograph at the total watershed outlet for storm event 7/15/14 of 0.38 inches

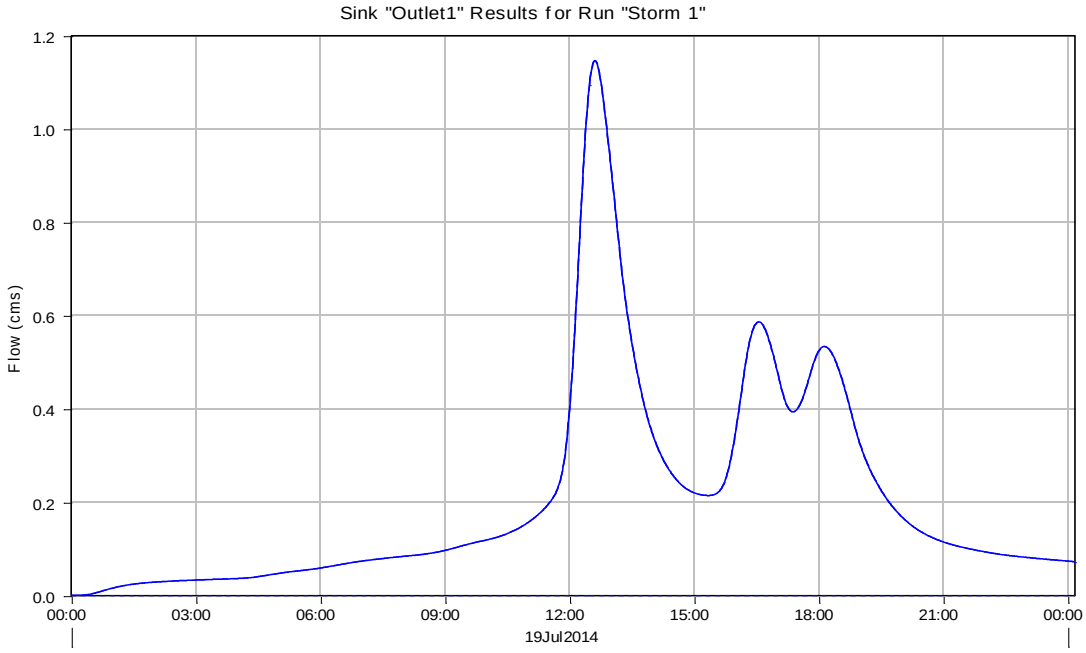

Figure A.75: HEC-HMS hydrograph at the total watershed outlet for storm event 7/19/14 of 0.51 inches

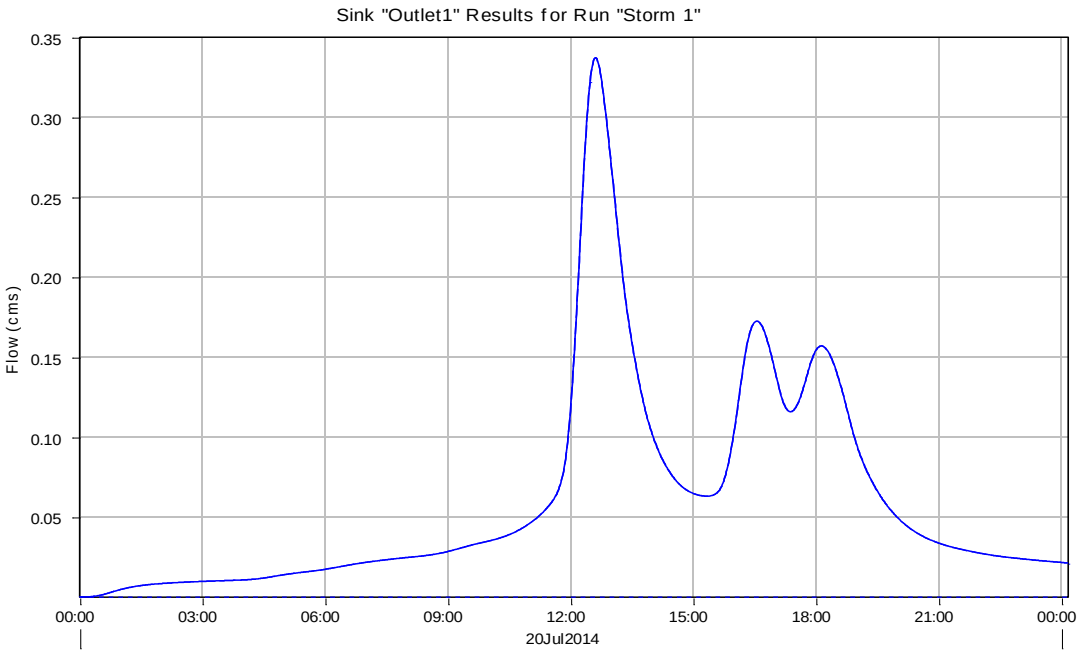

Figure A.76: HEC-HMS hydrograph at the total watershed outlet for storm event 7/20/14 of 0.15 inches

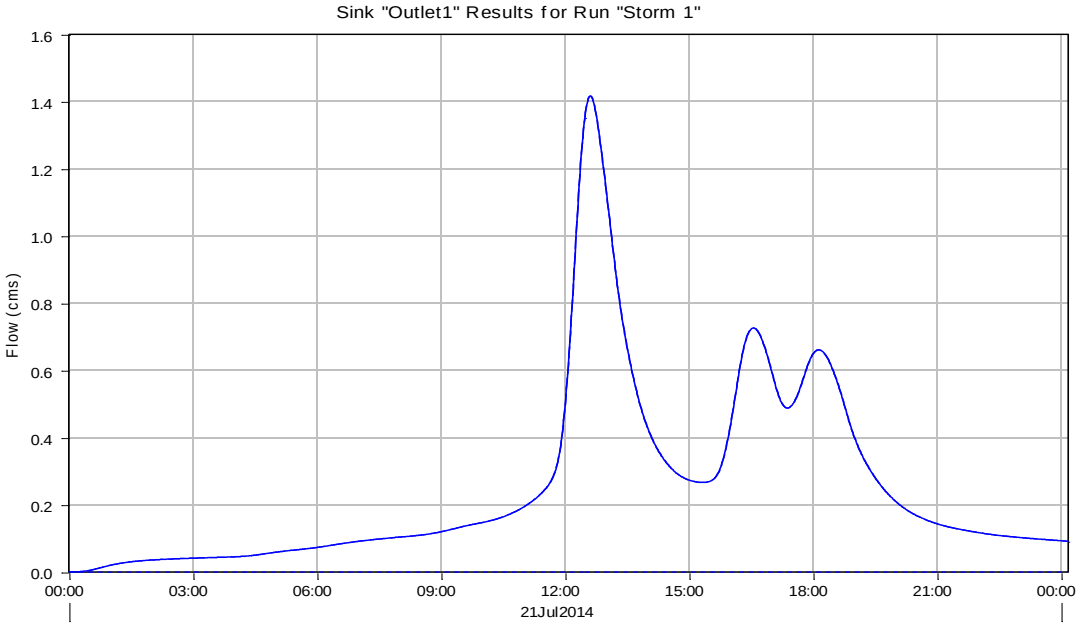

Figure A.77: HEC-HMS hydrograph at the total watershed outlet for storm event 7/21/14 of 0.63 inches

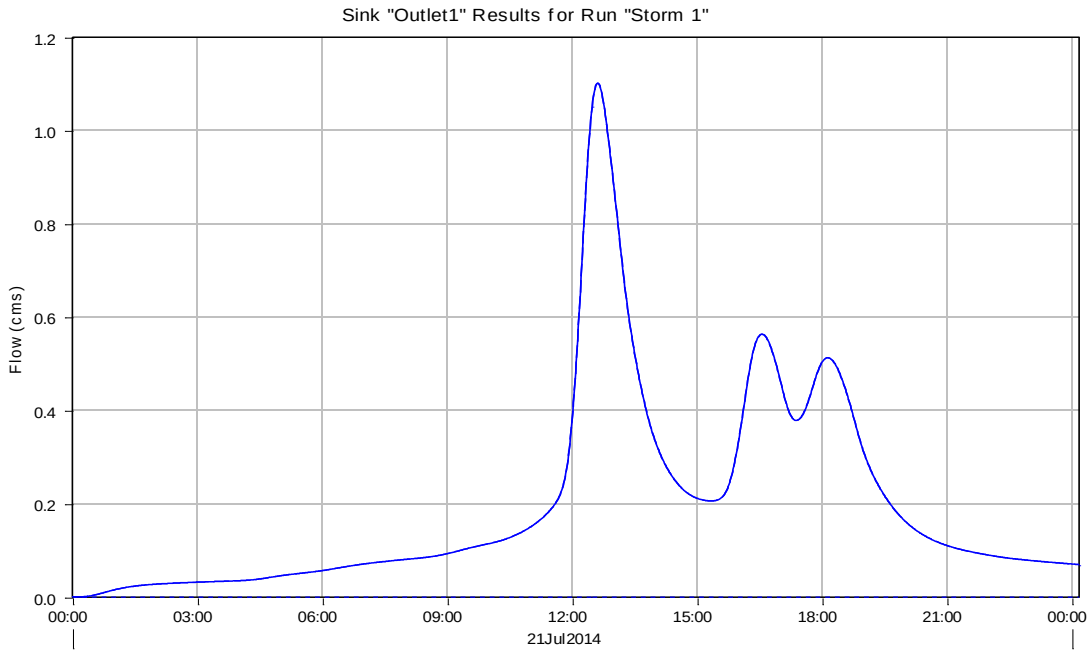

Figure A.78: HEC-HMS hydrograph at the total watershed outlet for storm event 7/21/14-7/22/14 of 0.49 inches

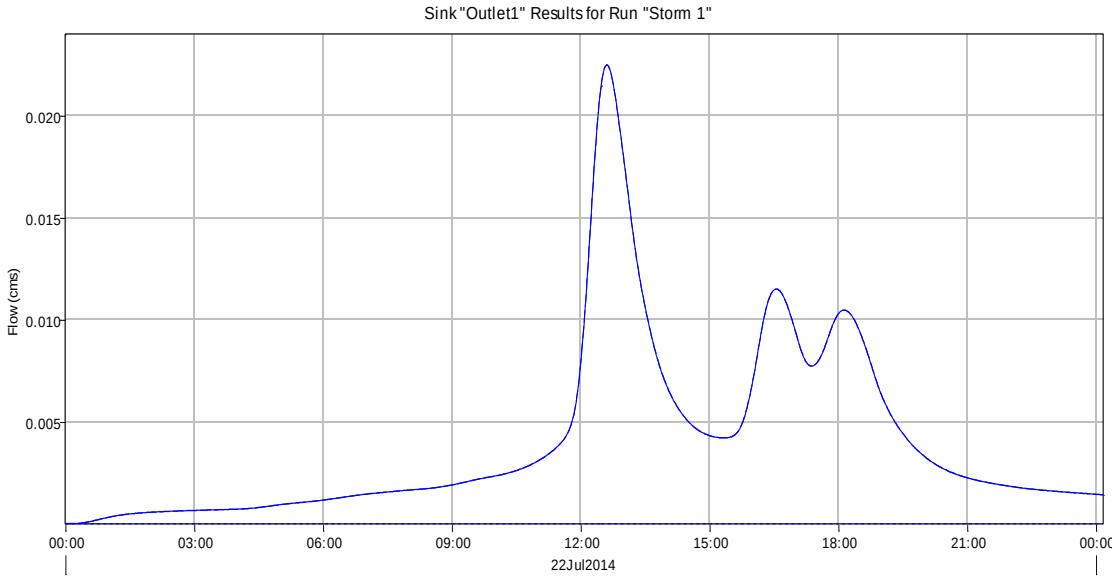

Figure A.79: HEC-HMS hydrograph at the total watershed outlet for storm event 7/22/14 of 0.01 inches

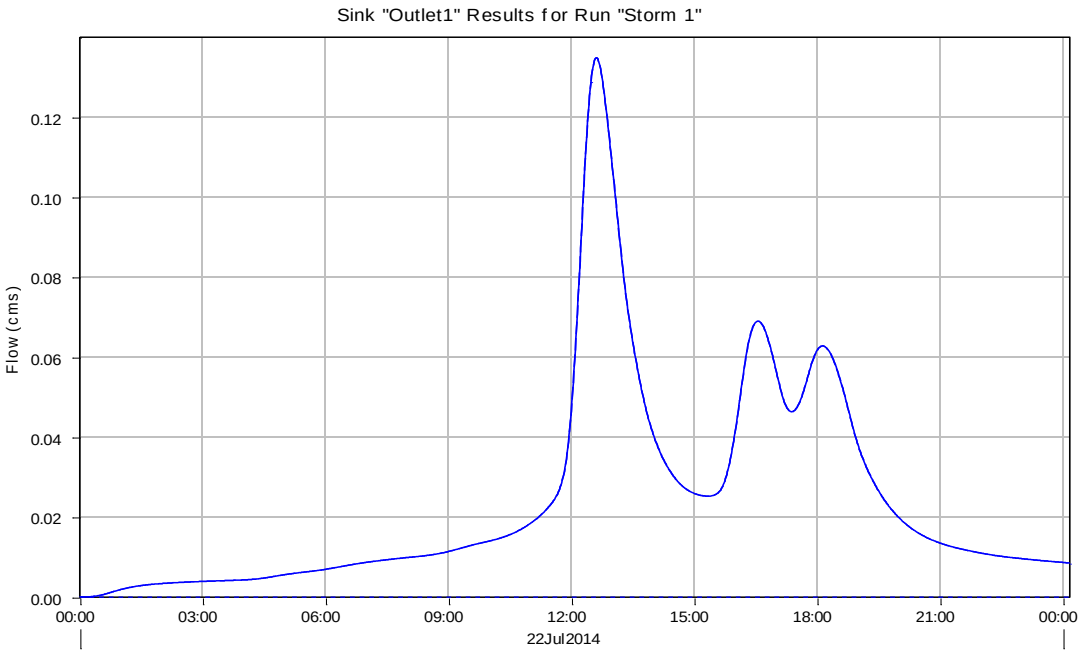

Figure A.80: HEC-HMS hydrograph at the total watershed outlet for storm event 7/22/14-7/23/14 of 0.06 inches

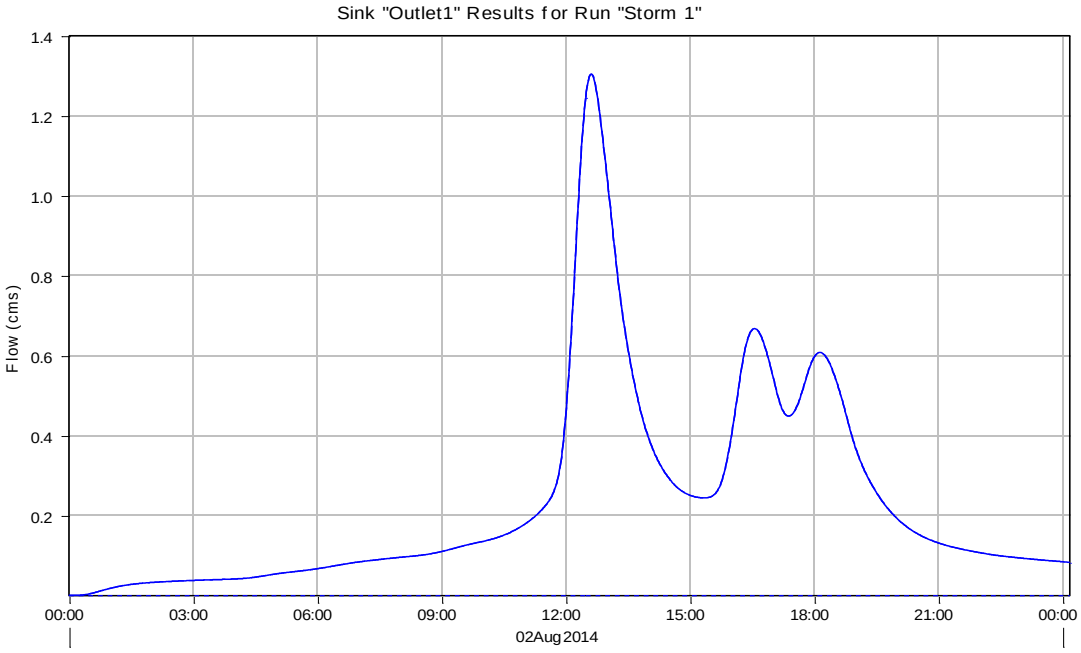

Figure A.81: HEC-HMS hydrograph at the total watershed outlet for storm event 8/2/14 of 0.58 inches

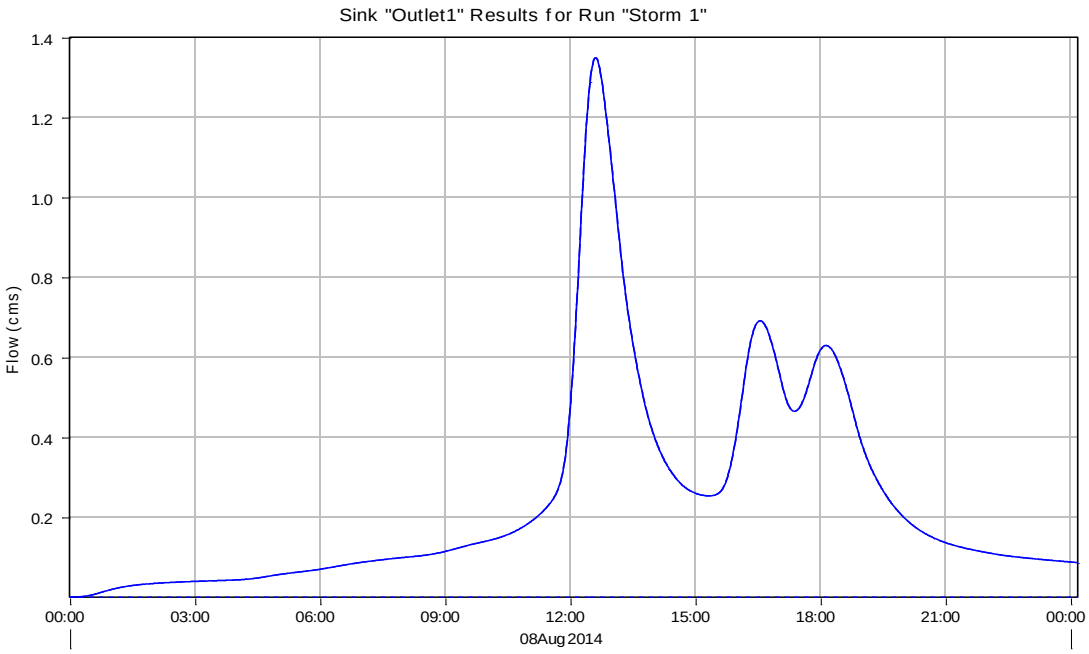

Figure A.82: HEC-HMS hydrograph at the total watershed outlet for storm event 8/8/14-8/9/14 of 0.60 inches

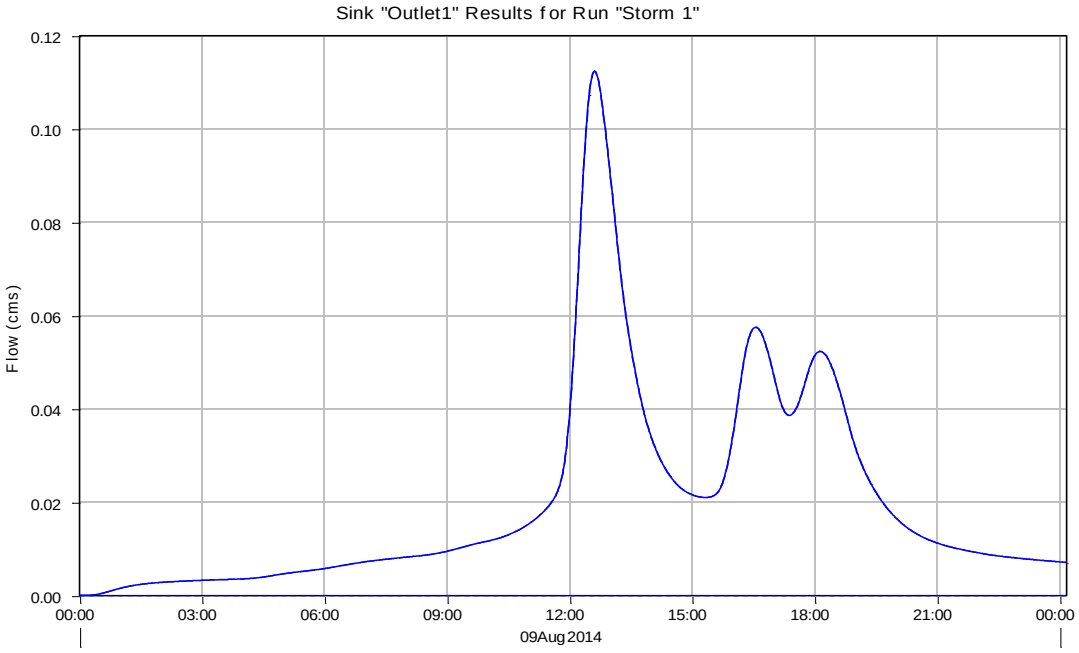

Figure A.83: HEC-HMS hydrograph at the total watershed outlet for storm event 8/9/14 of 0.05 inches

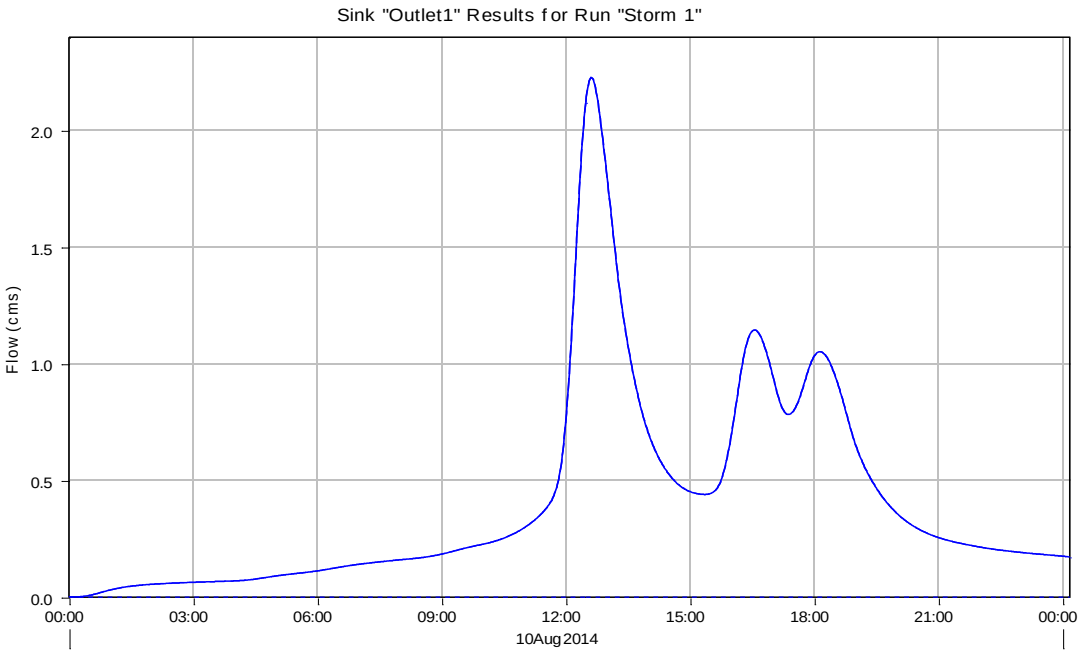

Figure A.84: HEC-HMS hydrograph at the total watershed outlet for storm event 8/10/14-8/11/14 of 0.97 inches

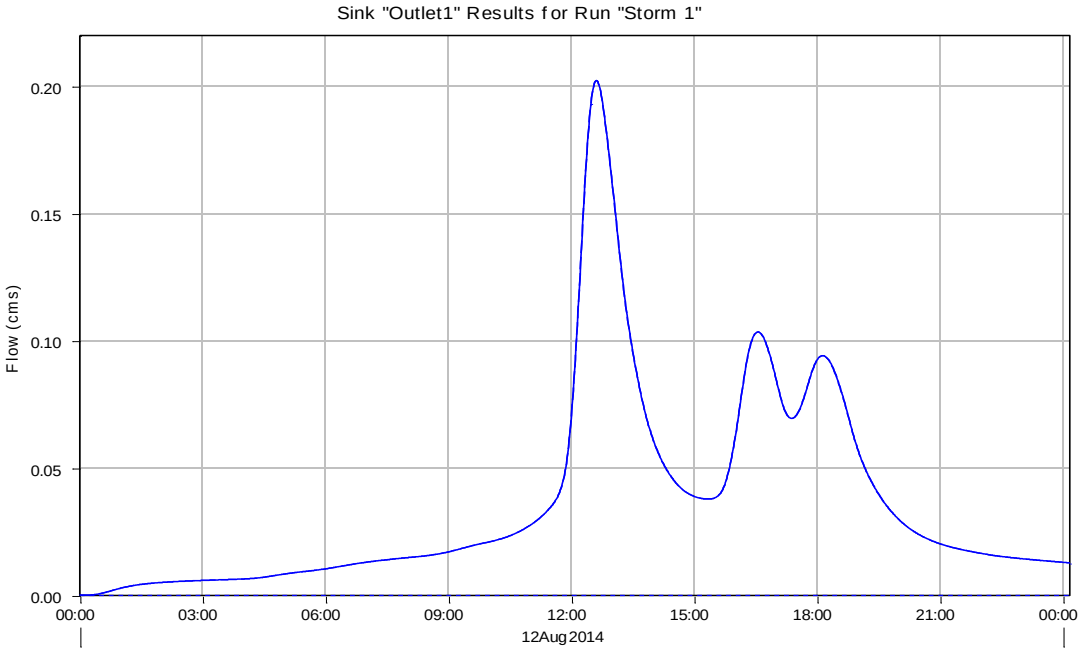

Figure A.85: HEC-HMS hydrograph at the total watershed outlet for storm event 8/12/14 of 0.09 inches

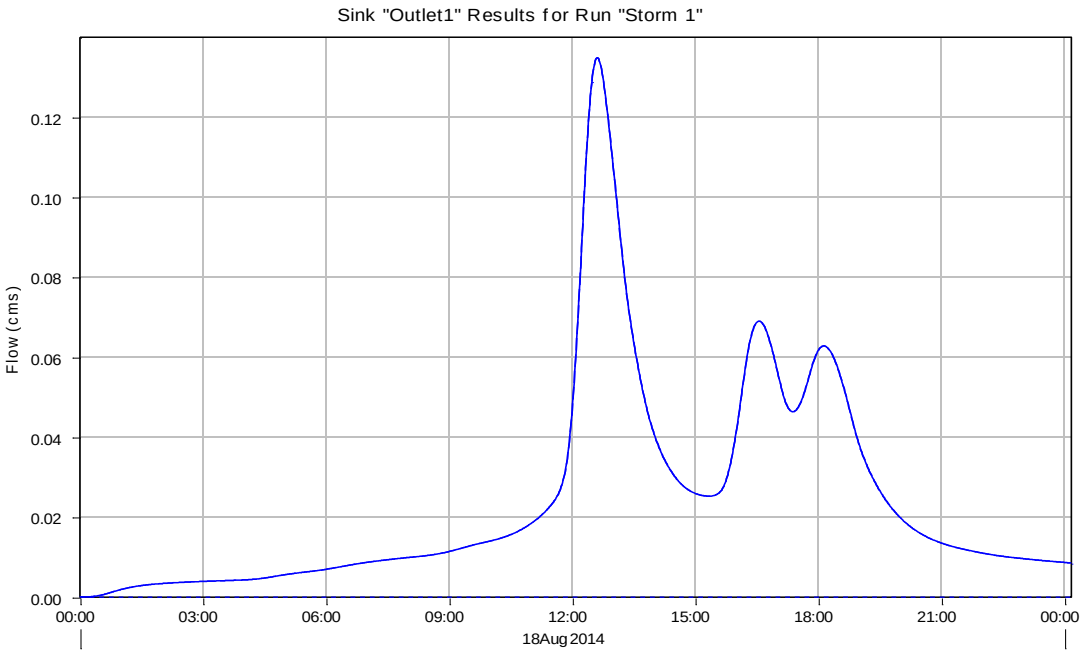

Figure A.86: HEC-HMS hydrograph at the total watershed outlet for storm event 8/18/14-8/19/14 of 0.06 inches

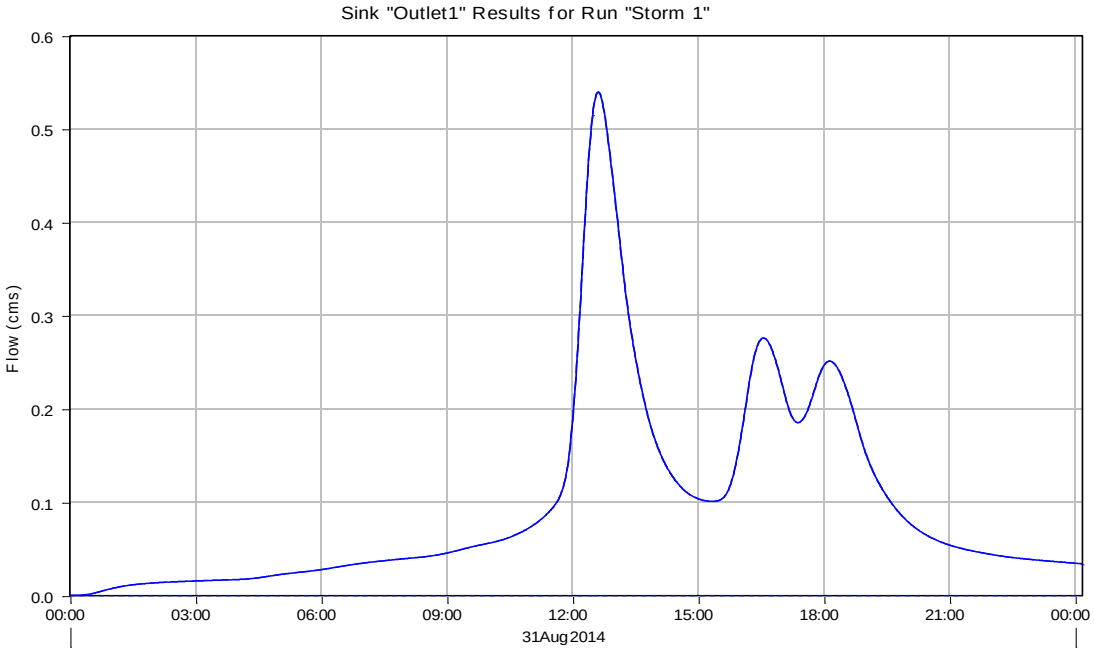

Figure A.87: HEC-HMS hydrograph at the total watershed outlet for storm event 8/31/14 of 0.24 inches

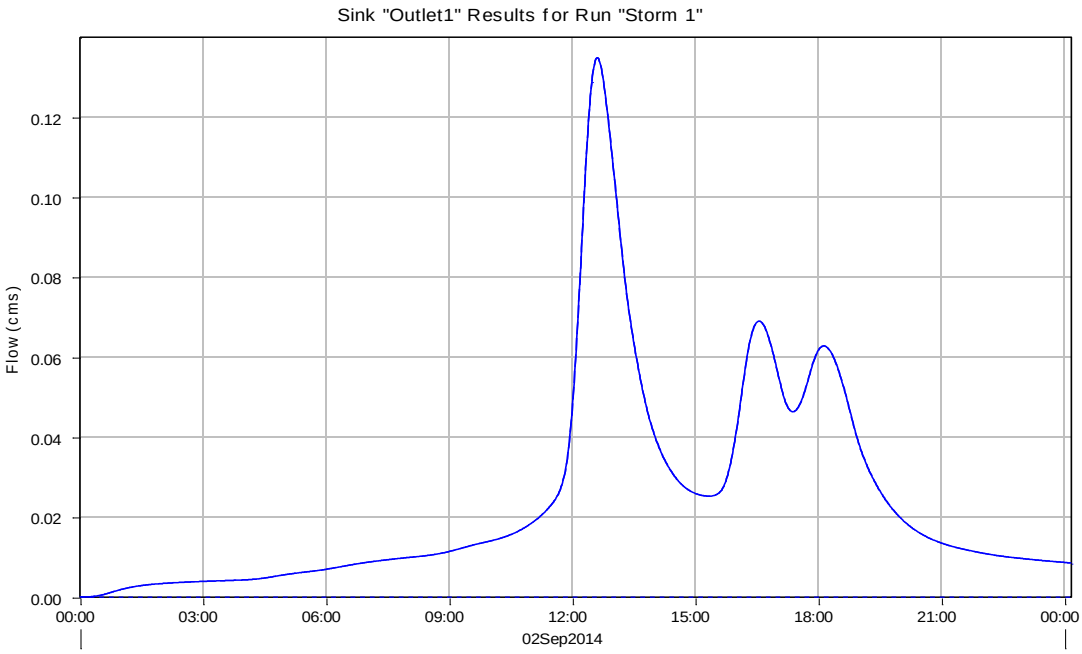

Figure A.88: HEC-HMS hydrograph at the total watershed outlet for storm event 9/2/14-9/3/14 of 0.06 inches

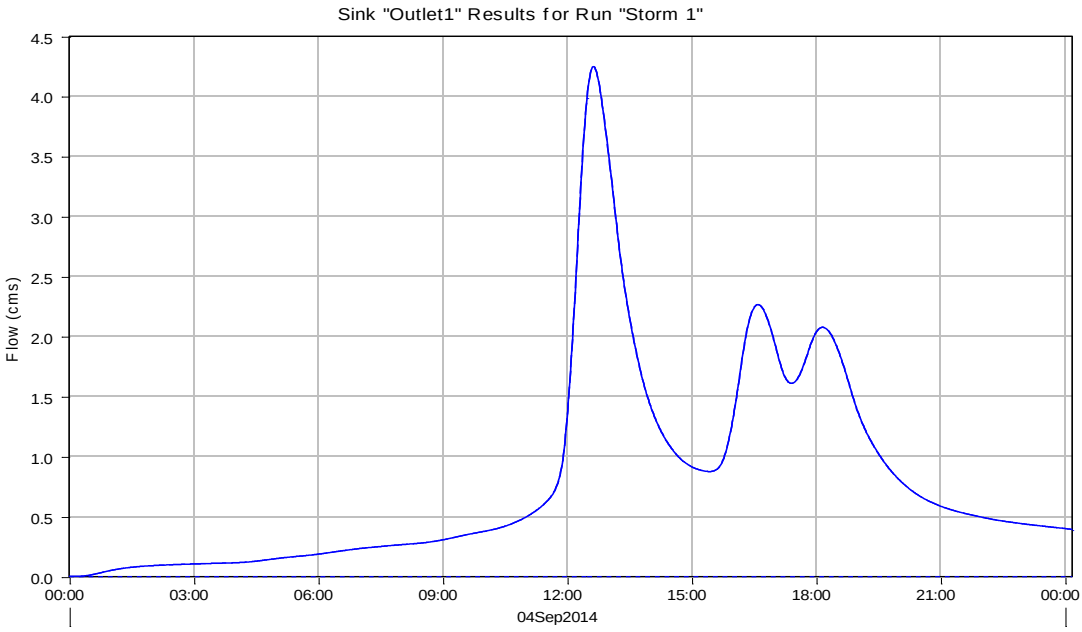

Figure A.89: HEC-HMS hydrograph at the total watershed outlet for storm event 9/4/14 of 1.61 inches

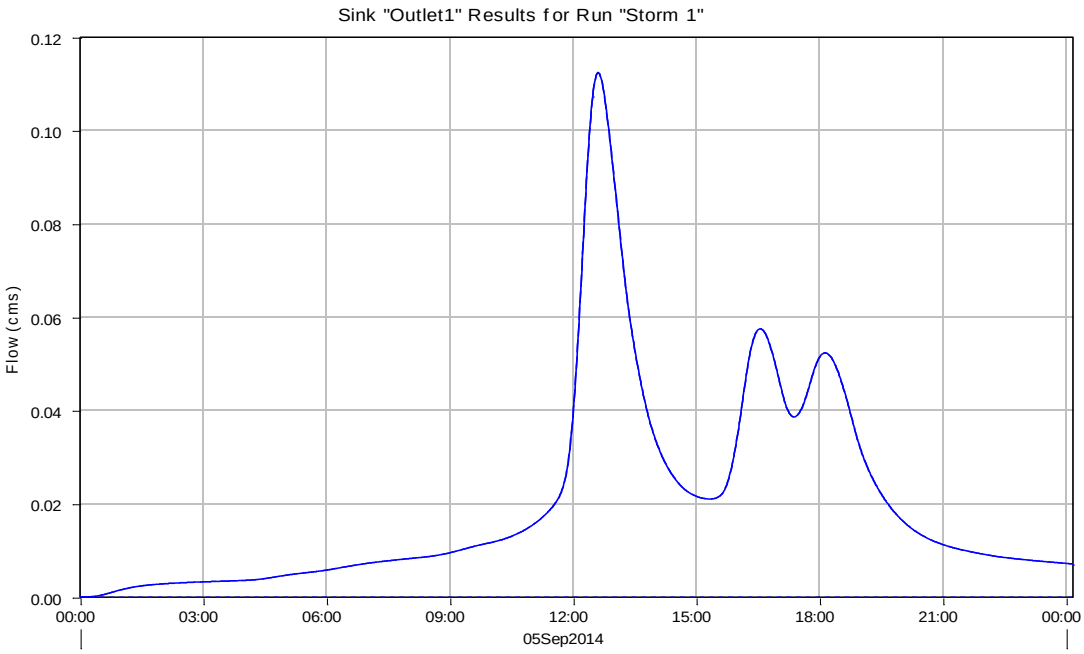

Figure A.90: HEC-HMS hydrograph at the total watershed outlet for storm event 9/5/14 of 0.05 inches

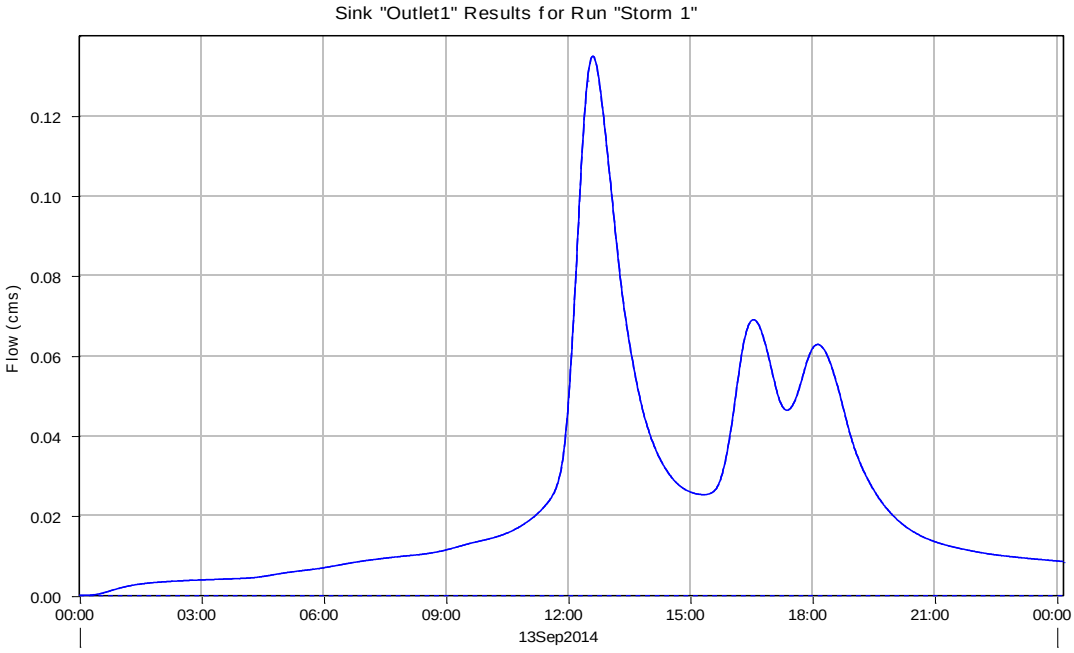

Figure A.91: HEC-HMS hydrograph at the total watershed outlet for storm event 9/13/14 of 0.06 inches

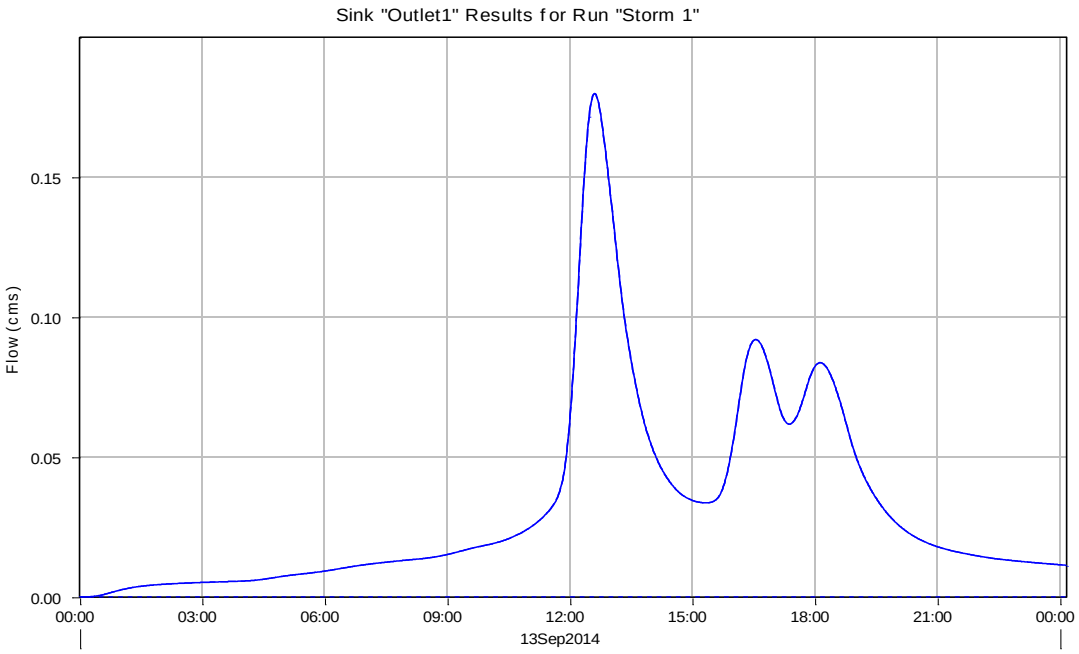

Figure A.92: HEC-HMS hydrograph at the total watershed outlet for storm event 9/13/14 of 0.08 inches

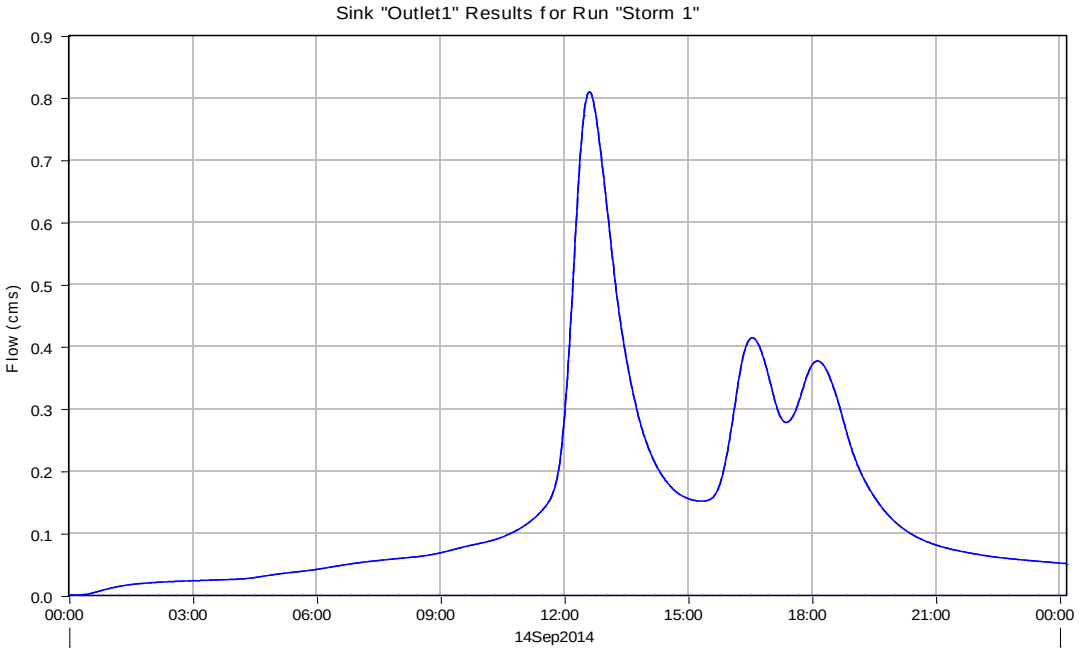

Figure A.93: HEC-HMS hydrograph at the total watershed outlet for storm event 9/14/14 of 0.36 inches

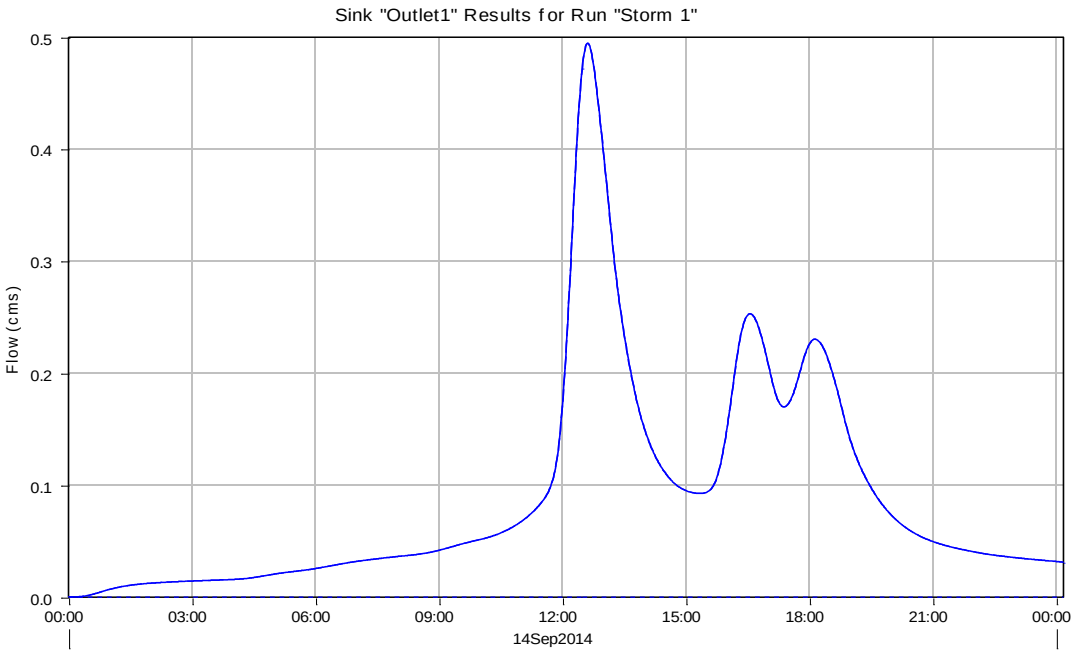

Figure A.94: HEC-HMS hydrograph at the total watershed outlet for storm event 9/14/14-9/15/14 of 0.22 inches

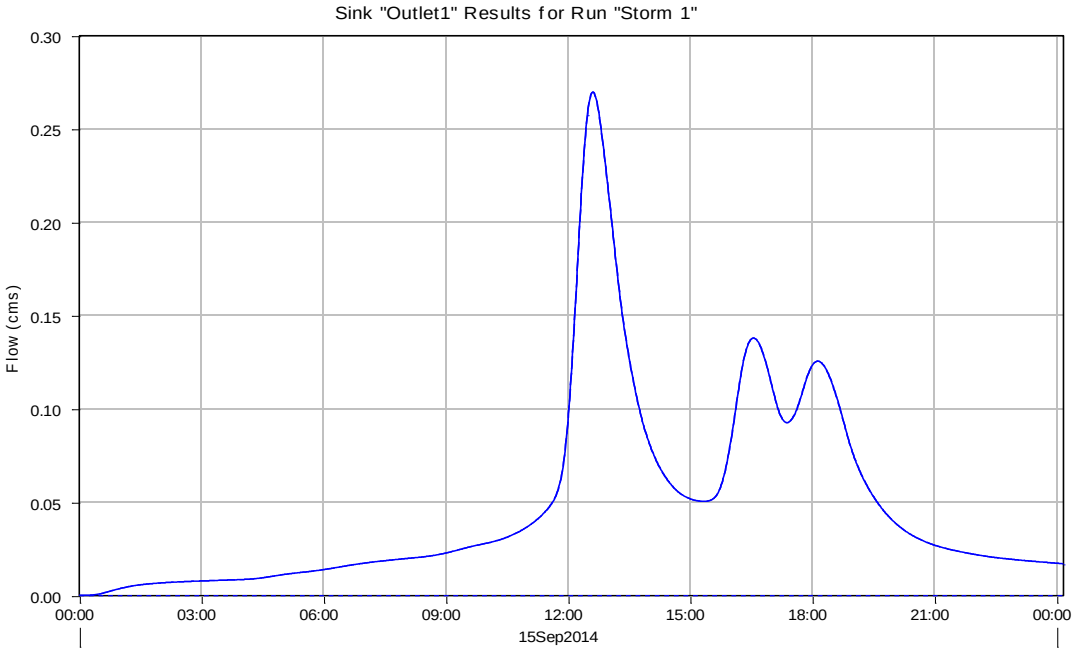

Figure A.95: HEC-HMS hydrograph at the total watershed outlet for storm event 9/15/14 of 0.12 inches

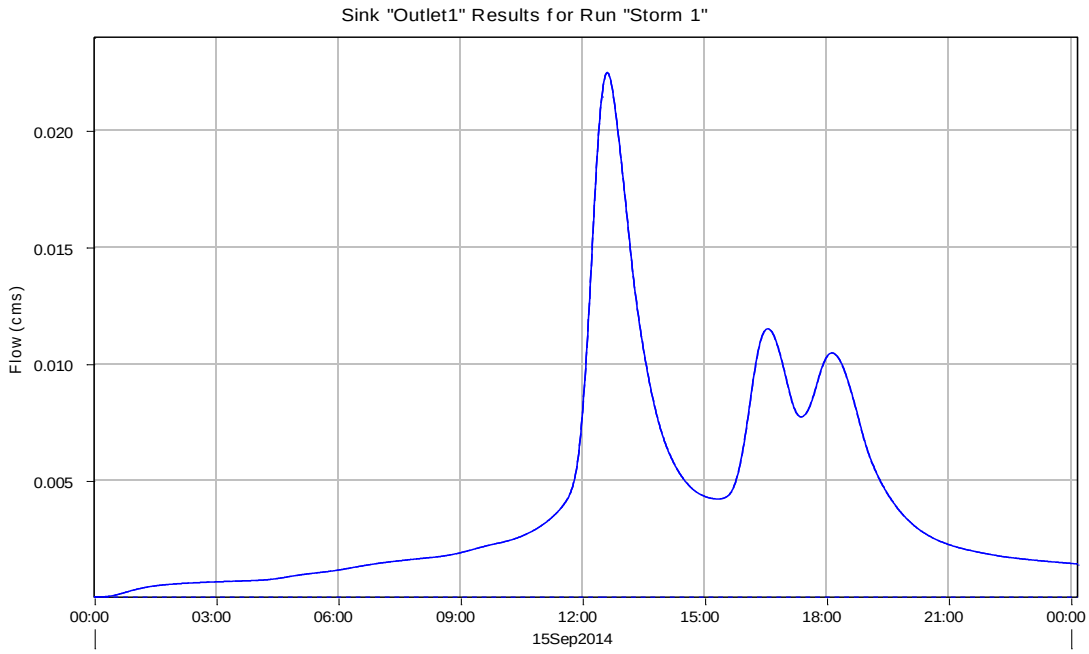

Figure A.96: HEC-HMS hydrograph at the total watershed outlet for storm event 9/15/14-9/16/14 of 0.01 inches

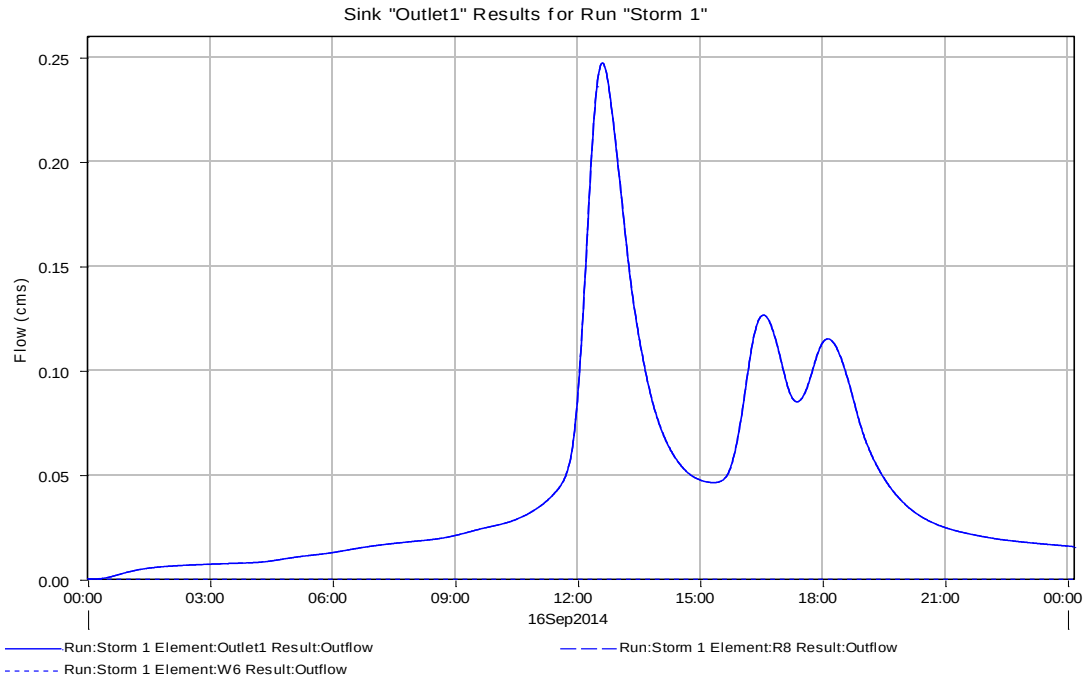

Figure A.97: HEC-HMS hydrograph at the total watershed outlet for storm event 9/16/14 of 0.11 inches

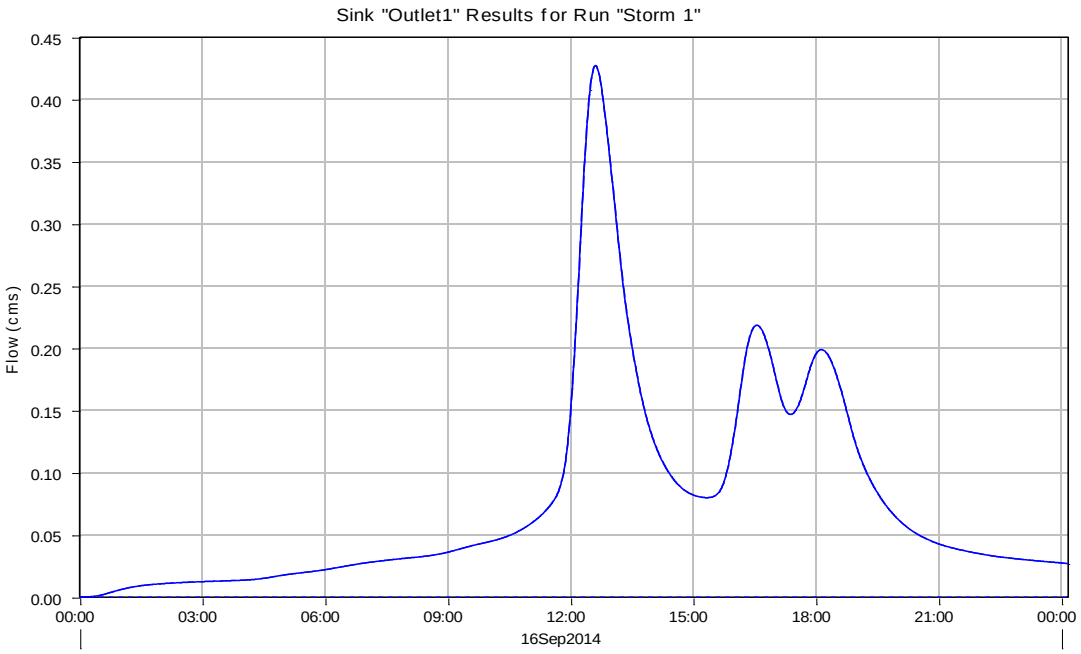

Figure A.98: HEC-HMS hydrograph at the total watershed outlet for storm event 9/16/14-9/17/14 of 0.19 inches

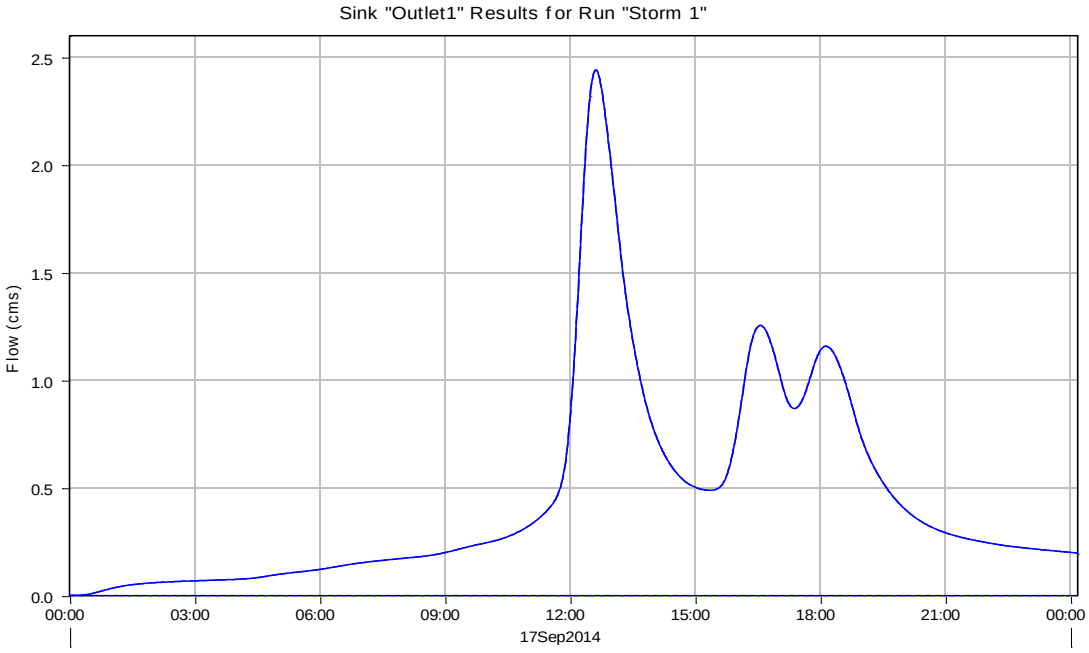

Figure A.99: HEC-HMS hydrograph at the total watershed outlet for storm event 9/17/14-9/18/14 of 1.05 inches

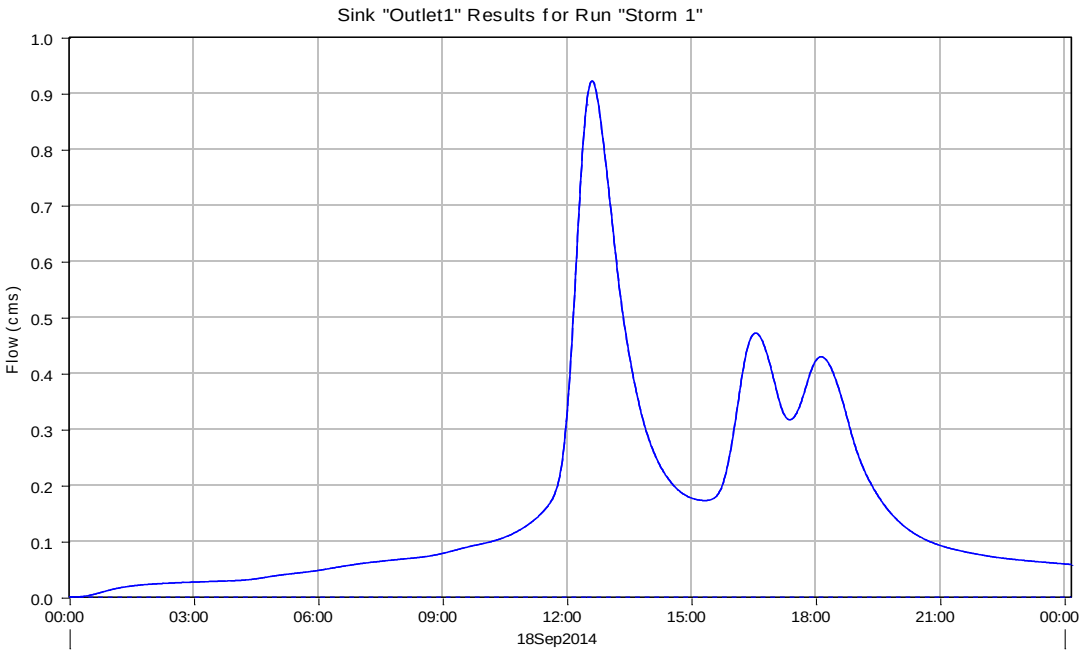

Figure A.100: HEC-HMS hydrograph at the total watershed outlet for storm event 9/18/14-9/19/14 of 0.41 inches

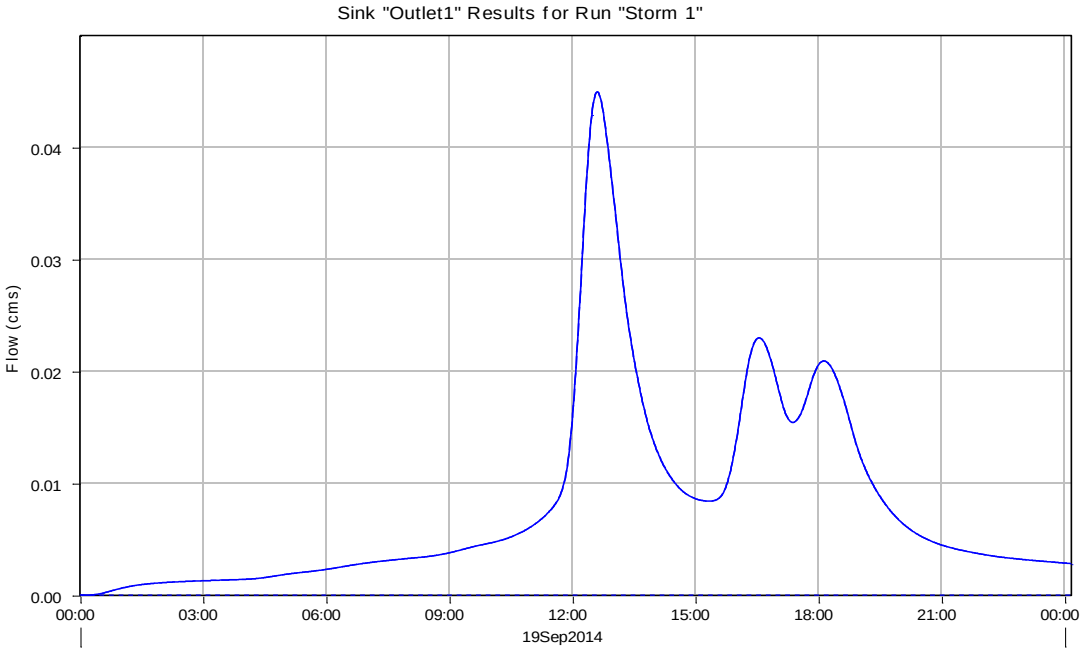

Figure A.101: HEC-HMS hydrograph at the total watershed outlet for storm event 9/19/14-9/20/14 of 0.02 inches

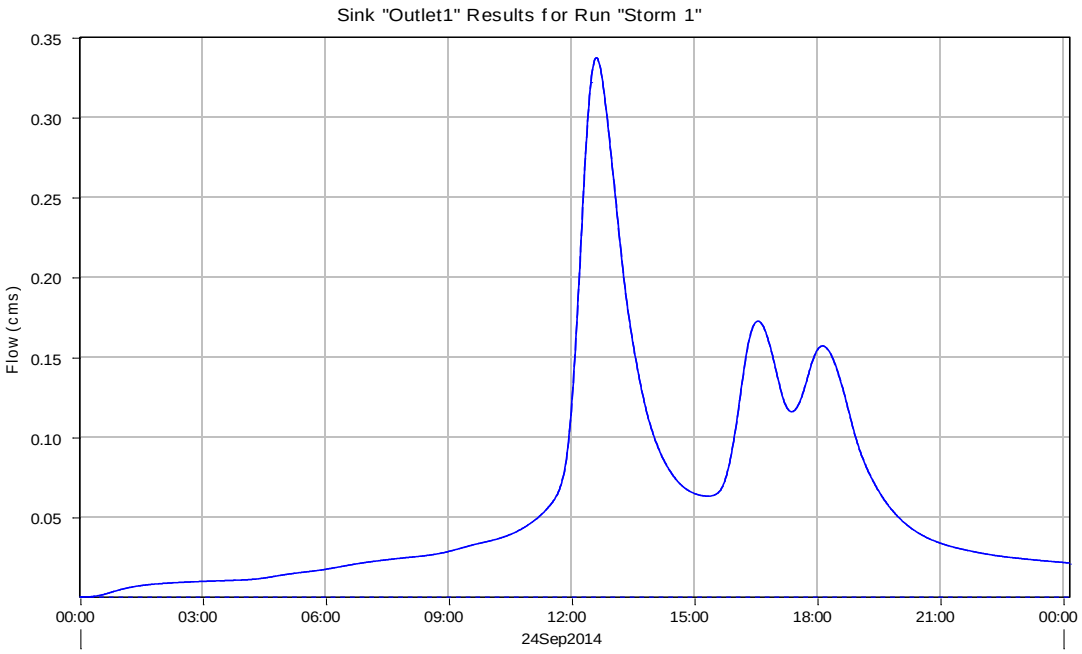

Figure A.102: HEC-HMS hydrograph at the total watershed outlet for storm event 9/24/14 of 0.15 inches

A.3 SENSOR HYDROGRAPHS

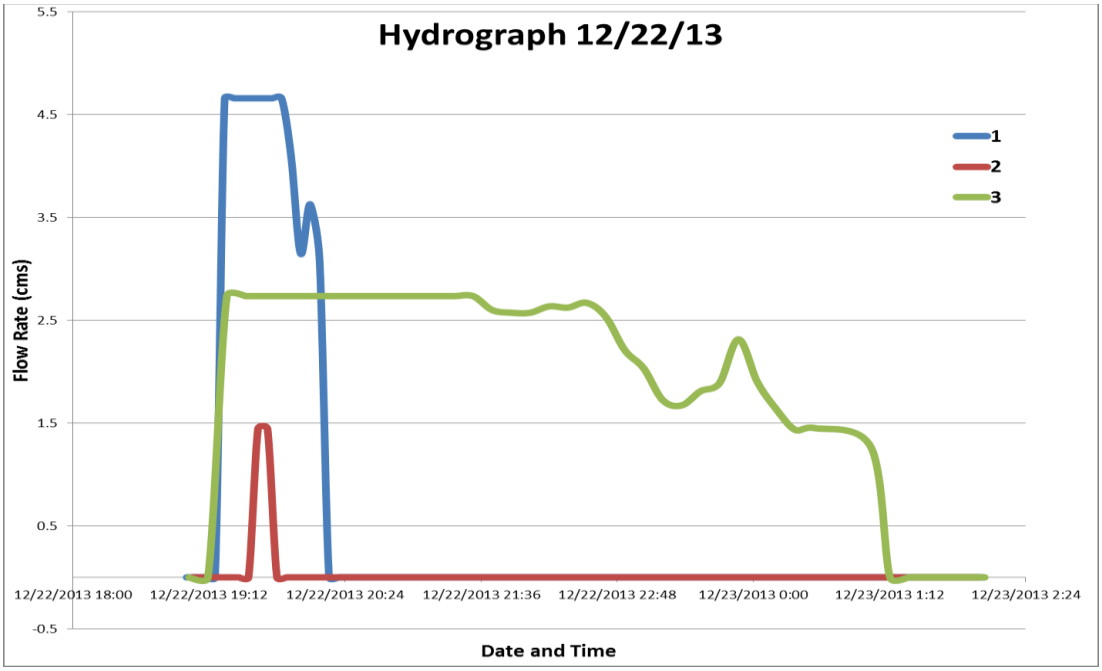

Figure A.103: Sensor hydrograph for all subwatersheds 1-11 for storm event 12/22/13 of 0.77 inches

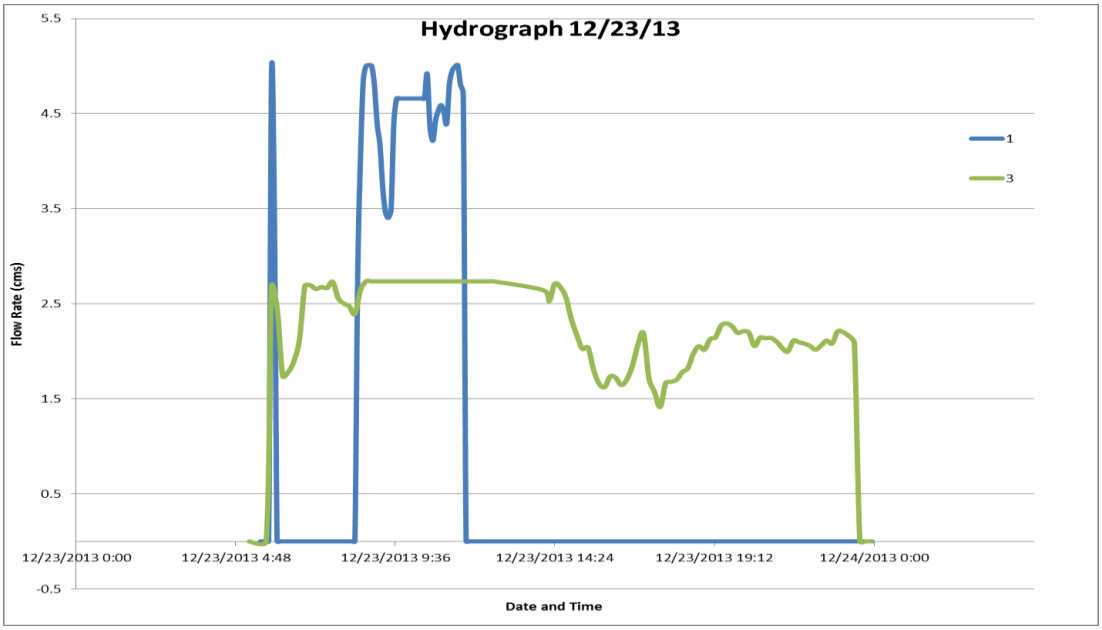

Figure A.104: Sensor hydrograph for all subwatersheds 1-11 for storm event 12/23/13 of 0.82 inches

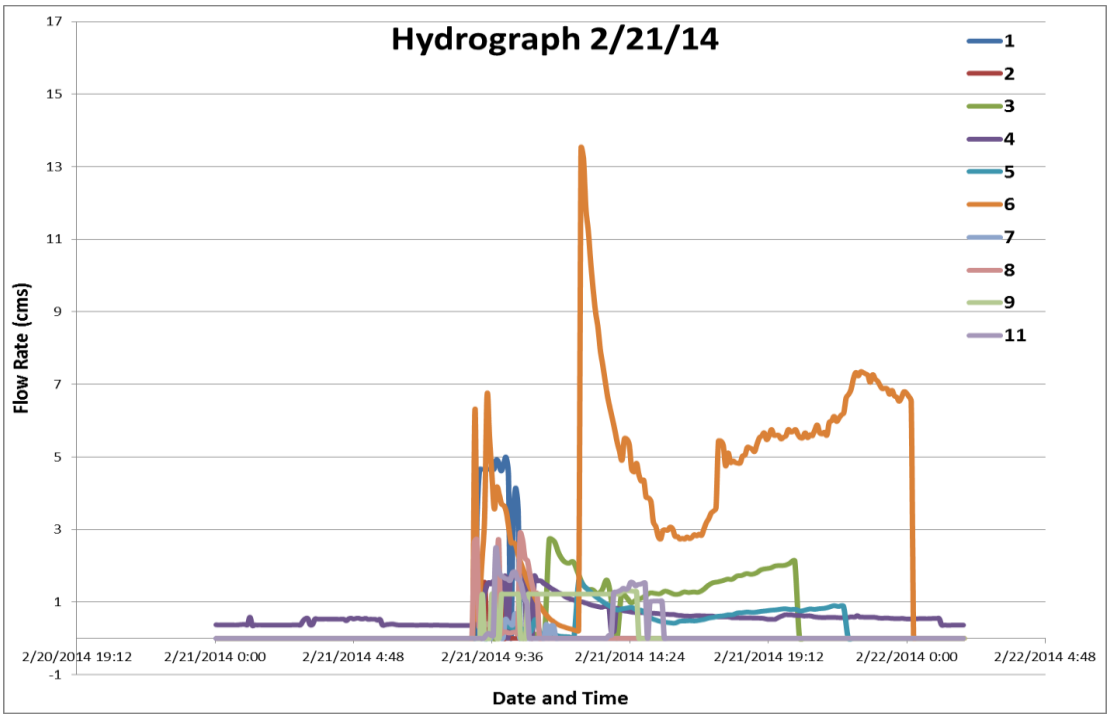

Figure A.105: Sensor hydrograph for all subwatersheds 1-11 for storm event 2/21/14 of 0.34 inches

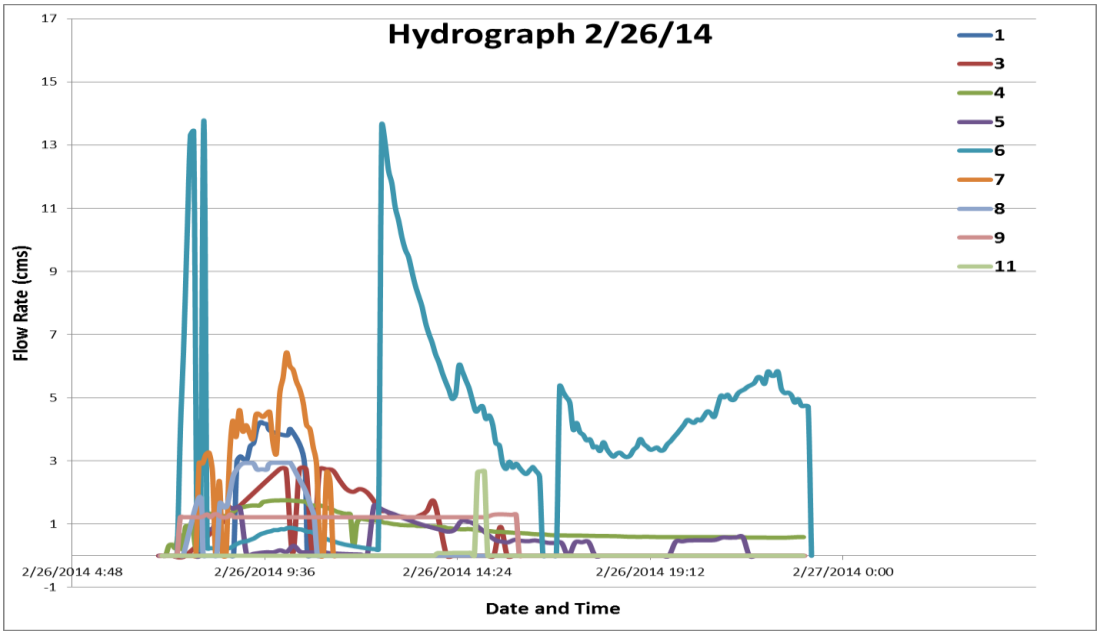

Figure A.106: Sensor hydrograph for all subwatersheds 1-11 for storm event 2/26/14 of 1.28 inches

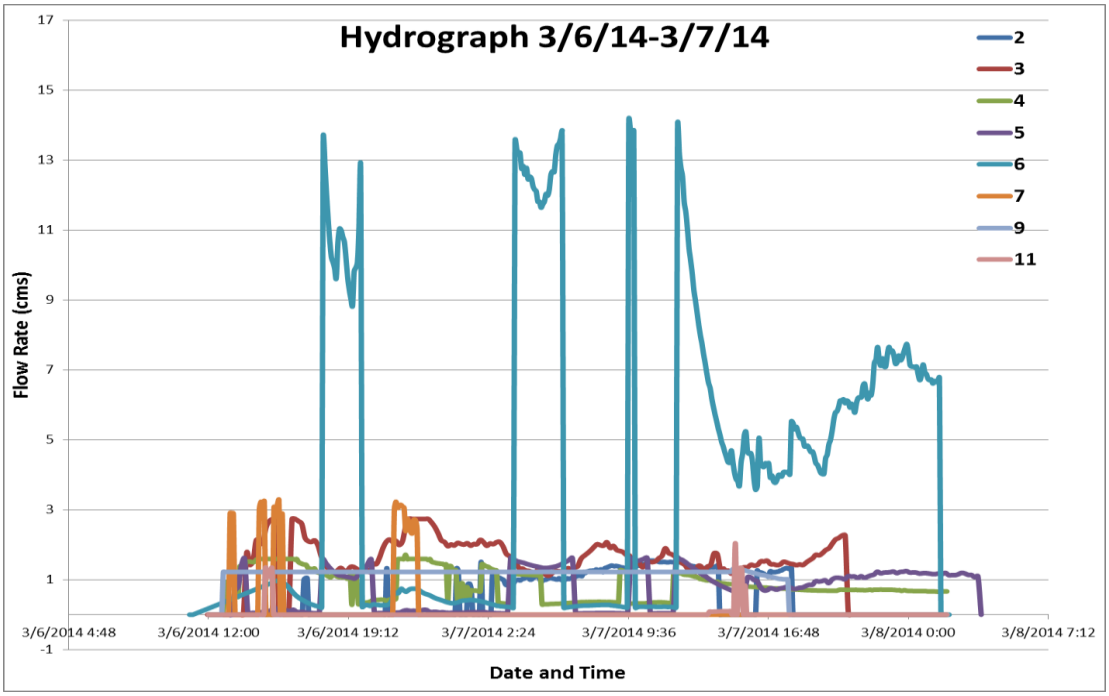

Figure A.107: Sensor hydrograph for all subwatersheds 1-11 for storm event 3/6/14-3/7/14 of 0.77 inches

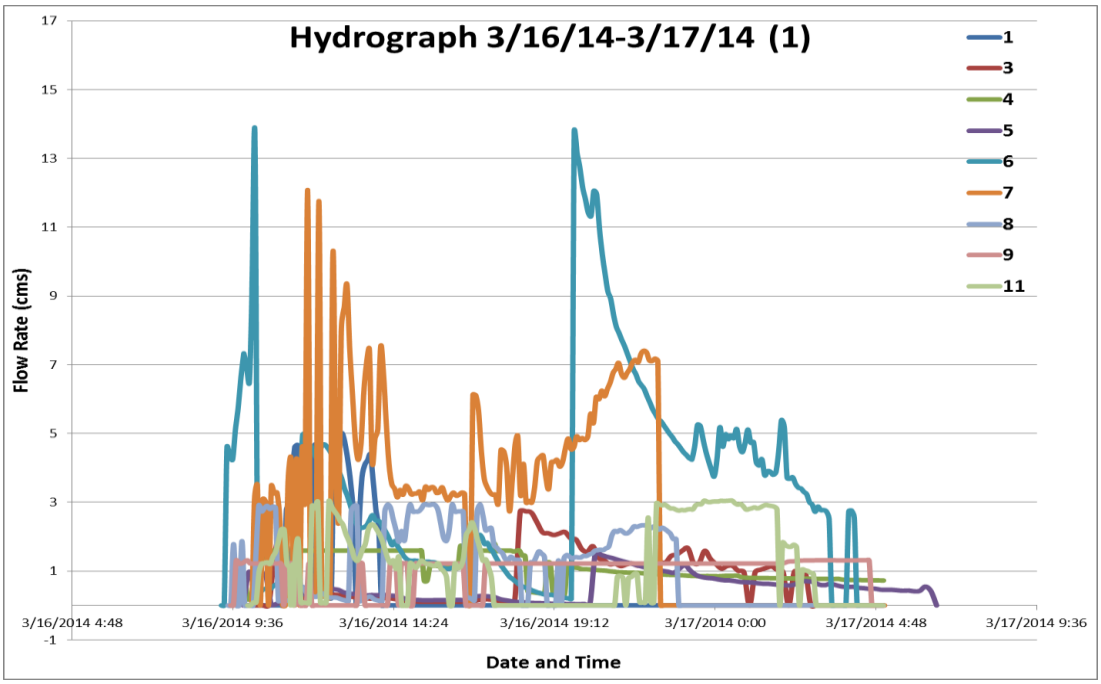

Figure A.108: Sensor hydrograph for all subwatersheds 1-11 for storm event 3/16/14-3/17/14 of 1.27 inches

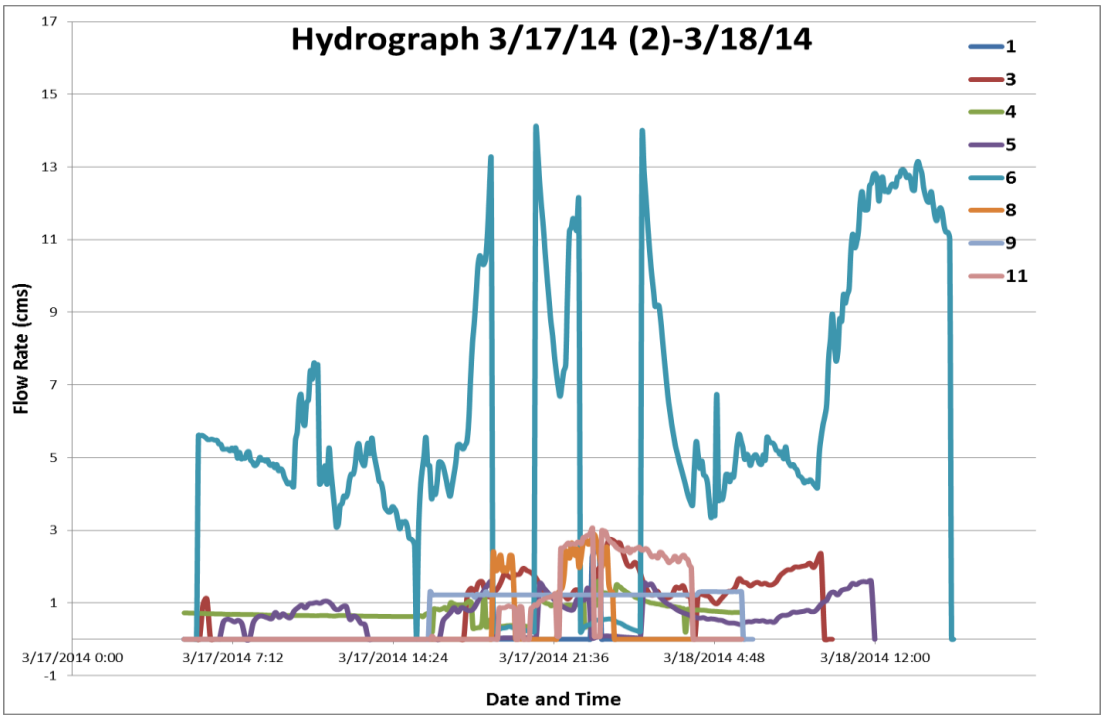

Figure A.109: Sensor hydrograph for all subwatersheds 1-11 for storm event 3/17/14-3/18/14 of 0.20 inches

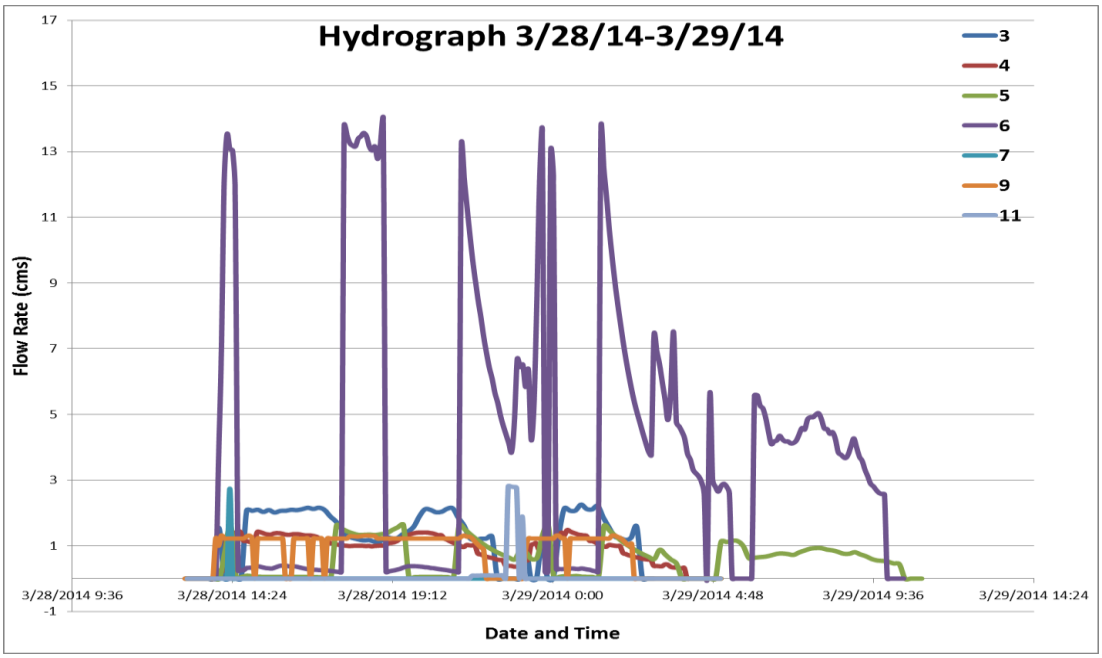

Figure A.110: Sensor hydrograph for all subwatersheds 1-11 for storm event 3/28/14-3/29/14 of 0.50 inches

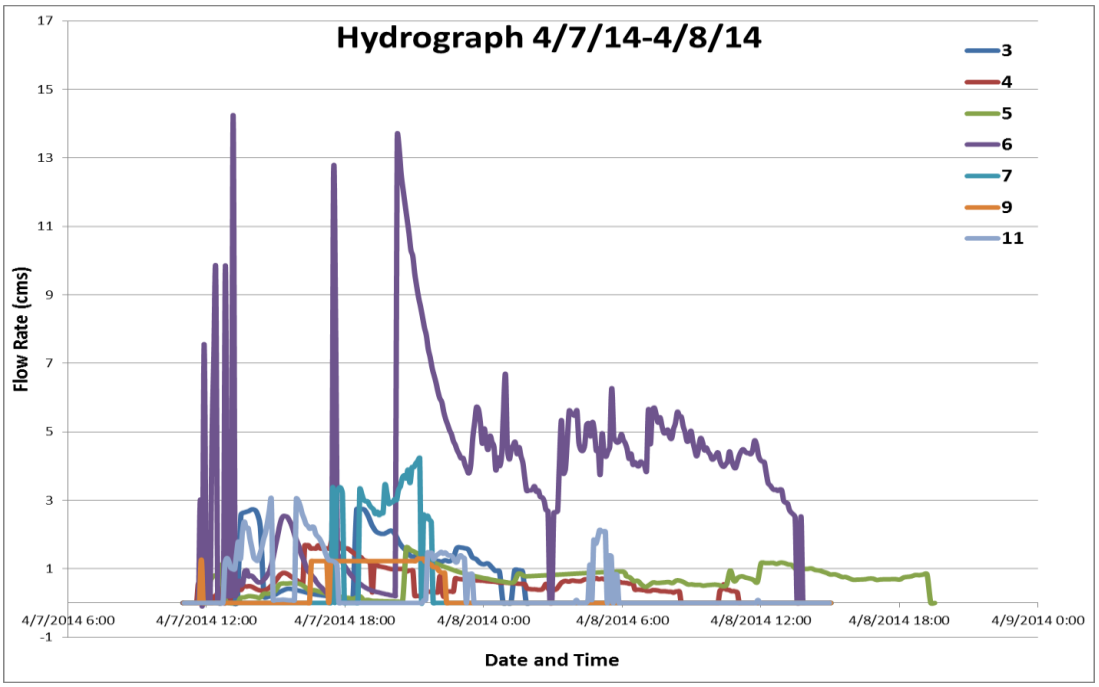

Figure A.111: Sensor hydrograph for all subwatersheds 1-11 for storm event 4/7/14-4/8/14 of 1.31 inches

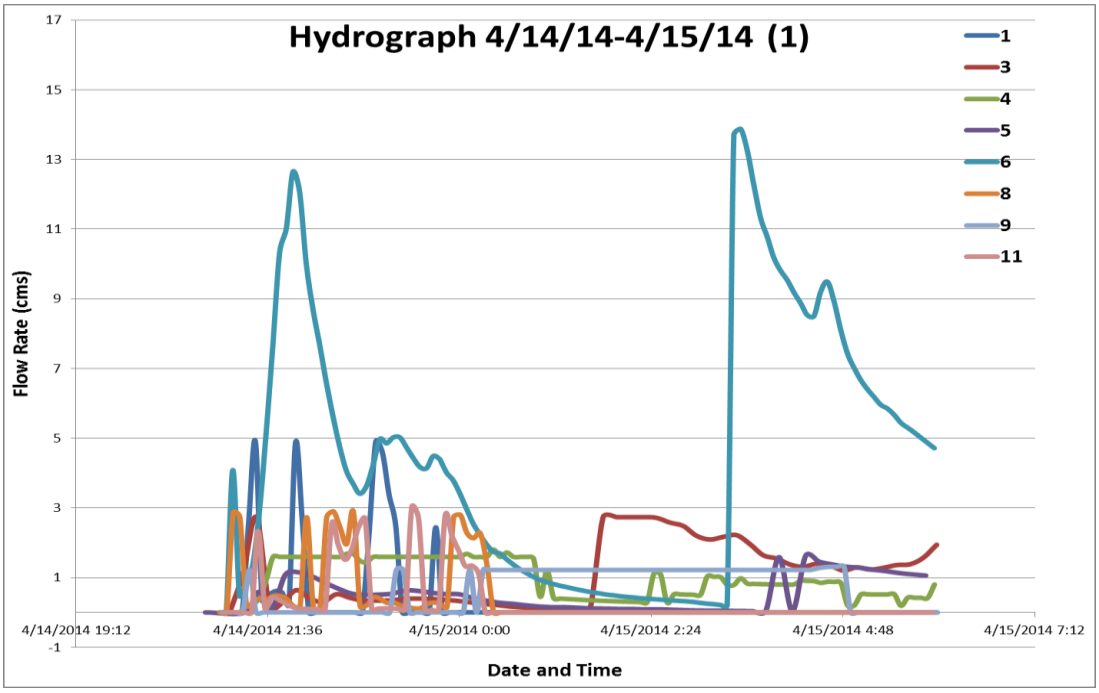

Figure A.112: Sensor hydrograph for all subwatersheds 1-11 for storm event 4/14/14-4/15/14 of 1.36 inches

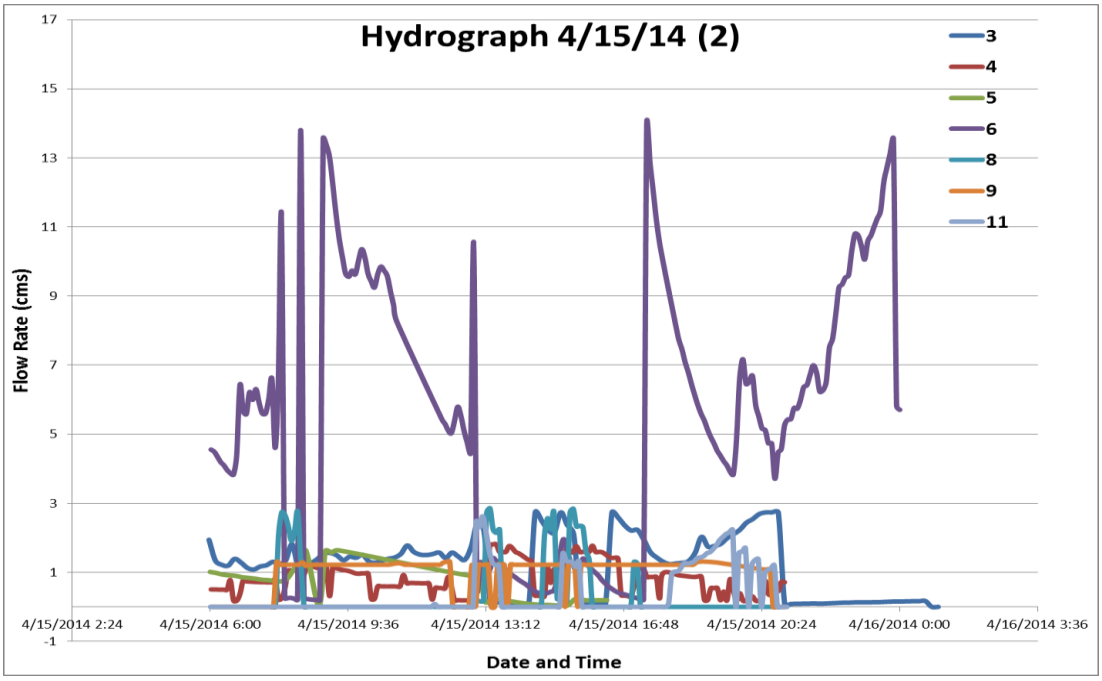

Figure A.113: Sensor hydrograph for all subwatersheds 1-11 for storm event 4/15/14 of 0.26 inches

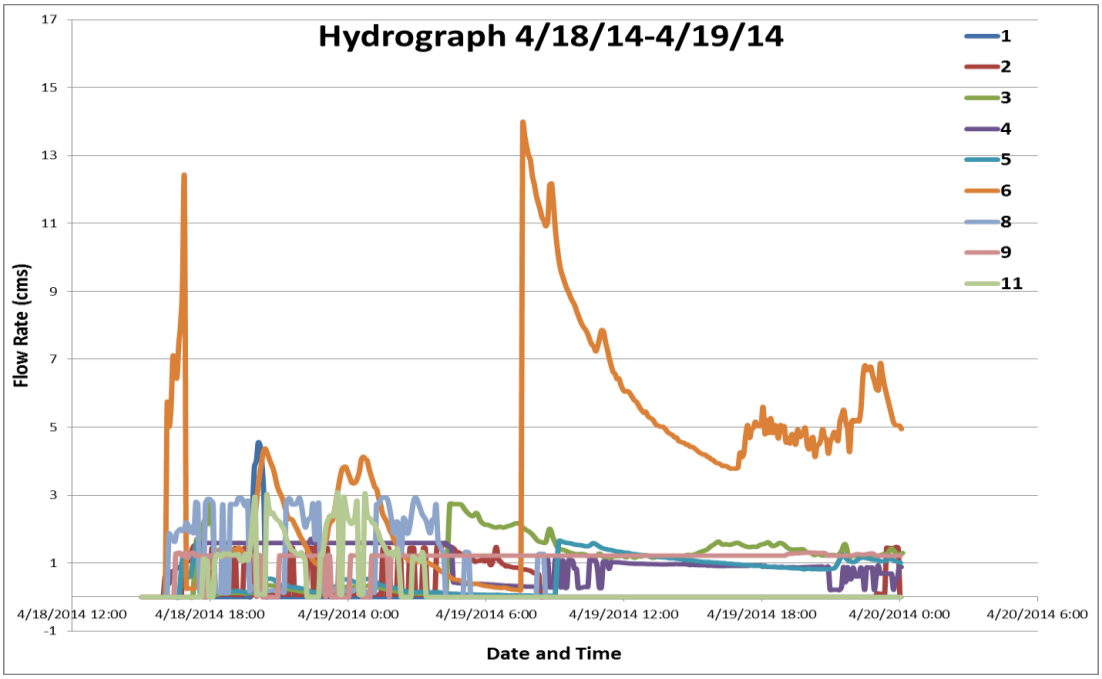

Figure A.114: Sensor hydrograph for all subwatersheds 1-11 for storm event 4/18/14-4/19/14 of 1.54 inches

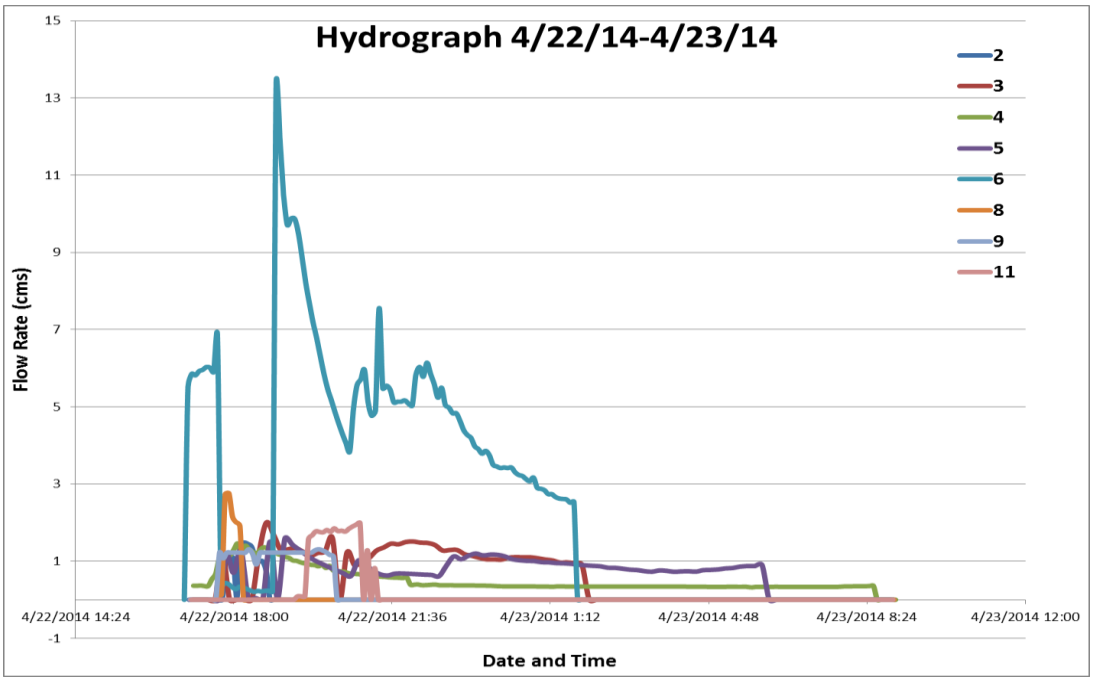

Figure A.115: Sensor hydrograph for all subwatersheds 1-11 for storm event 4/22/14-4/23/14 of 0.16 inches

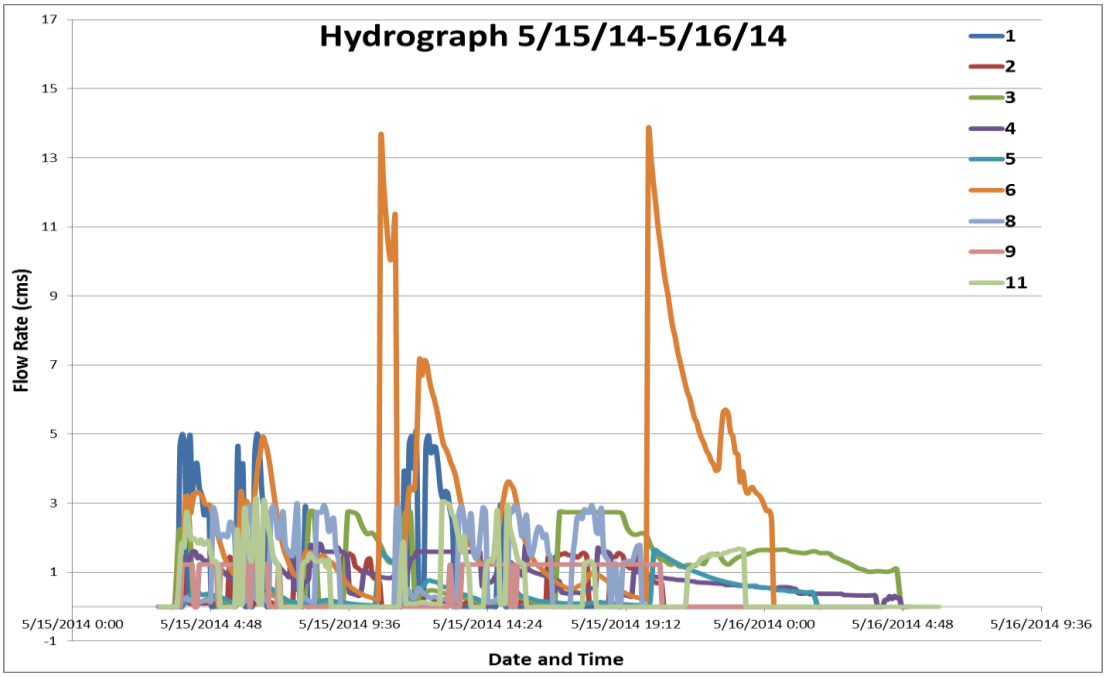

Figure A.116: Sensor hydrograph for all subwatersheds 1-11 for storm event 5/15/14-5/16/14 of 2.32 inches

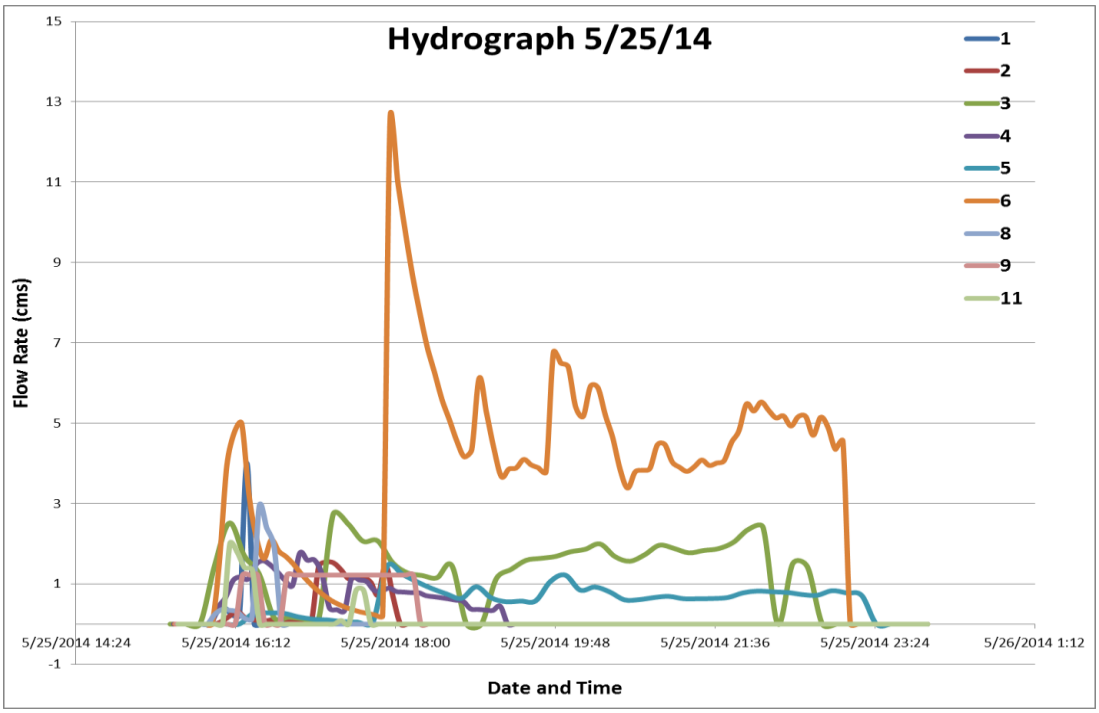

Figure A.117: Sensor hydrograph for all subwatersheds 1-11 for storm event 5/25/14 of 0.15 inches

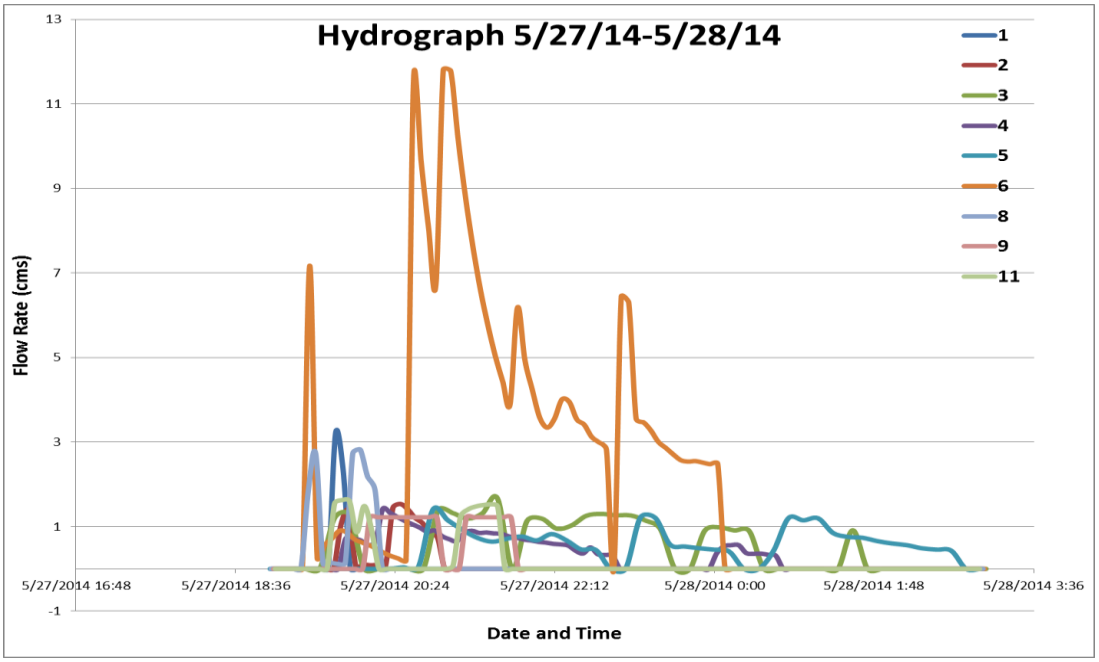

Figure A.118: Sensor hydrograph for all subwatersheds 1-11 for storm event 5/27/14-5/28/14 of 0.54 inches

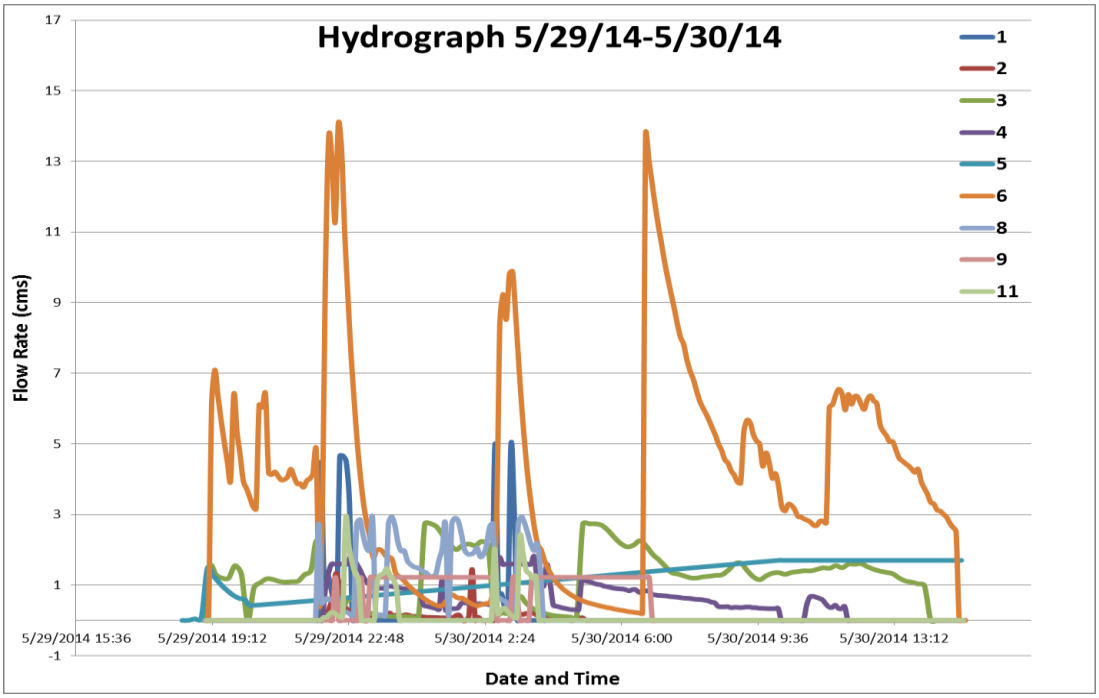

Figure A.119: Sensor hydrograph for all subwatersheds 1-11 for storm event 5/29/14-5/30/14 of 1.59 inches

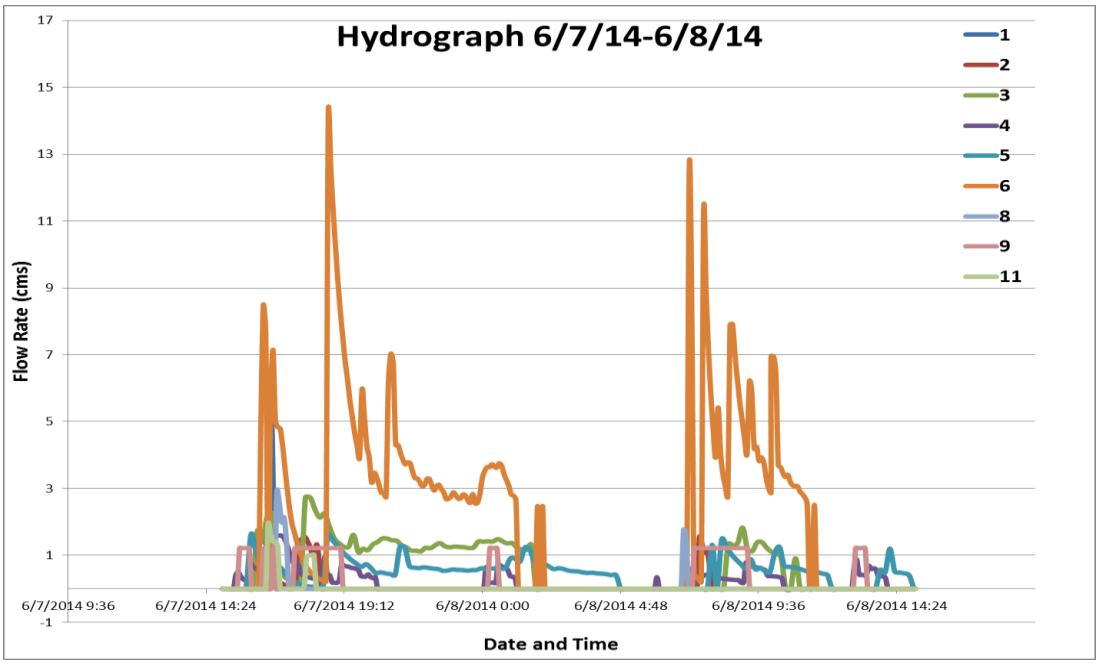

Figure A.120: Sensor hydrograph for all subwatersheds 1-11 for storm event 6/7/14-6/8/14 of 0.31 inches

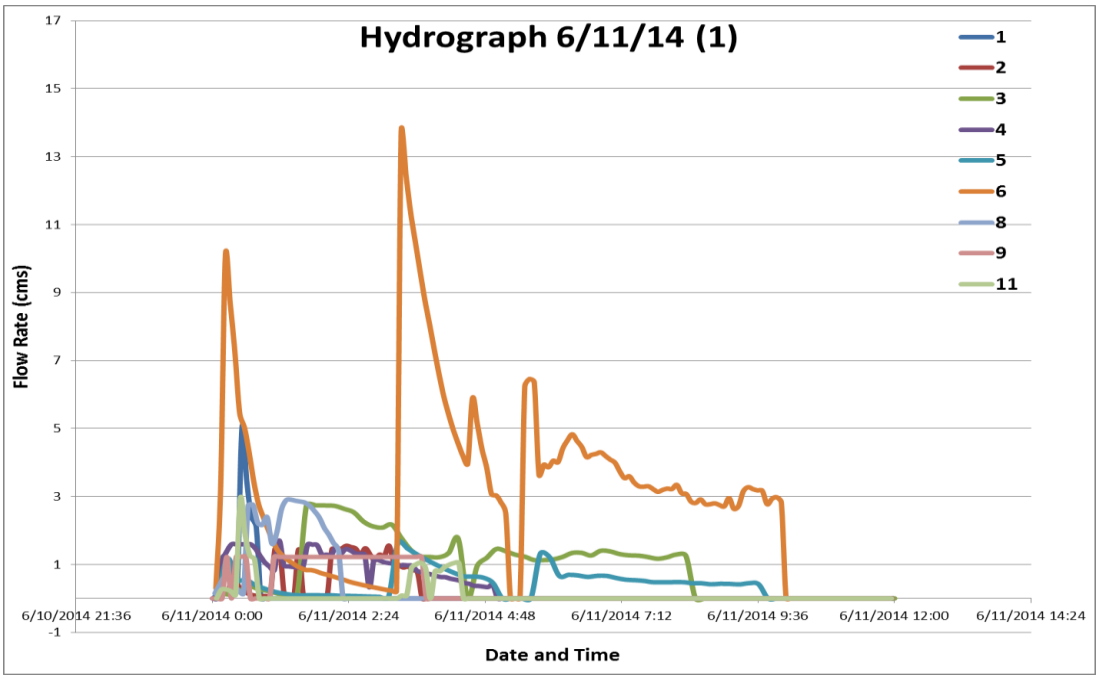

Figure A.121: Sensor hydrograph for all subwatersheds 1-11 for storm event 6/11/14 of 0.70 inches

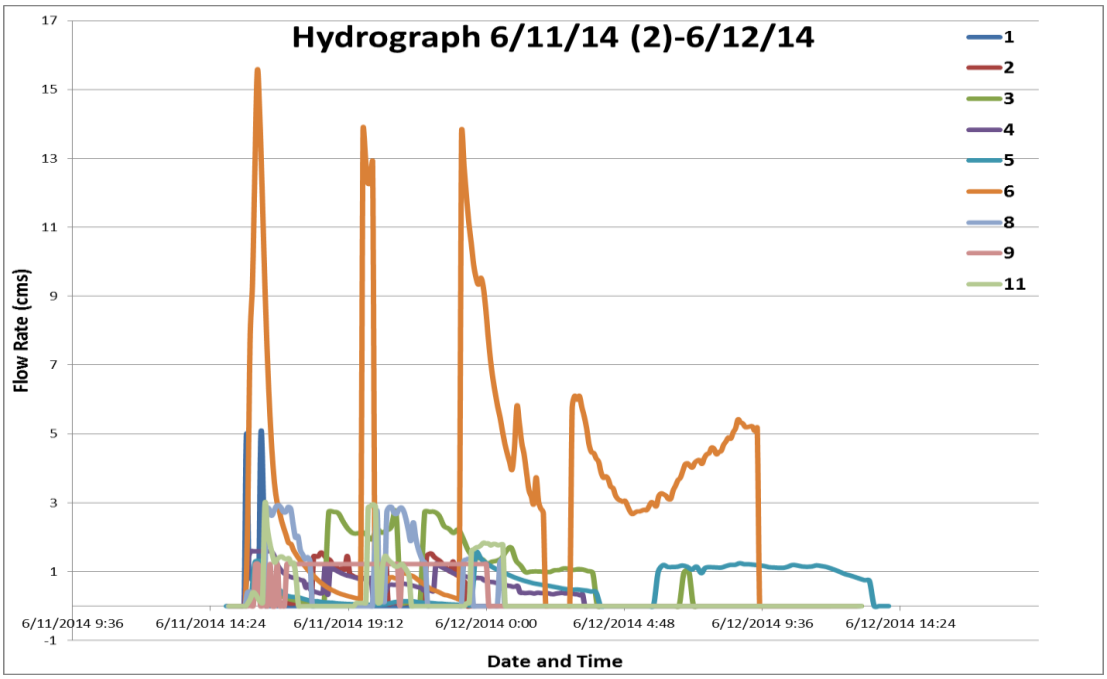

Figure A.122: Sensor hydrograph for all subwatersheds 1-11 for storm event 6/11/14-6/12/14 of 0.10 inches

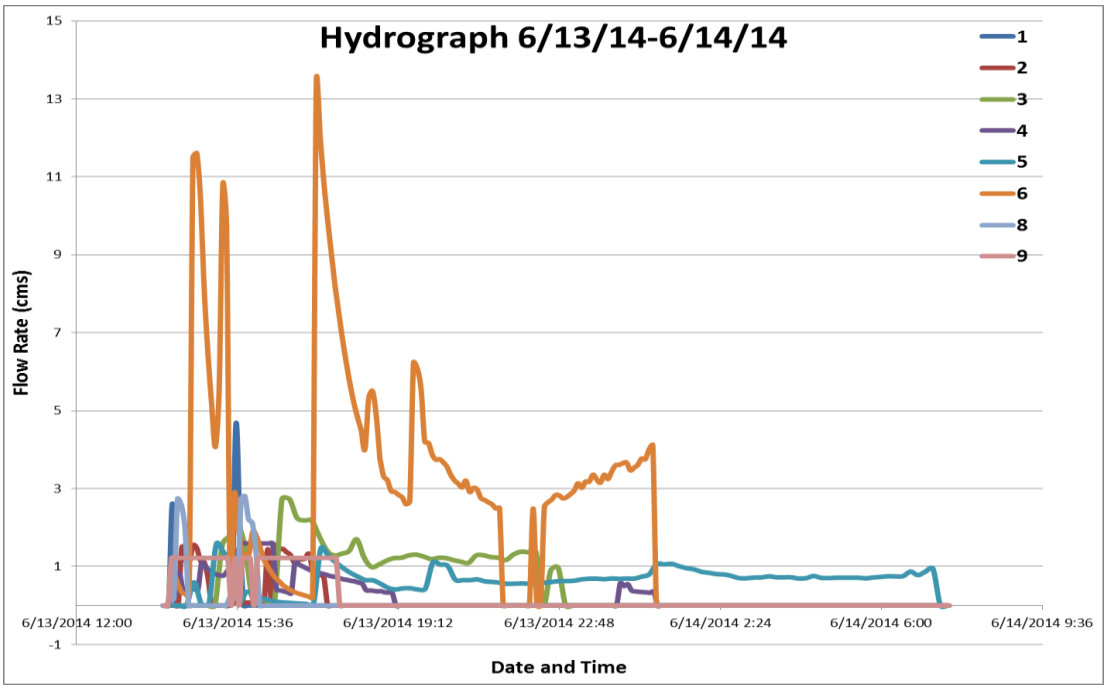

Figure A.123: Sensor hydrograph for all subwatersheds 1-11 for storm event 6/13/14-6/14/14 of 0.13 inches

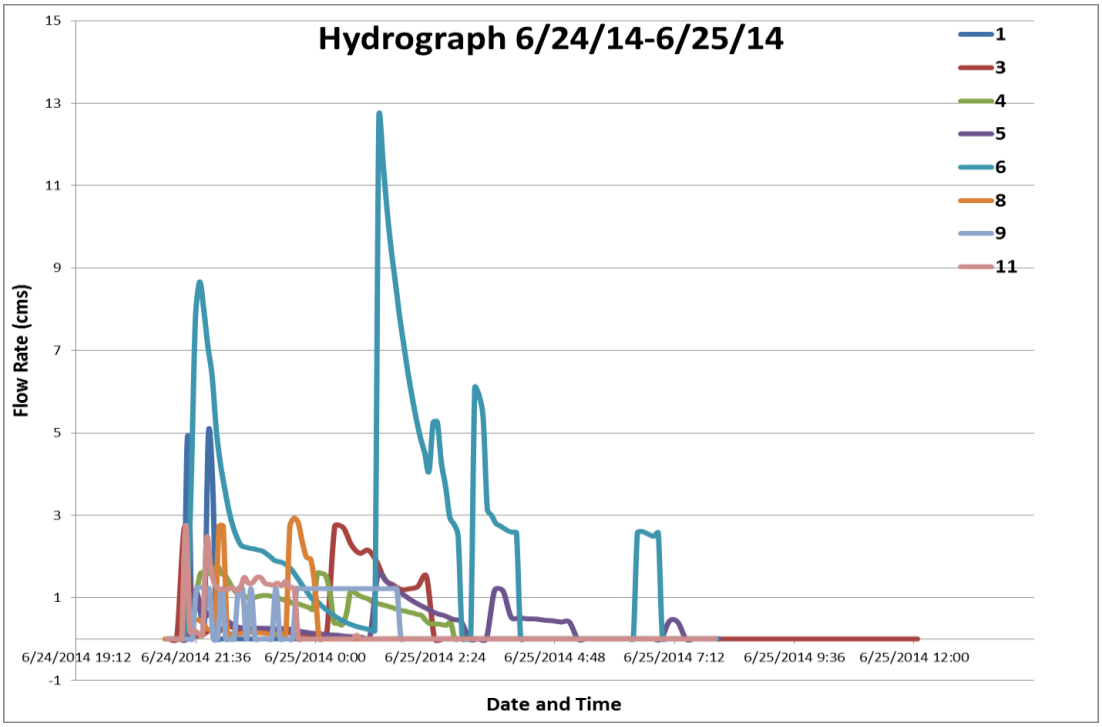

Figure A.124: Sensor hydrograph for all subwatersheds 1-11 for storm event 6/24/14-6/25/14 of 0.71 inches

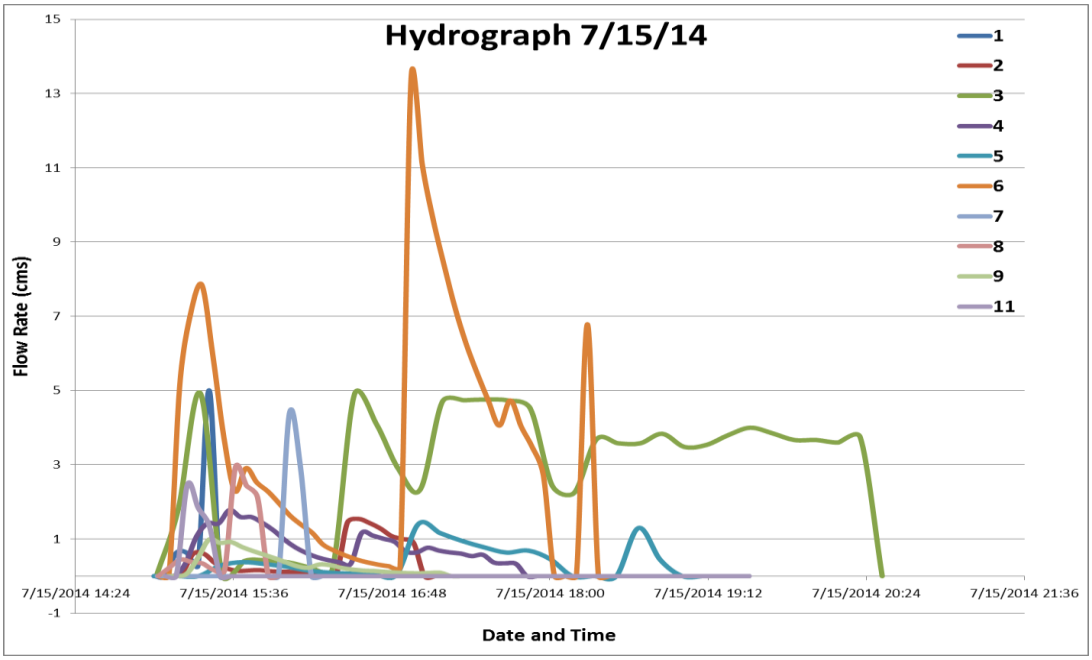

Figure A.125: Sensor hydrograph for all subwatersheds 1-11 for storm event 7/15/14 of 0.38 inches

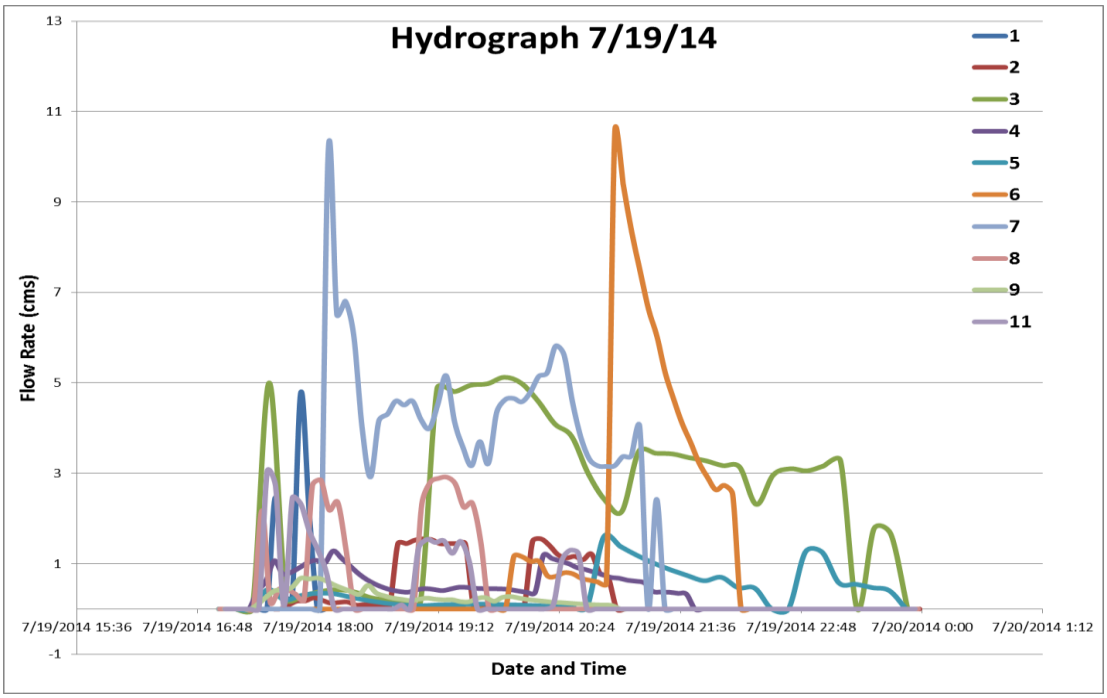

Figure A.126: Sensor hydrograph for all subwatersheds 1-11 for storm event 7/19/14 of 0.51 inches

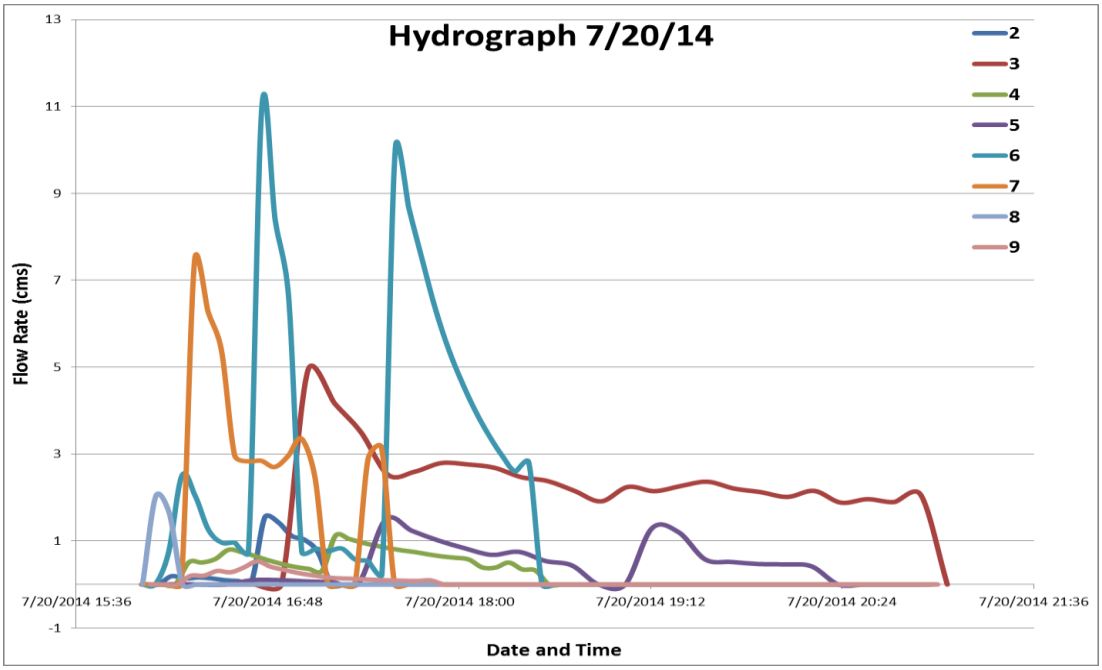

Figure A.127: Sensor hydrograph for all subwatersheds 1-11 for storm event 7/20/14 of 0.15 inches

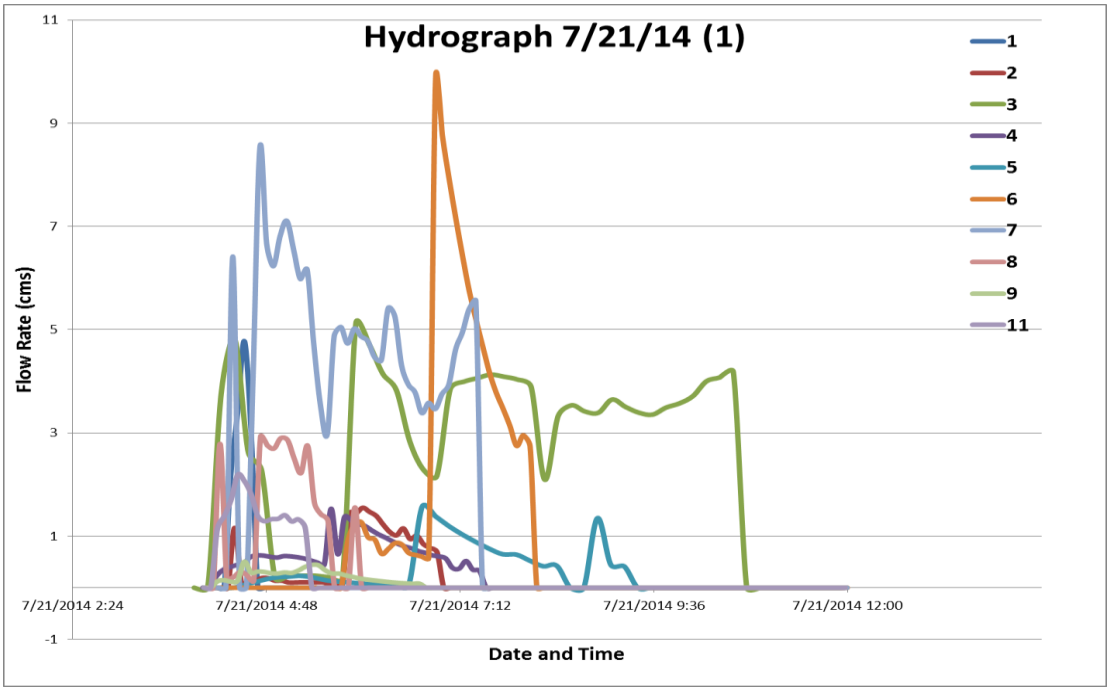

Figure A.128: Sensor hydrograph for all subwatersheds 1-11 for storm event 7/21/14 of 0.63 inches

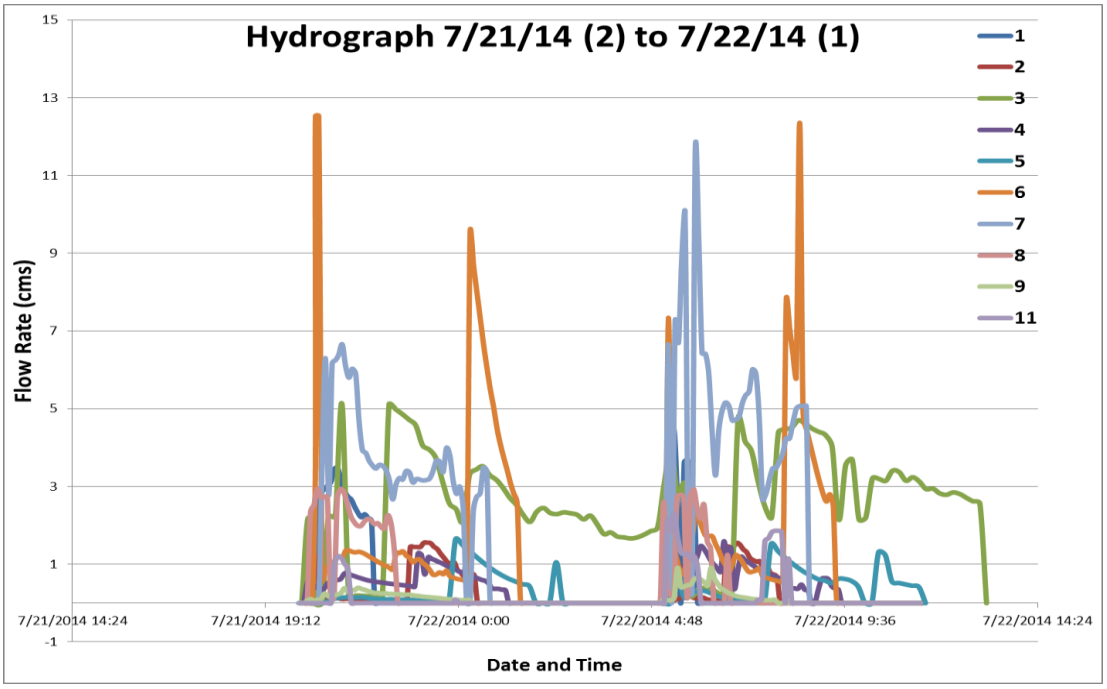

Figure A.129: Sensor hydrograph for all subwatersheds 1-11 for storm event 7/21/14-7/22/14 of 0.49 inches

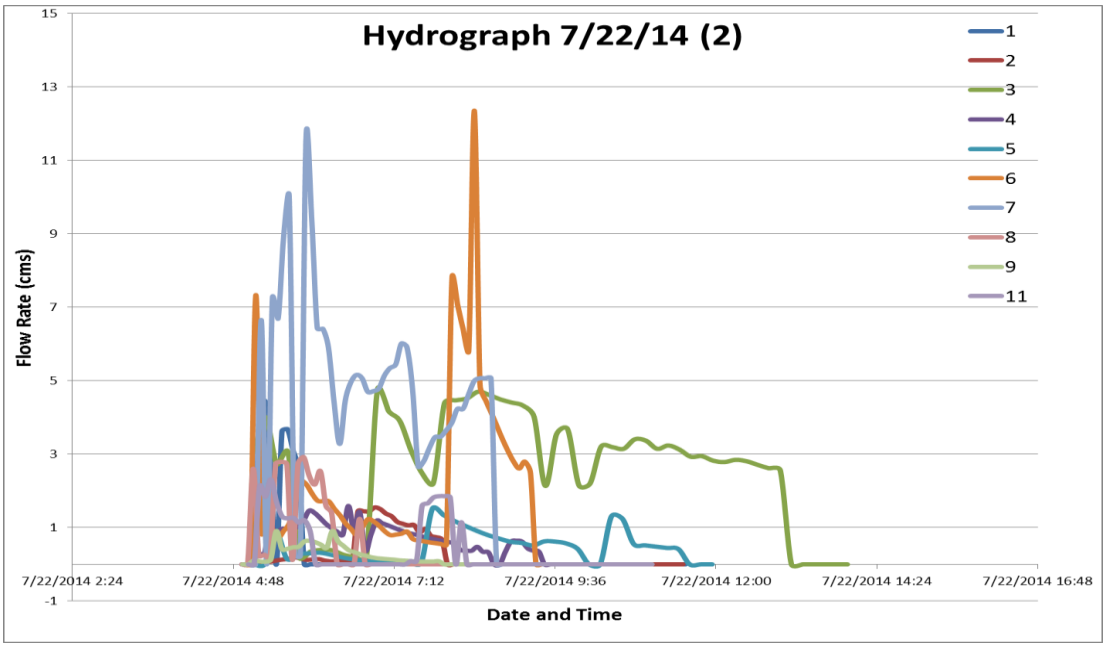

Figure A.130: Sensor hydrograph for all subwatersheds 1-11 for storm event 7/22/14 of 0.01 inches

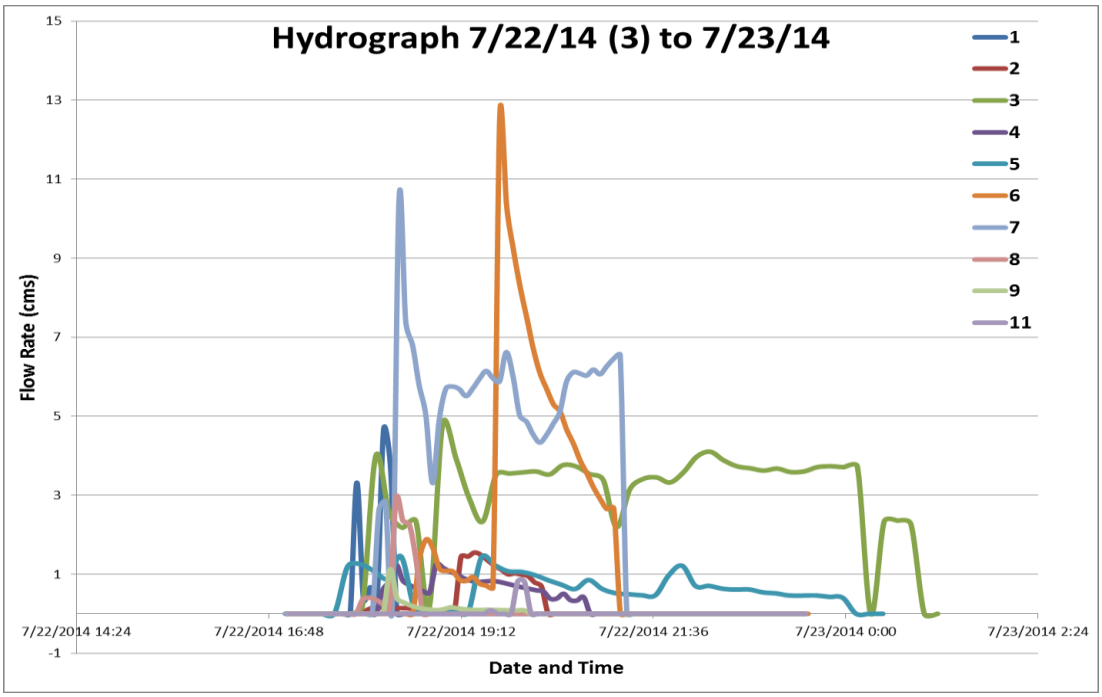

Figure A.131: Sensor hydrograph for all subwatersheds 1-11 for storm event 7/22/14-7/23/14 of 0.06 inches

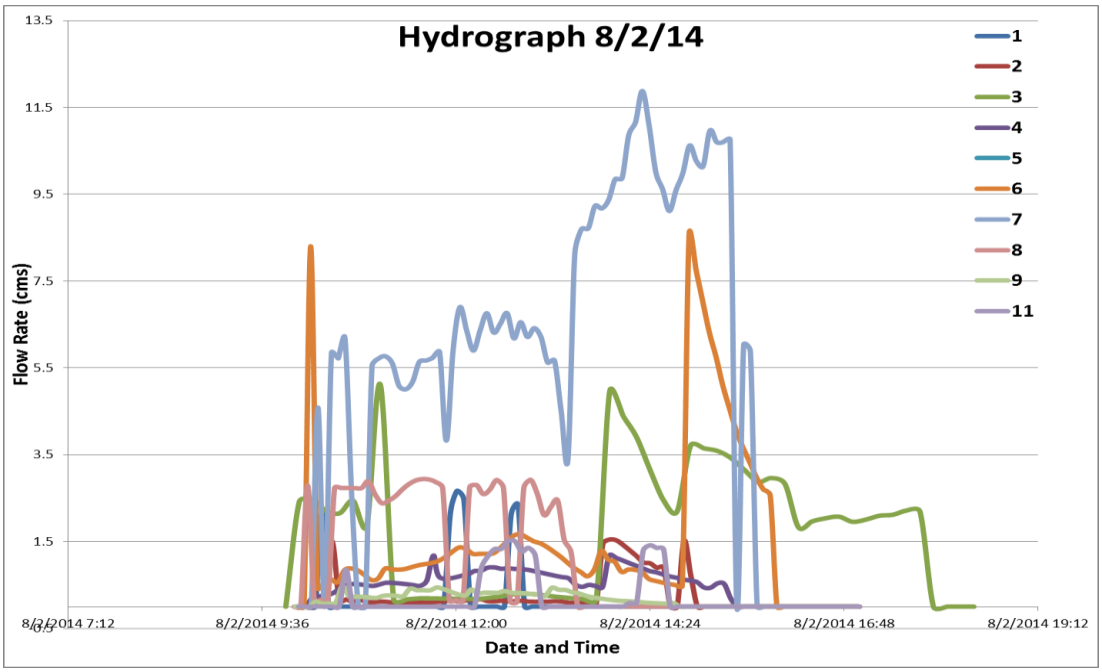

Figure A.132: Sensor hydrograph for all subwatersheds 1-11 for storm event 8/2/14 of 0.58 inches

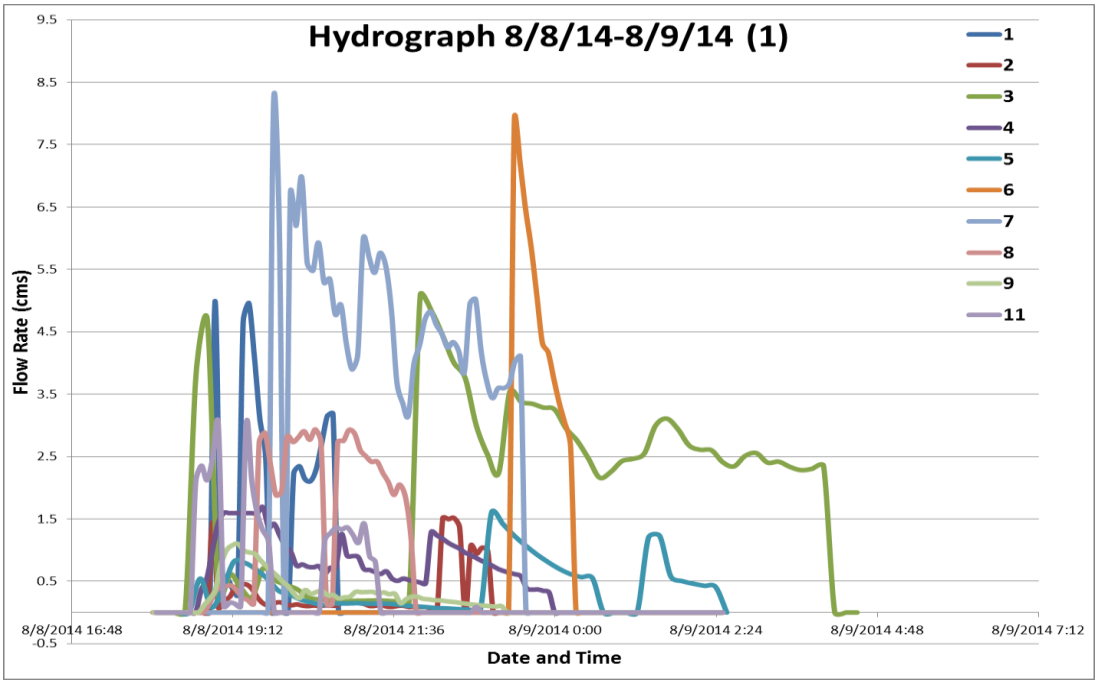

Figure A.133: Sensor hydrograph for all subwatersheds 1-11 for storm event 8/8/14-8/9/14 of 0.60 inches

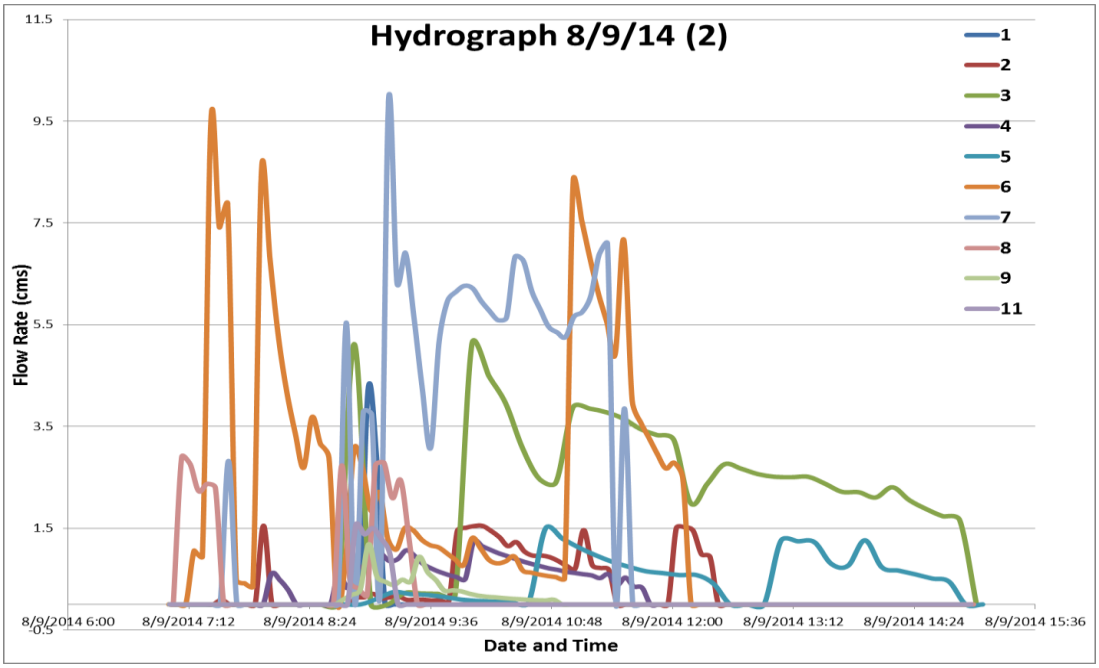

Figure A.134: Sensor hydrograph for all subwatersheds 1-11 for storm event 8/9/14 of 0.05 inches

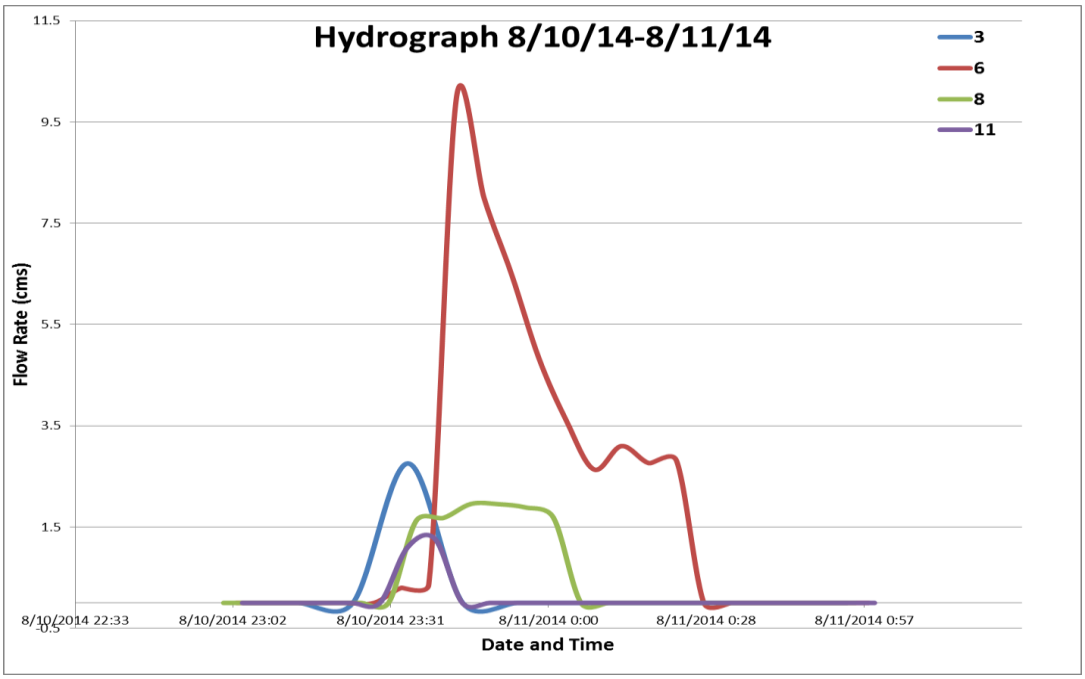

Figure A.135: Sensor hydrograph for all subwatersheds 1-11 for storm event 8/10/14-8/11/14 of 0.97 inches

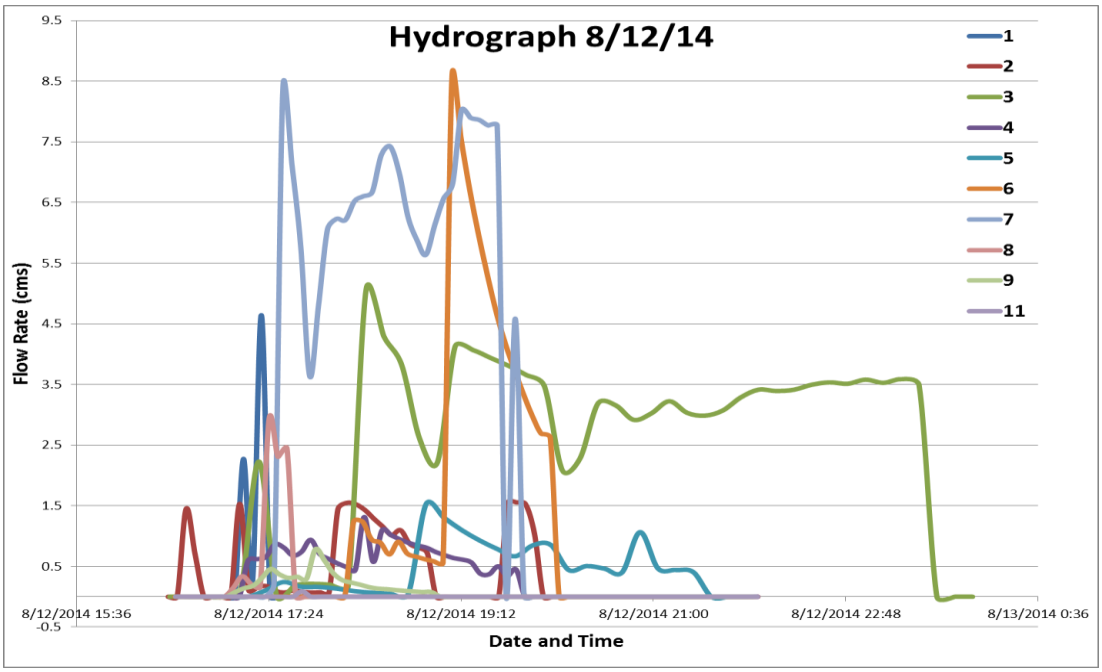

Figure A.136: Sensor hydrograph for all subwatersheds 1-11 for storm event 8/12/14 of 0.09 inches

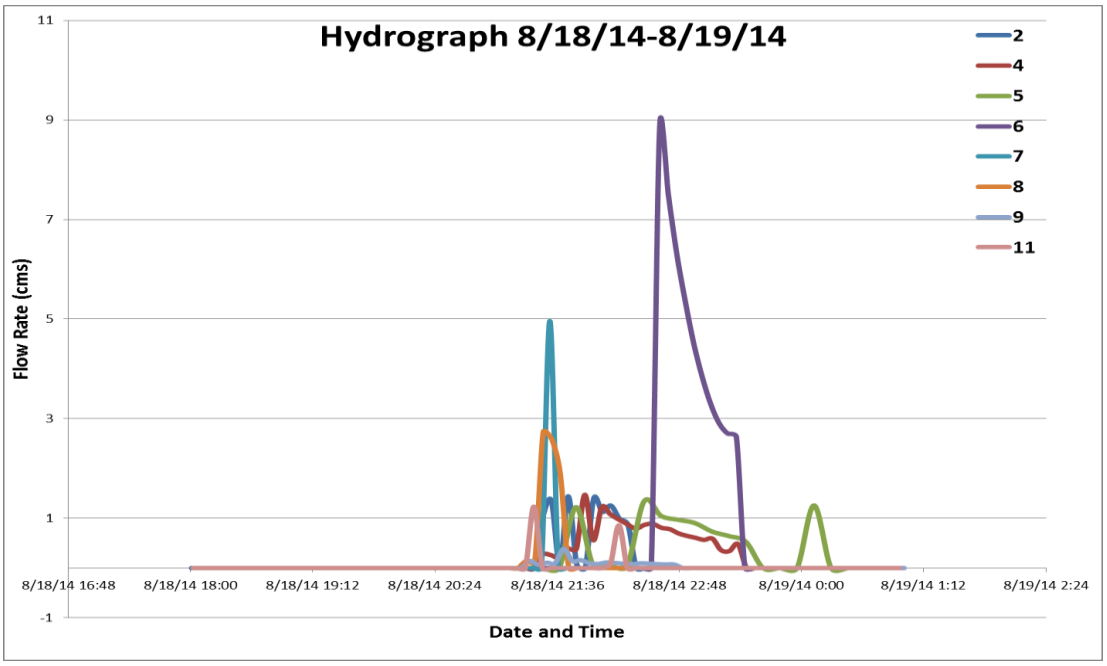

Figure A.137: Sensor hydrograph for all subwatersheds 1-11 for storm event 8/18/14-8/19/14 of 0.06 inches

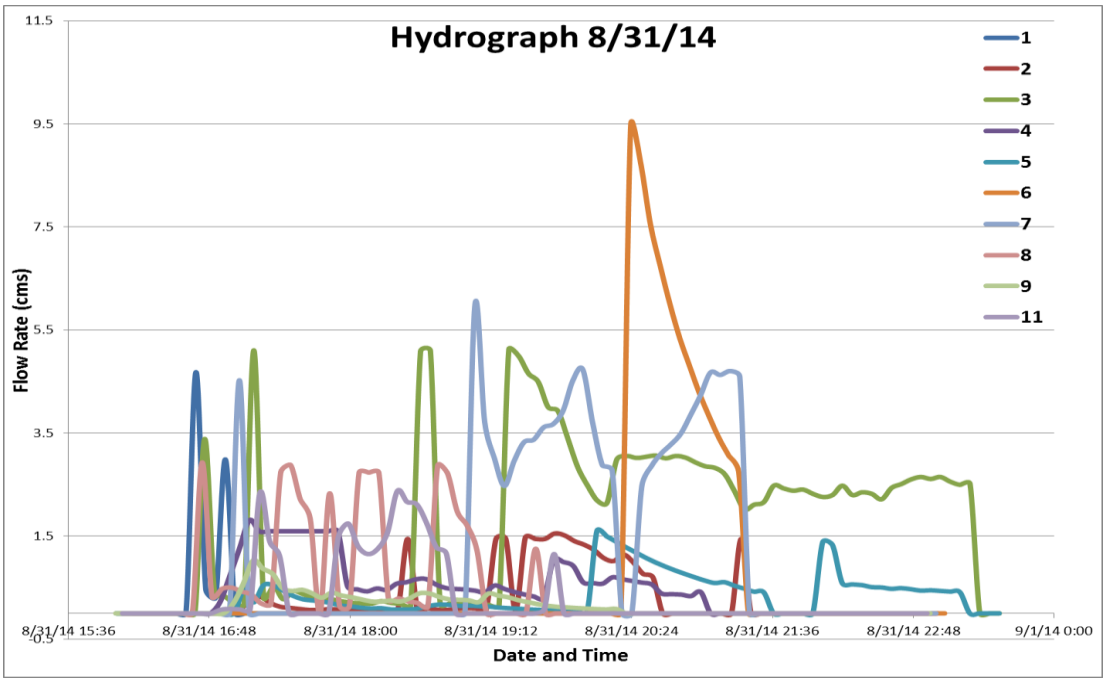

Figure A.138: Sensor hydrograph for all subwatersheds 1-11 for storm event 8/31/14 of 0.24 inches

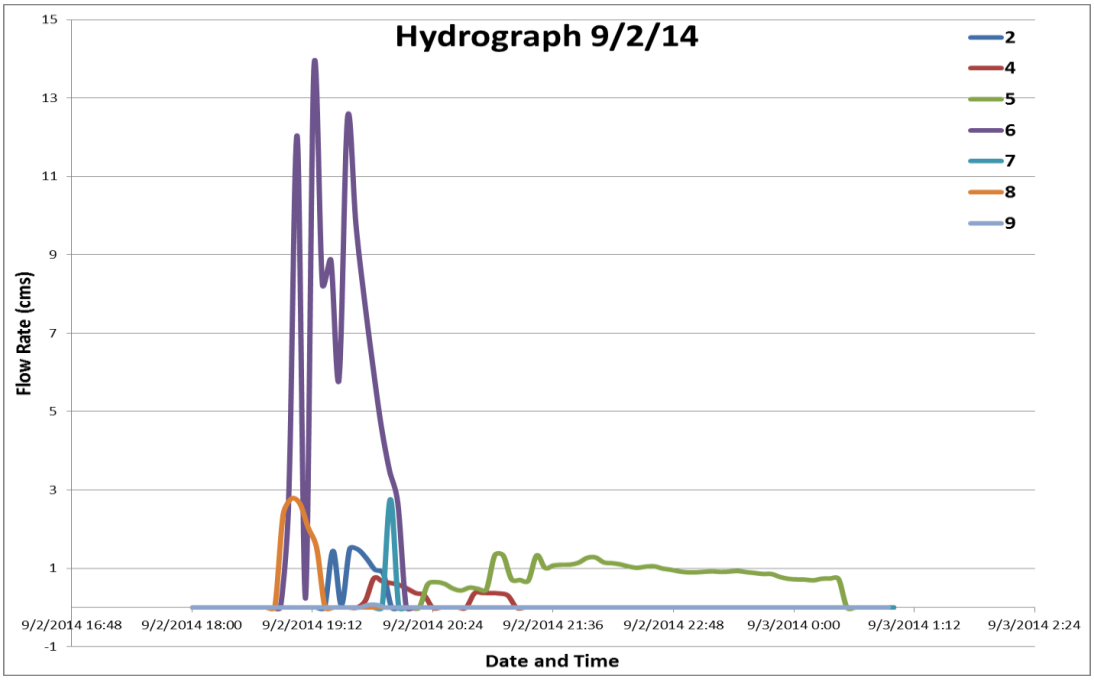

Figure A.139: Sensor hydrograph for all subwatersheds 1-11 for storm event 9/2/14-9/3/14 of 0.06 inches

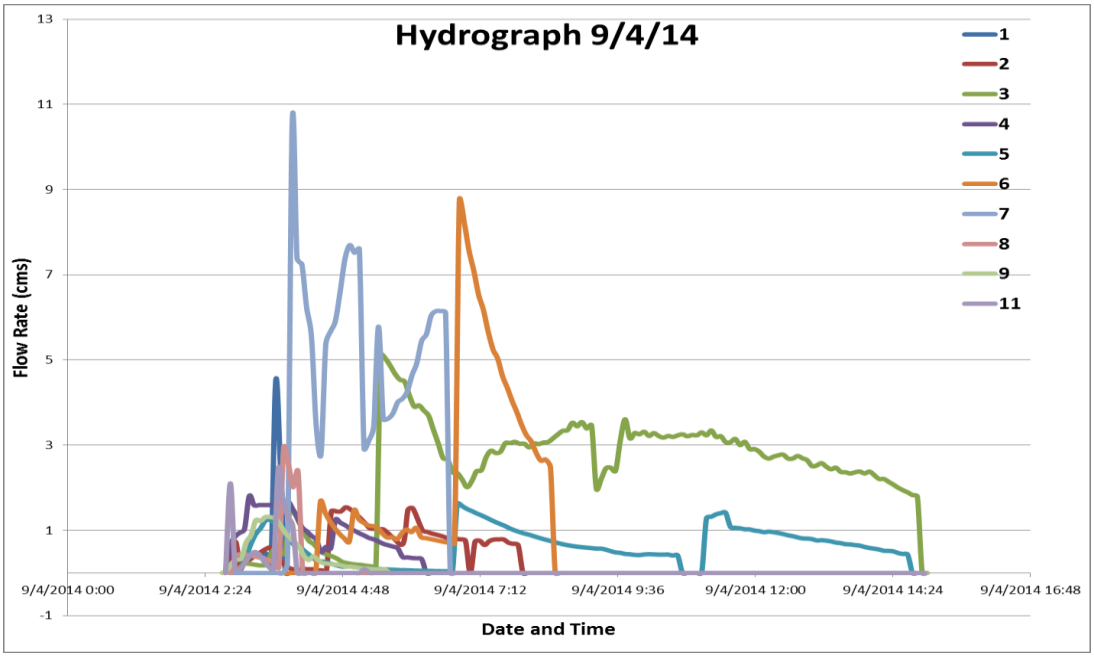

Figure A.140: Sensor hydrograph for all subwatersheds 1-11 for storm event 9/4/14 of 1.61 inches

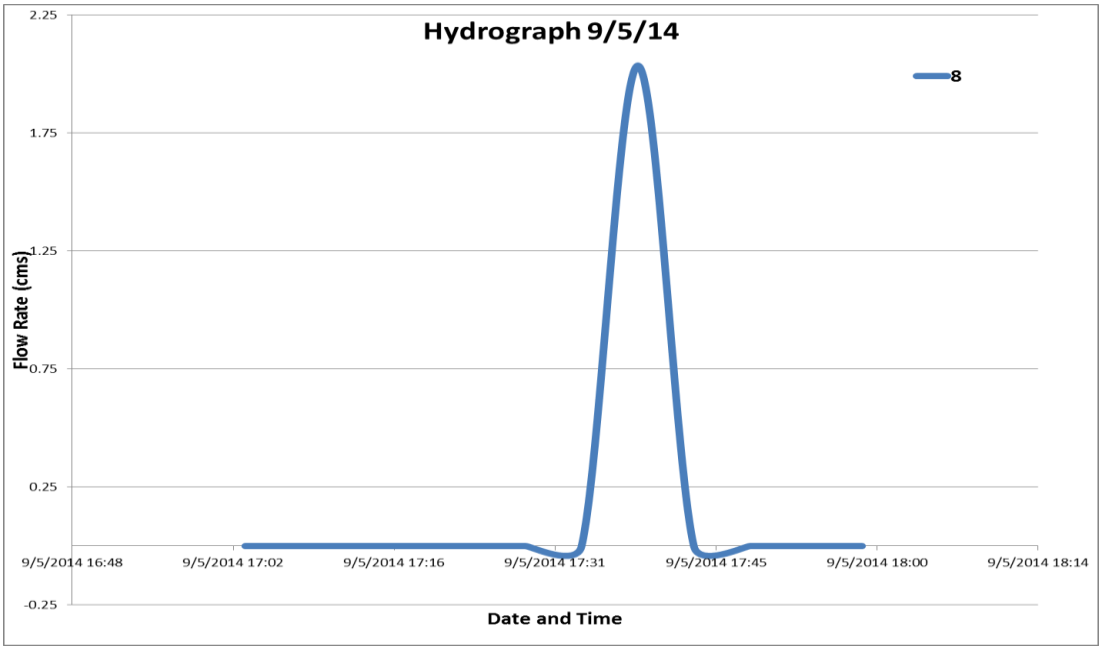

Figure A.141: Sensor hydrograph for all subwatersheds 1-11 for storm event 9/5/14 of 0.05 inches

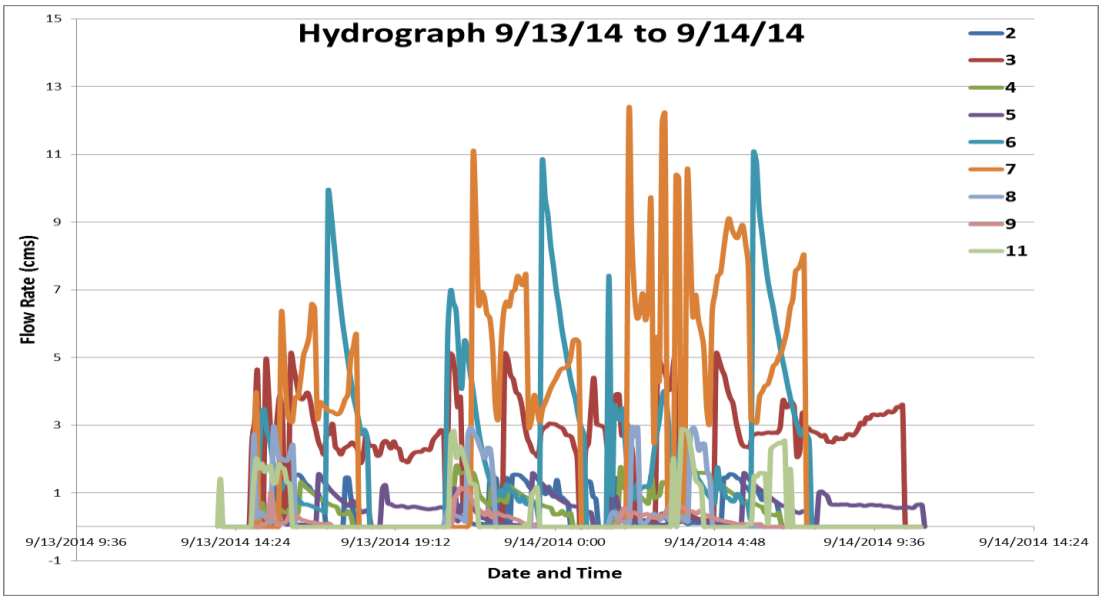

Figure A.142: Sensor hydrograph for all subwatersheds 1-11 for storm events 9/13/14 of 0.06 inches, 9/13/14 of 0.08 inches, and 9/14/14 of 0.36 inches

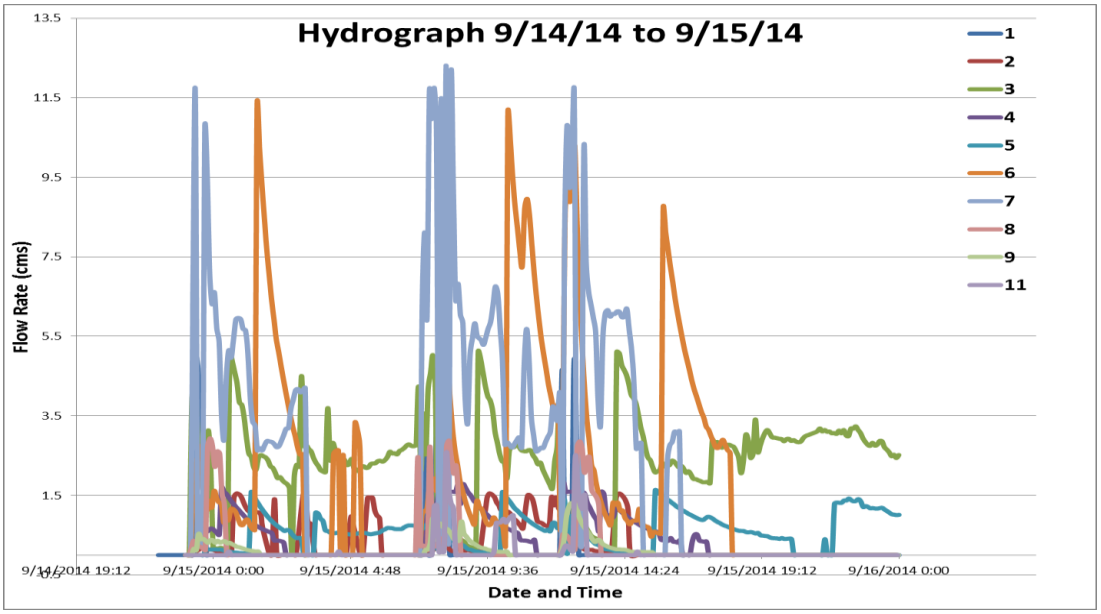

Figure A.145: Sensor hydrograph for all subwatersheds 1-11 for storm events 9/14/14-9/15/14 of 0.22 inches, 9/15/14 of 0.12 inches, and 9/15/14-9/16/14 of 0.01 inches

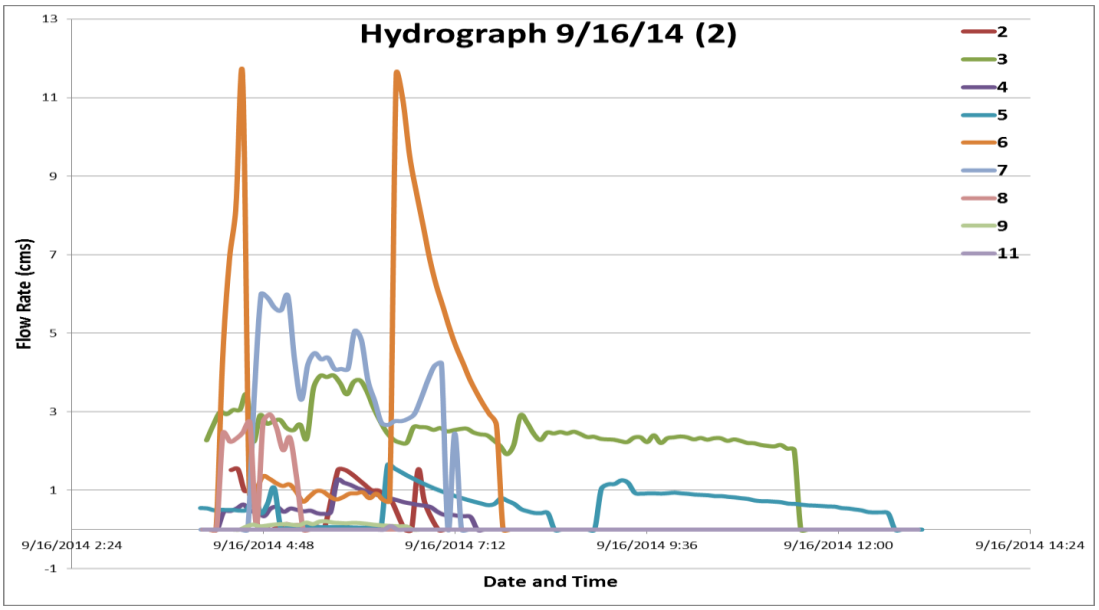

Figure A.148: Sensor hydrograph for all subwatersheds 1-11 for storm event 9/16/14 of 0.11 inches

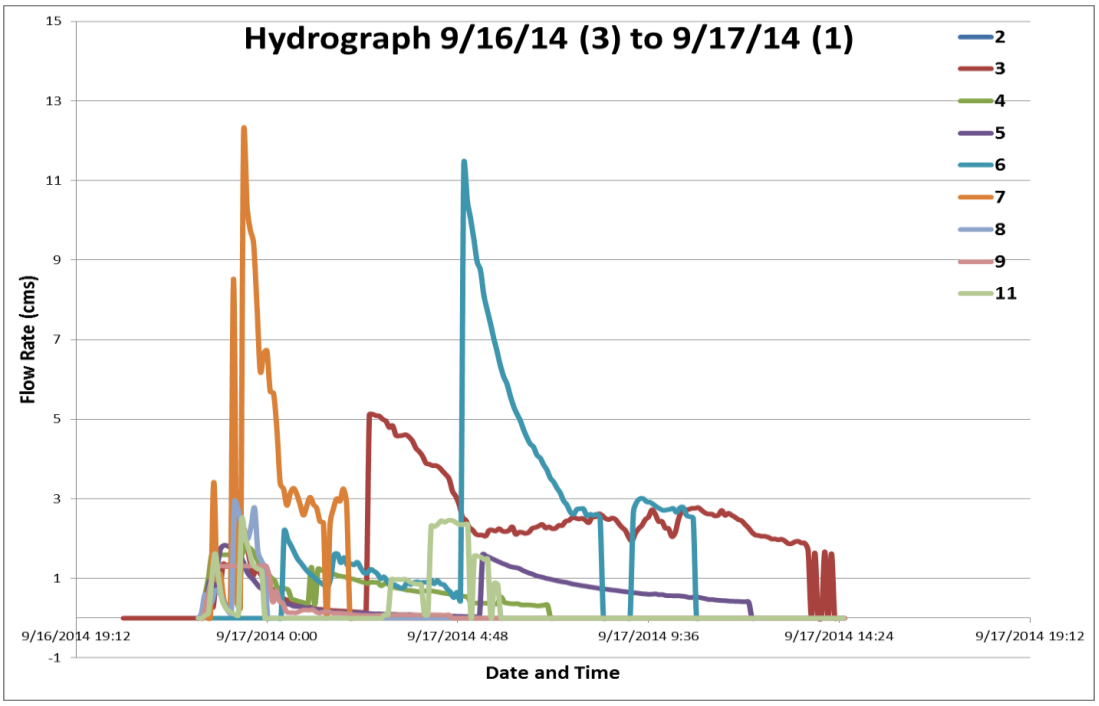

Figure A.149: Sensor hydrograph for all subwatersheds 1-11 for storm event 9/16/14-9/17/14 of 0.19 inches

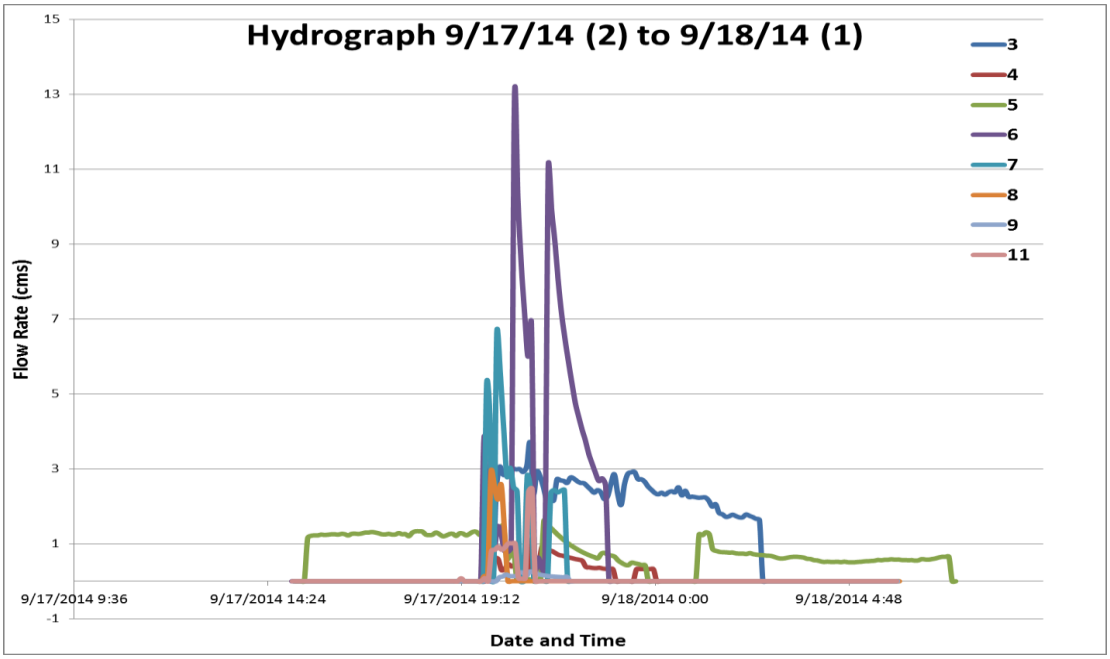

Figure A.150: Sensor hydrograph for all subwatersheds 1-11 for storm event 9/17/14-9/18/14 of 1.05 inches

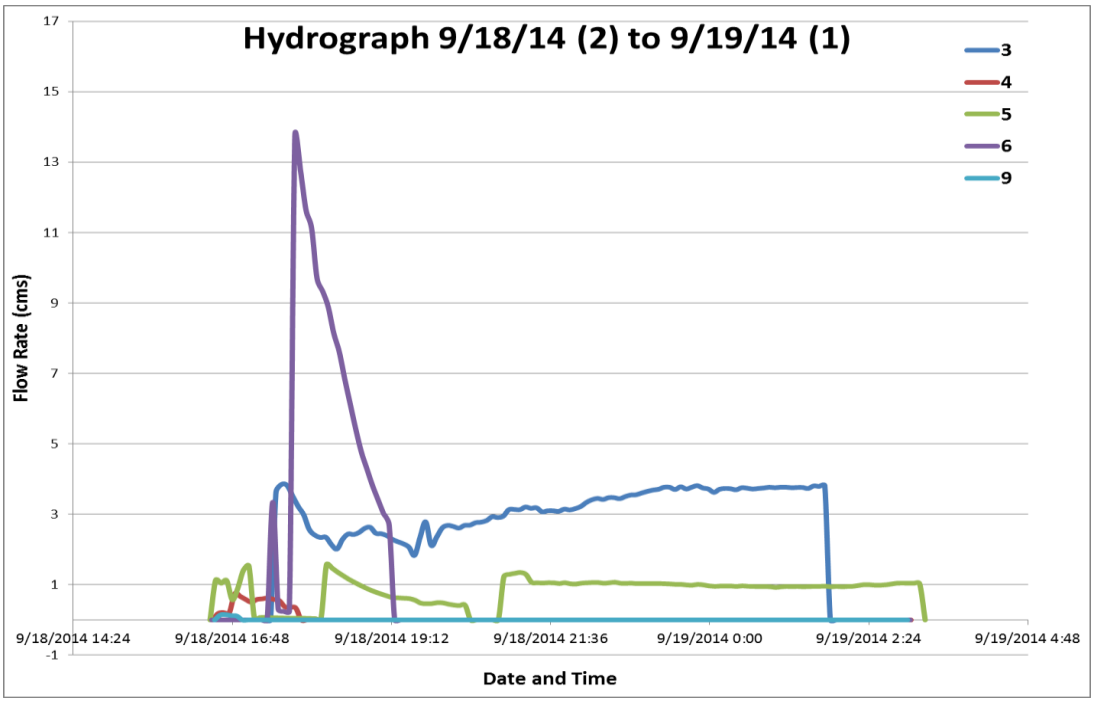

Figure A.151: Sensor hydrograph for all subwatersheds 1-11 for storm event 9/18/14-9/19/14 of 0.41 inches

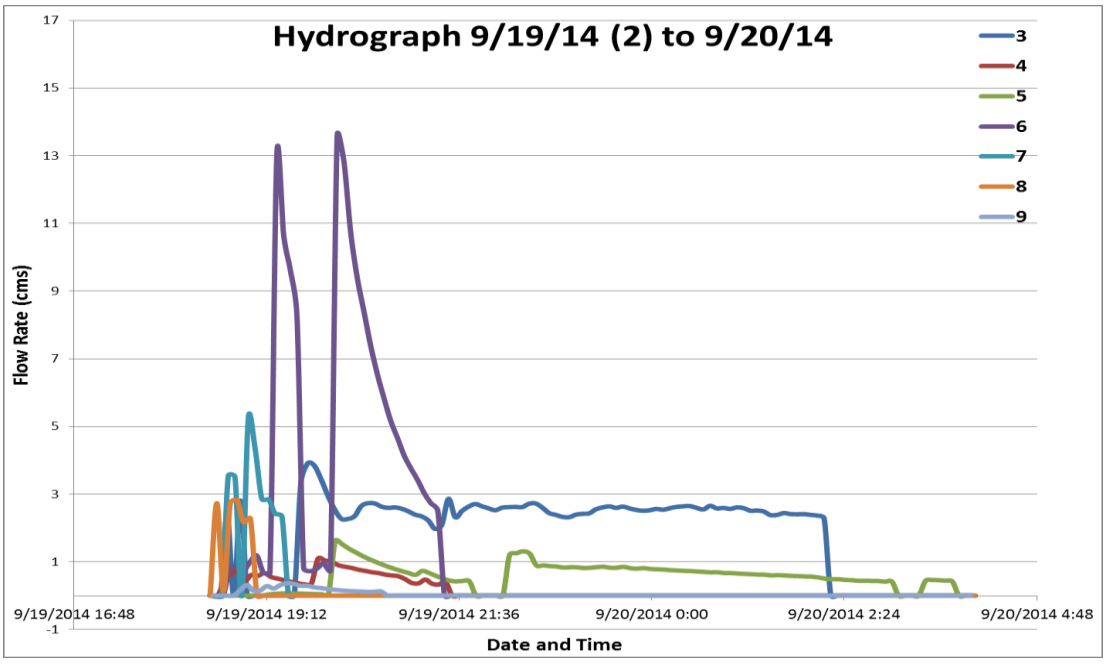

Figure A.152: Sensor hydrograph for all subwatersheds 1-11 for storm event 9/19/14-9/20/14 of 0.02 inches

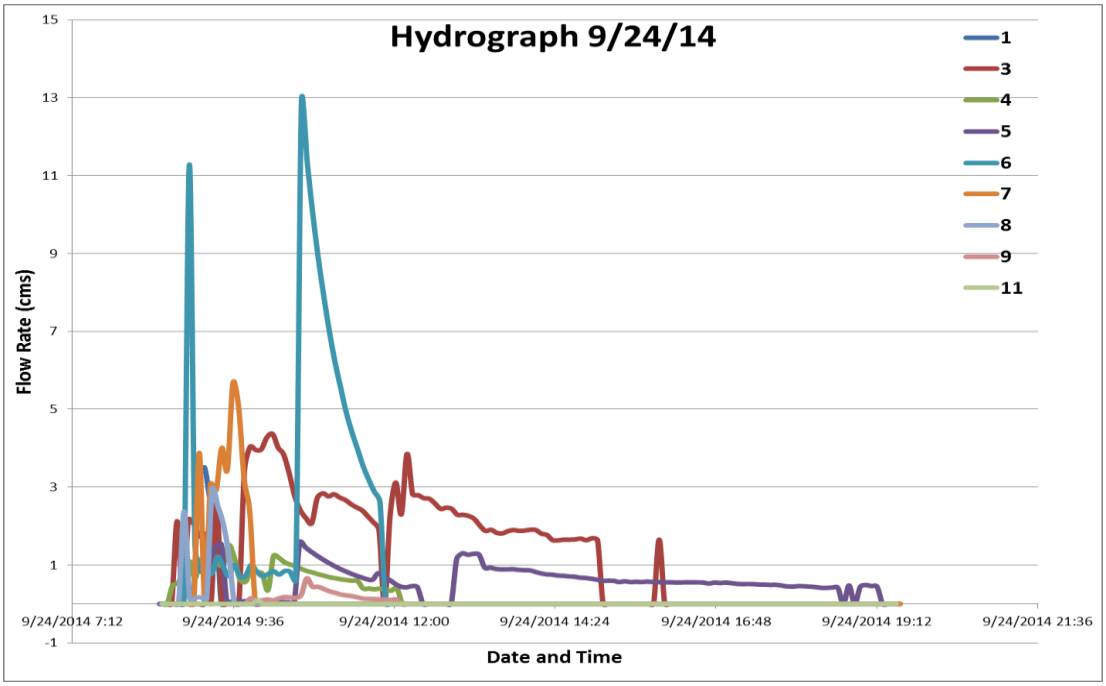

Figure A.153: Sensor hydrograph for all subwatersheds 1-11 for storm event 9/24/14 of 0.15 inches